BACKFILL EFFECTS ON RESPONSE OF BURIED REINFORCED CONCRETE SLABS

by

Pamela G. Hayes

Structures Laboratory

DEPARTMENT OF THE ARMY
Waterways Experiment Station, Corps of Engineers
3909 Halls Ferry Road, Vicksburg, Mississippi 39180-6199

US Army Corps of Engineers

AD-A215 823

STRUCTURES LABORATORY

DTIC
ELECTE
DEC 21 1989
S
B
D

September 1989
Final Report

89 12 21 032

REPORT DOCUMENTATION PAGE

Form Approved
OMB No. 0704-0188

1a. REPORT SECURITY CLASSIFICATION	1b. RESTRICTIVE MARKINGS
Unclassified	

2a. SECURITY CLASSIFICATION AUTHORITY	3. DISTRIBUTION/AVAILABILITY OF REPORT
	Approval for public release; distribution unlimited.
2b. DECLASSIFICATION/DOWNGRADING SCHEDULE	

4. PERFORMING ORGANIZATION REPORT NUMBER(S)	5. MONITORING ORGANIZATION REPORT NUMBER(S)
Technical Report SL-89-18	

6a. NAME OF PERFORMING ORGANIZATION	6b. OFFICE SYMBOL (If applicable)	7a. NAME OF MONITORING ORGANIZATION
USAEWES Structures Laboratory	CEWES-SS-E	

6c. ADDRESS (City, State, and ZIP Code)	7b. ADDRESS (City, State, and ZIP Code)
3909 Halls Ferry Road Vicksburg, MS 39180-6199	

8a. NAME OF FUNDING/SPONSORING ORGANIZATION	8b. OFFICE SYMBOL (If applicable)	9. PROCUREMENT INSTRUMENT IDENTIFICATION NUMBER
Defense Nuclear Agency		

8c. ADDRESS (City, State, and ZIP Code)	10. SOURCE OF FUNDING NUMBERS See reverse.			
Washington, DC 20305-1000	PROGRAM ELEMENT NO.	PROJECT NO.	TASK NO.	WORK UNIT ACCESSION NO.

11. TITLE (Include Security Classification)

Backfill Effects on Response of Buried, Reinforced Concrete Slabs

12. PERSONAL AUTHOR(S)
Hayes, Pamela G.

13a. TYPE OF REPORT	13b. TIME COVERED	14. DATE OF REPORT (Year, Month, Day)	15. PAGE COUNT
Final Report	FROM Oct 88 TO Sep 89	September 1989	240

16. SUPPLEMENTARY NOTATION

Available from National Technical Information Service, 5285 Port Royal Road, Springfield, VA 22161

17. COSATI CODES			18. SUBJECT TERMS (Continue on reverse if necessary and identify by block number)
FIELD	GROUP	SUB-GROUP	Backfill effects; Seismic velocity;
			Blast response; Shear strength;
			Protective structures; Wave speed. (EDC)

19. ABSTRACT (Continue on reverse if necessary and identify by block number)

The Backfill Effects tests were conducted in various backfill materials and provided data on the response of buried structures to localized point-source loadings. Four tests were conducted in this test series. To represent realistic backfill materials, two low seismic velocity materials, a high-shear-strength flume sand and a low-shear-strength reconstituted clay were used. The high seismic velocity material was obtained by using an in situ clay layer. The test articles were inforced concrete slabs mounted on a reaction structure for testing. The test slabs had L/t ratios of 5 and 10.

The results of this test series show that backfill material makes a significant difference in the response of buried structures. The tests conducted in the low seismic velocity materials had drastically different responses. A breach occurred in the test with the low-shear-strength, low seismic velocity reconstituted clay backfill, and light damage occurred in the test with the high-shear-strength, low seismic velocity sand backfill. Significant damage also occurred in the test with the high seismic velocity backfill.

20. DISTRIBUTION/AVAILABILITY OF ABSTRACT	21. ABSTRACT SECURITY CLASSIFICATION
☐ UNCLASSIFIED/UNLIMITED ☒ SAME AS RPT ☐ DTIC USERS	Unclassified
22a. NAME OF RESPONSIBLE INDIVIDUAL	22b. TELEPHONE (Include Area Code) 22c. OFFICE SYMBOL

DD Form 1473, JUN 86 *Previous editions are obsolete.* SECURITY CLASSIFICATION OF THIS PAGE

Key Words: Construction materials; structural response;

A

10. SOURCE OF FUNDING NUMBERS (Continued).

Headquarters, US Army Corps of Engineers, Project No. 4A762719AT40, Task HS, Work Unit 004, "Critical EAC Facilities/Sand Backfill Test," and Defense Nuclear Agency, Task Code RS/RC Structural Response, Work Unit/Conventional Weapons Backfill Test.

PREFACE

This report documents research conducted by members of the staff of the Structural Mechanics Division (SMD), Structures Laboratory (SL), US Army Engineer Waterways Experiment Station (WFS). The research was jointly sponsored by the Defense Nuclear Agency (DNA), under Task Code RS/RC Structural Response, Work Unit/Conventional Weapons Backfill Test, and Headquarters, US Army Corps of Engineers, under Project No. 4A762719AT40, Task HS, Work Unit 004, "Critical EAC Facilities/Sand Backfill Test." LTC Carlos Rubio was Technical Monitor, DNA.

This work was accomplished during the period October 1988 through September 1989 under the general supervision of Messrs. Bryant Mather, Chief, SL; James T. Ballard, Assistant Chief, SL; and Dr. Jimmy P. Balsara, Chief, SMD. Project Manager was Dr. Sam Kiger, and the Principal Investigator was Ms. Pamela G. Hayes, both of SMD. This report was published by the Information Technology Laboratory, WES.

COL Larry B. Fulton, EN, is the Commander and Director of WES. Dr. Robert W. Whalin is Technical Director.

Accession For	
NTIS GRA&I	☑
DTIC TAB	☐
Unannounced	☐
Justification	
By	
Distribution/	
Availability Codes	
Dist	Avail and/or Special
A-1	

1

CONTENTS

LIST OF ILLUSTRATIONS

3

LIST OF TABLES

CONVERSION FACTORS, NON-SI TO SI (METRIC)
UNITS OF MEASUREMENT

Non-SI units of measurement used in this report can be converted to SI (metric) units as follows:

Multiply	By	To Obtain
cubic feet	0.02831685	cubic metres
inches	25.4	millimetres
feet	0.3048	metres
feet per second (fps)	0.3048	metres per second
pounds (mass)	0.45359237	kilograms
pounds (force) per square inch (psi)	0.006895	megapascals

BACKFILL EFFECTS ON RESPONSE
OF BURIED REINFORCED CONCRETE SLABS

CHAPTER 1
INTRODUCTION

1.1 BACKGROUND

Soil-Structure interaction (SSI) is an important consideration in calculating the response of buried structures to blast effects. Results from the Shallow-Buried-Structures (SBS) research program, sponsored jointly by the Defense Nuclear Agency (DNA) and the Office, Chief of Engineers, have shown that the response of identical buried test slabs varies from slight damage to severe damage in different backfills when loaded with identical plane-wave type dynamic loads. The slabs buried as shallow as 50 percent of the roof span in a high shear strength sand sustained about ten times higher peak dynamic pressures than predicted when SSI effects were neglected. The unexpected hardness of the buried test slabs resulted because the effects of SSI had been underestimated. Data from the SBS research have resulted in significant revisions in vulnerability and design calculations for buried protective structures.

The SBS tests have shown that SSI is an important consideration in the prediction of buried structure response, and that the SSI effects vary based on the specific backfill material around the structure. The SBS test program involved testing reinforced concrete structures in a shallow-buried configuration using a HEST (High Explosive Simulation Technique) test which produced a plane-wave type dynamic load. The first test in this series, Foam HEST 1, was conducted in a sand backfill material with a charge density which resulted in a peak pressure of 1,900 psi[1]. The structure suffered only minor damage, with a center roof deflection of 0.5 inch. The interface pressure records for this test are shown in Figure 1.1. The third test of this series, Foam HEST 3, was conducted on an identical structure using the same test configuration with a clay backfill material. The charge density and HEST configuration was the same as that used in Foam HEST 1. However,

---

[1] A table of factors for converting from non-SI to SI (metric) units of measure can be found on page 5.

damage to the structure was approximately 6 inches of permanent deflection at the center of the roof. Interface pressure records for this test are shown in Figure 1.2. References 1 and 2 have summaries of all tests in the SBS program, while References 3 and 4 document the details of Foam HEST 1 and Foam HEST 3.

These tests show that when the same charge density is detonated in the HEST configuration above shallow-buried structures the loading on the structure and the response of the structure vary with different types of backfill material. Reference 2 documents the procedures developed during this test program to predict buried structure response for this type of loading considering the effects of SSI.

There has been a great deal of uncertainty in attempts to extrapolate the analytical methods developed in the SBS research program for a plane-wave type loading to compute buried structure response to a point-source type loading. For example, the curves shown in Figure 1.3 indicate about the same predicted structural response in a backfill with low seismic velocity (about 1,000 fps), but show a considerable difference at higher seismic velocities when using two different analytical methods. Before this test program virtually all experiments were conducted in a sand backfill, and there was no data from tests using a localized point-source load on buried structures in backfill materials with seismic velocities outside the range of about 800 fps to 1,500 fps. Differences indicated by the curves in Figure 1.3 are important since the analytical methods for the design of hardened structures from the Army Technical Manual #5-855-1 (Reference 5) predict increasing structural response with increasing seismic velocity, and analytic' methods presen'd by Hinman, et al, (Reference 6) predict structural response to be very nearly independent of seismic velocity. Based on the SBS test results and the differences presented by these two analytical methods, it is important to obtain test data on the response of buried structures to localized loading in various backfill materials to assure proper evaluation of the analytical methods for predicting buried structure response.

The Backfill Effects test series was proposed and conducted to provide the data base necessary to allow evaluation of the analytical methods depicted by the curves in Figure 1.3 and provide the information necessary

for the development of better predictive methods for ground shock and structural response from nearby point-source loadings.

1.2 OBJECTIVES

The objectives of this test program are to develop a consistent set of data for ground shock and structural response from localized loadings in various backfills. The data is used to evaluate the accuracy of current analytic methods for predicting structural loadings and response for buried structures. Data from this test program was prepared and presented in a manner which will aid the development of improved methods for calculating the loading and response of buried structures subjected to ground shock generated by nearby point-source loadings.

1.3 SCOPE OF WORK

The Backfill Effects tests were conducted in various backfill materials and provided data on the response of buried structures to localized point-source loading in each backfill material. These tests were conducted in one material with a relatively low seismic velocity and one with a relatively high seismic velocity. To represent realistic backfill materials, two low seismic velocity materials, a high shear strength flume sand and a low shear strength reconstituted clay, were used. For the high seismic velocity material, an in-situ clay layer with a seismic velocity of approximately 3,000 fps was used.

The test series consisted of four tests of buried structures with cylindrical charges in various backfill materials. Two of the tests were in the reconstituted clay backfill; one test on a relatively flexible test slab and one on a relatively stiff test slab. Two additional tests were conducted on flexible test slabs in backfills of compacted flume sand and in-situ clay. The test slabs were constructed with L/t ratios of 5 and 10, using designs corresponding to those used in previous localized loading tests with flume sand backfills (Reference 7). The test slabs were tested on a reaction structure also designed for previous flume sand tests. Instrumentation included structural and free-field accelerometers, interface pressure gages, deflection gages, and soil stress gages.
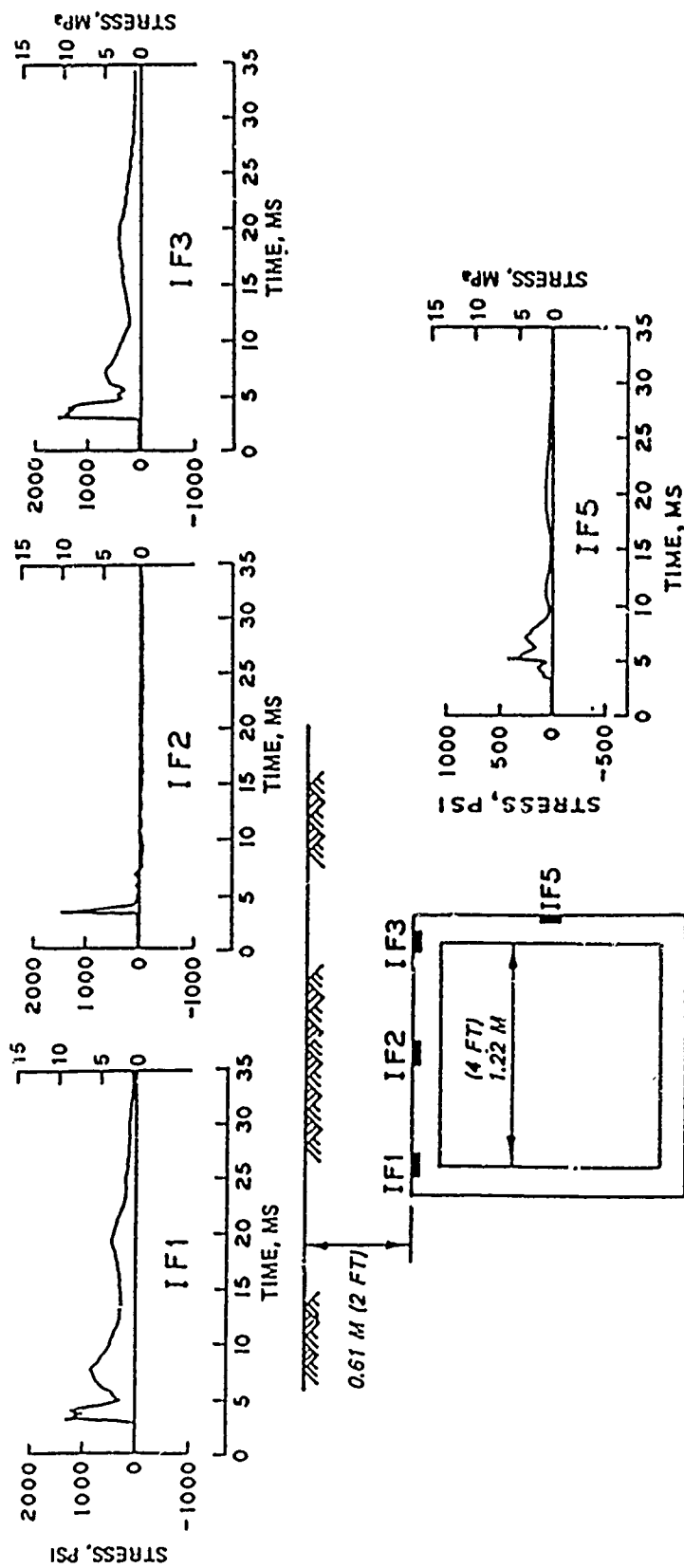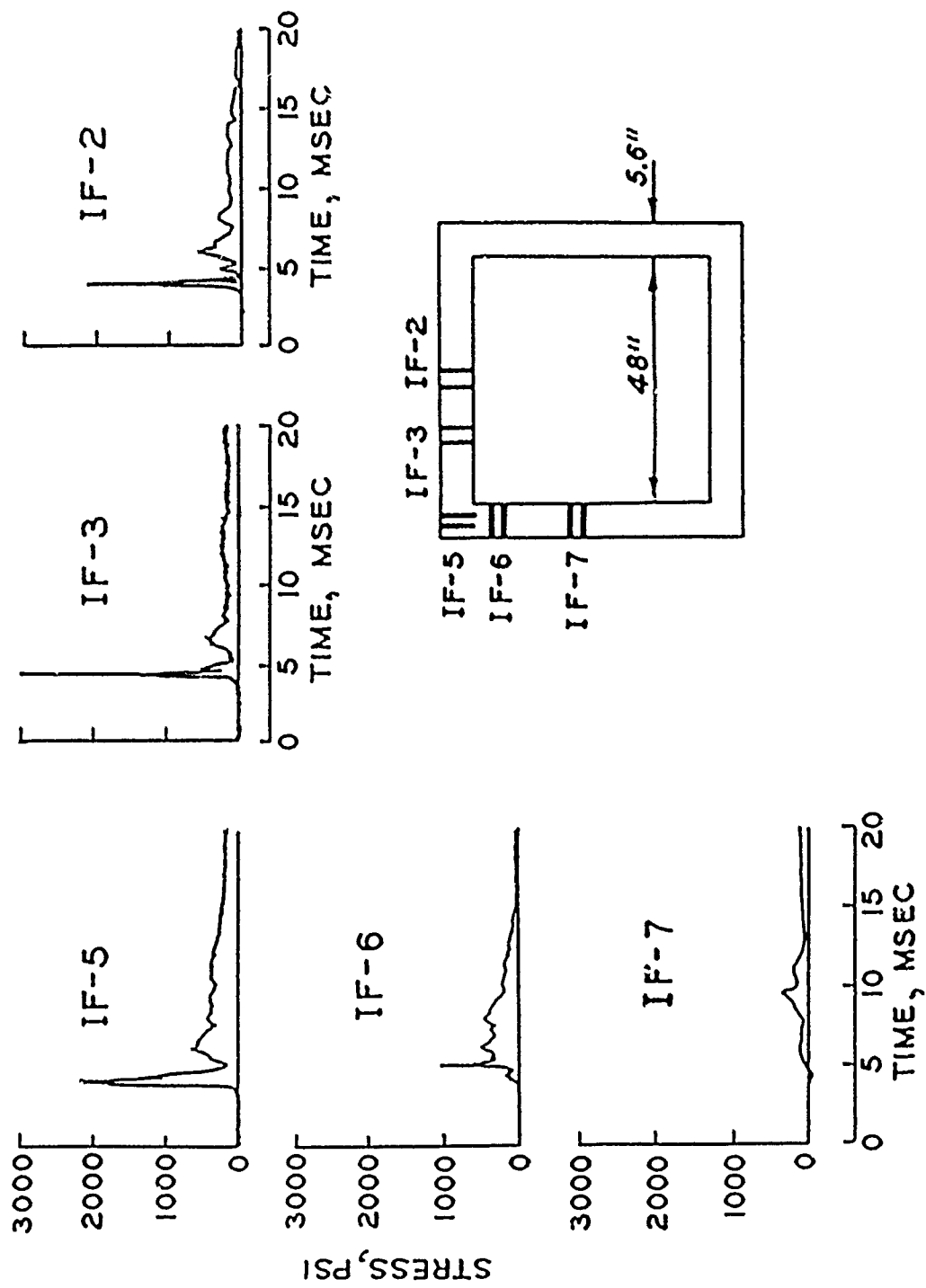
8

Figure 1.1. Interface pressure records, Foam HEST 1.
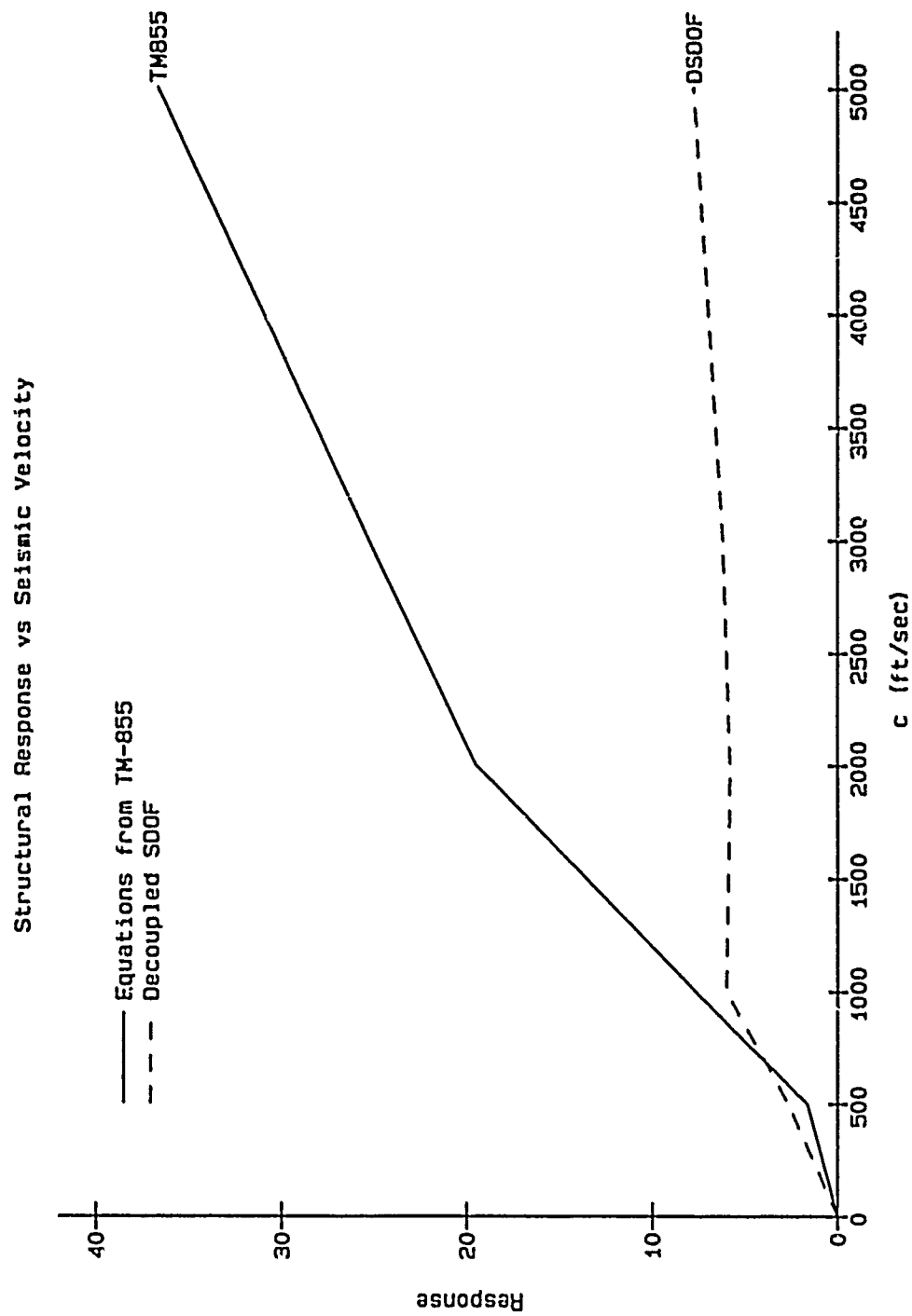
Figure 1.2. Interface pressure records, Foam HEST 3.

Figure 1.3. Comparison of structural response vs. seismic velocity.

11

CHAPTER 2

RELATED TESTS

All of the tests conducted previously using localized loading and buried structures have had backfill materials with seismic velocities in the range of 800 fps to 1,500 fps. An example of this type of test was conducted at Fort Polk, LA in 1983, by the Structural Mechanics Division, Structures Laboratory, US Army Engineer Waterways Experiment Station (WES) and used a buried reaction structure with various test slabs against the detonation of a a cased explosive charge. All of the tests were conducted with a backfill material of compacted flume sand having a seismic velocity of approximately 1,000 fps. These tests were sponsored by the Air Force Engineering and Services Center (AFESC), Tyndall Air Force Base, FL. The Backfill Effects test series was designed around the AFESC tests conducted at Fort Polk so that the results of these two tests could be compared. The results of the Fort Polk tests are documented in Reference 7. Reference 8 has a summary of the results of the AFESC tests from which the following information was taken.

2.1 TEST PARAMETERS

The AFESC tests at Fort Polk, LA consisted of eleven explosive tests conducted to study the response of structures buried in sand to the loading from a point-source detonation. Each test involved a reinforced concrete test slab and a cylindrical-cased charge. The parameters varied in this series of tests included the charge orientation, standoff distance, span-to-thickness ratio, and the percentage of reinforcing steel in the test slab.

The test articles used in the AFESC tests were reinforced concrete slabs. In each test slab, the percentage of reinforcing steel in the front face of the slab was equal to that of the back face. The steel ratios used for the steel in the vertical direction in each face of the test slab and L/t ratios for each slab are given in Table 2.1. The test slabs were 65 inches high and 15 feet long. The reaction structure was a reinforced concrete box open on one side to allow mounting of a test slab. After mounting on the reaction structure, each test slab had a clear span of 43.2 inches.

2.2 FIELD TEST PROCEDURES

A test bed was excavated, and the reaction structure was placed at one end of the test bed. A test slab was then attached to the reaction structure for each test. The structural instrumentation was then installed on the test slab and in the reaction structure. In this test series, a structural accelerometer was placed at the center of the back side of the test slab to monitor the motion of that point on the structure. An interface pressure gage was placed on the front face of the slab at this location to measure the structure loading. Free-field accelerometers and soil stress gages were located in the free-field at locations which were mirror images from the charge of the locations of the structural accelerometer and the interface pressure gage. A passive deflection gage was used to measure the deflection at the center of the test slab. The test bed was backfilled with compacted flume sand so that the center of the test slab and the center of gravity of the charge were 5 feet beneath the ground surface. A hole was excavated in the test bed at the proper location for the test charge. The charge was placed at the proper orientation and elevation with the center of the charge opposite the center of the test slab. The casing for the test charge was a cylinder 27 inches long with an inside diameter of 3.548 inches and a wall thickness of 0.166 inches. The casing was filled with 15 ' pounds of C4 and closed off by end caps.

2.3 TEST RESULTS

The tests of most importance for comparison with the Backfill Effects tests are those in which the charge was detonated at a range of 5 feet from the structure with either a horizontal or vertical orientation. The tests meeting these specifications were Tests No. 5, 6, 7, and 9.

Test No. 5 was a retest of a test slab having an L/t ratio of 10 and 0.5 percent steel. The charge was detonated in a horizontal orientation parallel to the long span of the structure. The response of the slab was significant with a center deflection of about 2.125 inches.

The slab tested in Test No. 6 had an L/t ratio of 10 with 1.0 percent steel. The charge was placed in a horizontal configuration and resulted in a center slab deflection of about 1.563 inches.

A test slab with an L/t ratio of 5 having 0.5 percent steel was tested in Test No. 7 with a horizontal charge orientation. The response of the test

13

slab was minimal with a maximum deflection at the center of the slab of about 0.62 inch.

In Test No. 9, a slab with an L/t of 10 having 0.5 percent steel was tested with a vertical charge orientation. The detonation of the charge in this configuration caused the most severe damage for this slab at the 5 foot range. The center span deflection was about 2.938 inches.

The parameters for each test and a summary of the damage to each test slab are shown in Table 2.2. Tests in this series were conducted on test slabs having both 0.5 and 1.0 percent steel with an L/t ratio of 10. A comparison of the damage occurring on these two test slabs when tested with the charge in the horizontal position was made. At a range of 5 feet both slabs sustained light damage, although deflections were slightly higher for the slab with 0.5 percent steel. At a range of 3.75 feet the slab with 0.5 percent steel was breached, and the slab with 1.0 percent steel sustained only moderate damage. The comparison of results between slabs with varying steel percentages is summarized in Table 2.3. This test series also investigated the differences in response when the charge orientation was varied. A comparison was made of the damage to test slabs having an L/t ratio of 10 and 0.5 percent steel tested at a range of 5 feet with vertical and horizontal charge orientations. The vertical charge orientation used in Test No. 9 caused the greatest response of the test slabs. The response was 38 percent greater than the response of the test slabs due to the horizontal charge orientation. The results of the charge orientation comparison are summarized in Table 2.4.

Table 2.1. Description of test slabs.

Test No.	Test Slab	Steel (%)	L/t
4	4	0.5	10
5	5	0.5	10
5A	8	0.5	10
6	6	1.0	10
6A	Retest 6	1.0	10
7	7	0.5	5
7A	Retest 7	0.5	5
8	Retest 4	0.5	10
8A	Retest 4	0.5	10
9	9	0.5	10
10	10	0.5	10

Table 2.2.   Summary of results.

FY 83 AFESC Test Series
(Sand)
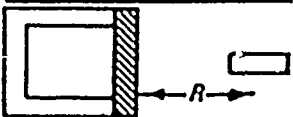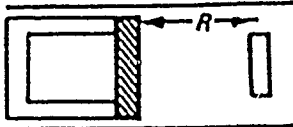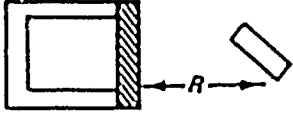
Test No.	p ↓	L/t	R ft.	Maximum Deflection in.	Charge Orientation
4	0.5	10	10	3/8	
5	0.5	10	5	2-1/8	
5A	0.5	10	3.75	Breach	
6	1.0	10	5	1-9/16	
6A	1.0	10	3.75	3-5/8	
7	0.5	5	5	5/8	
7A	0.5	5	2.5	3-1/2	
8	0.5	10	5	1	
8A	0.5	10	5	15/16	
9	0.5	10	5	2-15/16	
10	0.5	10	5	1-11/16	

Table 2.3. Effects of steel percentage on structural response.

Test No.	p %	L/t	Range (ft)	Maximum Deflection (in.)
5	0.5	10	5.00	2.13
5A	0.5	10	3.75	Breach
6	1.0	10	5.00	1.56
6A	1.0	10	3.75	3.63

Table 2.4. Effects of charge orientation on structural response.

Test No.	p %	L/t	Range (ft)	Charge Orientation	Maximum Deflection (in.)
5	0.5	10	5.0		2.13
9	0.5	10	5.0		2.94

17

CHAPTER 3
TEST ARTICLES

Since very little data was available from previous tests on the response of buried structures to localized loadings in higher seismic velocity backfill materials, it was decided to pattern the Backfill Effects tests after those conducted in the standard compacted sand backfill. This allowed more tests in the higher seismic velocity backfill for comparison with the tests in the sand backfill. The test articles used in the Backfill Effects test series included a reaction structure and reinforced concrete test slabs with L/t ratios of 5 and 10. These test articles were constructed using the same designs as the test articles used in the AFESC sand backfill tests at Fort Polk, LA.

3.1 REACTION STRUCTURE

The reaction structure was a heavily reinforced rectangular concrete box open on one side to allow mounting of a test slab. The reaction structure was approximately 65 inches high, 15 feet long, and 4 feet deep and had been constructed for a previous test. The roof, walls, and floor of the structure were each 11 inches thick. A 5/8-inch-thick steel plate was cast on the exposed surfaces of the roof, floor, and end walls of the structure to provide a hard smooth bearing surface for the test slabs and to protect the reaction structure. To provide for mounting of the test slabs, 1.25-inch-diameter bolt holes were drilled in the bearing plates with 1-inch nuts welded to the back side of the plates. Openings were provided on each end of the reaction structure with hinged steel plates as doors to provide access to the interior of the reaction structure after the test slab had been mounted. Gage mounts were attached to the reaction structure for deflection gages and structural accelerometers. The mount for the passive deflection gage was placed in the center of the rear wall of the reaction structure. The mounts for active deflection gages were placed along the centerline of the reaction structure 5 inches from the roof and floor. The mounts for the structural accelerometers were placed on the centerline 1.5 feet and 2.5 feet from the front edge of the reaction structure. Figure 3.1 shows the dimensions of the reaction structure and the locations of the instrumentation mounts.

3.2 TEST SLAB CONSTRUCTION

Six test slabs were cast for the Backfill Effects test series. The first three test slabs constructed had L/t ratios of 5 and contained 0.5 percent steel, while the second three test slabs constructed had L/t ratios of 10 with 1.0 percent steel. Both sets of test slabs were constructed using a concrete mix corresponding to the mix used in the AFESC tests. The concrete mix used a Type II Portland cement and was designed to produce a 28-day unconfined compressive strength of 5,000 psi. The aggregate was a crushed limestone no greater than 3/8-inch in diameter. The specifications for the concrete mix for these test slabs are shown in Table 3.1. Test cylinders were collected during placement of the concrete for each set of test slabs. These cylinders were tested to obtain unconfined compressive strengths with test dates 28 days after placement and again for each slab on test day. The average 28 day compressive strength of the test slabs with an L/t of 5 was 6,258 psi. The test slabs with an L/t of 10 had an average 28 day compressive strength of 5,128 psi. The compressive strengths for the test slabs on the days of the dynamic tests varied from 5,855 psi to 6,398 psi. The results of the concrete compressive strength tests are summarized in Table 3.2.

Construction first began with three test slabs having an L/t of 5 and 0.5 percent steel. These test slabs were 65 inches high, 15 feet long, and 8.6 inches thick. The reinforcement layout used a Grade 60 No. 3 deformed reinforcing bar as the principal steel in the slab. The temperature and shear steel were D2 wire neat treated to conform as closely as possible to Grade 60. The results of the tensile pull tests for the steel used in construction of these slabs are shown in Table 3.3. The principal steel and shear steel were bent and tied together to form the reinforcing mat according to the layout in Figure 3.2. The reinforcing mat was placed in the wooden formwork for the slabs and the appropriate gage mounts were positioned and tied in place. Mounts were positioned in the reinforcing mat for interface pressure gages and structural accelerometers. Nine interface pressure mounts were tied to the reinforcing mat such that the interface pressure gages would measure the pressure distribution on the outside face of the test slab. The positions of the interface pressure gages are shown in Figure 3.3. Figure 3.4 shows a typical gage mount for the interface pressure gages tied to the reinforcing mat. The 2-inch by 2-inch steel plates used for mounting

19

the structural accelerometers to the rear face of the test slab had D2 wire bent at a 90-degree angle and welded to the plate to assure proper bonding to the concrete slab. The D2 wire on the plate was then tied into the mat to secure the plates during concrete placement at the locations shown in Figure 3.3. Figure 3.5 shows a typical steel plate tied into the reinforcing mat. The bolt holes were formed using 1-3/4-inch-diameter PVC plastic pipe. The pipe was held in place by holes drilled in the bottom of the formwork at the proper positions and by boards with holes drilled in them attached on the top side of the form. Figure 3.6 shows the reinforcing mat for a slab with an L/t of 5 just before concrete placement. After placement and curing of the concrete, the formwork was removed.

Construction was then started on three test slabs with L/t ratios of 10 and 1.0 percent steel. These test slabs were 65 inches high, 15 feet long, and 4.3 inches thick. The reinforcement layout used Grade 60 No. 3 deformed reinforcing bar for the principal steel. The temperature steel was D1 wire, and the shear steel was D2 wire which had been heat treated to conform as closely as possible to Grade 60. The results of the tensile pull tests for the steel used in construction of these slabs are shown in Table 3.3. The principal steel and shear steel were bent and tied together to form the reinforcing mat according to the layout in Figure 3.7. The reinforcing mat was placed in the wooden formwork for the slabs, and the appropriate gage mounts were positioned and tied in place. The gage mounts for the interface pressure gages and the structural accelerometers were the same as those described previously for the test slabs with L/t ratios of 5. The locations of these gages are also the same and are shown in Figure 3.3. The bolt holes used in attaching the test slab to the reaction structure were again formed with the 1-3/4-inch-diameter PVC plastic pipes secured at the proper locations. Figure 3.8 shows the reinforcing mat for the slabs with an L/t ratio of 10 before concrete placement. The concrete was placed and cured, and the formwork was removed.

Table 3.1. Specifications for concrete mix.

JOB NAME		CONCRETE MIXTURE PROPORTIONS (WORK SHEET) (CRD-C 3)	DATE	
JOB. NO.	MIXTURE SER. NO. 5,000 psi		INITIALS	

PORTLAND CEMENT TYPE II		POZZOLAN SER. NO.		A. C. ADMIX SER. NO.	
SER. NO. ADDITION		TYPE		NAME D-Air	
BRAND AND MILL		SOURCE		AMOUNT 0.05 percent mL	

OTHER CEMENT SER. NO		CHEMICAL ADMIX SER. NO. HPS-HRWRA SP 2.8 oz/units	
BRAND AND MILL		NAME HPSR 8 oz/amount	

FINE AGGREGATE			COARSE AGGREGATE		
TYPE Limestone	SER. NO. CL-43 HS-10		TYPE Limestone		SER. NO. CL-43 HS-09
SOURCE			SOURCE		SIZE 3/8

MATERIALS

MATERIAL	SIZE RANGE	BULK SPECIFIC GRAVITY	UNIT WEIGHT (SOLID), LB/CU FT	ABSORPTION, PERCENT	TOTAL MOISTURE CONTENT, PERCENT	NET MOISTURE CONTENT, PERCENT
CEMENT						
F. AGGREGATE			169.10	0.9	0.2	-0.7
C. AGGREGATE (A)			171.60	0.5		-0.4
C. AGGREGATE (B)						
C. AGGREGATE (C)						
C. AGGREGATE (D)						
POZZ/OTHER CEMENT						

PROPORTIONS

MATERIAL		CALCULATED BATCH DATA (1 CU YD)			ACTUAL BATCH DATA CU FT		
		SOLID VOLUME CU FT/BATCH	SAT. SURF DRY BATCH WT. LB	FACTOR	SAT. SURF DRY BATCH WT. LB	WATER CORRECTION, LB	ACTUAL BATCH WT
CEMENT		3.053	600				600
F. AGGREGATE		8.992	1520.5				1509
C. AGGREGATE (A)		8.992	1543.0				1537
C. AGGREGATE (B)							
C. AGGREGATE (C) Super			16.9 oz				500 ml
C. AGGREGATE (D) D Air			0.3 lb				0.3
POZZ/OTHER CEMENT HPSR			48 oz				1420 ml
WATER		5.288	330			+17.5	347.5
AIR		.675					
TOTAL	AIR FREE	26.325					
	YIELD						

MIXTURE DATA

SLUMP _____ IN.	AIR CONTENT (D) _____ %	MIXING WATER _____ F	TH CF _____ LB/CU YD
REMOLD EFF _____ DROPS	AIR CONTENT (C) _____ %	AMBIENT _____ F	ACT CF _____ LB/CU YD
TH UW _____ LB/CU FT	AIR CONTENT (F) _____ %	CONCRETE _____ F	W/C 0.55 WT
ACT UW _____ LB/CU FT	BLEEDING _____ %	S/A 50 PERCENT VOL	

WES FORM NO 476
REV MAR 1977

(OVER)

21

Table 3.2. Concrete compressive strengths.

Test No.	Date Cast	Cylinder Test Date	Age	Sample No.	f'c (psi)
2	1/19/89	2/16/89	28	1	5,310
				2	5,980
				3	6,260
				4	6,080
				5	6,600
				6	6,510
				7	6,460
				8	6,540
				9	6,190
				10	6,650
				Avg.	6,258
1,3,4	2/10/89	3/10/89	28	1	4,700
				2	5,020
				3	5,660
				4	5,060
				5	4,990
				6	5,340
				Avg.	5,128
1		3/28/89		1	6,070
				2	6,120
				Avg.	6,095
2		4/12/89		1	5,960
				2	6,120
				3	6,380
				4	7,020
				5	6,510
				Avg.	6,398
3		4/18/89		1	5,910
				2	5,800
				Avg.	5,855
4		4/1'/89		Avg.	5,855

Table 3.3. Tensile test results for reinforcement steel.

Type of Steel	L/t	Use	Avg. Yield Stress (psi)
No. 3 reinforcing bar	5,10	Principal steel	67,424
D1 wire	10	Temperature steel	81,667
D2 wire	5	Temperature steel & Shear steel	58,125
D3 wire	10	Shear steel	73,232
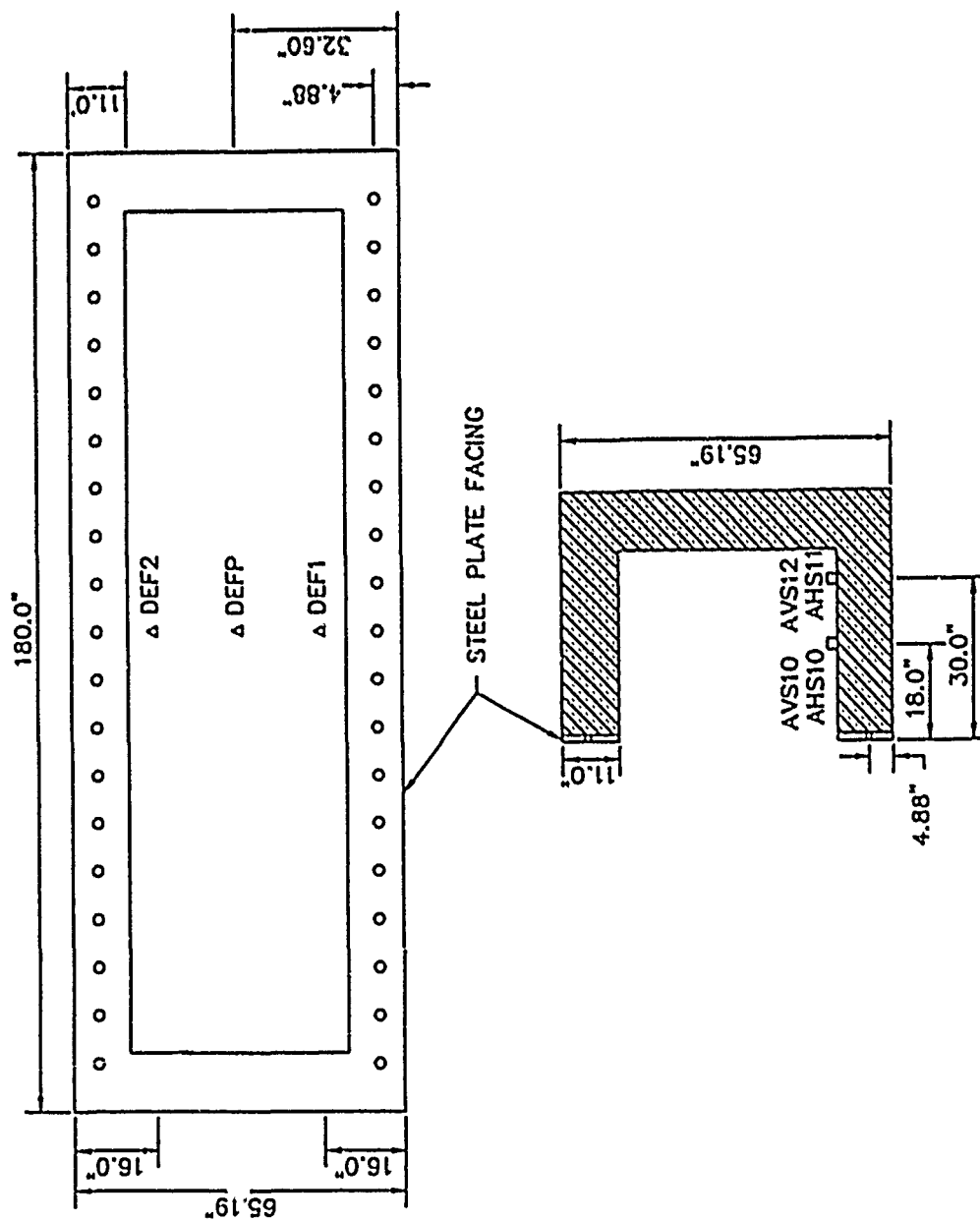
Figure 3.1. Reaction structure dimensions and instrumentation layout.

PLAN

SECTION A-A

SHEAR STEEL DETAIL

PRINCIPAL STEEL DETAIL (BOTH ENDS)

SECTION B-B

NOTE: TEMPERATURE STEEL, 0.160" DIA WIRE @ 14'–11" LENGTH
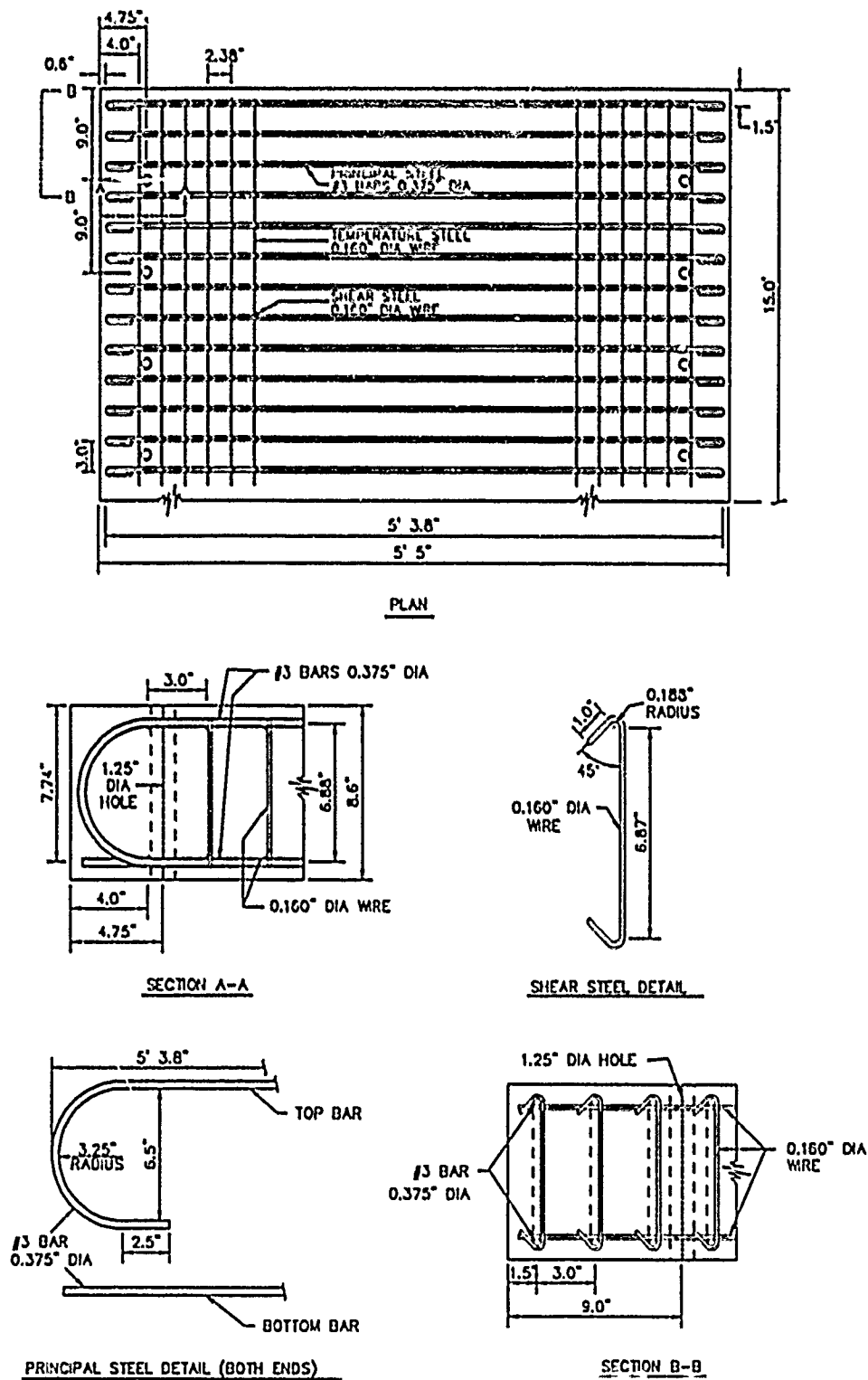
Figure 3.2.   Reinforcing steel layout for test slab with L/t of 5.

25

FRONT VIEW

O INTERFACE PRESSURE

□ ACCELEROMETER

△ DEFLECTION

REAR VIEW

Figure 3.3.   Structural instrumentation for test slabs.
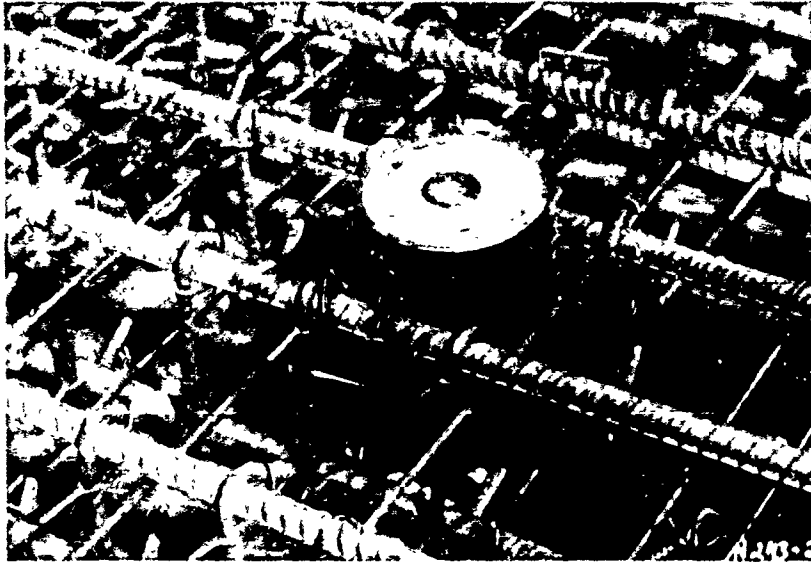
Figure 3.4. Interface pressure gage mount.

Figure 3.5. Mounting plate for structural accelerometer.
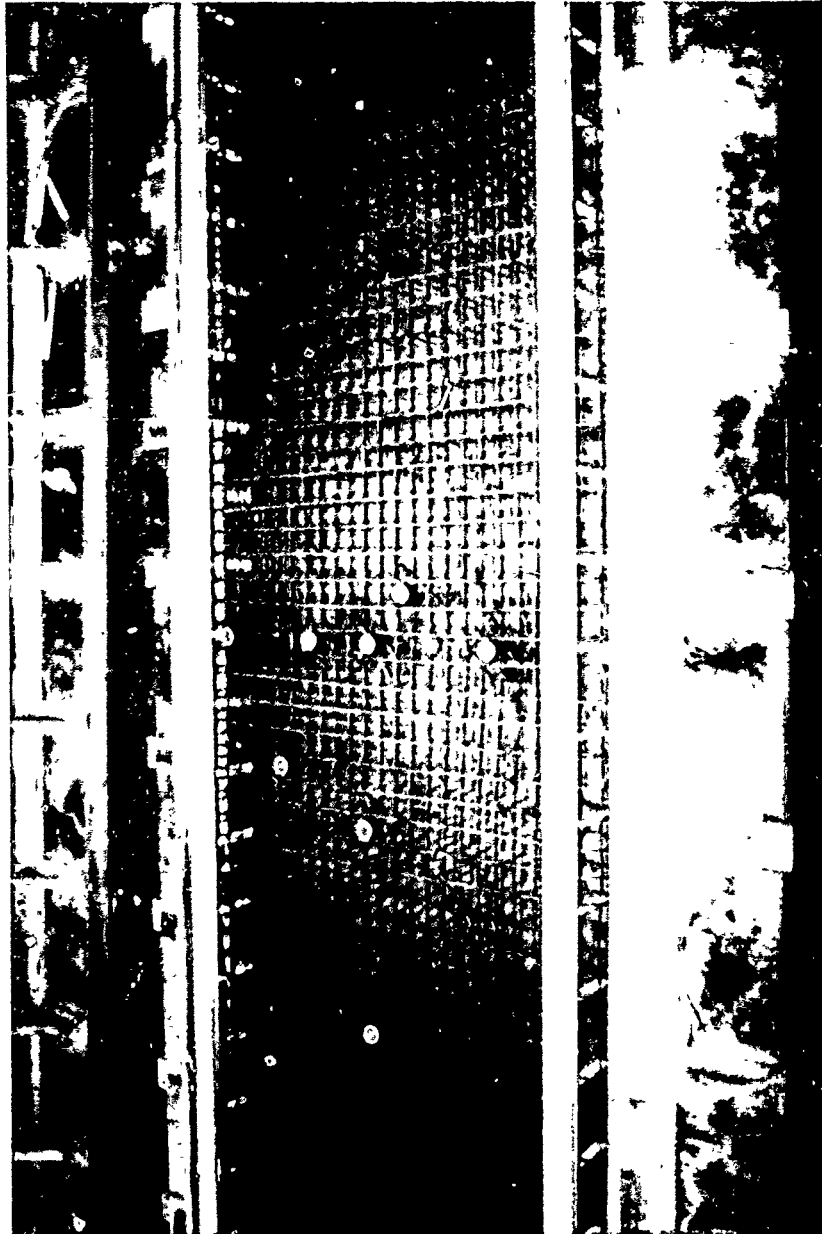
Figure 3.6. Reinforcing mat for test slab with L/t of 5.

PLAN

SECTION A-A

SHEAR STEEL DETAIL

PRINCIPAL STEEL DETAIL (BOTH ENDS)

SECTION B-B

NOTE: TEMPERATURE STEEL, 0.113" DIA @ 14'-11" LENGTH
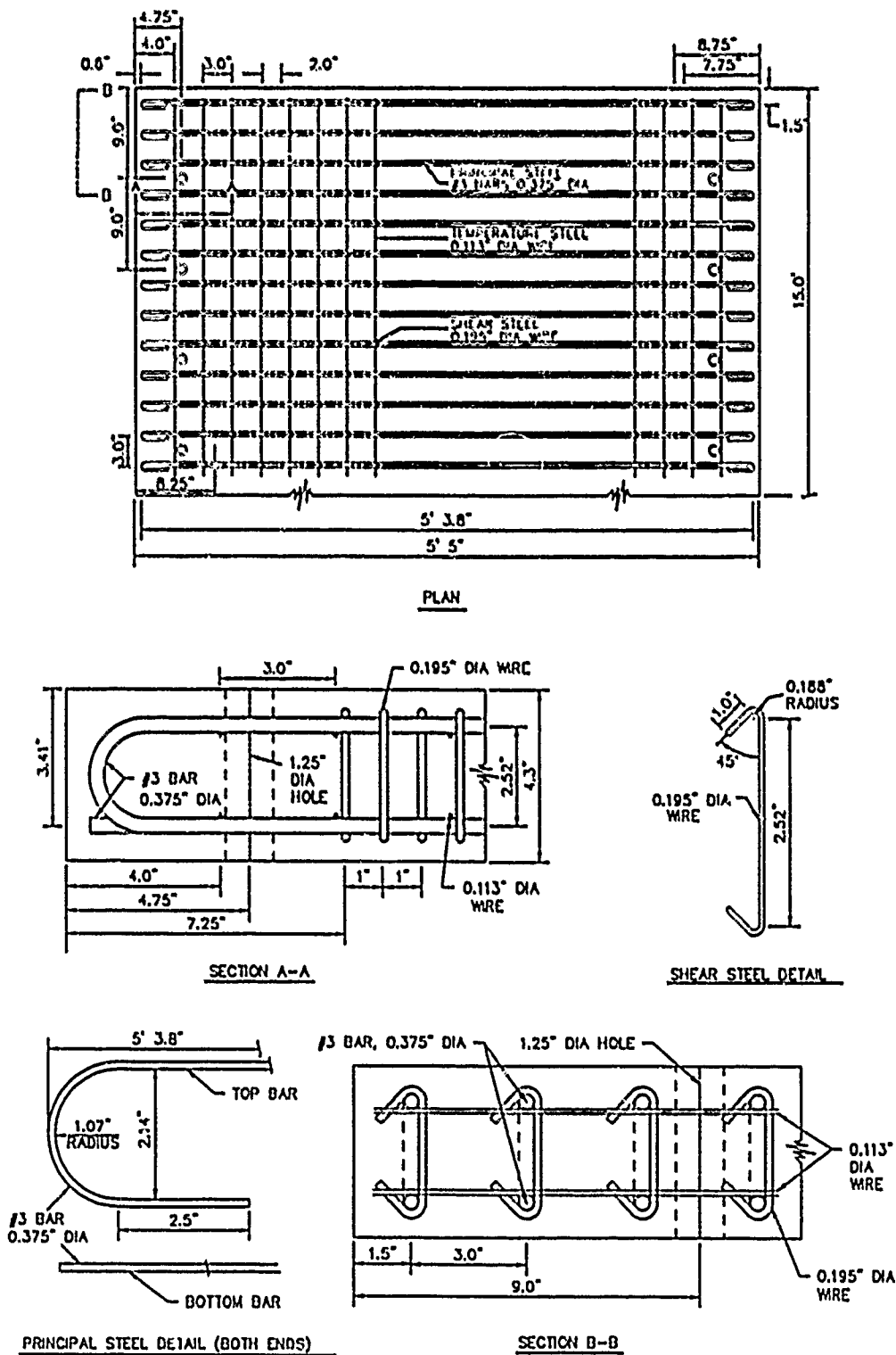
Figure 3.7.   Reinforcing steel layout for test slab with L/t of 10.

29
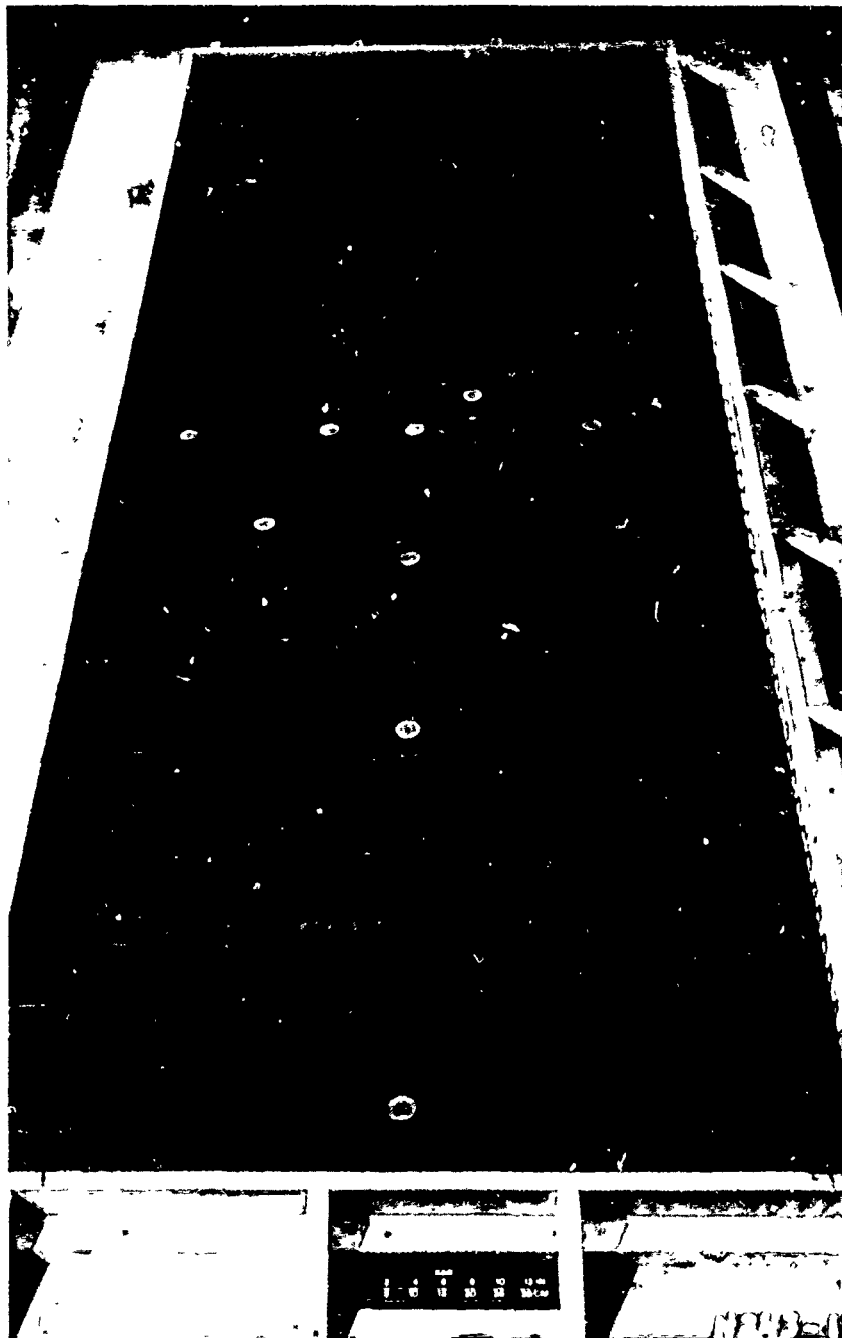
Figure 3.8. Reinforcing mat for test slab with L/t of 10.

CHAPTER 4

FIELD TEST PROCEDURES

The four tests of the Backfill Effects test series were conducted to determine the response of buried structures to localized point-source loadings in various backfill materials. The first two tests were conducted in a reconstituted clay backfill material, one test on a relatively flexible test slab and the other on a relatively stiff test slab. The clay backfill material was characterized by a low shear strength and a low seismic velocity. The third test was conducted in a compacted sand backfill material on a relatively flexible test slab. This test had the same parameters as the tests conducted in the AFESC test series and provided a good measure for comparison between the tests in this series and the AFESC tests. The sand backfill was characterized by a high shear strength and a low seismic velocity. The fourth test in the CONWEB test series was again on a relatively flexible test slab in an in-situ clay backfill material having a low shear strength and a high seismic velocity.

The charge for these tests was a cylindrical cased charge containing 15.4 pounds of C4 and enclosed by end caps on each end. The casing was 27 inches long with an inside diameter of 3 548 inches and a case thickness of 0.165 inch. The charge was detonated in either a horizontal or vertical orientation in each of the tests with the charge cylinder parallel to the long span of the test slab. The Backfill Effects test series was conducted at the Rodgers Hollow test site at Fort Knox, KY during the period March through May 1989.

4.1 SITE SELECTION

In March 1989, the Rodgers Hollow test site at Fort Knox, KY was prepared for testing for the Backfill Effects test series. The test slabs and reaction structure were shipped from WES to the test site. The results of geotechnical studies of the Rodgers Hollow test site conducted during previous test programs were examined to determine possible locations for the Backfill Effects test beds (References 9 and 10). The location for the test beds required that the water table be relatively close to the ground surface, and that no distinct gravel layers were in the area of the test bed to a depth of approximately 8 feet. It was also necessary to locate the in-situ

31

test bed in a location which had not been previously used for explosive
testing. Excavation was conducted at several possible locations on the test
range to determine an approximate location of the water table and if there
were distinct gravel layers at that site. The site which best satisfied the
desired conditions was selected for the backfill and in-situ tests.

A geotechnical study was conducted to characterize the site selected for
the two test beds. Twelve locations around the two Backfill Effects test
beds were assigned for drilling bore holes. One of the twelve holes was
designated for the installation of a piezometer. A seismic survey was also
conducted for the area surrounding the test beds, with emphasis on the area
to be used for the in-situ test bed. Figure 4.1 shows the locations of the
geophones used for the surface seismic refraction survey to determine the
seismic velocities of the various layers of soil in the area and to determine
the depth of the water table. This figure also shows the locations of the
bore samples taken in this area and the location of the piezometer. In each
of the four Backfill Effects tests, soil samples were taken for geotechnical
tests which would characterize the backfill material in the test beds.

4.2 BACKFILL TEST 1

The first backfill test was the test of a slab with an L/t ratio of 10
having 1.0 percent steel. The backfill material was reconstituted clay
having a low shear strength and a low seismic velocity. This test was
conducted with a vertical charge orientation.

4.2.1 STRUCTURE PLACEMENT

The 20 foot by 20-foot test bed selected for the reconstituted backfill
tests was excavated to a depth of approximately 8 feet. A sump hole was dug
on one side to collect the water which was constantly seeping into the test
bed. The bottom of the test bed was leveled and compacted, and the reaction
structure, with test slab already attached, was then set in place. The four
accelerometers in the reaction structure and the six accelerometers on the
rear face of the test slab were mounted in the locations shown in Figure 3.1
and Figure 3.2, respectively. There were two vertical and two horizontal
accelerometers in the reaction structure. The accelerometers on the test
slab were oriented to measure horizontal accelerations. Seven interface
pressure gages were mounted on the front face of the test slab. The active

deflection gages were attached to the rear face of the test slab, and the passive deflection gage was mounted. The locations for the interface pressure gages and the deflection gages are shown in Figure 3.3. When all of the structural instrumentation was prepared, the instrumentation cables were run out of the structure through a 4-inch-diameter, Schedule 40, PVC plastic pipe. Figure 4.2 shows the reaction structure and test slab with the instrumentation cables exiting the structure through the PVC pipe. The inside of the test structure with the gages mounted is shown in Figure 4.3.

4.2.2 BACKFILL PROPERTIES AND PLACEMENT

The backfill material used in this test was a low shear strength, low seismic velocity reconstituted clay. After placement of the reaction structure and preparation of the instrumentation, the backfill procedure began. Geotechnical studies had determined that to achieve the desired seismic velocity of approximately 1,000 fps, the reconstituted clay backfill should have 4.0 percent or less air voids. The clay was placed in the test bed and compacted with hand-held mechanical tampers (Figure 4.4) to form 6-inch lifts which had approximately 4.0 percent air voids. Nuclear moisture-density measurements were taken at four different locations in the test bed and gave the wet and dry densities and water content of the clay material. Figure 4.5 was used in the field to relate the density and water content of the clay to the percent air voids in the backfill. When the density of the backfill material did not correspond to an air void percent of approximately 4.0 or less, the mechanical tampers were run over the backfill again. The process was repeated until the correct air void content was obtained. The average wet density of the reconstituted clay backfill for Test 1 was 122.5 lb/ft^3 with a standard deviation of 2.00 lb/ft^3, while the average dry density was 99.4 lb/ft^3 with a standard deviation of 2.5 lb/ft^3. The backfill procedure was repeated to an elevation approximately 2.29 feet above the reaction structure.

Pint jar samples were taken from two locations in the test bed on each 6-inch lift to determine oven-dried water contents. This was necessary since the nuclear density gages measured the absorbed and adsorbed water in the clay producing a slightly higher than accurate water content reading. The oven-dried water content readings from the pint jar samples were compared to the nuclear density gage water content readings, and a correction factor was

33

developed. The average corrected water content of the backfill for this test was 23.3 percent with a standard deviation of 2.3 percent.

Gallon jar samples were taken from the test bed after placement of every foot of backfill material. These samples were submitted for laboratory testing to determine the specific gravity of the clay backfill. Two 55-gallon drums of the backfill material were collected, and the material was used to classify the soil using the Unified Soil Classification System.

4.2.3 FREE-FIELD INSTRUMENTATION

The free-field gages, including accelerometers, soil stress gages, and time of arrival (TOA) gages were placed in the test bed as the proper elevations were reached in the backfill process. These gages were placed at the locations and elevations shown in Figure 4.6 and Figure 4.7. Figure 4.8 shows the ranges of the free-field gages to the explosive charge. All of the gages in the free-field were oriented toward the charge except AHF6 and SE6, which were positioned parallel to the structure.

The free-field accelerometers were mounted in shock isolated canisters which were 4 inches wide and 9 inches long. Each end of the canister was sloped to form a wedge shape. The free-field accelerometer which was located 3 feet from the charge was mounted in a log canister having a 6-inch diameter and 12-inch length. Steel tubing was attached to the gage canisters to protect the instrumentation cable until it exited the test bed. The soil stress gages were mounted in a paddle mount which was 4 inches wide and 8 inches long. The steel tubing was also attached to these gage mounts. Figure 4.9 shows placement of both free-field accelerometers and soil stress gages in the clay backfill material. Fifty-two time of arrival gages were placed at the 5 foot depth in an array around the charge. The placement of these gages is shown in Figure 4.10. The test bed was also instrumented with ten geophones, five on each side of the charge at various depths. The geophones were to be used in downhole seismic tests to determine the seismic velocity of the test bed before detonation of the charge. The locations of the geophones are shown in Figure 4.11.

During placement of the backfill, a 6-inch-diameter PVC pipe was place at the location and depth required for the charge cylinder. After completion of the backfill procedure, the PVC pipe was removed and the charge cylinder was inserted in the hole with the cap and firing line attached. The charge

34

was buried with a vertical orientation at a depth of 5.03 feet at the center of the charge and at a range of 5 feet from the test panel. The hole above the charge was filled with the clay backfill material which was compacted around the charge cylinder.

4.3 BACKFILL TEST 2

The second backfill test was the test of a slab with an L/t of 5 with 0.5 percent steel. The backfill material was reconstituted clay having a low shear strength and a low seismic velocity. The test was conducted with a horizontal charge orientation.

4.3.1 STRUCTURE PLACEMENT

The reconstituted clay backfill material was completely excavated from the test bed after the first backfill test, and the damaged test slab was removed from the reaction structure. The next test slab with an L/t of 5 was attached to the reaction structure. Silicone sealant was used between the reaction structure and the test slab to prevent water entering the structure. The structural instrumentation, including accelerometers, deflections gages, and interface pressure gages, was prepared in the same manner described for Backfill Test 1. The locations of these gages on the reaction structure and test slab are shown in Figures 3.1 and 3.3. The instrumentation cables again exited the reaction structure through a 4-inch-diameter, Schedule 40, PVC plastic pipe. Figure 4.12 shows a pretest view of the test slab mounted to the reaction structure. A pretest view of the inside of the reaction structure with the instrumentation installed is shown in Figure 4.13.

4.3.2 BACKFILL PROPERTIES AND PLACEMENT

The backfill material used Test No. 2 was the same low shear strength, low seismic velocity reconstituted clay used in Test No. 1. After mounting the test slab and preparation of the instrumentation, the backfill procedure began. The reconstituted clay was placed in the test bed and compacted to form 6-inch lifts which had approximately 4.0 percent air voids. Nuclear moisture-density gage readings were taken at four locations in each lift. These readings were used to verify that the proper compaction was achieved to have 4.0 percent or less air voids in the backfill material. The average wet density of the reconstituted clay backfill for Test 2 was 123.7 lb/ft^3 with a

standard deviation of 1.9 lb/ft^3. The average dry density for this test was 100.6 lb/ft^3 with a standard deviation of 2.5 lb/ft^3. Pint jar samples were taken from two locations in the test bed on each 6-inch lift. The correction factor for the water contents from the nuclear density gage was determined using the oven-dried water contents obtained from these samples. The average corrected water content of the backfill for Test No. 2 was 23.0 percent with a standard deviation of 2.4 percent. Gallon jar samples of the backfill material were collected after placement of each foot of material. The samples were used to determine the specific gravity of the clay backfill. Two 55-gallon drums of the backfill material were collected, and the material was used to classify the soil using the Unified Soil Classification System. The backfill procedure continued to an elevation approximately 2.29 feet above the reaction structure.

4.3.3 FREE-FIELD INSTRUMENTATION

The free-field gages in Backfill Test 2 included soil stress gages, accelerometers, and interface pressure gages. The gages were placed in the test bed when the proper elevations were reached in the backfill process. The locations and elevations for the gages in this test are shown in Figure 4.14. All of the gages in the free-field were oriented toward the charge except AHF6 and SE6, which were positioned parallel to the structure.

The free-field accelerometers were mounted in shock isolated canisters. Steel tubing was attached to the canisters to protect the cable until it exited the test bed. The soil stress gages were mounted in paddle mounts and also had steel tubing attached to protect the instrumentation cable. Both the soil stress gages and the accelerometers were placed in the backfill material using a gage placement tool. The tool allowed the gages to be pushed into the backfill material as shown in Figure 4.15. This placement method allowed the gages to be placed in the backfill without disturbing the surrounding soil.

During placement of the backfill material, a wooden formwork approximately 6 inches thick and 30 inches long was placed parallel to the structure in the proper location for the test charge. The formwork was tall enough so that it could be removed after completion of the backfill process. When the formwork was removed, the charge cylinder, with firing line attached, was lowered in a horizontal orientation to a depth of 4.81 feet at

36

the center of the charge (Figure 4.16). The charge was positioned parallel
to the test slab at a distance of 5 feet from the front face of the test
slab. The clay backfill material was then compacted around the charge
cylinder to the top of the test bed.

4.4 BACKFILL TEST 3

The third backfill test was the test of a slab with an L/t of 10 having
1.0 percent steel. The backfill material was a compacted concrete sand
having a high shear strength and a low seismic velocity. The test was
conducted with vertical charge orientation.

4.4.1 STRUCTURE PLACEMENT

The reconstituted clay material was completely removed from the test bed
after the second backfill test, and the damaged test slab was removed. The
next test slab with and L/t of 10 was mounted on the reaction structure and
sealed with silicone sealant. The structural instrumentation, including
accelerometers, deflection gages, and interface pressure gages, was prepared
in the same manner described for Backfill Test 1. The locations of these
gages on the reaction structure and test slab are shown in Figures 3.1 and
Figure 3.3. The instrumentation cables exited the structure through a
4-inch-diameter, Schedule 40, PVC plastic pipe. Figure 4.17 shows a pretest
view of the test slab mounted to the reaction structure. The interior of the
reaction structure with the instrumentation installed in shown in
Figure 4.18.

4.4.2 BACKFILL PROPERTIES AND PLACEMENT

The backfill material for Test 3 was a compacted concrete sand having a
high shear strength and a low seismic velocity. The backfill procedure began
after mounting of the test slab and installation of the structural gages.
The sand was placed in the test bed and compacted to form 6-inch lifts to an
elevation of approximately 2.29 feet above the reaction structure. Previous
experience in tests with compacted sand backfill showed that the backfill
should have an average wet density in the range of 116 lb/ft^3 to 118 lb/ft^3
to have a seismic velocity of approximately 1,000 fps. Nuclear moisture-
density readings were taken from four locations in the test bed for each
6-inch lift to ensure proper compaction of the sand. The average wet density

of the compacted sand backfill in Test 3 was 116.4 lb/ft^3 with a standard deviation of 1.3 lb/ft^3. The average dry density of the compacted sand backfill was 110.8 lb/ft^3 with a standard deviation of 1.3 lb/ft^3. Pint jar samples were taken from two locations in the test bed for each 6-inch lift. The jar samples were used to determine oven-dried water contents which were used as verification for the nuclear density gage. The average water content for the compacted sand backfill in Test 3 was 5.0 percent with a standard deviation of 0.7 percent. Gallon jar samples of the sand backfill were collected after placement of each foot of backfill material. These samples were used to determine the specific gravity of the sand backfill. Two 55-gallon drums of the backfill material were collected, and the material was used to classify the soil using the Unified Soil Classification System.

4.4.3 FREE-FIELD INSTRUMENTATION

The free-field gages in Backfill Test 3 included soil stress gages, accelerometers, and interface pressure gages. The gages were placed in the test bed when the proper elevations were reached in the backfill process. The locations and elevations for the gages in this test are shown in Figure 4.19. All of the gages in the free-field were oriented toward the charge except AHF6 and SE6, which were positioned parallel to the structure.

The free-field accelerometers were mounted in the same shock isolated canisters used in the previous clay backfill tests. A 6-inch long piece of steel tubing was attached to the canister to protect the instrumentation cable as it exited the gage mount. The instrumentation cable was run from the gages out of the test bed. Low-pressure soil stress gages were used in Backfill Test 3. The instrumentation cable was protected with refrigeration tubing for approximately 3 feet from the connection to the gage. The accelerometers and soil stress gages were placed in the test bed as shown in Figure 4.20 and Figure 4.21. The test bed was also instrumented with ten geophones, five on each side of the charge at various depths. The geophones were to be used in downhole seismic tests to determine the seismic velocity of the sand backfill in this test. The locations of the geophones are shown in Figure 4.22.

A vertical charge orientation was used in Backfill Test 3. A 6-inch-diameter PVC plastic pipe was placed in the backfill at the proper depth for charge placement. After the completion of the backfill, the charge was

lowered into the PVC pipe to a depth of 4.90 feet at the center of the charge. The PVC pipe was then removed. Sand was then compacted around the test charge.

4.5 IN-SITU TEST 4

The in-situ test was the test of a slab with an L/t of 10 having 1.0 percent steel. The in-situ clay backfill material was undisturbed by previous explosive testing and had an average seismic velocity of approximately 3,000 fps and a low shear strength. The test was conducted with a vertical charge orientation.

4.5.1 STRUCTURE PLACEMENT

The test bed for the in-situ test was located a short distance from the test bed used for the backfill tests. The 20-foot by 20-foot area to be used for the test bed was excavated and leveled to a depth of approximately 2 feet exposing a clay soil. The removal of this soil also helped to ensure that the structure was placed beneath the depth of the water table. While the reaction structure and test slab were being removed from the test bed used in the backfill tests, a hole the approximate size of the reaction structure and test slab was excavated. The next test slab with an L/t of 10 was mounted on the reaction structure before placement in the test bed. The slab was sealed with the silicone sealant, and the structural instrumentation was prepared with the cables exiting the structure through the 4-inch-diameter PVC pipe. The reaction structure was then set in the test bed. A soil-matching grout was placed in front of and on the sides of the reaction structure. It also covered approximately 6 inches over the top of the reaction structure. The GM-7 Barite grout was determined in several other test series to be a good match for the clay at the Fort Knox test site. It has the properties of 2,750 fps average seismic velocity, 86 psi average compressive strength, and 115 lb/ft^3 density. Sand was compacted on the back side of the reaction structure and from the soil-matching grout on top of the reaction structure to the top of the test bed which was approximately 2.29 feet from the top of the reaction structure.. The properties of the test bed for the in-situ test were determined from the seismic survey and the bore hole samples.

4.5.2 FREE-FIELD INSTRUMENTATION

The free-field gages in the In-Situ Test 4 included soil stress gages, accelerometers, and interface pressure gages. The accelerometers were mounted in shock isolated canisters which had steel tubing attached to protect the instrumentation cable until it exited the test bed. The soil stress gages were mounted in the paddle mount and also had steel tubing attached to protect the cable.

Five of the soil stress gages and two of the accelerometers were placed in the grout surrounding the reaction structure. A formwork was constructed over the reaction structure to hold the gages at the proper location and elevation while the soil-matching grout cured. The locations of these gages are shown in Figure 4.23.

The remaining accelerometers and soil stress gages were placed in the test bed on the opposite side of the charge from the reaction structure. A small drilling machine was used to dig 6-inch-diameter holes for the gages at the proper locations. The gages were suspended in the holes by the steel tubing at the proper elevations and a quick set grout was used to secure the gage in place. The rest of the hole was filled with the soil matching grout. The locations of these gages are also shown in Figure 4.23. The test bed after installation of all the free-field gages is shown in Figure 4.24.

The charge was placed in the test bed in a 6-inch-diameter hole drilled with the drilling machine. The charge was positioned, with the firing line and cap attached, at a depth of 5.00 feet at the center of the charge and at a range of 5 feet from the front face of the test slab. The hole was then filled with the soil-matching grout.
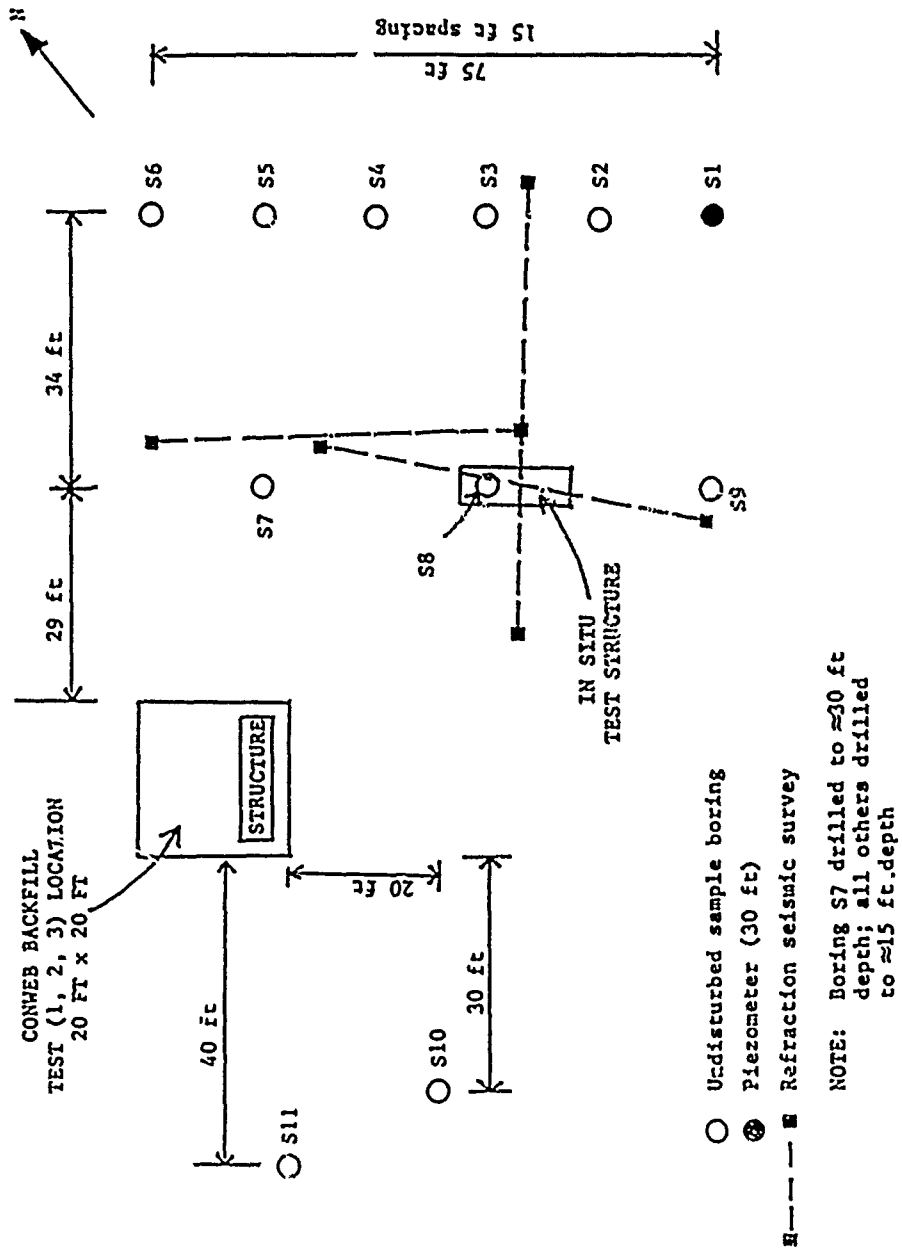
Figure 4.1. Seismic survey and bore hole locations.
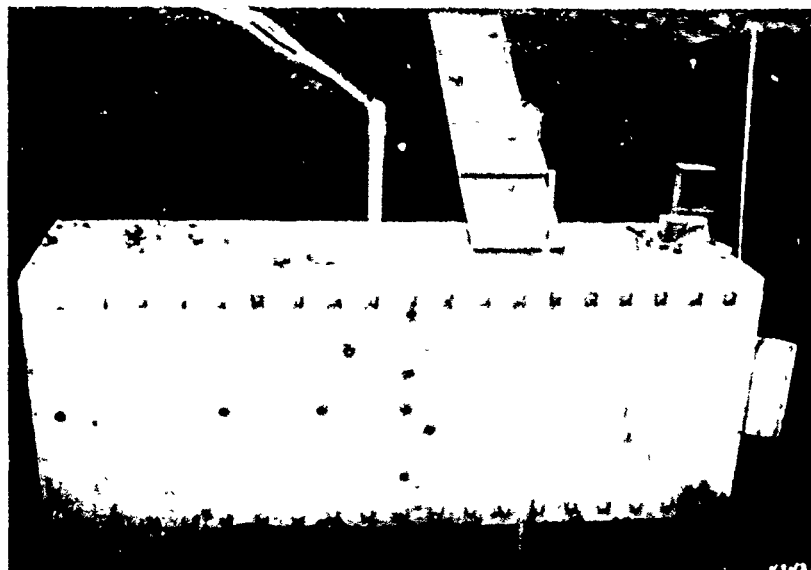
Figure 4.2. Reaction structure and test slab before Backfill Test 1.

Figure 4.3. Interior face of test slab before Backfill Test 1.

Figure 4.4.   Compaction of clay backfill with
mechanical tampers.
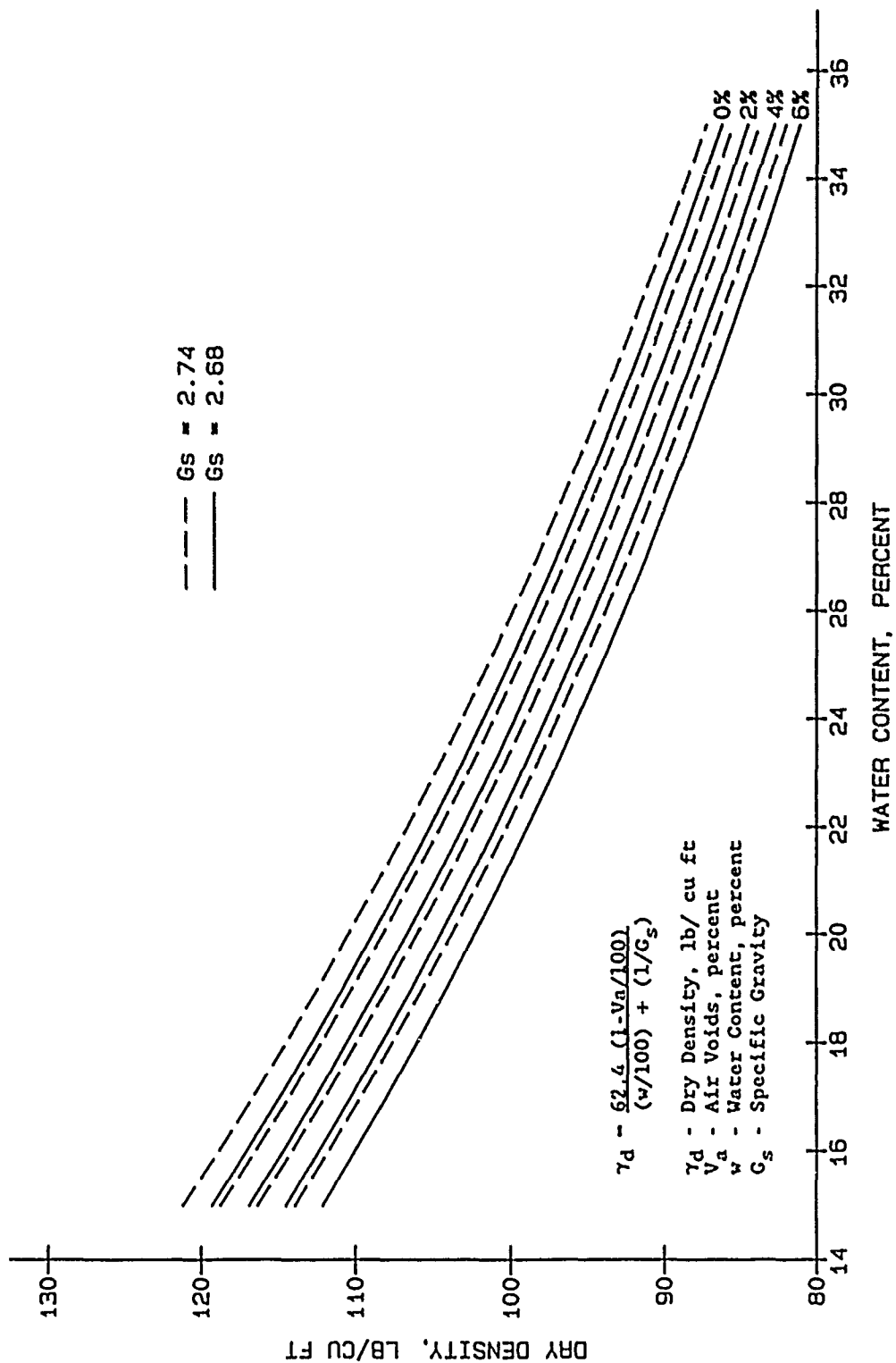
Figure 4.5. Chart for determination of air voids in soil.
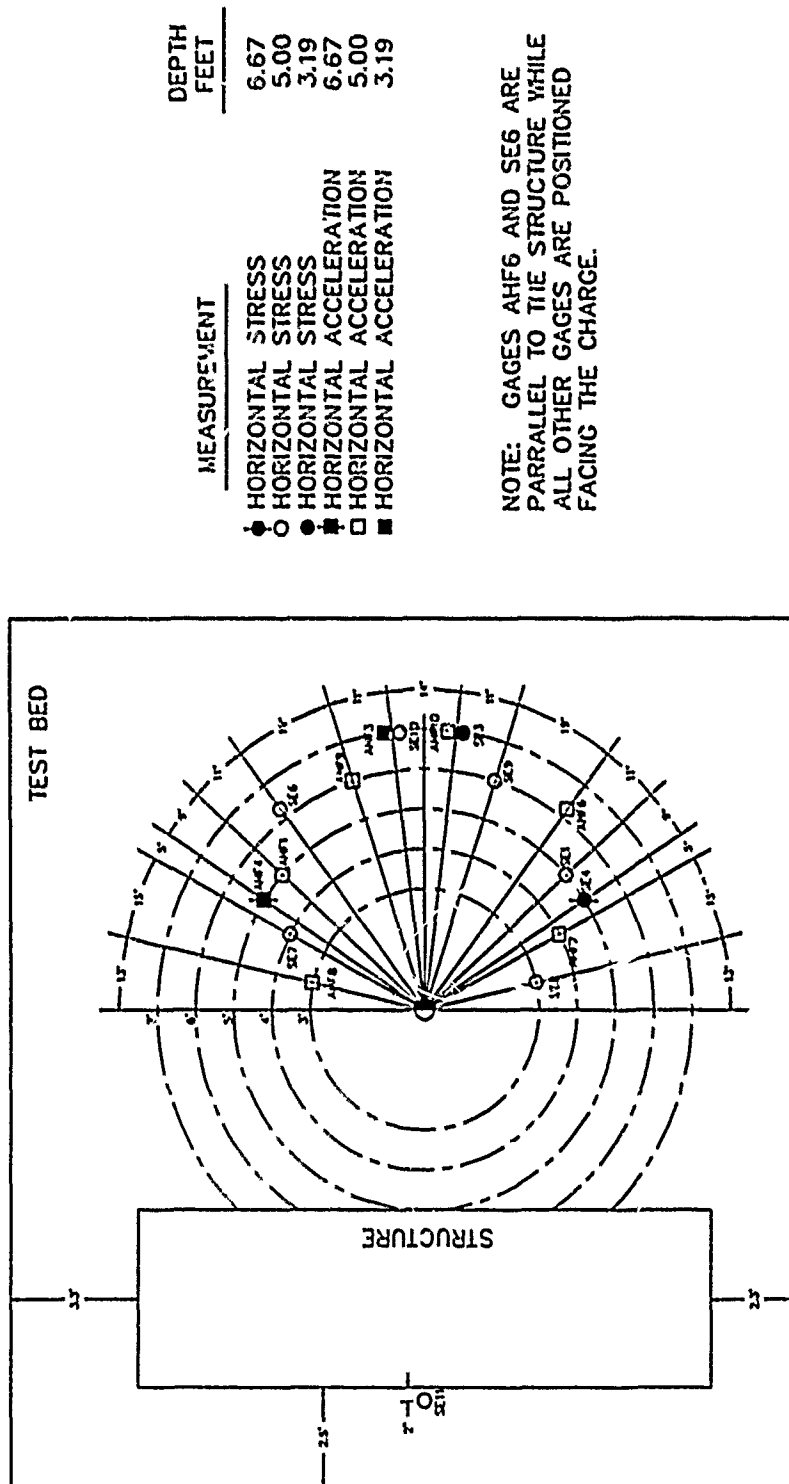
Figure 4.6. Free-field instrumentation layout, Backfill Test 1.

45
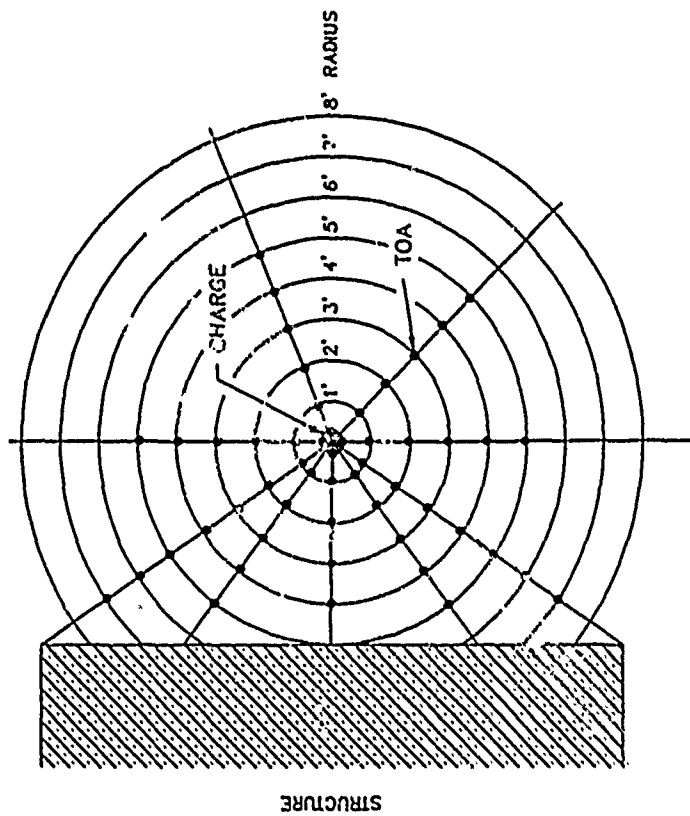
Depth: 5 feet from surface.

Figure 4.7. Time of arrival gage layout.

Figure 4.8   Free-field instrumentation layout showing
gage range from charge.
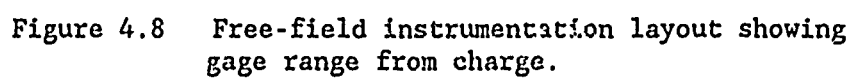
Figure 4.9. Placement of free-field gages in Backfill Test 1.

Figure 4.10. Placement of time of arrival gages in
Backfill Test 1.
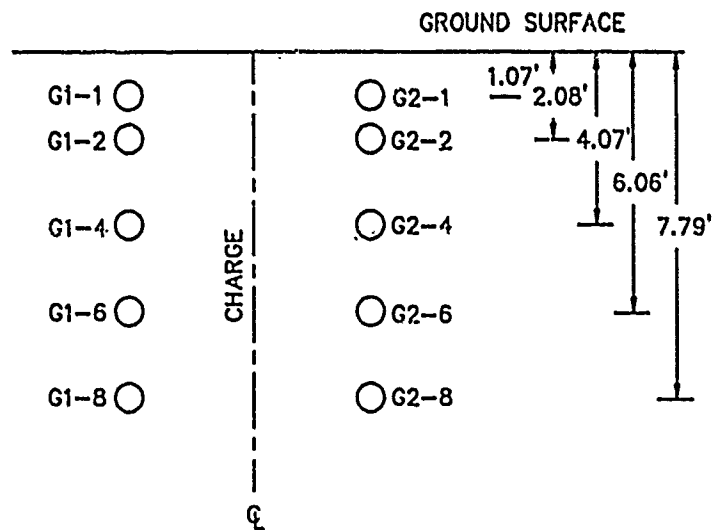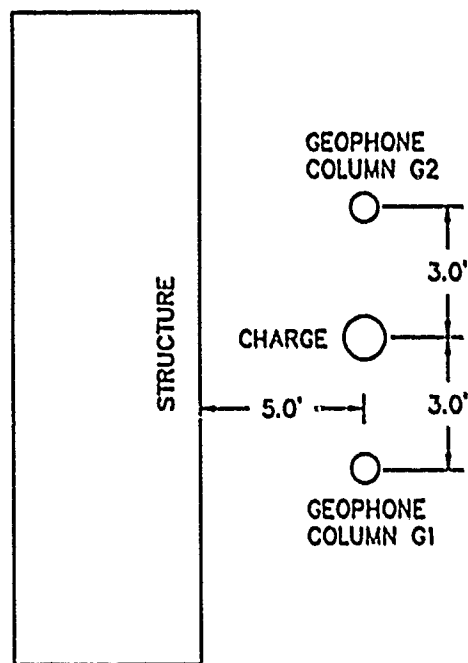
Figure 4.11. Layout for geophones used in downhole seismic tests, Backfill Test 1.
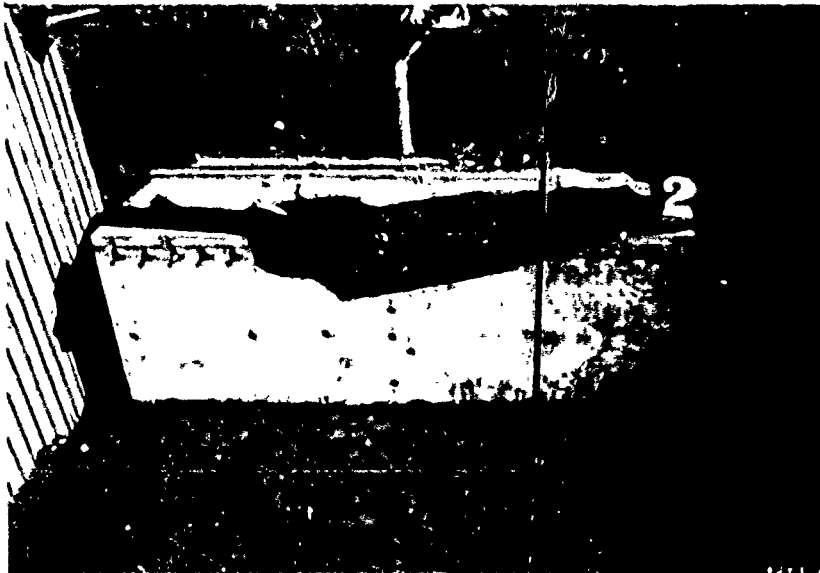
Figure 4.12. Reaction structure and test slab
before Backfill Test 2.

Figure 4.13. Interior face of test slab
before Backfill Test 2.

50
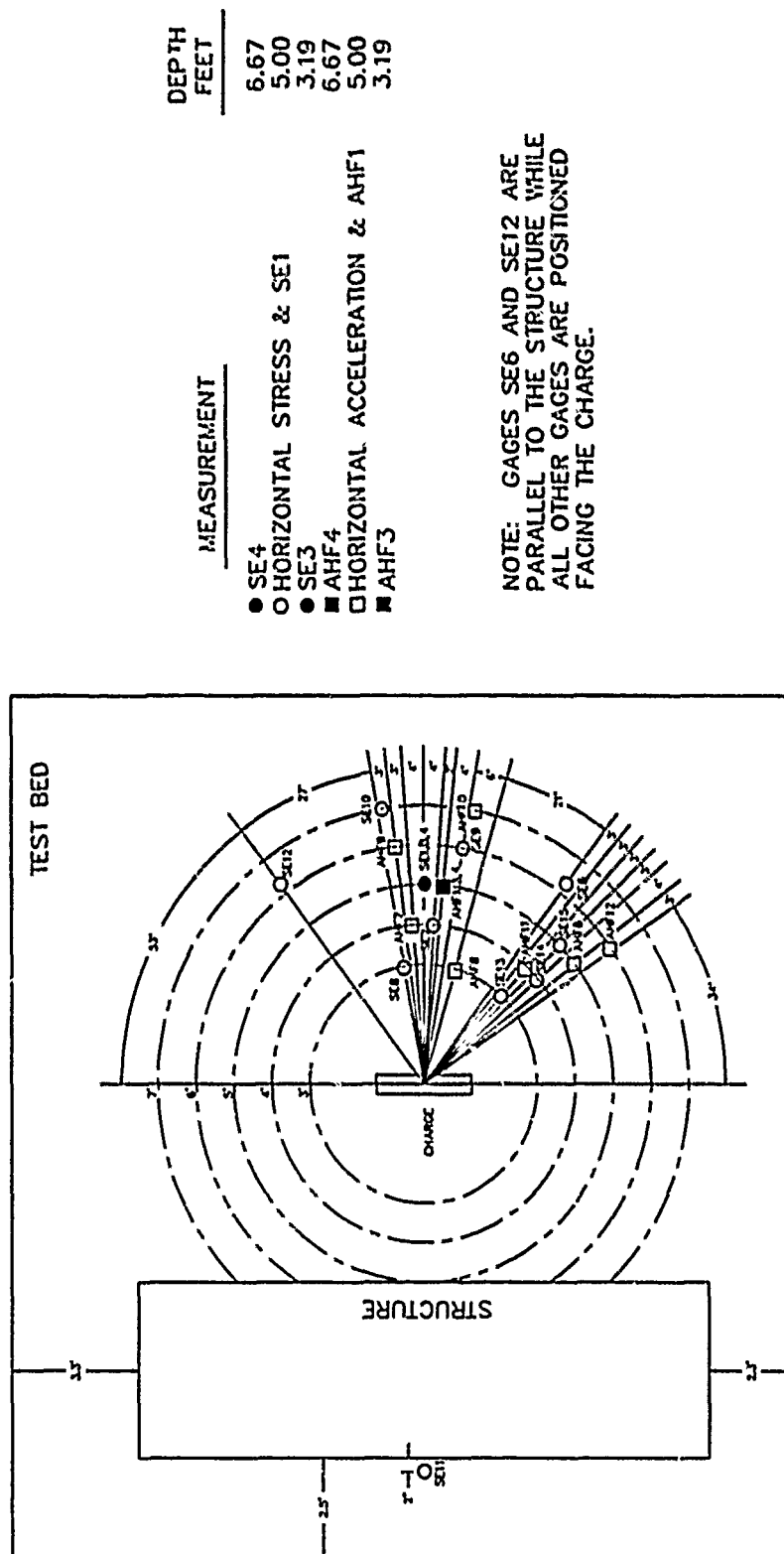
Figure 4.14. Free-field instrumentation layout, Backfill Test 2.

MEASUREMENT	DEPTH FEET
● SE4	6.67
○ HORIZONTAL STRESS & SE1	5.00
● SE3	3.19
■ AHF4	6.67
□ HORIZONTAL ACCELERATION & AHF1	5.00
▨ AHF3	3.19

NOTE: GAGES SE6 AND SE12 ARE PARALLEL TO THE STRUCTURE WHILE ALL OTHER GAGES ARE POSITIONED FACING THE CHARGE.

Figure 4.15. Placement of free-field gages in Backfill Test 2.

Figure 4.16. Charge placement in Backfill Test 2.

Figure 4.17. Reaction structure and test slab
before Backfill Test 3.
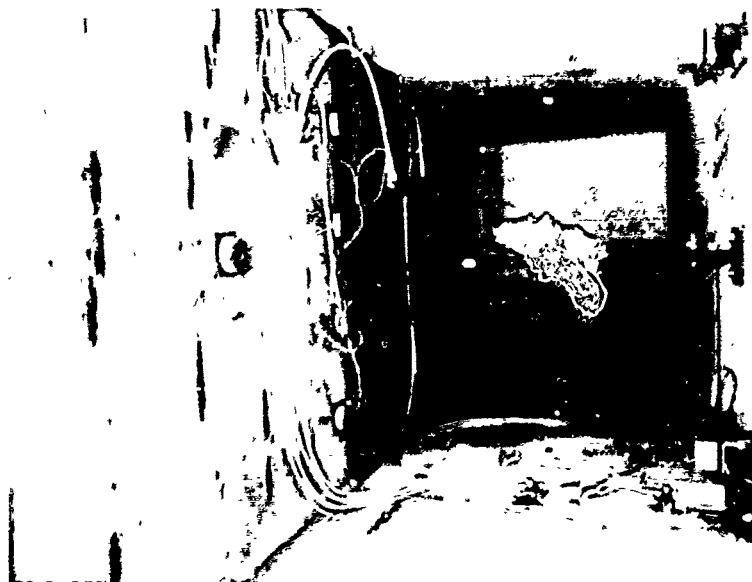
Figure 4.18. Interior face of test slab
before Backfill Test 3.

Figure 4.19. Free-field instrumentation layout, Backfill Test 3.
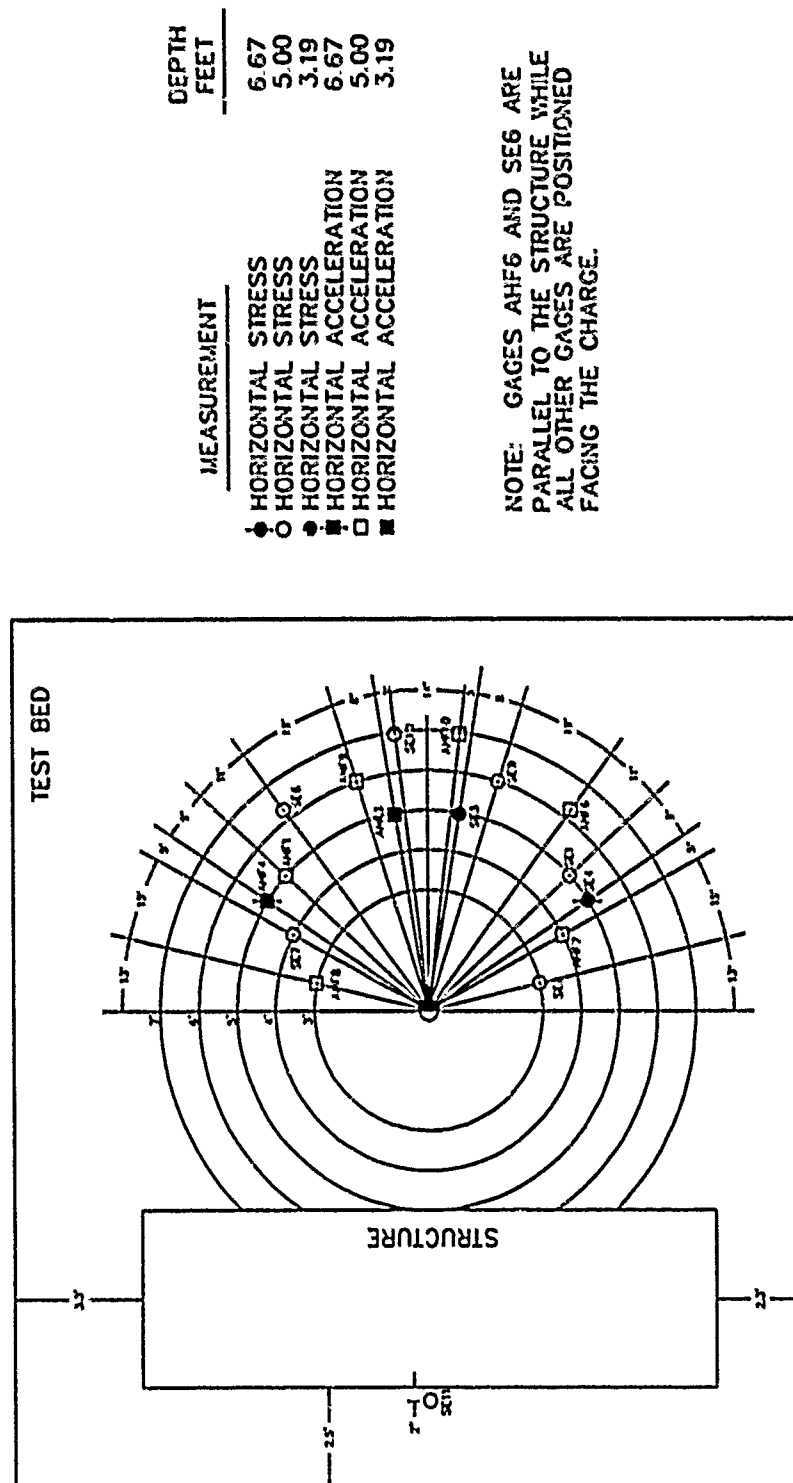
Figure 4.20. Accelerometer placement in Backfill Test 3.

Figure 4.21. Placement of soil stress gage in Backfill Test 3.
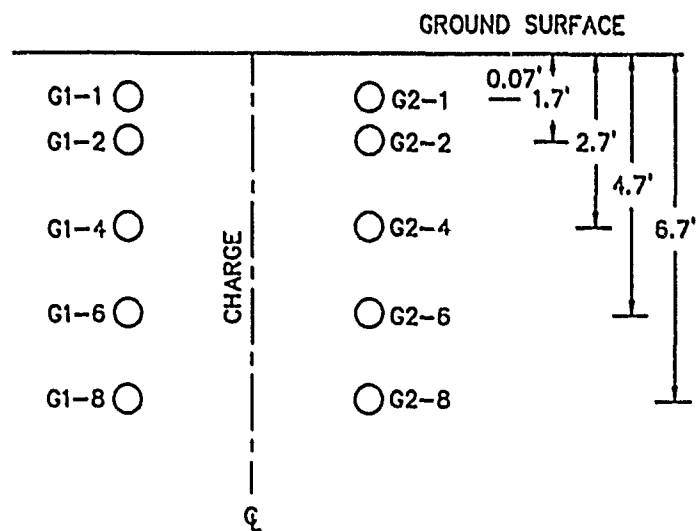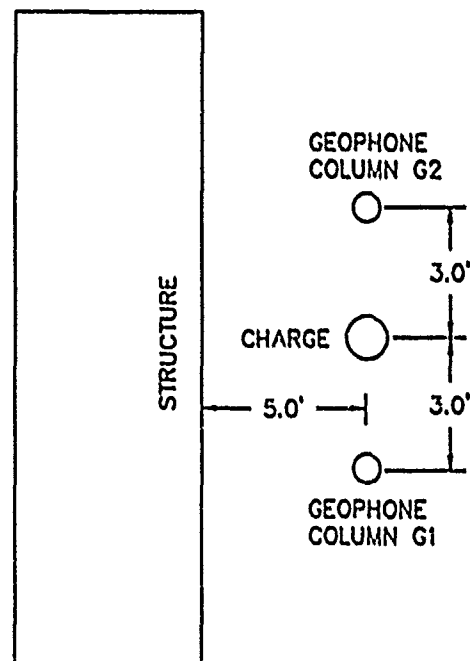
Figure 4.22. Geophone locations in Backfill Test 3.
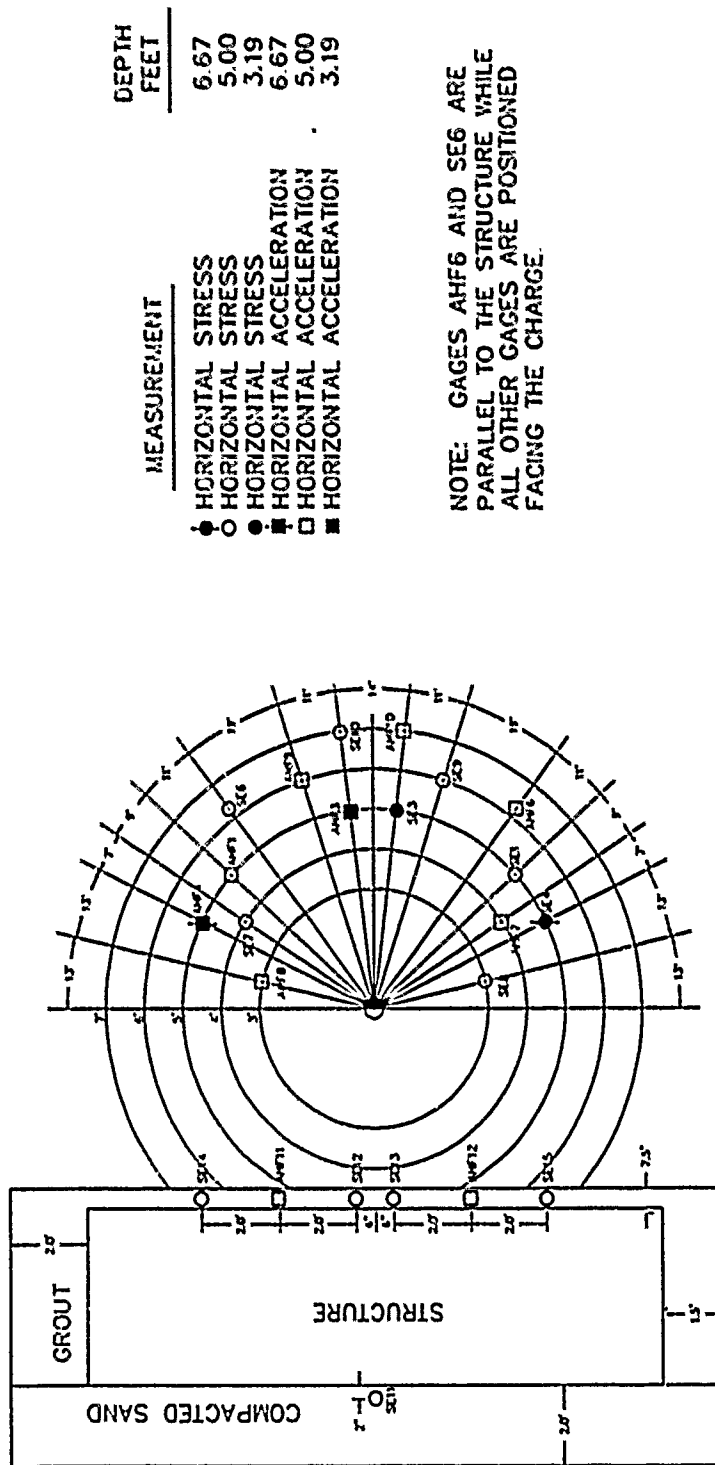
Figure 4.23. Free-field instrumentation layout, In-Situ Test 4.

Figure 4.24. In-Situ test bed after placement of reaction structure and free-field gages.

CHAPTER 5

FIELD TEST RESULTS

5.1 GEOPHYSICAL SITE CHARACTERIZATION

Surface seismic refraction tests were conducted over the area used for the two test beds in the Backfill Effects test series. These tests were conducted to determine the depth of the water table and the seismic velocity of the various layers of soil in the area. Twelve sites were also selected for bore holes to collect undisturbed samples of the soil to a depth of 30 feet. The results of the seismic survey and the boring samples show that the soil from ground surface to a depth of 5 feet was classified as a brown gravelly clay. The seismic velocity of this layer of soil ranged from 1,280 fps to 1,370 fps. The water table was located at a depth of 2 feet with 100 percent saturation at the 5 foot level. From a depth of 5 feet to 12 feet, the soil was classified as brown to gray gravelly clay, and from 12 feet to 24 feet as a gray soft clay. The seismic velocity from 5 feet to 24 feet ranged from 4,570 fps to 4,700 fps. Below the 24 foot depth, the soil was classified as clay with rock and gravel.

5.1.1 BACKFILL TEST 1

Several types of samples were taken from the clay backfill material used for Backfill Test 1. The gallon can samples of soil taken from the test bed every 2 feet during the backfill procedure were used to determine the specific gravity of the clay was 2.71. After applying the correction factor to the water content readings and determining the specific gravity of the clay, the mean air voids in the backfill for Test 1 were calculated to be 4.4 percent with a standard deviation of 2.45 percent. The two 55-gallon drums of backfill material were used to classify the soil based on the Unified Soil Classification System. The backfill material has the gradation curve shown in Figure 5.1 and was classified as brown gravelly clay.

Surface seismic refraction tests and downhole seismic tests were conducted to determine the seismic velocity of the test bed in Backfill Test 1. The time of arrival versus depth from the geophones in the downhole seismic survey for this test are shown in Figure 5.2. The average seismic velocity for the backfill material in this test was determined to be

1,100 fps. A summary of the properties of the test bed for Backfill Test 1 and the surrounding in-situ soil are shown in Figure 5.3.

5.1.2 BACKFILL TEST 2

The properties of the backfill material used in Test 2 were very similar those of the backfill material used in Test 1. The pint jar samples were taken to determine the correct water content for the backfill material, and the gallon can samples were taken to determine the specific gravity of this material was also 2.71. The mean air voids were calculated on the basis of this information and were found to be 3.7 percent with a standard deviation of 2.5 percent. The two 55-gallon drums of backfill material were used to classify the clay as a brown gravelly clay with the gradation curve shown in Figure 5.1. The backfill procedure was identical in the first and second backfill tests, and the seismic velocity was assumed to be approximately the same. Since the other properties of the backfill were not significantly different, that assumption was valid. A summary of the properties of the test bed in Backfill Test 2 and the surrounding in-situ soil are shown in Figure 5.4.

5.1.3 BACKFILL TEST 3

Several types of samples were taken to determine the properties of the sand backfill material used in Backfill Test 3. The pint jar samples were used to determine oven-dried water contents of the sand as a check for the nuclear density gage. The gallon can samples were used to determine the specific gravity of the sand was 2.70. This information was then used to calculate the mean air voids in the test bed. The mean air voids were 25.3 percent with a standard deviation of 1.1 percent. The two 55-gallon drums of the sand backfill material were used to develop the gradation curve shown in Figure 5.1. Figure 5.5 shows a comparison of the gradation curves for the concrete sand used for the backfill material in Backfill Test 3 at Fort Knox, KY, the Socorro plaster sand, and the flume sand used in the AFESC backfill tests at Fort Polk, LA.

Surface seismic refraction surveys and downhole seismic surveys were conducted to determine the seismic velocity of the test bed in Backfill Test 3. The time of arrival versus depth from the geophones in the downhole seismic survey are shown in Figure 5.6. The average seismic velocity for the

sand backfill in the test bed was determined to be 1,100 fps also. A comparison of the time of arrivals versus depth from the geophones in Backfill Test 1 and Backfill Test 3 are shown in Figure 5.7. This comparison shows that the results of the downhole seismic surveys for each of these backfill materials are very similar and that the 1,100 fps average seismic velocity agrees well with the results of both tests. A summary of the properties of the test bed in Backfill Test 3 and the surrounding in-situ soil are shown in Figure 5.8.

5.1.4 IN-SITU TEST 4

The in-situ test bed had the same properties described above for the area surrounding the two test beds. The water table was located 2 feet below the elevations taken for the ground surface of the test bed, and the level of 100 percent saturation was 5 feet below ground surface. The first 5 feet of soil in the in-situ test bed had a seismic velocity in the range of 1,280 fps to 1,370 fps, and the soil was classified as a brown gravelly clay. Below this level the seismic velocity of the test bed was in the range of 4,570 fps to 4,700 fps, and the soil was classified as brown to gray gravelly clay. The average seismic velocity over the depth of the in-situ test bed was approximately 3,400 fps. A summary of the properties of the test bed in the In-Situ Test 4 are shown in Figure 5.9.

5.2 BACKFILL TEST 1

The reconstituted clay backfill test of an L/t of 10 slab having 1.0 percent steel was conducted on 24 March 1989 with a vertical charge orientation. A reading was taken from the piezometer immediately before the test was conducted and showed that the water table was approximately 6 inches below ground surface. Figure 5.10 shows the crater formed after detonation of the charge. The crater was approximately 7.87 feet deep with a width parallel to the structure of 13 feet and a length perpendicular to the structure of 13 feet.

The detonation of the cased charge at a range of 5 feet from the front face of the test slab caused severe damage. Figure 5.11 shows the 18-inch by 51-inch hole in the front face of the test slab. There was a 19-inch deflection from the outside face of the slab to the deformed reinforcement bars at the center of the slab. The reinforcement bars were broken at the

top and bottom supports near the center of the slab. Cracks were formed on both the front and rear face along the entire length of the slab. The rear face of the slab is shown in Figure 5.12.

The differences between the pretest and posttest elevations taken on top of the reaction structure show that the structure settled an average of 1.89 inches, and the top of the reaction structure rotated toward the charge. The average rigid body motion measured at the top of the reaction structure was 0.66 inches in the direction of the charge. This was due in part to the rotation of the reaction structure. Table 5.1 shows the pretest and posttest structural elevations and the rigid body motion of the structure.

Appendix A contains the digitized data for the free-field and structural gages in this test. No data has been included in the appendix for the TOA gages. The first four TOA gages which were placed on the charge cylinder gave a reading of 0.1 microseconds. The remaining TOA gages stopped at a reading of 0.4 microseconds. The soil stress and interface pressure records provided in this report have been filtered with a low pass 20 kHz filter. They were then filtered with a 5 to 17 kHz band rejection filter. The filtering processes was designed to reduce the noise on the data record due to the instrumentation system. The structural accelerometers, AHS-10 and AHS-11, were shifted with a constant baseline shift to zero velocity at 1.0 second. The other accelerometer records were modified using a constant baseline shift to account for errors in picking zero by shifting the velocity at time of arrival to zero. Some of the accelerometers were shifted with a constant baseline shift to conform more closely to the waveform projected by the free-field gages.

The peak pressure recorded by the soil stress gage, SE-1, at 5 feet from the charge was 1,000 psi. The peak particle velocity from the free-field accelerometer at the 5-foot range was 325 in/sec. The peak interface pressure at the center of the test slab was 1,900 psi. The loading wave speed of the backfill was determined from the time of arrival to the free-field gages. An average of the wave speeds determined from the gages at a range of 3 feet from the charge to a range of 5 feet from the charge gave a loading wave speed for the backfill material of 1,400 fps. An average of the wave speeds determined from the free-field gages at a range of 5 feet from the charge gave a loading wave speed of 2,900 fps. These values of the

loading wave speed are considerably different from the seismic velocity of 1,100 fps for this backfill material.

5.3 BACKFILL TEST 2

The reconstituted clay backfill test of the L/t of 5 slab was conducted on 7 April 1989 with a horizontal charge orientation. Immediately before this test was conducted a reading was taken at the piezometer. The water table was shown to be 8 inches below ground surface. The detonation of the charge created the crater shown in Figure 5.13. The crater had a depth of 6.65 feet and a width parallel to the reaction structure of 11 feet. The length of the crater perpendicular to the reaction structure was 13.17 feet.

Light to moderate damage with cracks on the front and rear face along the entire length of the test slab was caused by the detonation of the 15.4-pound cased charge at a range of 5 feet from the front face of the test slab. Figure 5.14 shows the front face of the test slab after excavation of the test bed and again after removal of the test slab from the reaction structure. The rear face of the test slab is shown attached to the reaction structure and also after removal from the reaction structure in Figure 5.15. The passive deflection gage measured a maximum deflection of 1.56 inches and a permanent deflection of 1.19 inches. The reaction structure suffered minor cracking on the rear wall and floor after Backfill Test 2. This damage is shown in Figure 5.16.

The pretest and posttest elevations taken on top of the reaction structure show that the reaction structure moved upward an average of 1.98 inches and rotated toward the charge. The rigid body motion measured at the top of the reaction structure showed an average movement of 0.28 inches toward the charge. Again this average movement of the top of the reaction structure toward the charge is in part due to the rotation of the reaction structure. Table 5.1 shows the pretest and posttest elevations of the reaction structure and the rigid body motion.

Appendix B contains the digitized data for the free-field and structural gages in this test. The soil stress and interface pressure records provided in this report have been filtered with a 20 kHz low pass filter. They were then filtered with a 5 to 17 kHz band rejection filter. The filtering processes was designed to reduce the noise on the data record due to the instrumentation system. The accelerometers have been shifted to set the

velocity to zero at the time of arrival for each gage using a constant baseline shift. Some of the accelerometers were shifted with a constant baseline shift to conform more closely to the waveform projected by the free-field gages.

The soil stress gage, SE-1, was placed at a range of 5 feet from the charge and measured a peak pressure of 1,000 psi. The free-field accelerometer at the same distance from the charge measured a peak particle velocity of 375 in/sec. The peak interface pressure at the center of the test slab was 2,400 psi. This data compares well with the same measurements in the reconstituted clay backfill in Backfill Test 1. The loading wave speed of the backfill determined from the average of the wave speeds from the gages up to a range of 5 feet was 1,400 fps. The wave speed determined from an average of the wave speeds from gages at a range of 5 feet was 2,800 fps. The seismic velocity for this backfill material was 1,100 fps.

Backfill Test 2 was conducted on identical test articles with the same charge configuration used in AFESC Test 7. The backfill material was changed from a high shear strength sand to a low shear strength reconstituted clay material with approximately the same seismic velocity as the sand backfill. The test slab in the sand backfill had a maximum deflection of 0.63 inches, while the test slab in the clay backfill had a maximum deflection of 1.56 inches. The differences in response of the tests slabs show that backfill can effect the response of buried structures.

5.4 BACKFILL TEST 3

The compacted sand backfill test of an L/t of 10 slab having 1.0 percent steel was conducted on 18 April 1989 with a vertical charge orientation. Before detonation of the charge in Backfill Test 3, readings were taken from the piezometer and the 2-inch-diameter PVC plastic pipes placed in each corner of the test bed. The peizometer showed that the water table was approximately 7 inches beneath the ground surface. The plastic pipes in each corner of the test bed gave an average reading of 1.5 feet of water in the bottom of the test bed. These readings may not indicate the true condition of the test bed as the pipes with the highest water level readings were located in positions where water was constantly flowing into the test bed. The was also no way to ensure that the pipes had not become clogged during the backfill procedure. The sump hole was continually draining water from

the test bed. Figure 5.8 shows the possible levels of water retained in the test bed.

The crater formed by the detonation of the 15.4-pound cased charge in the sand backfill is shown in Figure 5.17. The crater had a depth of 4.96 feet and a width parallel to the reaction structure of 14.5 feet. The length of the crater perpendicular to the reaction structure was 16.83 feet.

The detonation of the charge at a range of 5 feet from the front face of the test slab caused light damage with small cracks along the length of the slab on the front and rear face. Figure 5.18 shows the front face of the test slab after excavation of the test bed. The rear face of the slab while mounted on the reaction structure and also after removal from the reaction structure is shown in Figure 5.19. The passive deflection gage in the reaction structure showed a maximum deflection of 1.44 inches and a permanent deflection of 1.13 inches.

The pretest and posttest elevations for the top of the reaction structure show that the structure moved upward 0.12 inches. The average rigid body motion at the top of the reaction structure was measured to be 0.79 inches away from the charge. Table 5.1 shows the pretest and posttest elevations and the rigid body motion of the structure.

Appendix C contains the digitized data for the free-field and structural gages in this test. The soil stress and interface pressure records in this report have been filtered with a 20 kHz low pass filter. They were then filtered with a 5 to 17 kHz band rejection filter. The filtering processes was designed to reduce the noise on the data record due to the instrumentation system. The accelerometers have been shifted to set the velocity to zero before the time of arrival at each gage using constant baseline shifts. Some of the accelerometers were shifted with a constant baseline shift to conform more closely to the waveform projected by the free-field gages.

The soil stress gage, SE-1, located 5 feet from the charge measured a peak stress of 450 psi. The peak interface pressure at the center of the test slab was 825 psi. The peak stress in the free-field for the reconstituted backfill material was 1,000 psi in Test 1 and Test 2, which is considerably higher than the peak stress in Test 3. The peak interface pressure at the center of the slab for Test 1 was 2,100 psi and was 2,400 psi for Test 2. The measured stresses were much less in the

sand backfill than in the reconstituted clay. The loading wave speed was found to be 1,300 fps from an average of all the gages up to a range of 5 feet from the charge. This value was not much different than the 1,400 fps loading wave speed calculated for the reconstituted clay in both tests. The loading wave speed from an average of the gages at a range of 5 feet from the charge was 1,800 fps. This compares to 2,900 fps and 2,800 fps in Backfill Test 1 and 2.

Backfill Test 3 was conducted on an identical test slab as the one used in Backfill Test 1 with the only changes in the test configuration being the backfill material. The response of the test slab in Backfill Test 1 was a breach of the slab, while the test slab in Backfill Test 3 suffered only light damage with a maximum deflection of 1.44 inches. The backfill effects made significant difference in the response of these two test slabs.

Backfill Test 3 was also conducted to provide a comparison between the tests conducted at Fort Knox, KY, and the AFESC tests conducted at Fort Polk, LA. The necessity for the comparison test was based on the differences in the water table at the two sites and the properties of the soil surrounding the test beds. The same test configuration and similar test articles were used in each set of tests. The test slab for Backfill Test 3 had an L/t of 10 and 1.0 percent steel, while the test slab for AFESC Test 9 had 0.5 percent steel. The test slab in the AFESC tests had a maximum deflection of 2.94 inches, and the test slab in Backfill Test 3 had a maximum deflection of 1.44 inches. The AFESC tests showed that there was a decrease in deflection when the steel percentage in the slab was increased. A test slab with 1.0 percent steel was tested in AFESC Test 6 with a horizontal charge orientation and had a maximum deflection of 1.56 inches. The AFESC tests showed that the vertical charge orientation caused greater maximum deflection in one test. The maximum deflection measured in Backfill Test 3 compares well with the results of the AFESC tests and showed that there were no significant effects caused by the differences in the test sites.

5.5 IN-SITU TEST 4

The in-situ test of an L/t of 10 slab having 1.0 percent steel was conducted on 28 April 1989 with a vertical charge orientation. Readings from the piezometer were taken immediately before the test, and the ground water table was approximately 1.79 feet below ground surface. The detonation of

the charge caused a crater which was 6.55 feet deep as shown in Figure 5.20. The crater had a 16 foot width parallel to the reaction structure and a 14.75 foot length perpendicular to the reaction structure.

The detonation of the 15.4-pound cased charge at a range of 5 feet from the front face of the test slab caused severe damage. Figure 5.21 shows damage to the front face of the test slab after excavation of the test bed. Principal steel was broken in the back layer of the reinforcing mat at the center of the slab and in the front layer of the mat just below the top supports and above the bottom supports. The rear face of the slab is shown in Figure 5.22. The passive deflection gage in the reaction structure showed a maximum deflection of 10.69 inches and a permanent deflection of 9.19 inches.

The pretest and posttest elevations on the top of the reaction structure show that the structure moved upward an average of 2.19 inches. The rigid body motion at the top of the reaction structure was 1.94 inches away from the charge. Table 5.1 shows the pretest and posttest structural elevations and the rigid body motion.

Appendix D contains the digitized data for the free-field and structural gages in this test. The soil stress interface pressure records in this report have been filtered with a 20 kHz low pass filter. They were then filtered with a 5 to 17 kHz band rejection filter. The filtering processes was designed to reduce the noise on the data record due to the instrumentation system. The accelerometers have been shifted to set the velocity to zero before the time of arrival at each gage using a constant baseline shift. Some of the accelerometers were shifted with a constant baseline shift to conform more closely to the waveform projected by the free-field gages.

The peak pressure recorded by the soil stress gage, SE-1, at a range of 5 feet from the charge was 1,000 psi. The peak interface pressure measured at the center of the test slab was 2,300 psi. The loading wave speed determined from the average of wave speeds from gages at a range up to 5 feet was 1,900 fps. The loading wave speed determined from wave speeds from gages at a range of 5 feet was 3,800 fps. The loading wave speed for the in-situ backfill material was considerably higher than the wave speeds for the backfill materials.

In-Situ Test 4 involved a test slab identical to the ones used in Test 1 and Test 3. The seismic velocity in the in-situ material was approximately 3,000 fps, and the material had a low shear strength. The test slab suffered severe damage from the detonation of the charge. These tests seem to show that the strength characteristics of the soil are important to the response of the buried structure.

Table 5.1. Structural elevations and rigid body motion.

Backfill Test 1

Position	Pretest Elevation	Posttest Elevation	Rigid Body Motion
1	94.64'	94.78'	A: -0.94"
2	94.76'	94.86'	B: -0.38"
3	94.69'	94.97'	Avg: -0.66"
4	94.75'	94.86'	

Backfill Test 2

Position	Pretest Elevation	Posttest Elevation	Rigid Body Motion
1	94.78'	95.02'	A: +1.06"
2	94.86'	94.97'	B: -0.50"
3	94.97'	95.04'	Avg: +0.28"
4	94.86'	95.10'	

Backfill Test 3

Position	Pretest Elevation	Posttest Elevation	Rigid Body Motion
1	95.02'	95.00'	A: +0.63"
2	94.97'	94.99'	B: +0.94"
3	95.04'	95.09'	Avg: +0.79"
4	95.10'	95.09'	

In-Situ Test 4

Position	Pretest Elevation	Posttest Elevation	Rigid Body Motion
1	95.05'	95.12'	A: +1.88"
2	95.06'	95.00'	B: +2.00"
3	94.88'	95.27'	Avg: +1.94"
4	94.86'	95.19'	

Test Bed

3	2
A 4	1 B

Reaction Structure

Figure 5.1. Gradation curves for bacfkfill materials.
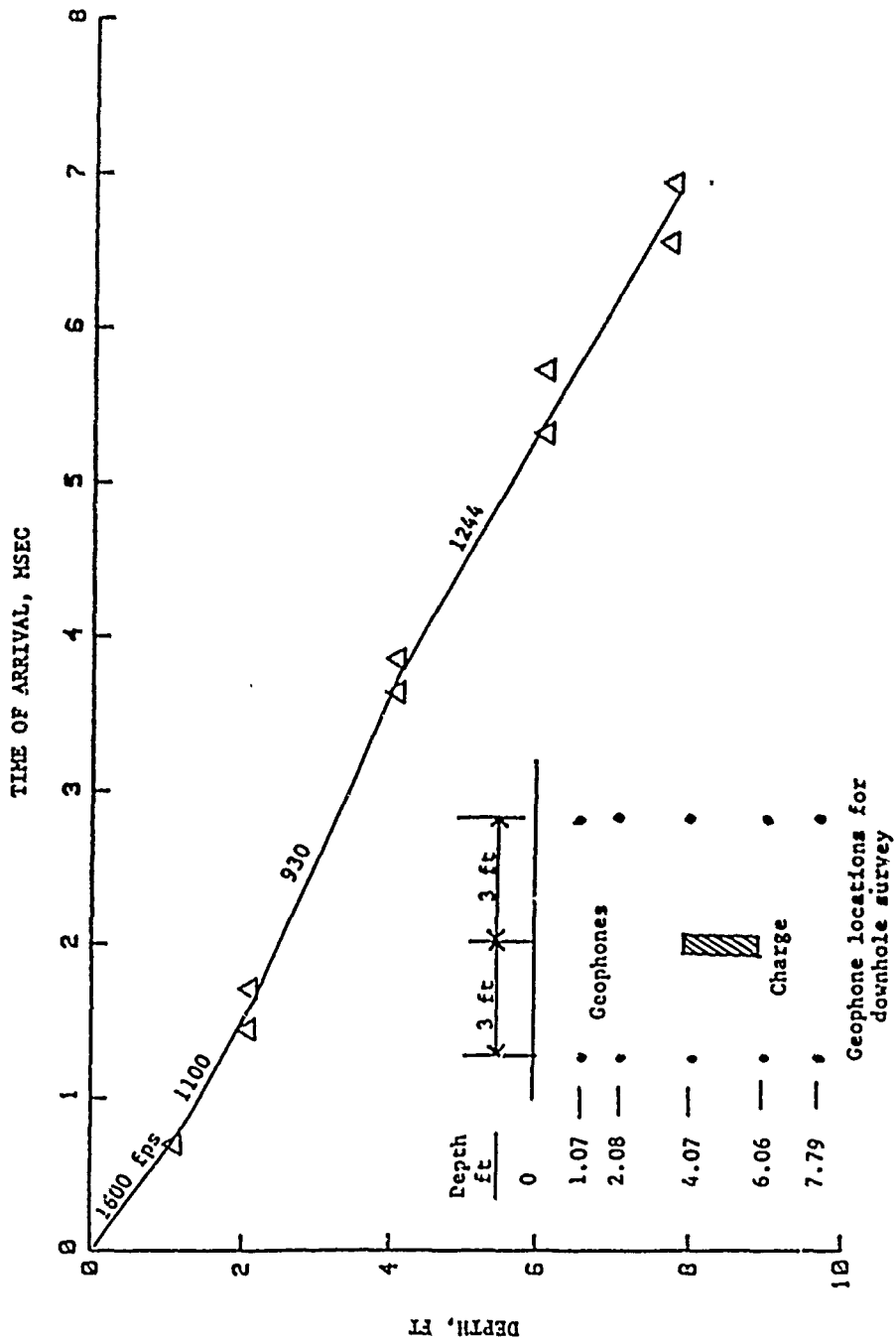
Figure 5.2. Time of arrival versus depth from geophones, Backfill Test 1.

71
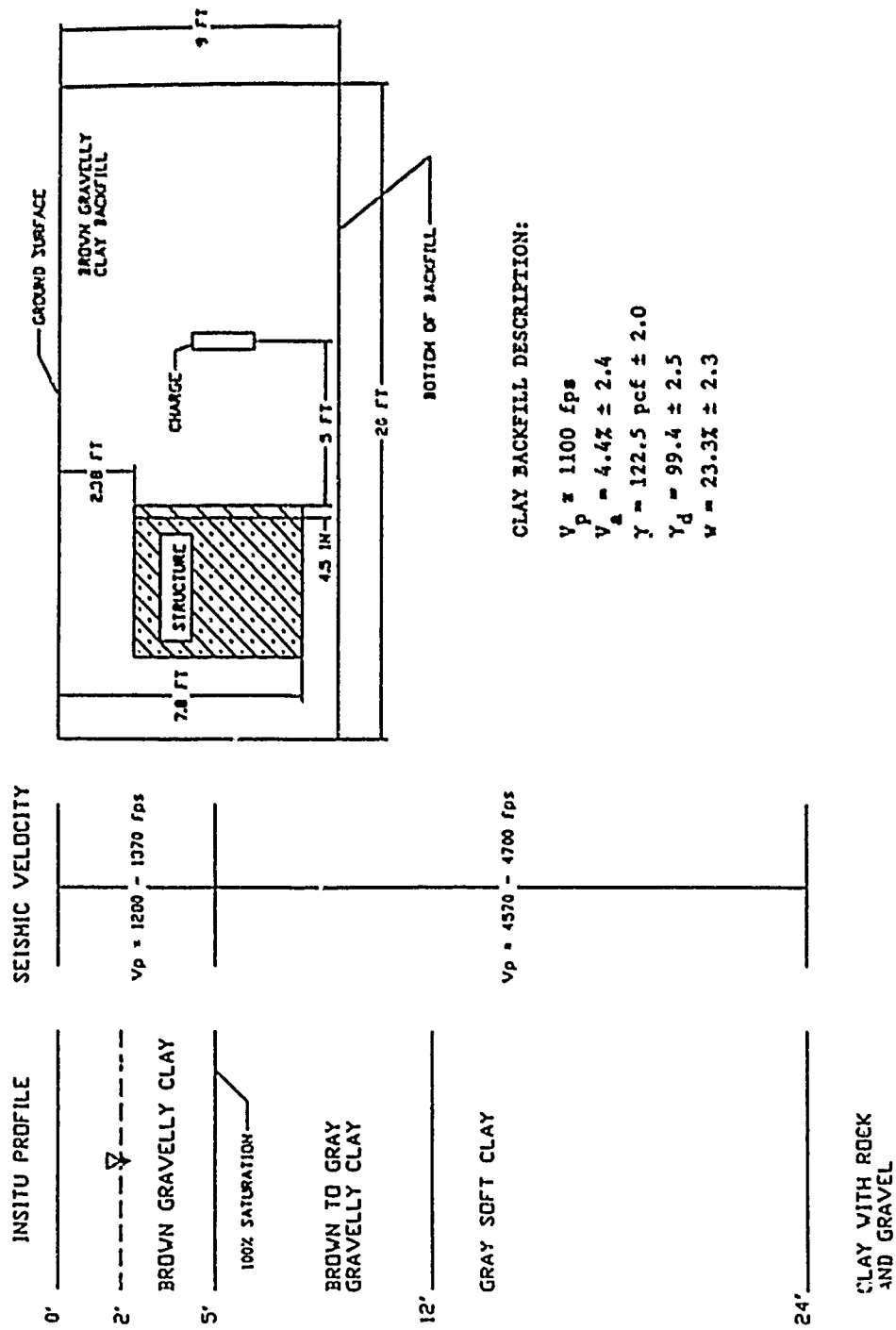
Figure 5.3. Section through Backfill Test 1 test bed and in-situ profile.
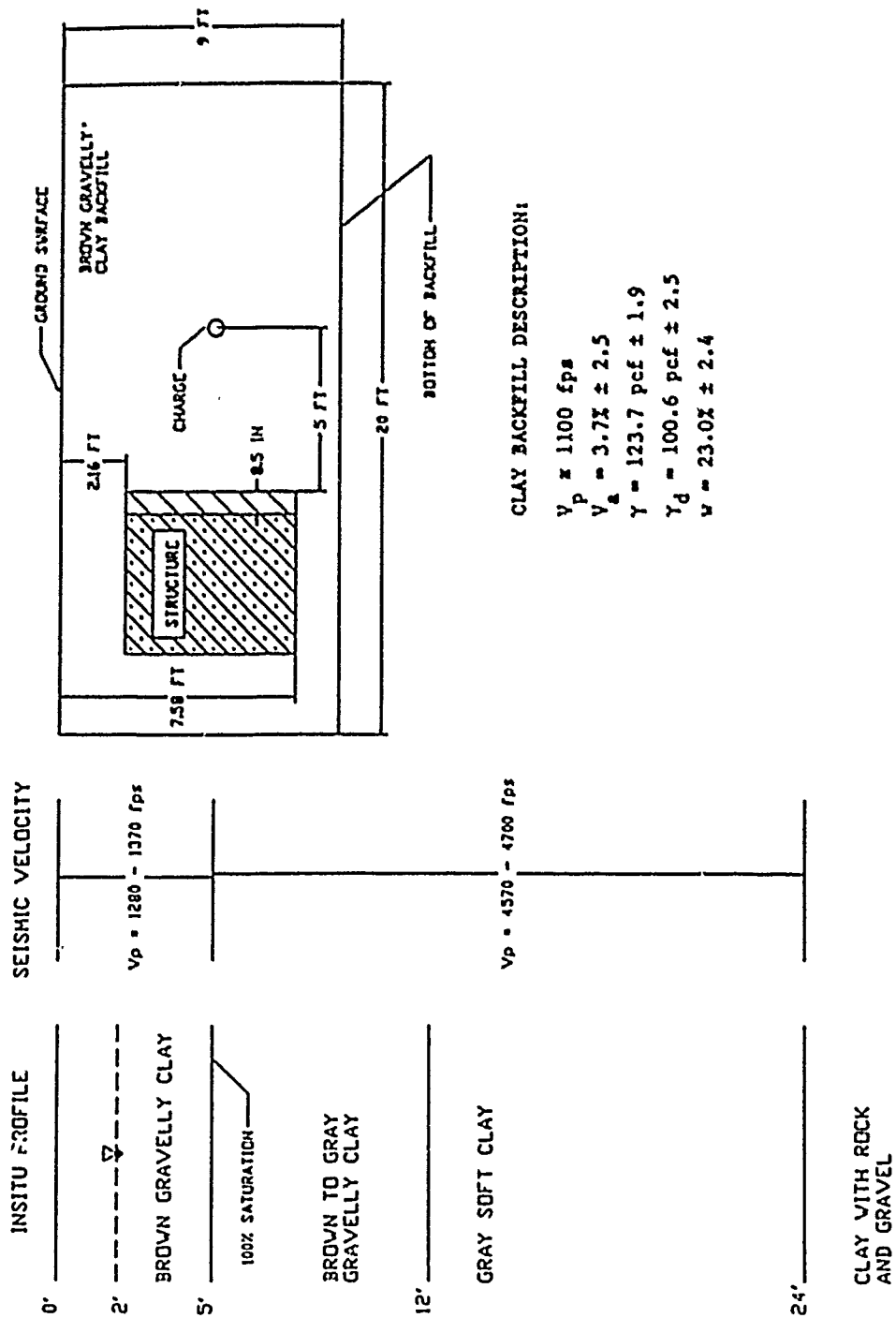
Figure 5.4. Section through Backfill Test 2 test bed and in-situ profile.

73
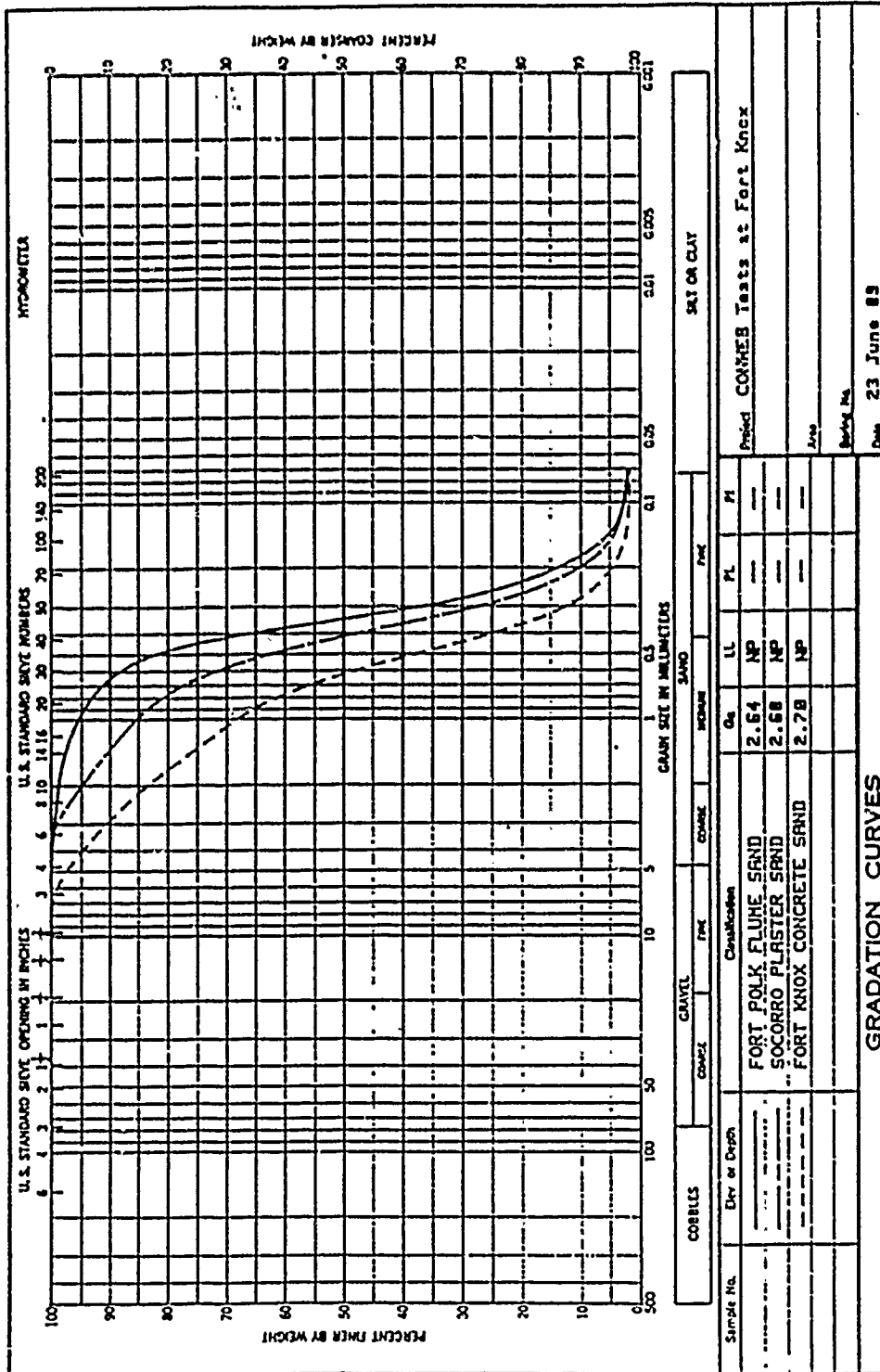
Figure 5.5. Comparison of gradation curves for sand.
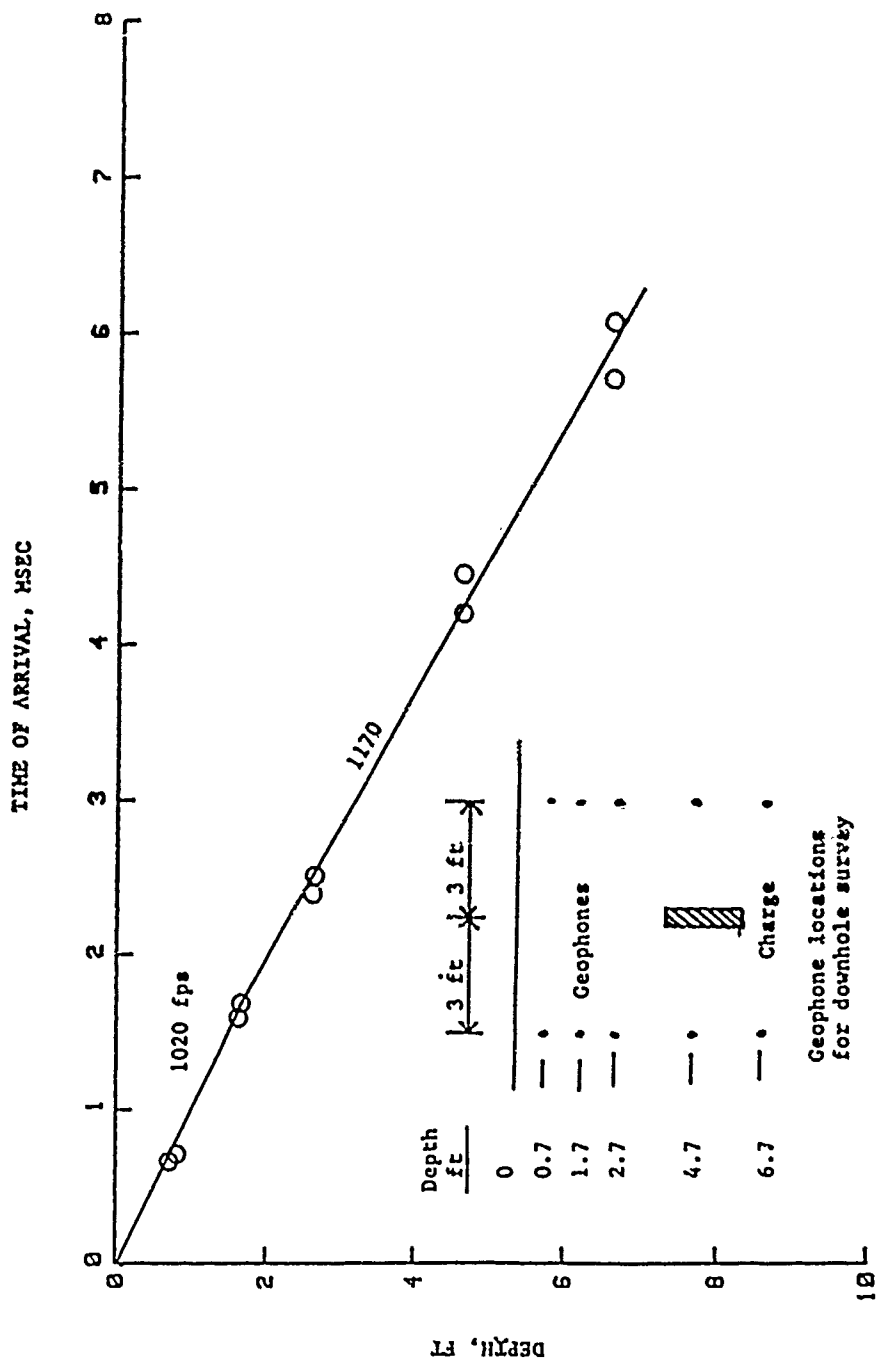
Figure 5.6. Time of arrival versus depth from geophones, Backfill Test 3.

TIME OF ARRIVAL, MSEC

△ CONNES Test 1 Clay Backfill
O CONNES Test 3 Sand Backfill

1100 fps
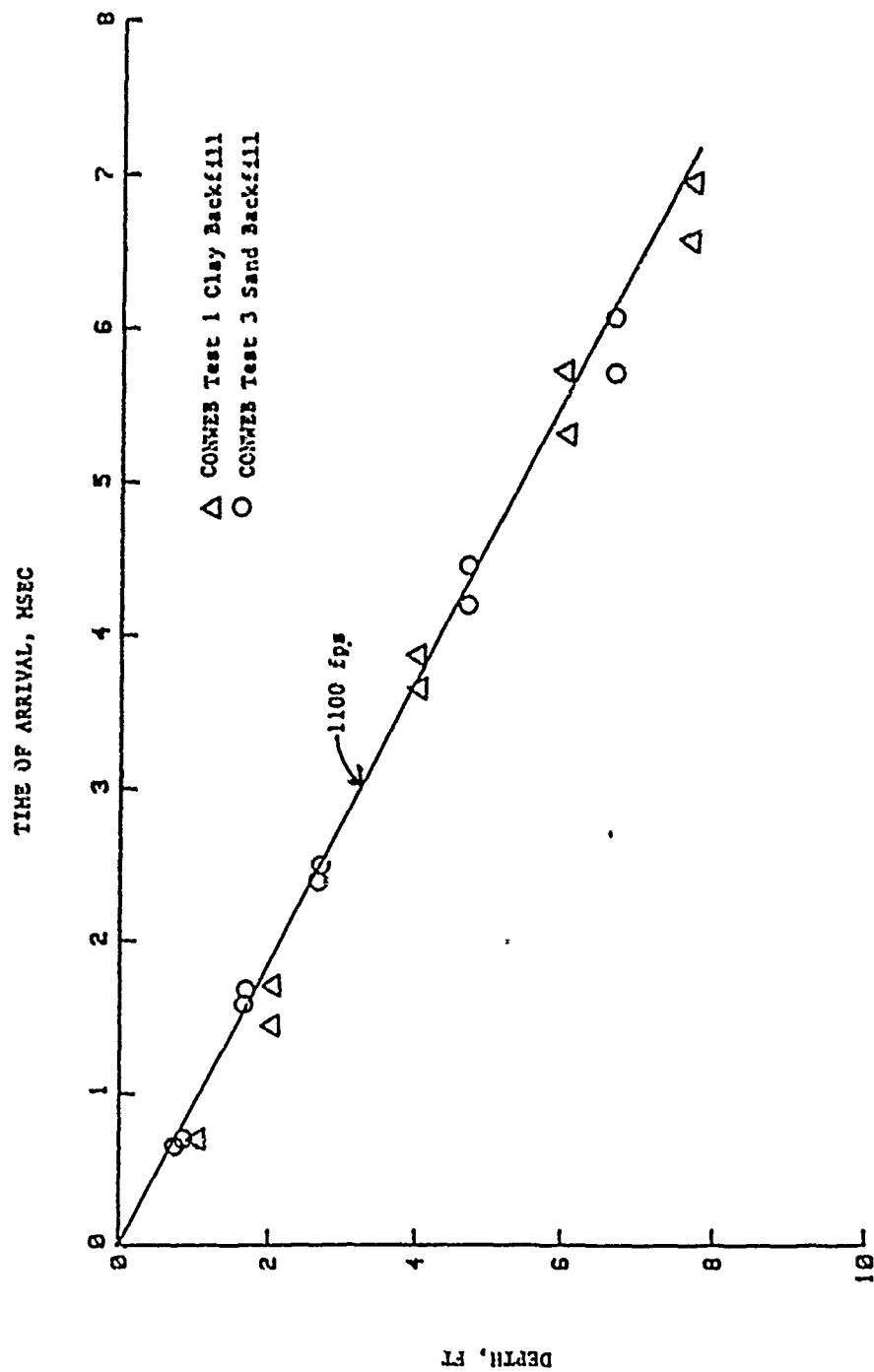
DEPTH, FT

Figure 5.7. Comparison of time of arrival versus depth from geophones
in Backfill Test 1 and Backfill Test 3.

76
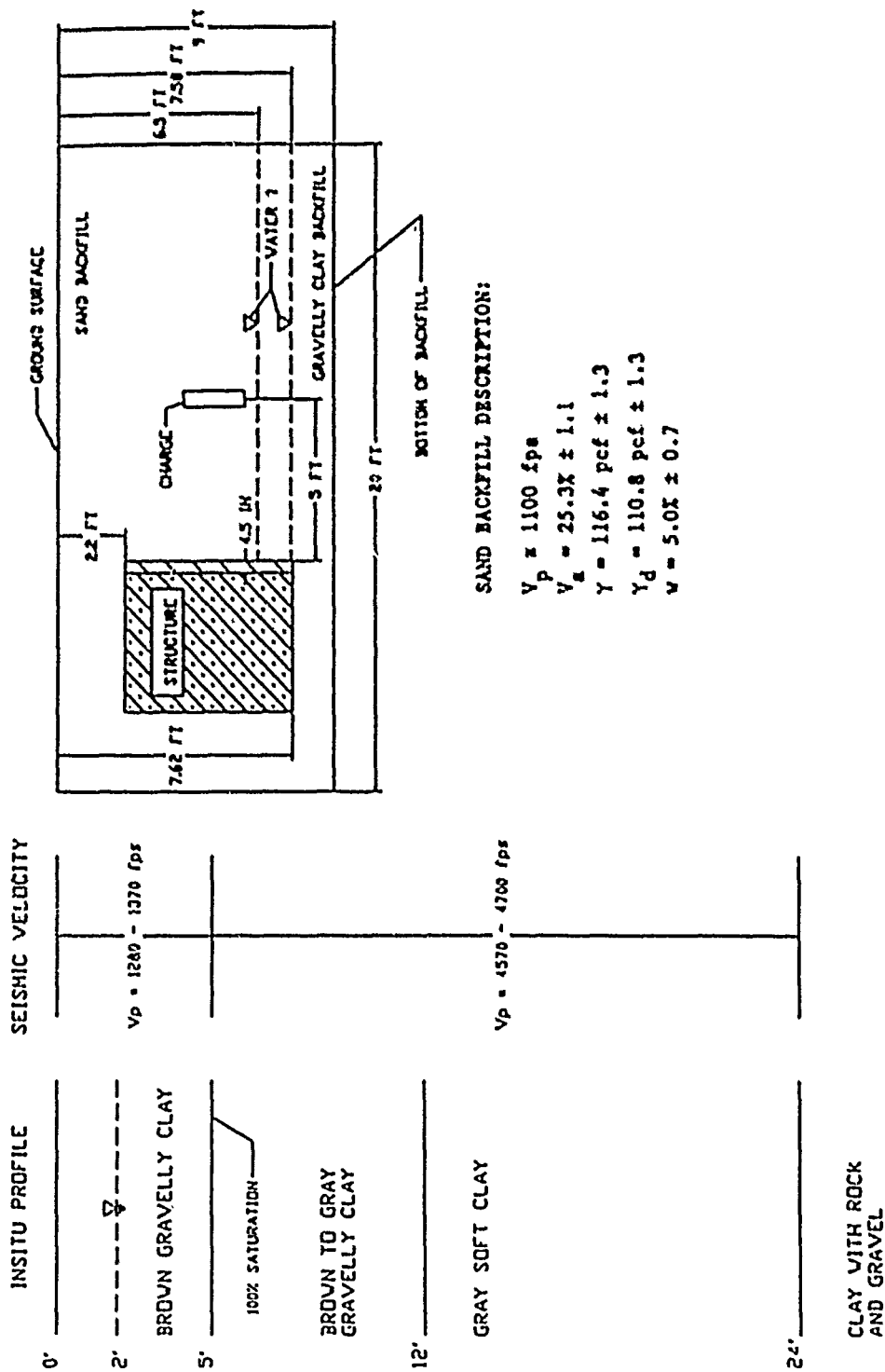
Figure 5.8. Section through Backfill Test 3 test bed and in-situ profile.
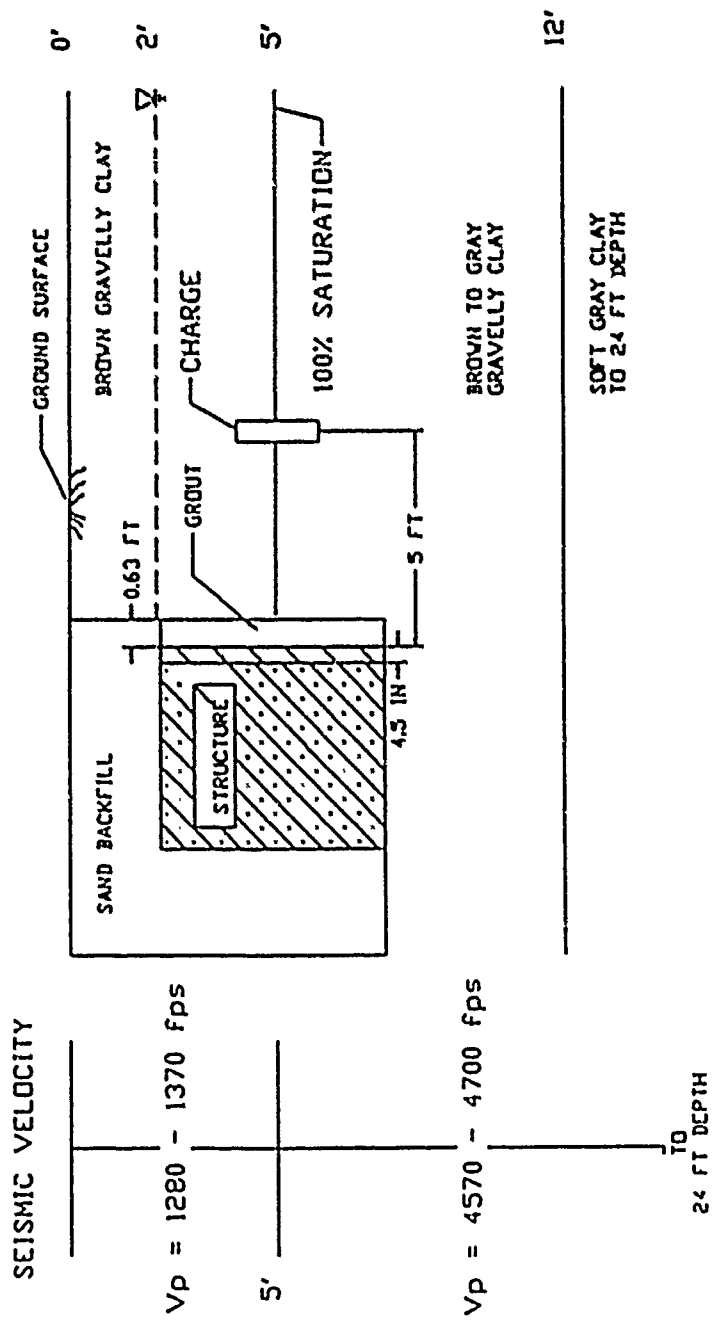
Figure 5.9. Section through In-Situ test bed.

Figure 5.10. Crater formed in Backfill Test 1.

Figure 5.11. Damage to the front face of test slab, Backfill Test 1.

Figure 5.12. Damage to inside of test slab,
Backfill Test 1.
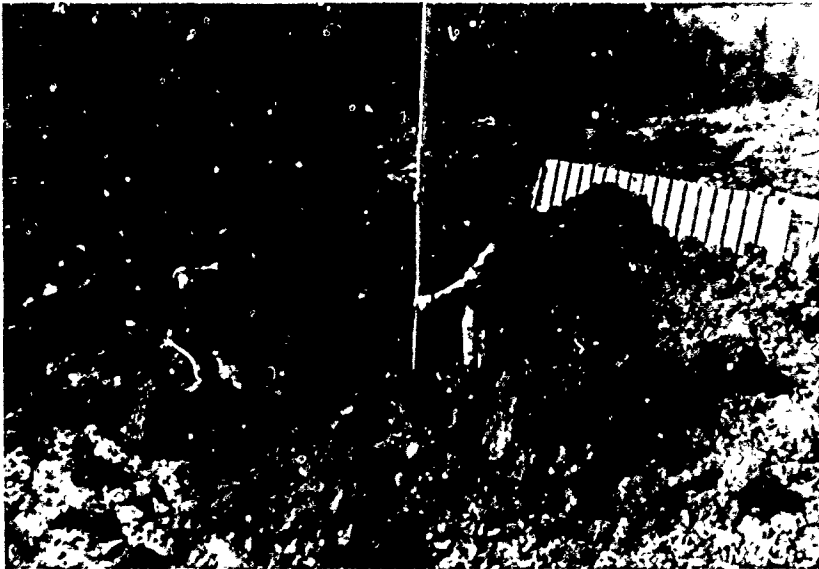
Figure 5.13. Crater formed in Backfill Test 2.
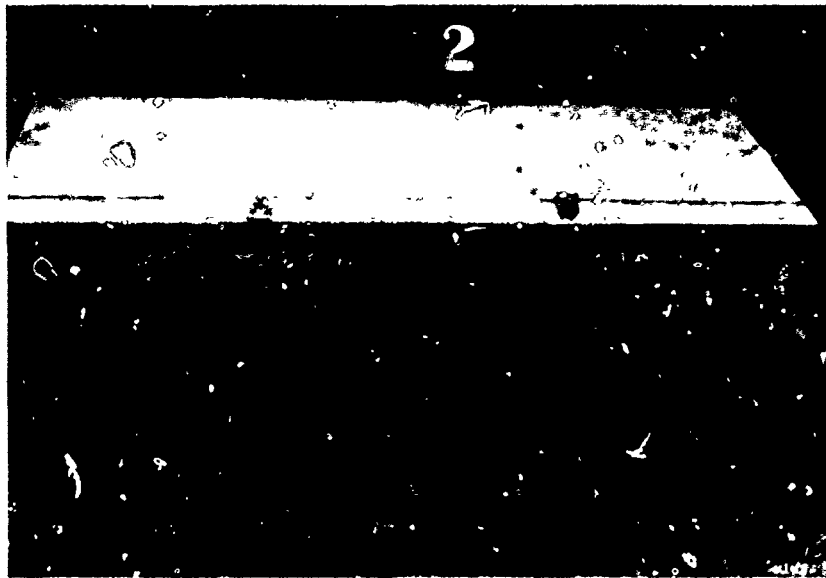
a. Attached to reaction structure.
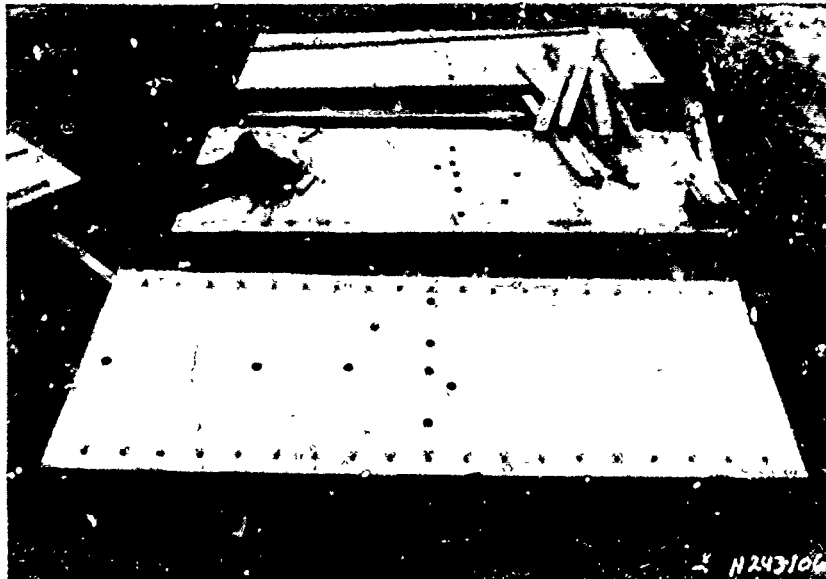
b. After removal from reaction structure.

Figure 5.14.   Damage to front face of test slab,
Backfill Test 2.

81

a. Attached to reaction structure.
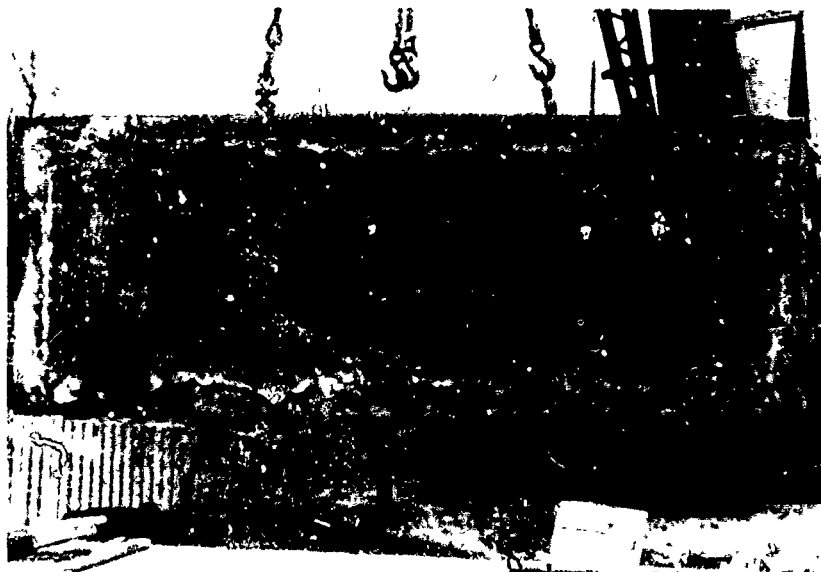
b. After removal from reaction structure.

Figure 5.15. Damage to interior face of test slab,
Backfill Test 2.
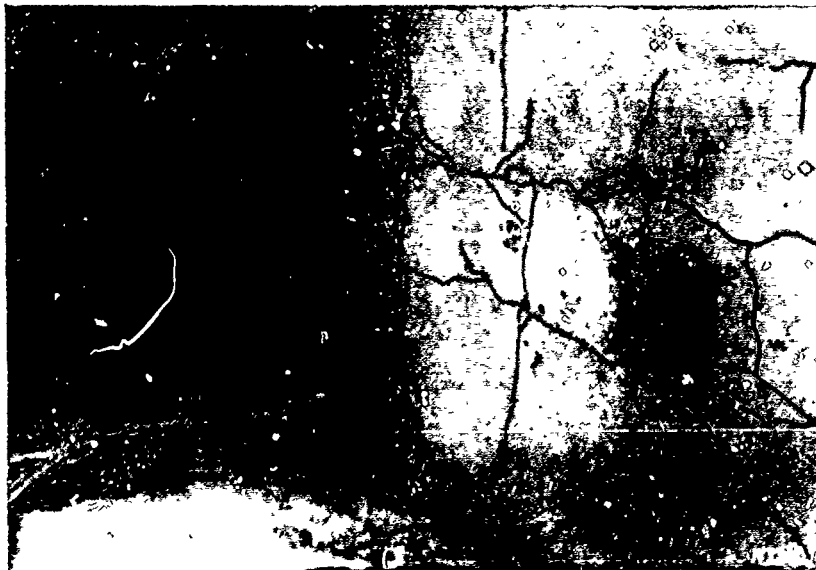
Figure 5.16. Damage to reaction structure after
Backfill Test 2.
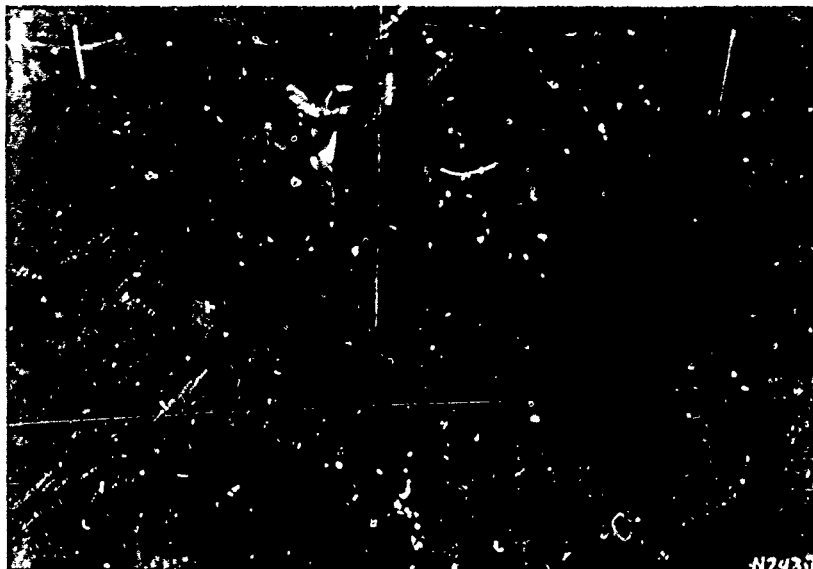
Figure 5.17. Crater formed in Backfill Test 3.
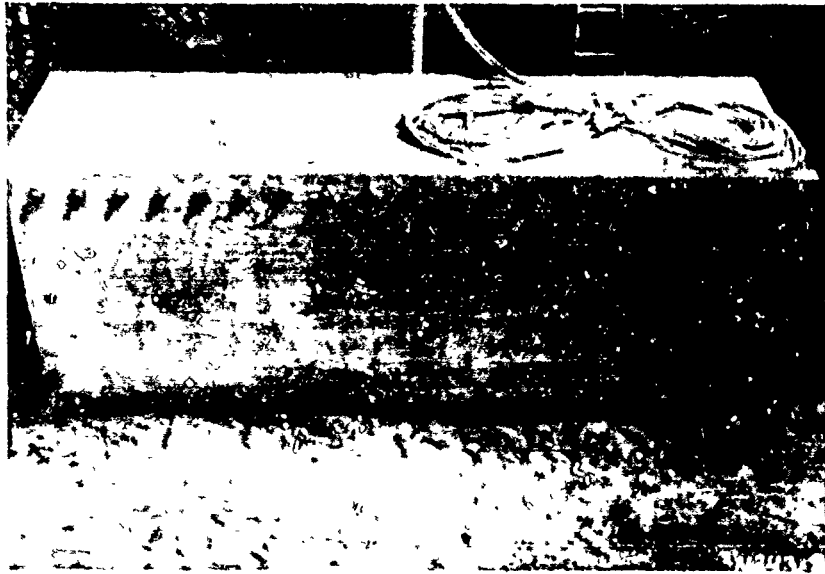
Figure 5.18. Damage to outside face of test slab,
Backfill Test 3.

N247·9(

a. Attached to reaction structure.

Figure 5.19. Damage to interior face of test slab,
Backfill Test 3 (Sheet 1 of 2).
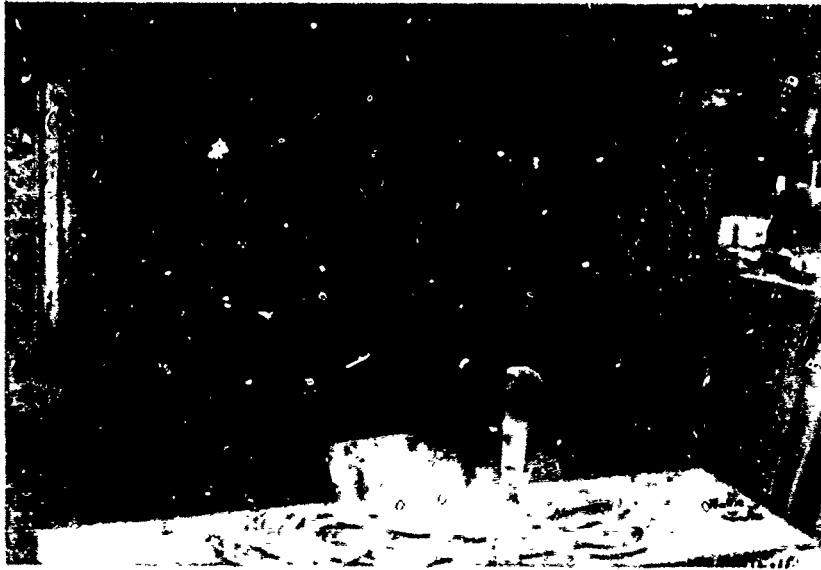
b.   After removal from reaction structure.

Figure 5.19.   Damage to interior face of test slab,
             Backfill Test 3 (Sheet 2 of 2).

Figure 5.20.   Crater formed in In-Situ Test 4.

Figure 5.21. Damage to outside face of test slab,
In-Situ Test 4.

Figure 5.22. Damage to interior face of test slab,
In-Situ Test 4.

CHAPTER 6
CONCLUSIONS AND RECOMMENDATIONS

6.1 CONCLUSIONS

The Backfill Effects tests have shown that the response of a buried structure when dynamically loaded with a localized load is significantly effected by the type of backfill material around the structure. One of the most common parameters used to describe a backfill material has been the seismic velocity of the backfill. These tests have shown that it is possible to have two completely different backfill materials with approximately the same seismic velocity. Backfill Test 1 and Backfill Test 3 were conducted on identical test slabs. Test 1 was conducted in a reconstituted clay backfill having a low shear strength and a seismic velocity of approximately 1,100 fps. Test 3 was conducted in a compacted sand backfill having a high shear strength and a seismic velocity of approximately 1,100 fps. The test slab in the reconstituted clay backfill material was breached by the detonation of the 15.4 pound cased charge at a distance of 5 feet from the front face of the test slab. The test slab in the compacted sand backfill suffered only light damage when subjected to the same test configuration used in Test 1. The responses of the test slabs in these two tests indicate that seismic velocity is not a valid parameter for determining backfill effects.

In-Situ Test 4 involved a test slab identical to the ones used in Test 1 and Test 3. The seismic velocity in the in-situ material was approximately 3,000 fps, and the material had a low shear strength. The test slab suffered severe damage from the detonation of the charge. These tests seem to show that the strength characteristics of the soil are important to the response of the buried structure.

Backfill Test 3 was conducted to provide a comparison between the tests conducted at Fort Knox, KY, and the AFESC tests conducted at Fort Polk, LA. The necessity for the comparison test was based on the differences in the water table at the two sites and the properties of the soil surrounding the test beds. The same test configuration and similar test articles were used in each set of tests. The test slab for Backfill Test 3 had an L/t of 10 and 1.0 percent steel, while the test slab for AFESC Test 9 had 0.5 percent steel. The test slab in the AFESC tests had a maximum deflection of 2.94 inches, and the test slab in Backfill Test 3 had a maximum deflection of

1.44 inches. The AFESC tests showed that there was a decrease in deflection when the steel percentage in the slab was increased. A test slab with 1.0 percent steel was tested in AFESC Test 6 with a horizontal charge orientation and had a maximum deflection of 1.56 inches. The AFESC tests did show that the vertical charge orientation caused greater maximum deflection in one test. The maximum deflection measured in Backfill Test 3 compares well with the results of the AFESC tests and showed that there were no significant effects caused by the differences in the test sites.

Backfill Test 2 was conducted on identical test articles with the same charge configuration used in AFESC Test 7. The backfill material was changed from a high shear strength sand to a low shear strength reconstituted clay material with approximately the same seismic velocity as the sand backfill. The test slab in the sand backfill had a maximum deflection of 0.63 inches, while the test slab in the clay backfill had a maximum deflection of 1.56 inches. The differences in response of the tests slabs show the extent to which backfill can effect the response of buried structures.

The free-field in the Backfill Effects tests were instrumented to determine the loading wave speeds of the different backfill materials. The loading wave speed was determined from the time of arrival to the free-field gages and their corresponding range to the charge. The loading wave speeds were determined using an average of the wave speeds calculated from the free-field gages up to and including a range of 5 feet. These data show that the loading wave speeds can be considerably higher than the seismic velocity of the backfill and are strongly dependent on peak stress levels. The loading wave speed were also calculated using an average of the wave speeds calculated from free-field gages at the 5-foot range. Again these values differed considerably from the seismic velocity of the backfill. The seismic velocity of a backfill material does not indicate the loading wave speed of the backfill material.

6.2 RECOMMENDATIONS

The results of these tests and preliminary analysis of the data show that further information can be obtained on backfill effects on buried structures with further analysis of the AFESC and Backfill Effects data. Two and tree dimensional finite element calculations should be performed to study the relative importance of backfill properties such as wave speed, shear

strength, and stress-strain relationships. The relative importance of the structural properties such as stiffness, strength, and rigid body motion should also be investigated.

REFERENCES

1. Krauthammer, T.; "Shallow-Buried RC Box-Type Structures"; Journal of Structural Engineering, Vol. 110, No. 3, March 1984; American Society of Civil Engineering.

2. Kiger, S. A., Slawson, T. R., and Hyde, D. W.; "Vulnerability of Shallow-Buried Flat-Roof Structures; Final Report: A Computational Procedure"; Technical Report SL-80-7, Report 6, September 1984; U.S. Army Engineer Waterways Experiment Station, Vicksburg, Mississippi.

3. Kiger, S. A. and Getchell, J. V.; "Vulnerability of Shallow-Buried Flat-Roof Structures; Foam HEST 1 and 2"; Technical Report SL-80-7, Report 1, September 1980; U.S. Army Engineer Waterways Experiment Station, Vicksburg, Mississippi.

4. Getchell, J. V. and Kiger, S. A.; "Vulnerability of Shallow-Buried Flat-Roof Structures; Foam HEST 3 and 6"; Technical Report SL-80-7, Report 4, U.S. Army Engineer Waterways Experiment Station, Vicksburg, Mississippi.

5. Headquarters, Department of the Army; "Fundamentals of Protective Design for Conventional Weapons;" Army Technical Manual 5-855-1, November 1985; U.S. Army Engineer Waterways Experiment Station, Vicksburg, Mississippi.

6. Hinman, E. E. and Weidlinger, P.; "Single-Degree-of-Freedom Solution of Structure-Medium Interaction", Proceedings from International Symposium on the Interaction of Conventional Munitions with Protective Structures, Mannheim, West Germany, 1987.

7. Baylot, J. T., Kiger, S. A., Marchand, K. A., and Painter, J. T.; "Response of Buried Structures to Earth-Penetrating Conventional Weapons;" Report ESL-TR-85-09, November 1985; Air Force Engineering and Services Laboratory, Air Force Engineering and Services Center, Tyndall Air Force Base, Florida.

8. Baylot, J. T. and Hayes, P. G.; "Ground Shock Loads on Buried Structures", Proceedings from Shock and Vibration Symposium, Virginia Beach, Virginia, 1989.

9. Zelasko, J. S.; "Executive Summary of Geotechnical Operations Conducted for FY 82 Silo Test/Combined Effects Program;" Miscellaneous Paper SL-86-17, November 1986; U.S. Army Engineer Waterways Experiment Station, Vicksburg, Mississippi.

10. Cargile, J. D. and Kean, T. B., II; "Cofferdam Concept Test Program, Geotechnical Investigation, Volume I: Main Text and Appendixes A Through C, Report 1;" Technical Report SL-88-33, August 1988; U.S. Army Engineer Waterways Experiment Station, Vicksburg, Mississippi.

APPENDIX A
DATA, BACKFILL TEST 1

Data from gages DEF-1 and DEF2 in Backfill Test 1 have not been included in this report.

CONWEB T1
IF-1-S
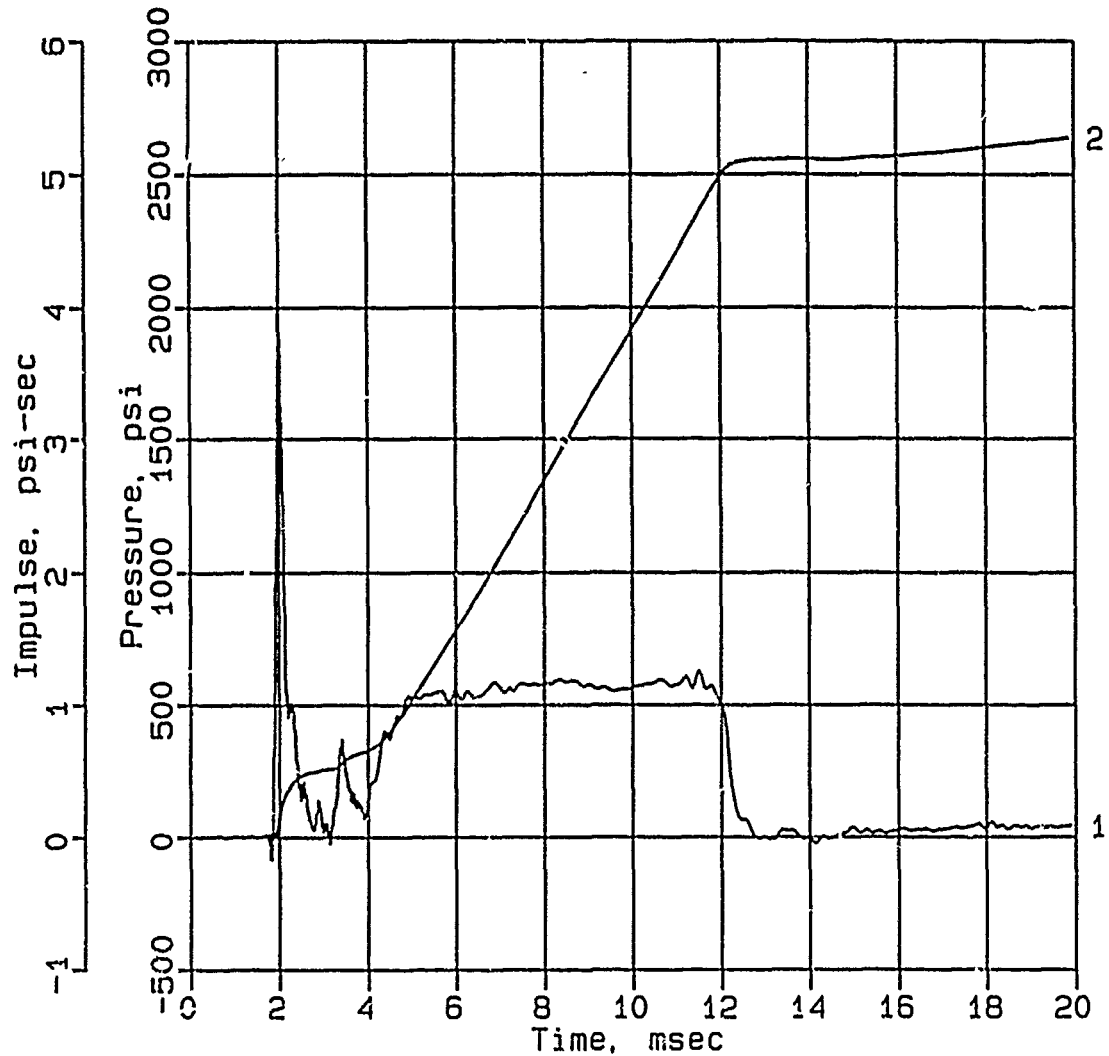
Digitizing rate: 200,000 Hz
Calibration: 2162
Filtering: 20 kHz low pass filter
        5 - 17 kHz band rejection filter

A3

CONWEB T1

IF-2-S
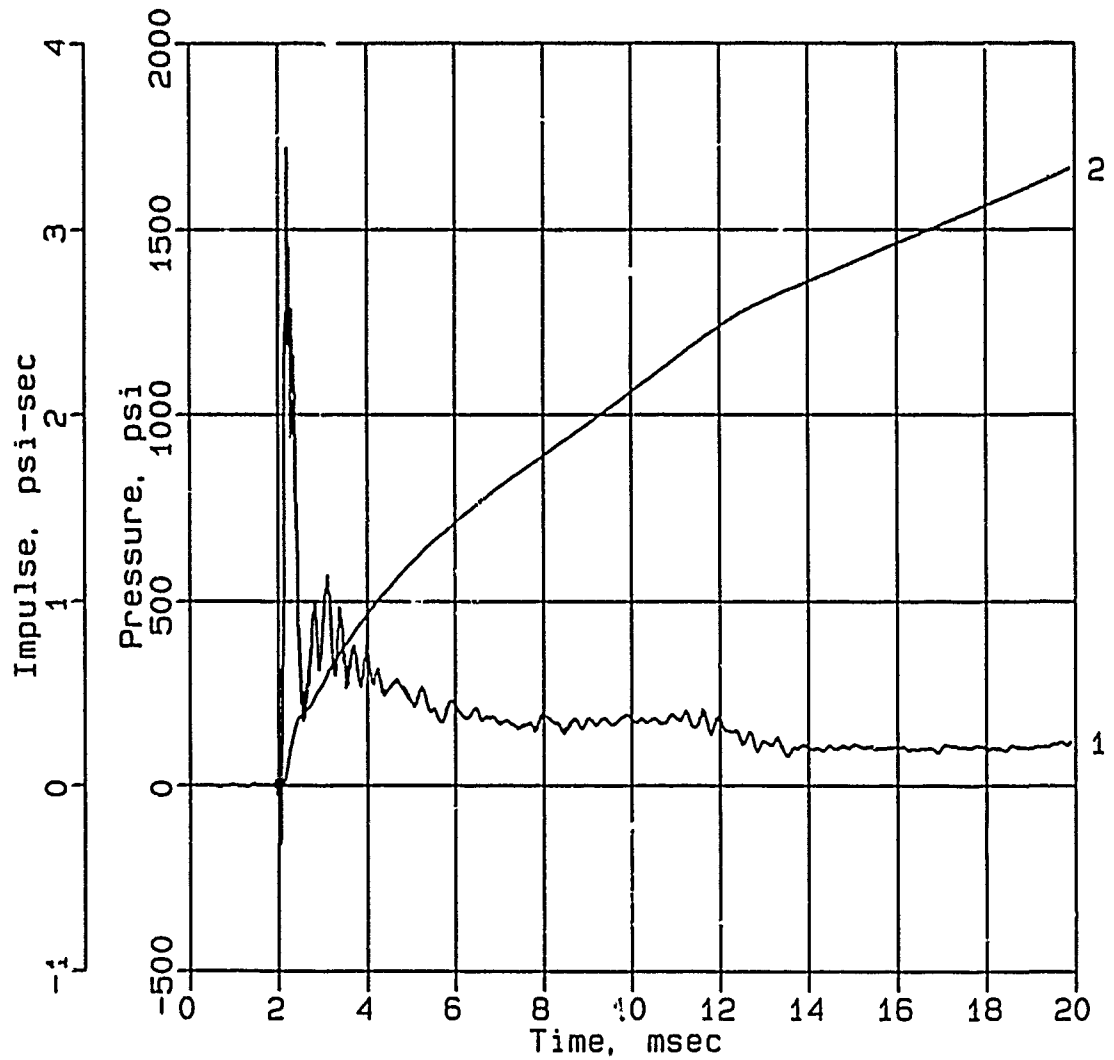
Digitizing rate: 200,000 Hz
Calibration: 2100
Filtering: 20 kHz low pass filter
5 - 17 kHz band rejection filter

A4

CONWEB T1

IF-3-S
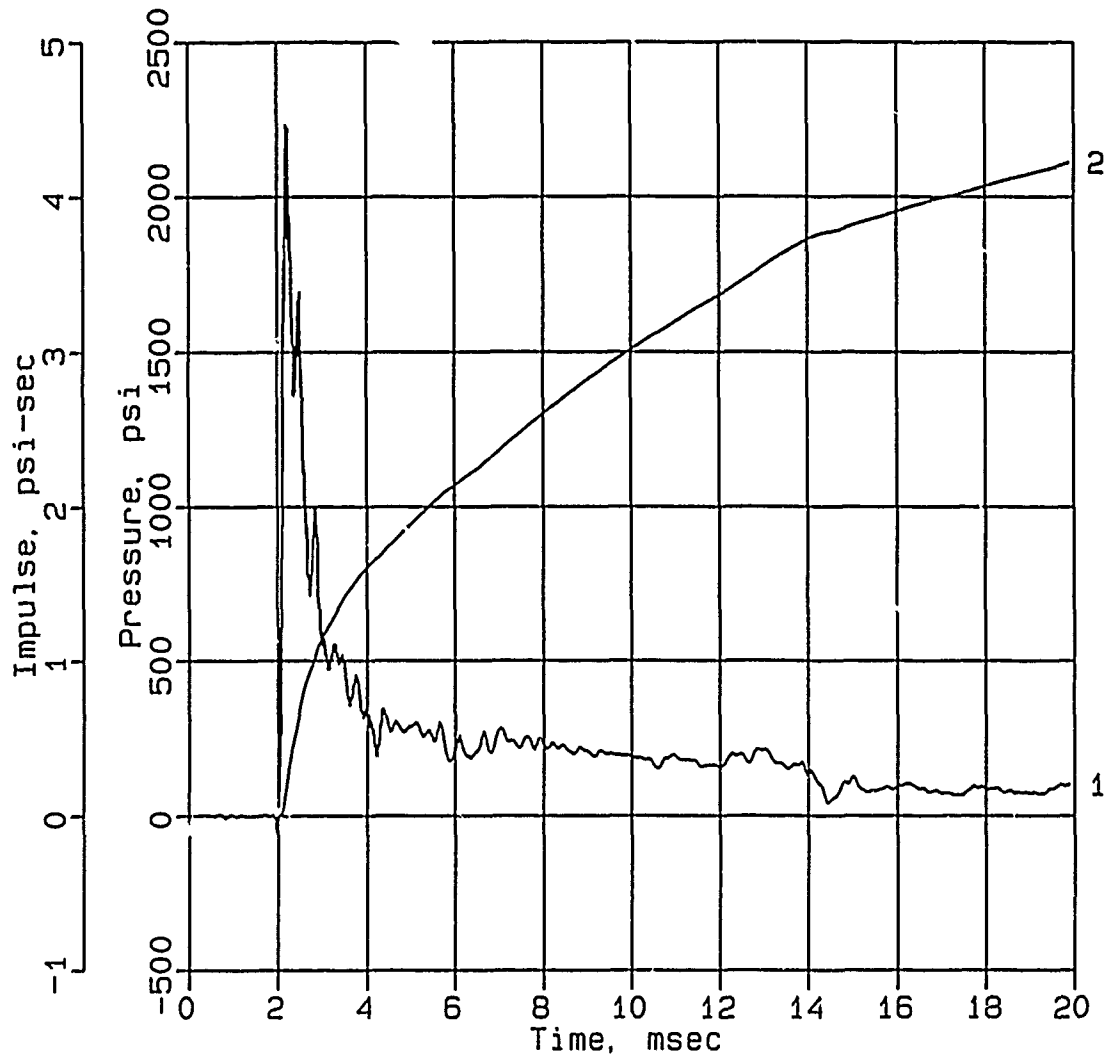
Digitizing rate: 200,000 Hz
Calibration: 2020
Filtering: 20 kHz low pass filter
            5 - 17 kHz band rejection filter

A5
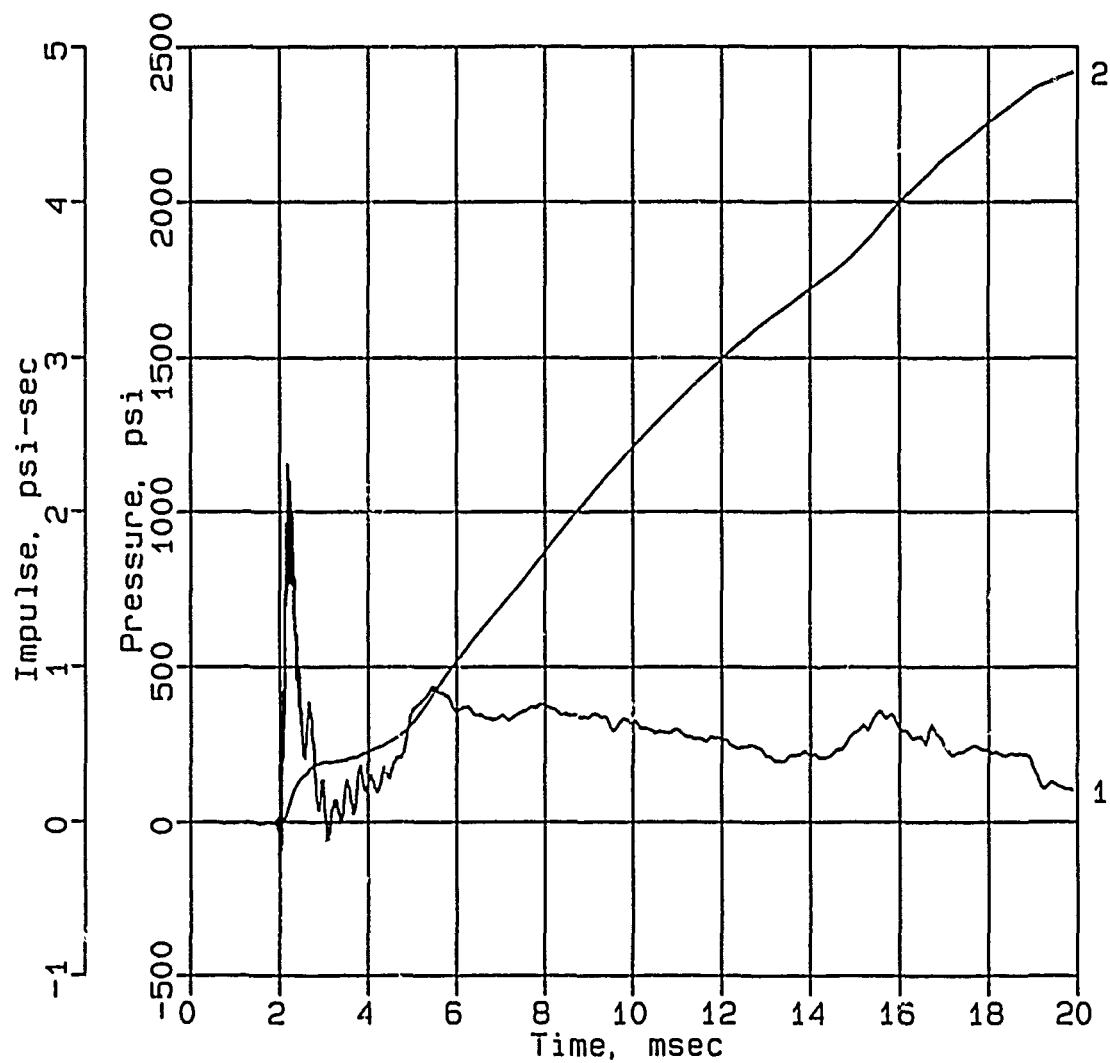
CONWEB T1
IF-5

Digitizing rate: 200,000 Hz
Calibration: 2107
Filtering: 20 kHz low pass filter
            5 - 17 kHz band rejection filter

A6

CONWEB T1

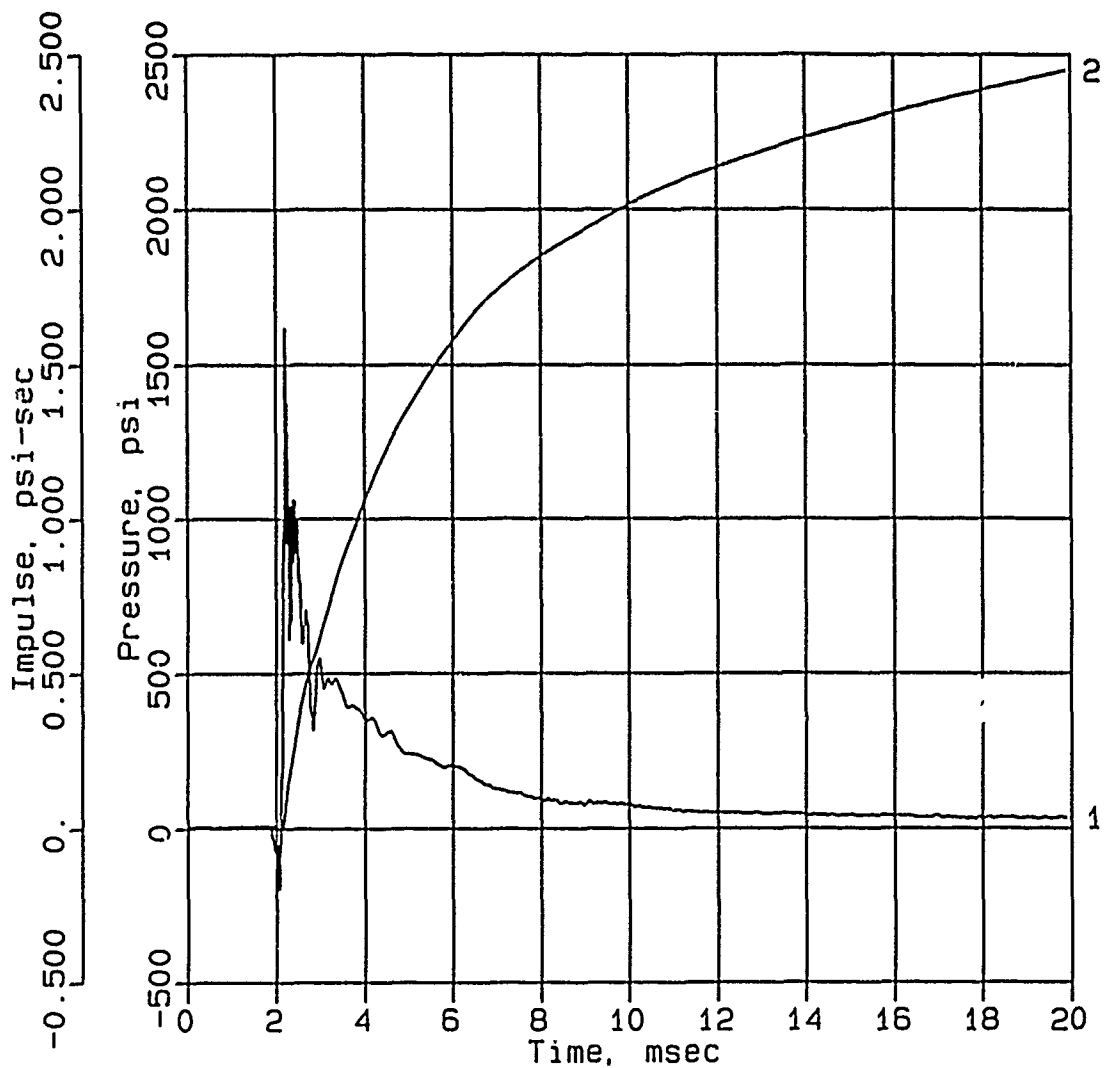## IF-6
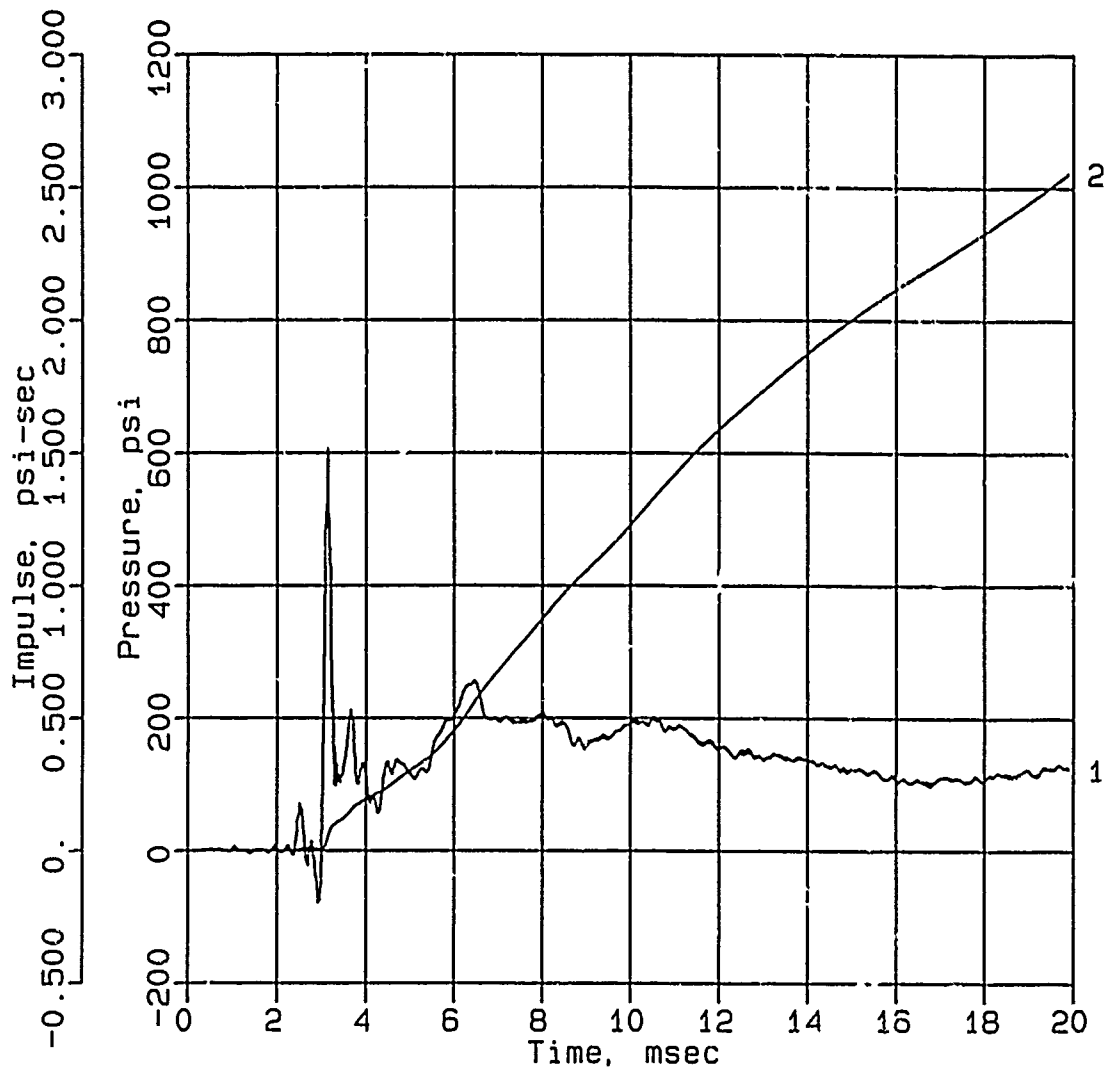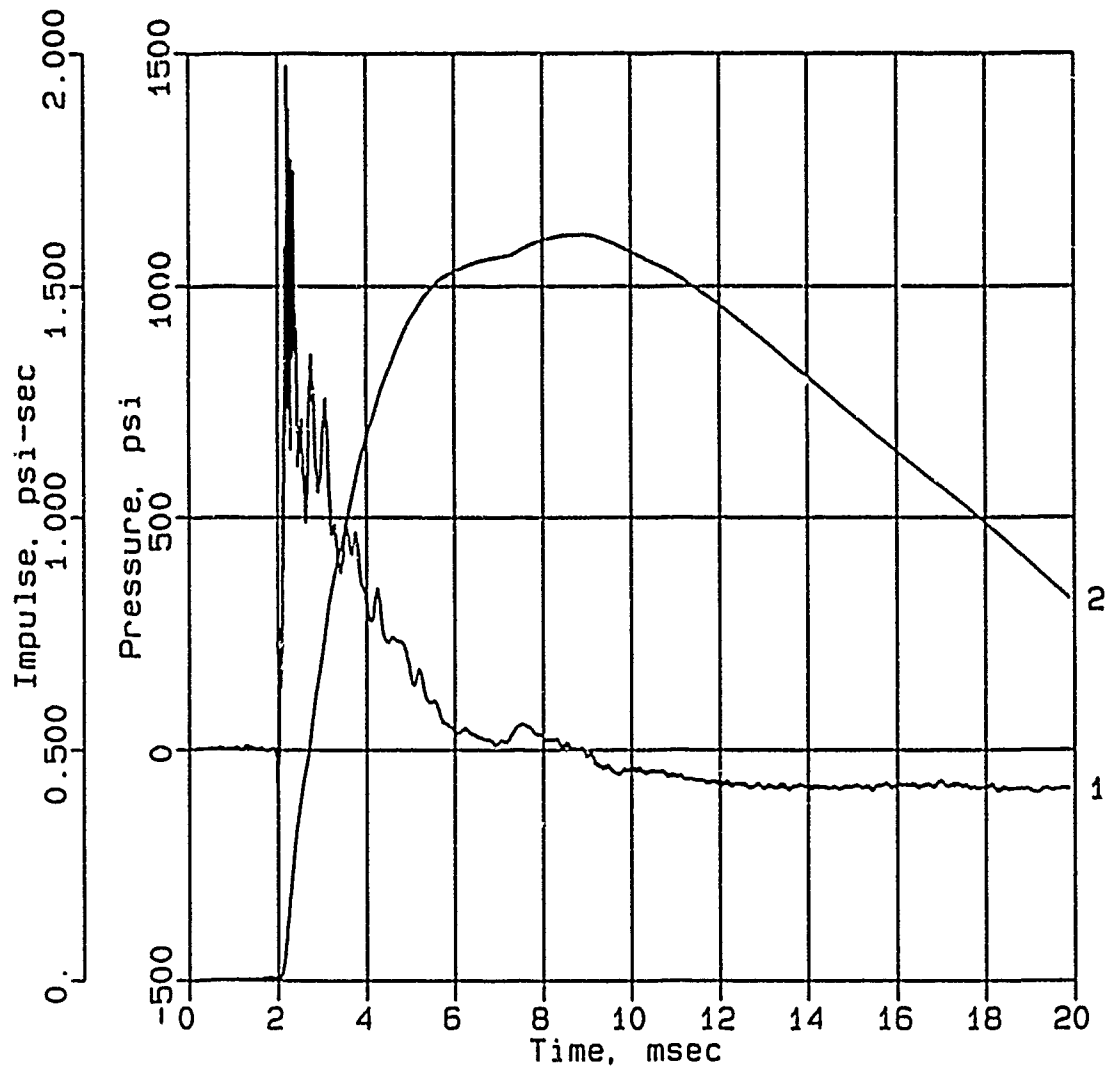

Digitizing rate: 200,000 Hz
Calibration: 1946
Filtering: 20 kHz low pass filter
            5 - 17 kHz band rejection filter

A7
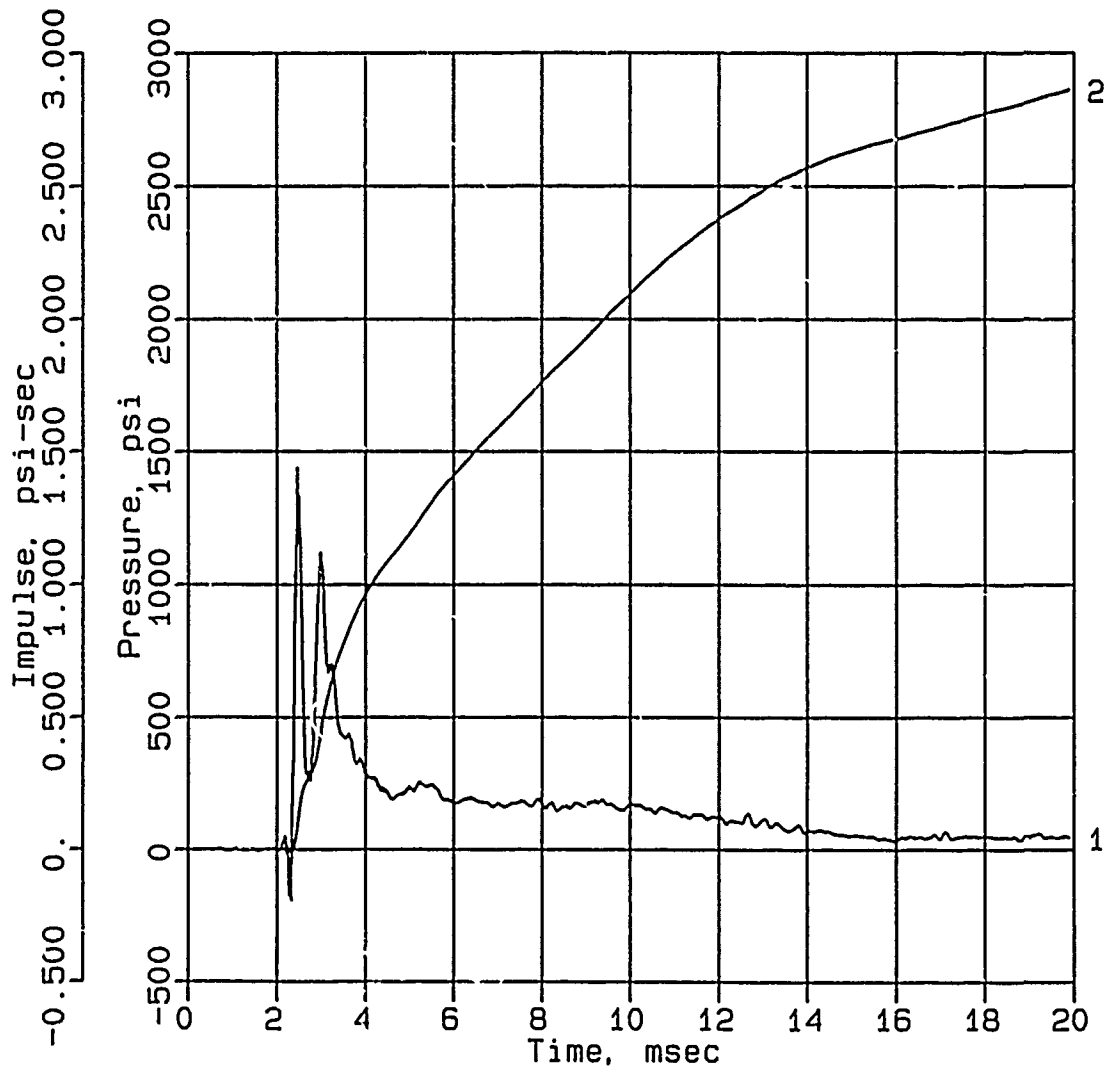
CONWEB T1
IF-8

Digitizing rate: 200,000 Hz
Calibration: 2675
Filtering: 20 kHz low pass filter
            5 - 17 kHz band rejection filter

A8
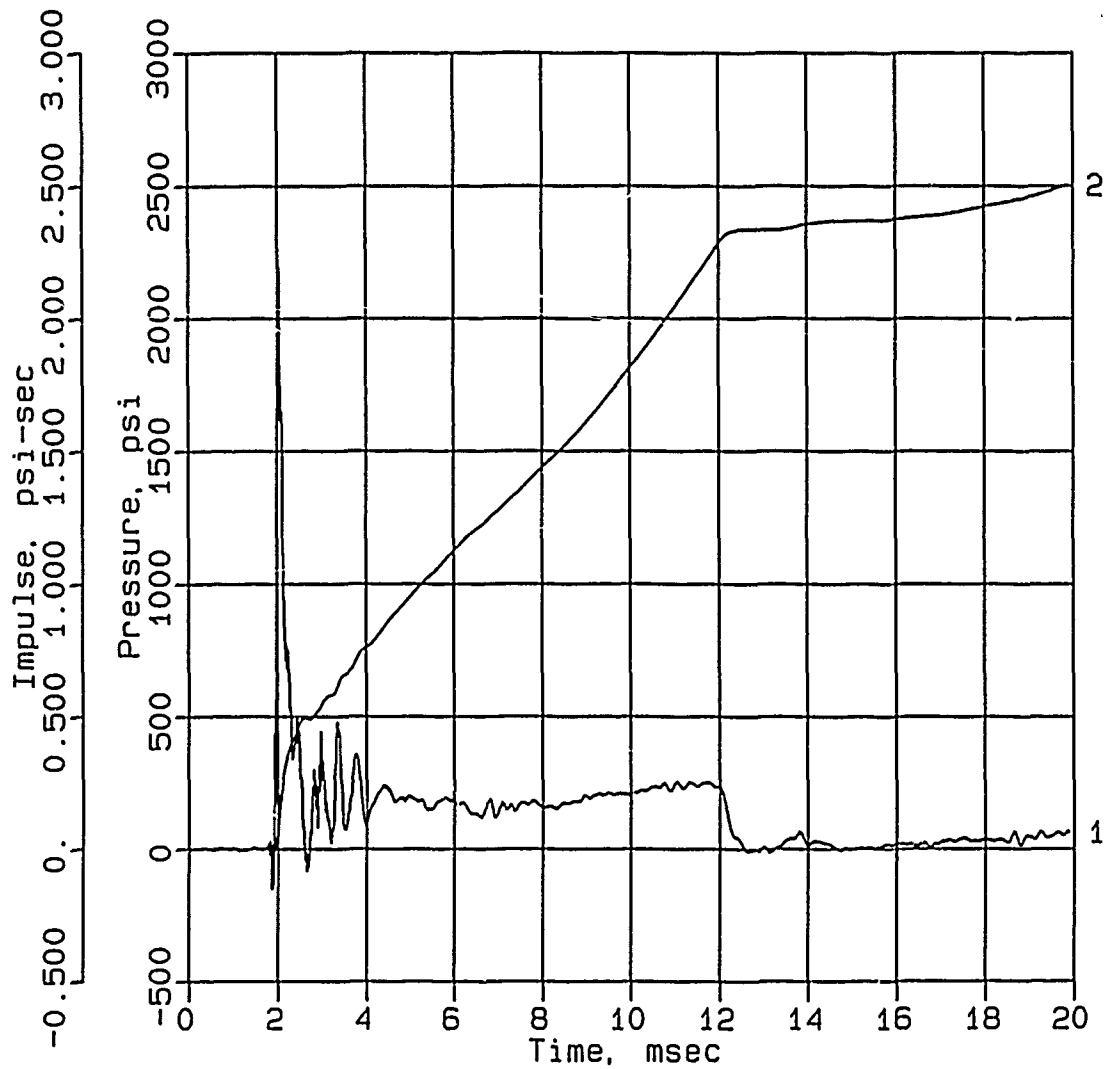
CONWEB T1
IF-9-S
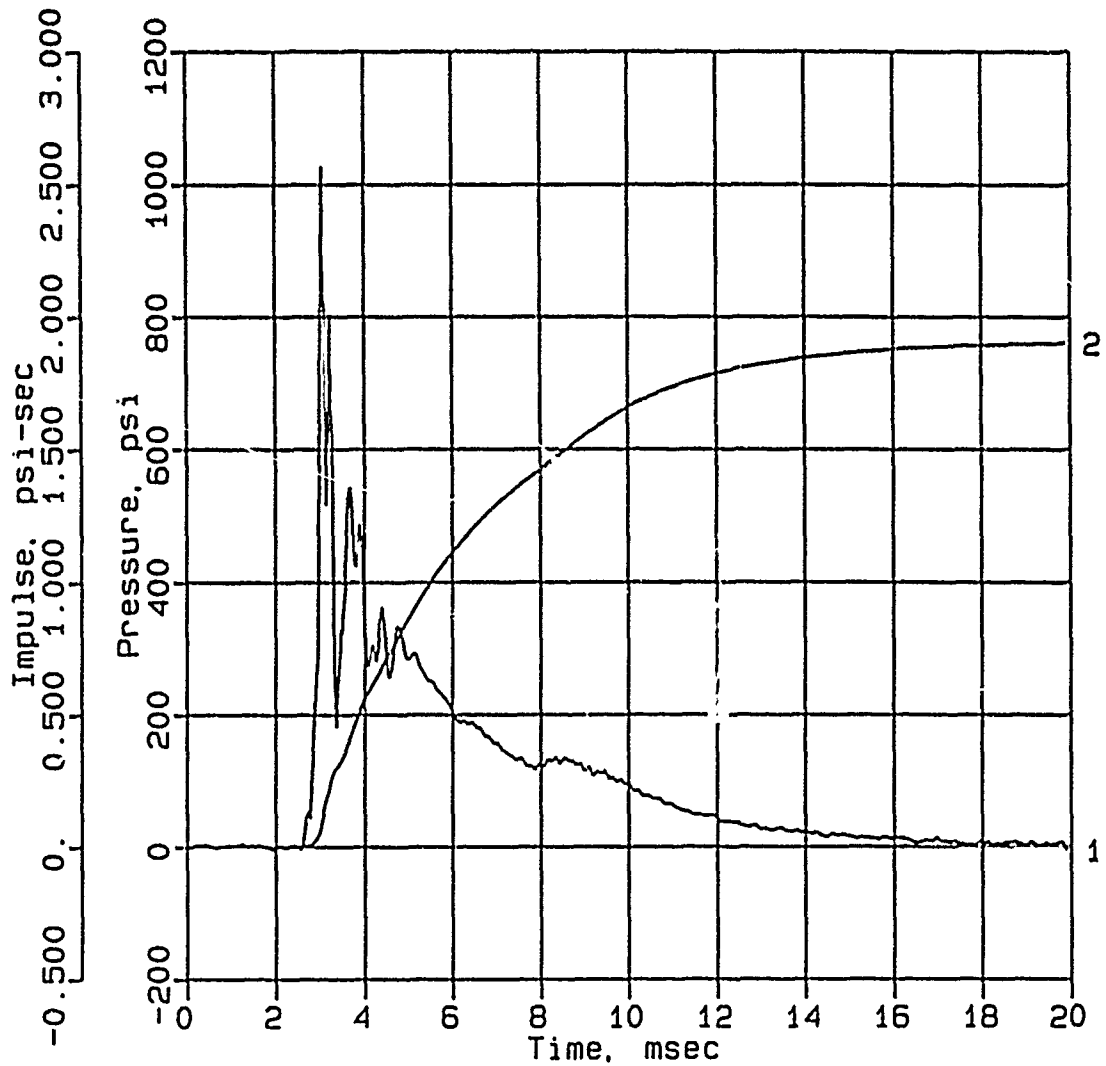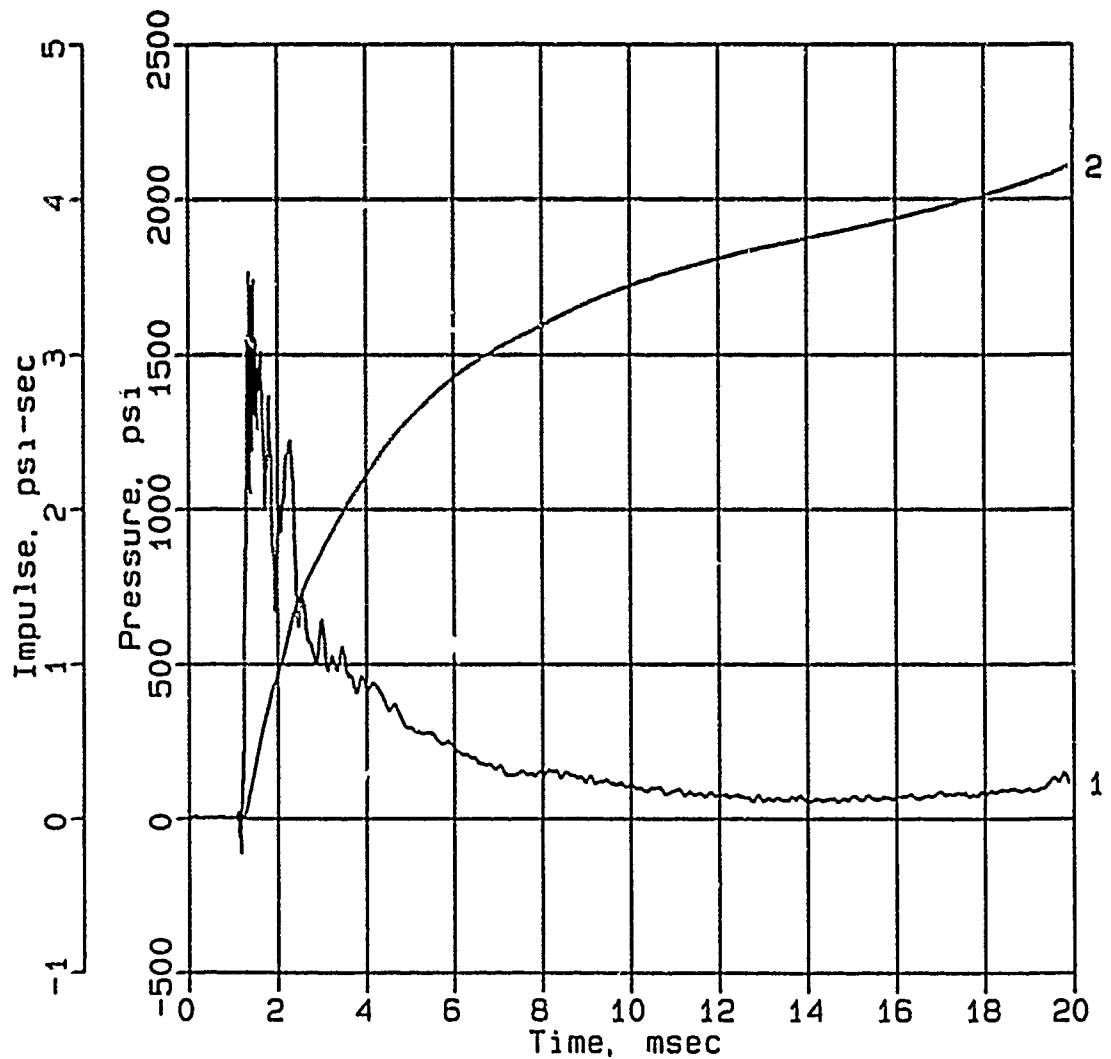

Digitizing rate: 200,000 Hz
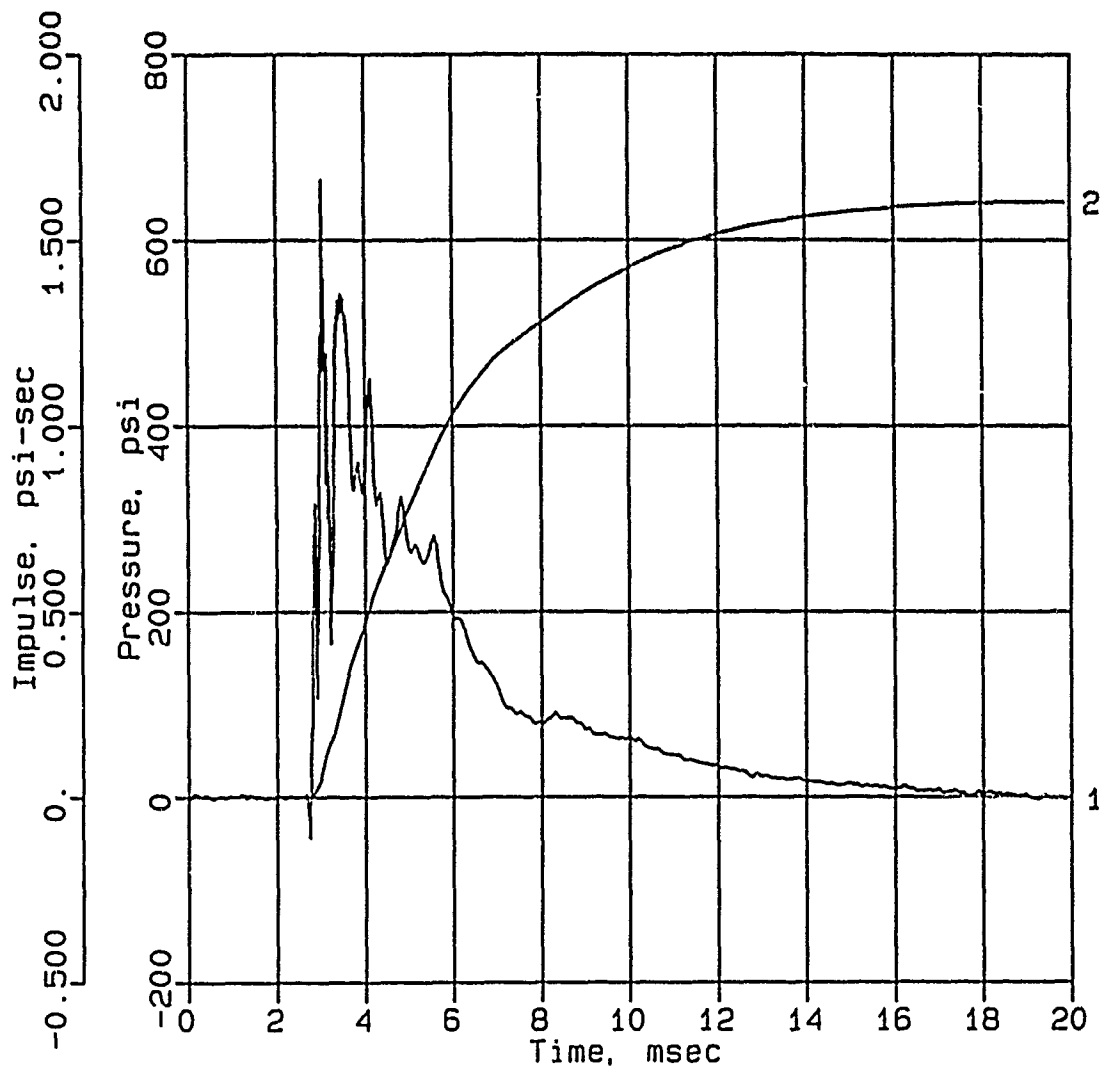Calibration: 1933
Filtering: 20 kHz low pass filter
          5 - 17 kHz band rejection filter

A9

CONWEB T1
AHS-0-S

Digitizing rate: 200,000 Hz
Calibration: 5376
Constant Baseline Shift

A10
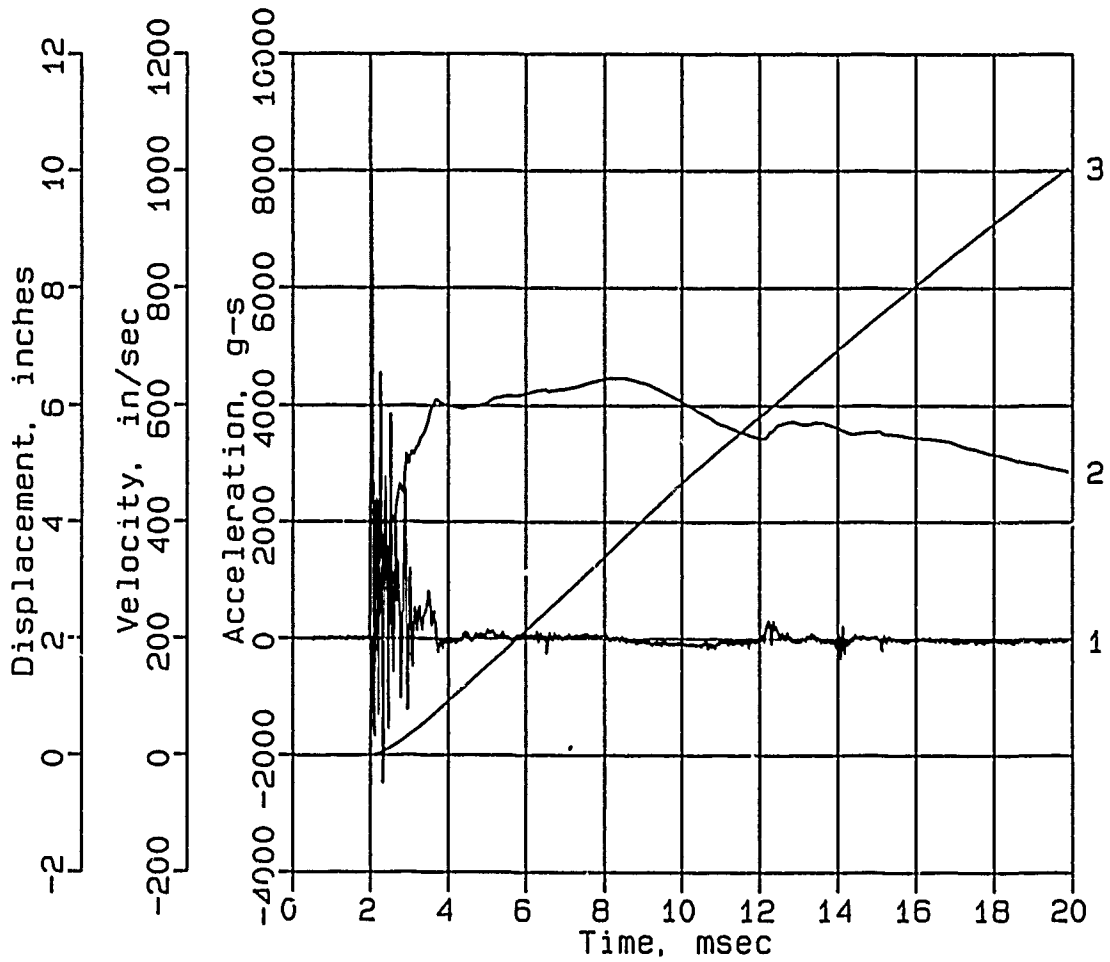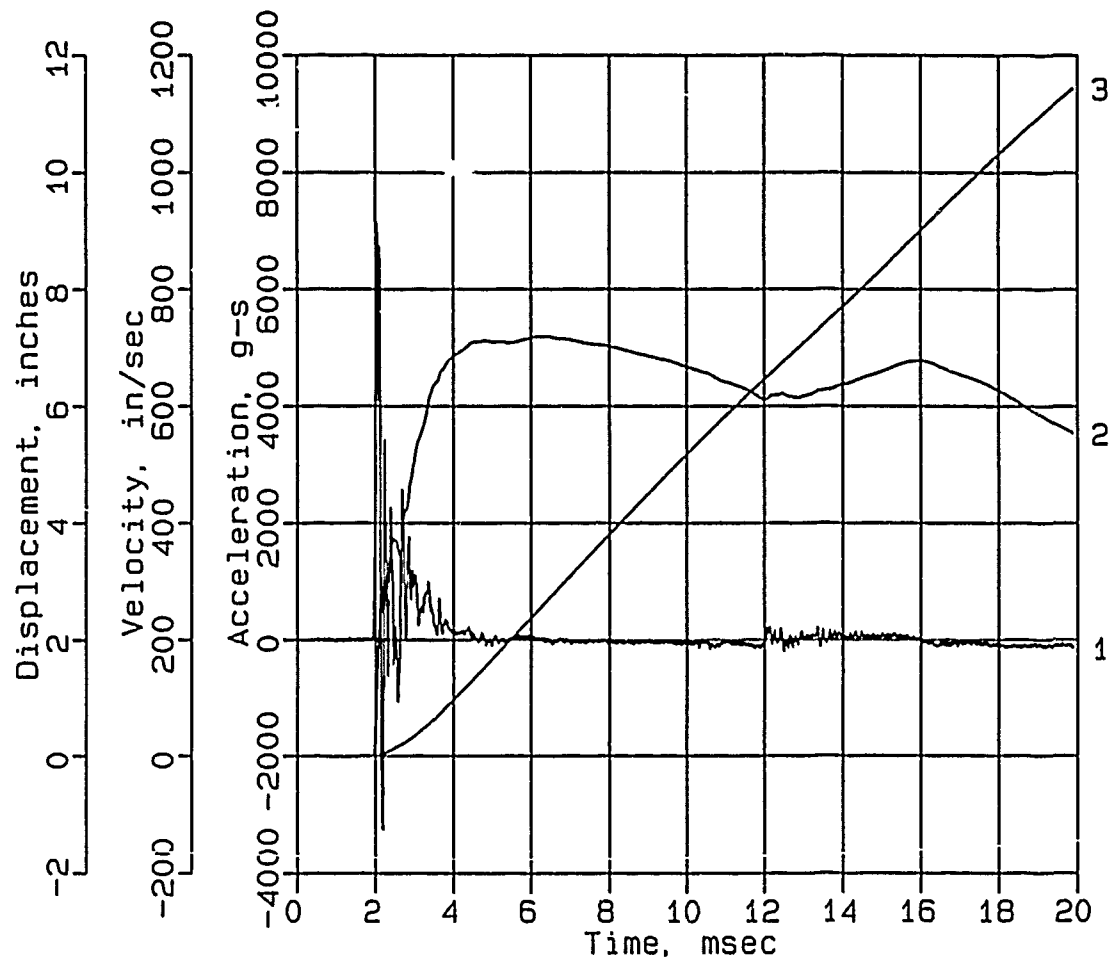
CONWEB T1
AHS-1

Digitizing rate: 200,000 Hz
Calibration: 5712
Constant Baseline Shift

CONWEB T1
AHS-2-S

Digitizing rate: 200,000 Hz
Calibration: 5275
Constant Baseline Shift

A12
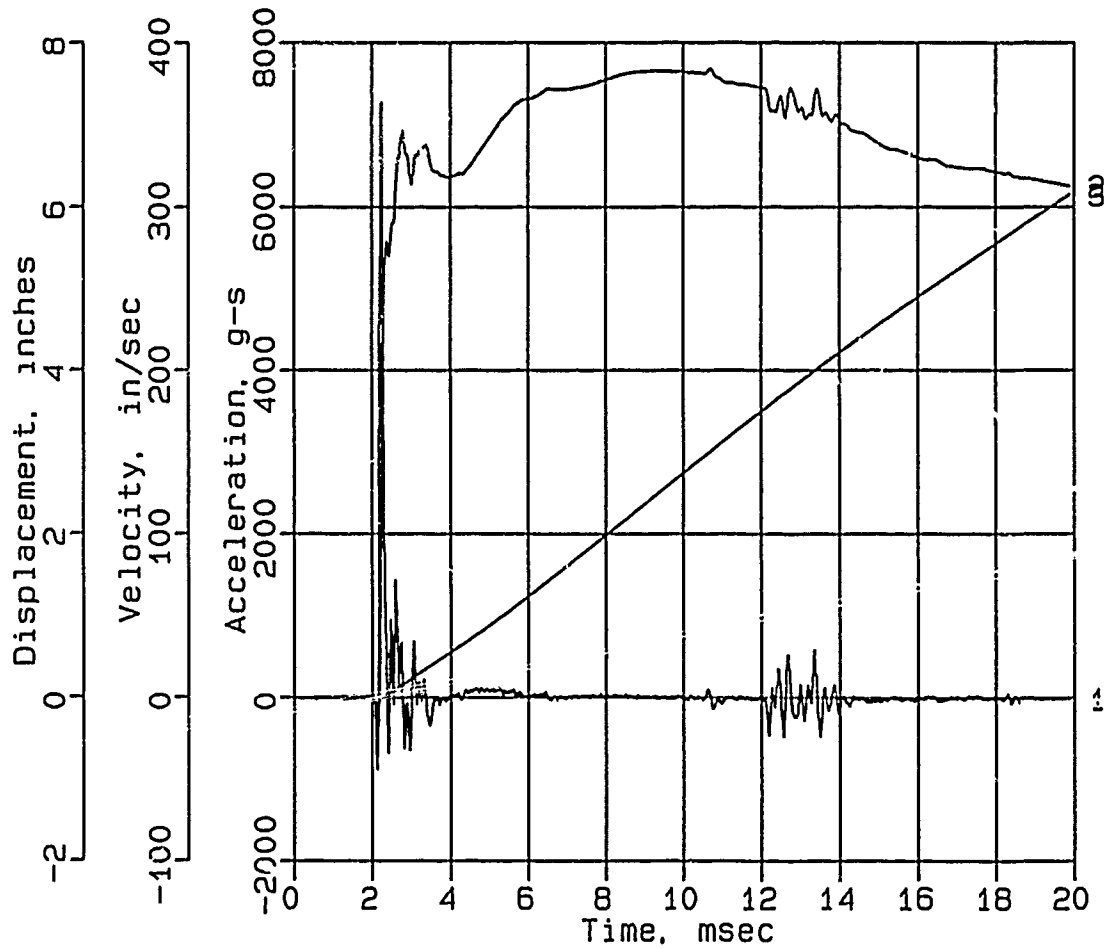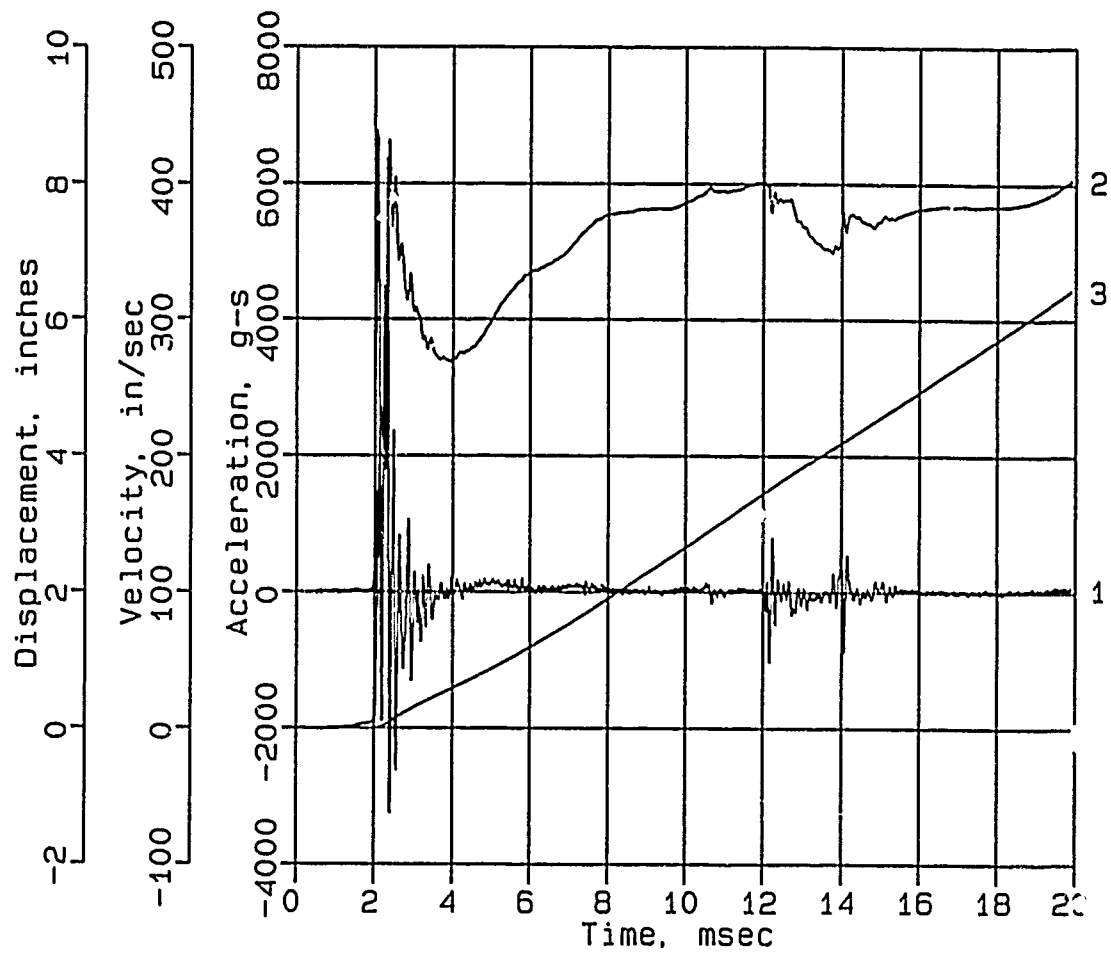
CONWEB T1
AHS-3

Digitizing rate: 200,000 Hz
Calibration: 5702
Constant Baseline Shift

A13

CONWEB T1
AHS-5

Digitizing rate; 200,000 Hz
Calibration: 5055
Constant Baseline Shift

A14
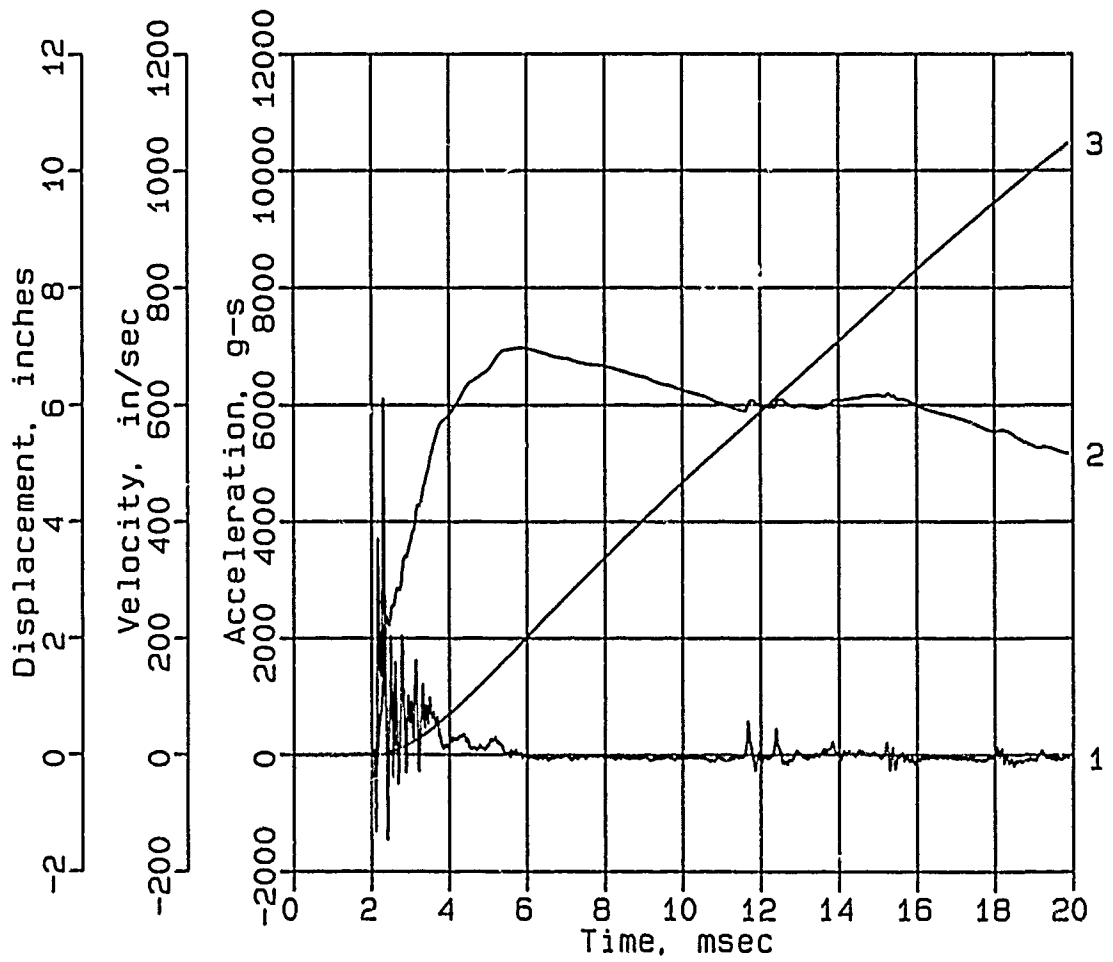
CONWEB T1
AHS-6

Digitizing rate: 200,000 Hz
Calibration: 1907
Constant Baseline Shift

A15
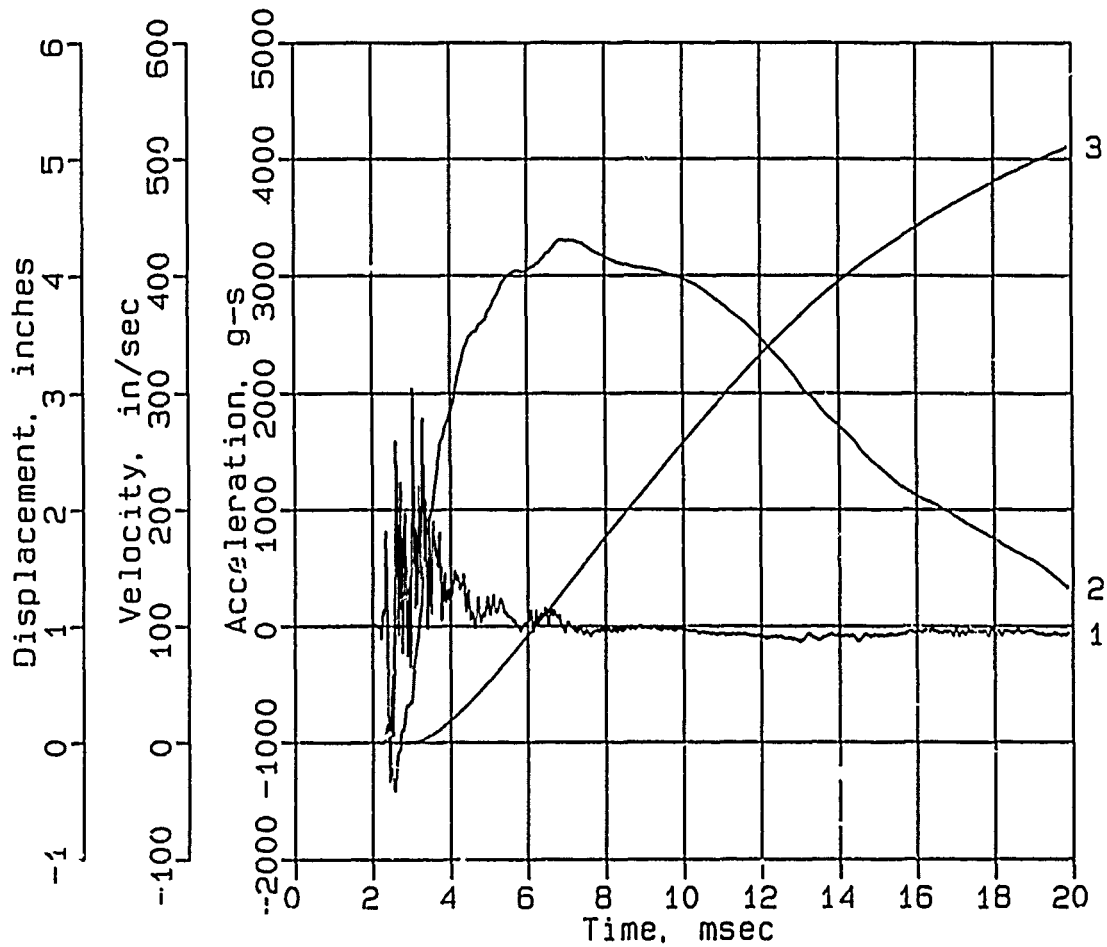
CONWEB T1
AHS-10

Digitizing rate: 200,000 Hz
Calibration: 871
Constant Baseline Shift

A16
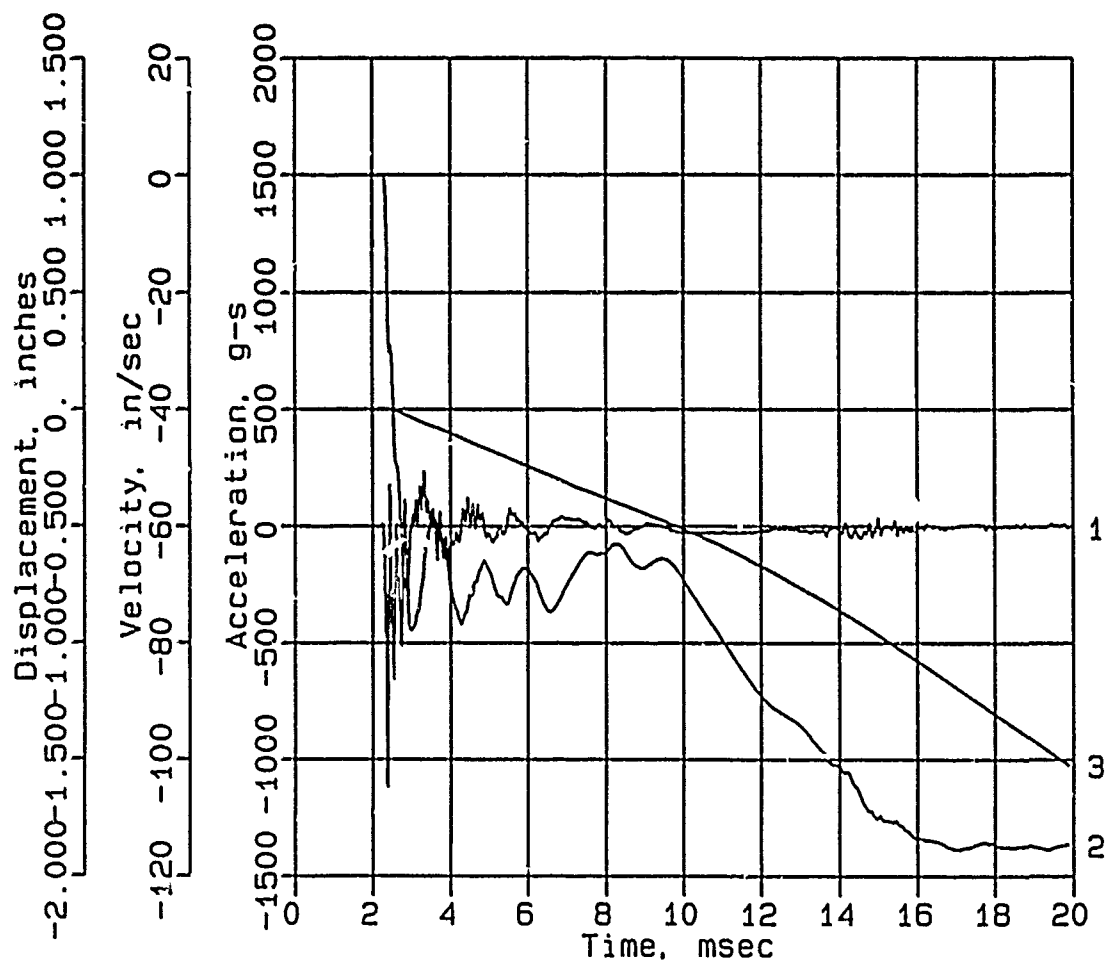
CONWEB T1
AHS-11

Digitizing rate: 200,000 Hz
Calibration: 1059
Constant Baseline Shift

A17
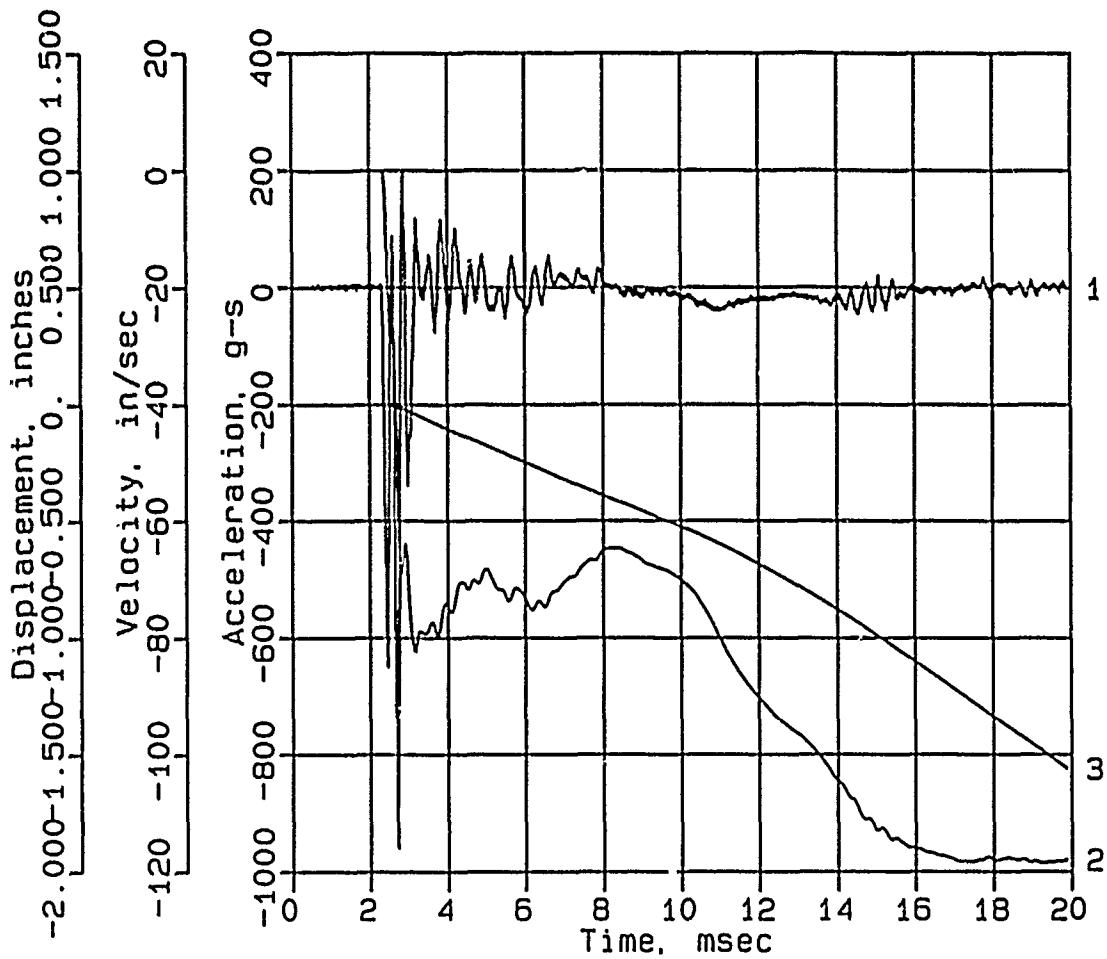
CONWEB T1
AVS-10

Digitizing rate: 200,000 Hz
Calibration: 942
Constant Baseline Shift

A18

CONWEB T1

AVS-12

Displacement, inches: -0.200, 0., 0.200, 0.400, 0.600, 0.800

Velocity, in/sec: -40, -20, 0, 20, 40, 60

Acceleration, g-s: -1000, -500, 0, 500, 1000, 1500

Time, msec: 0, 2, 4, 6, 8, 10, 12, 14, 16, 18, 20

Digitizing rate: 200,000 Hz
Calibration: 1062
Constant Baseline Shift

A19
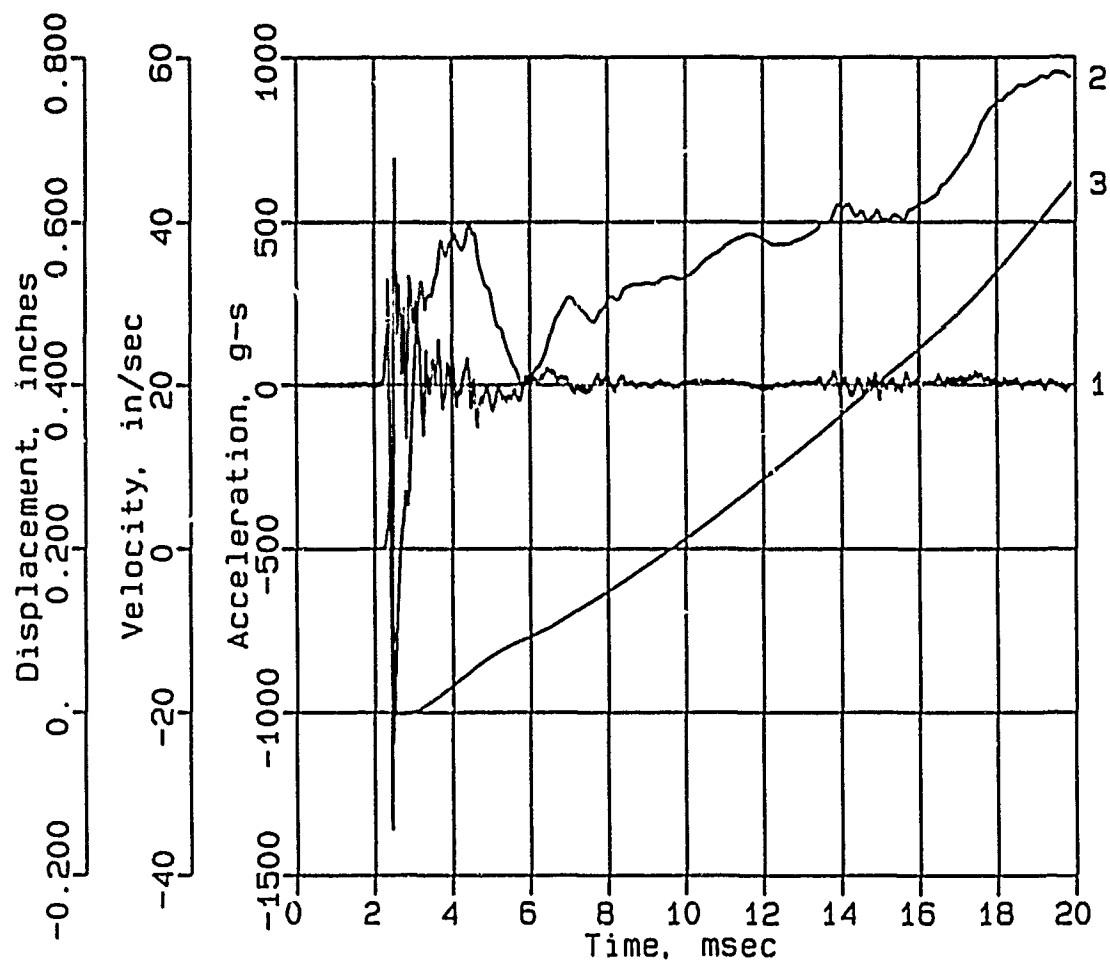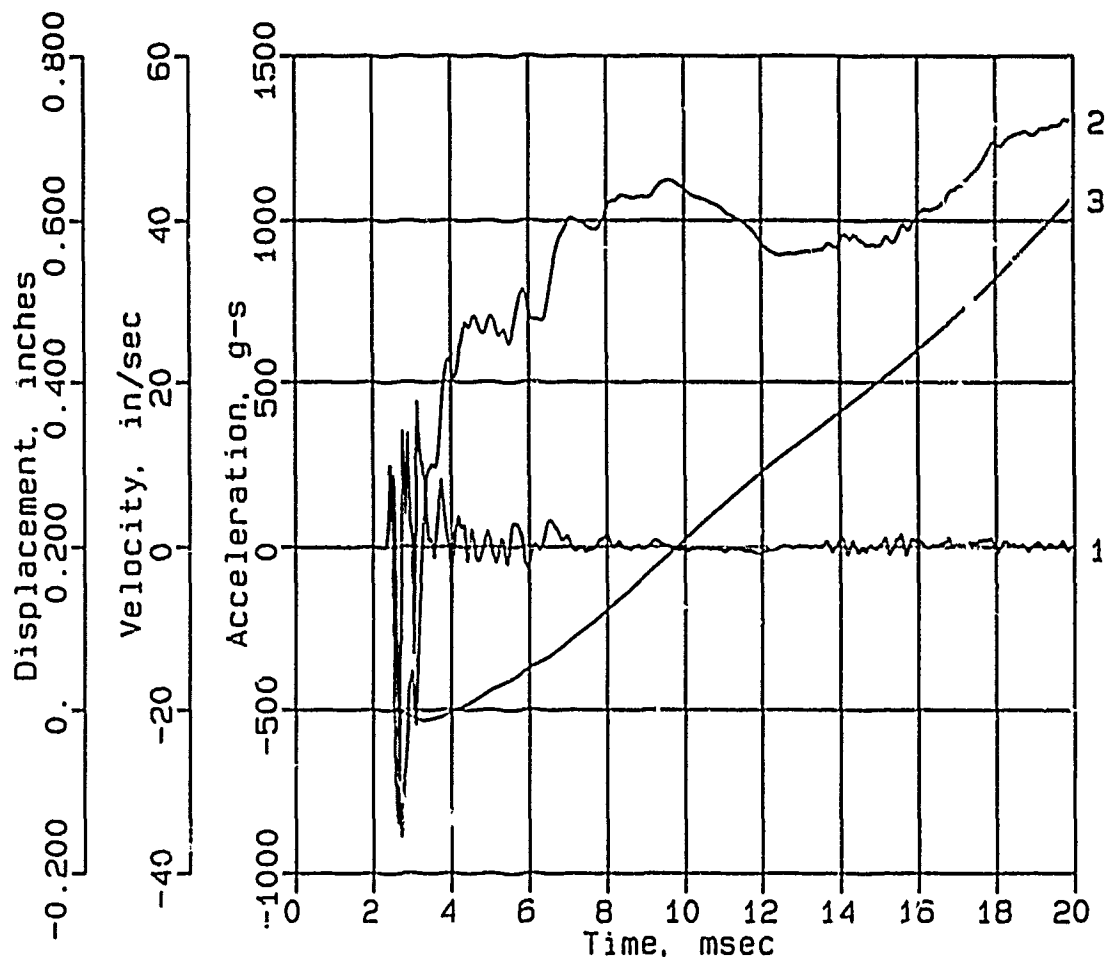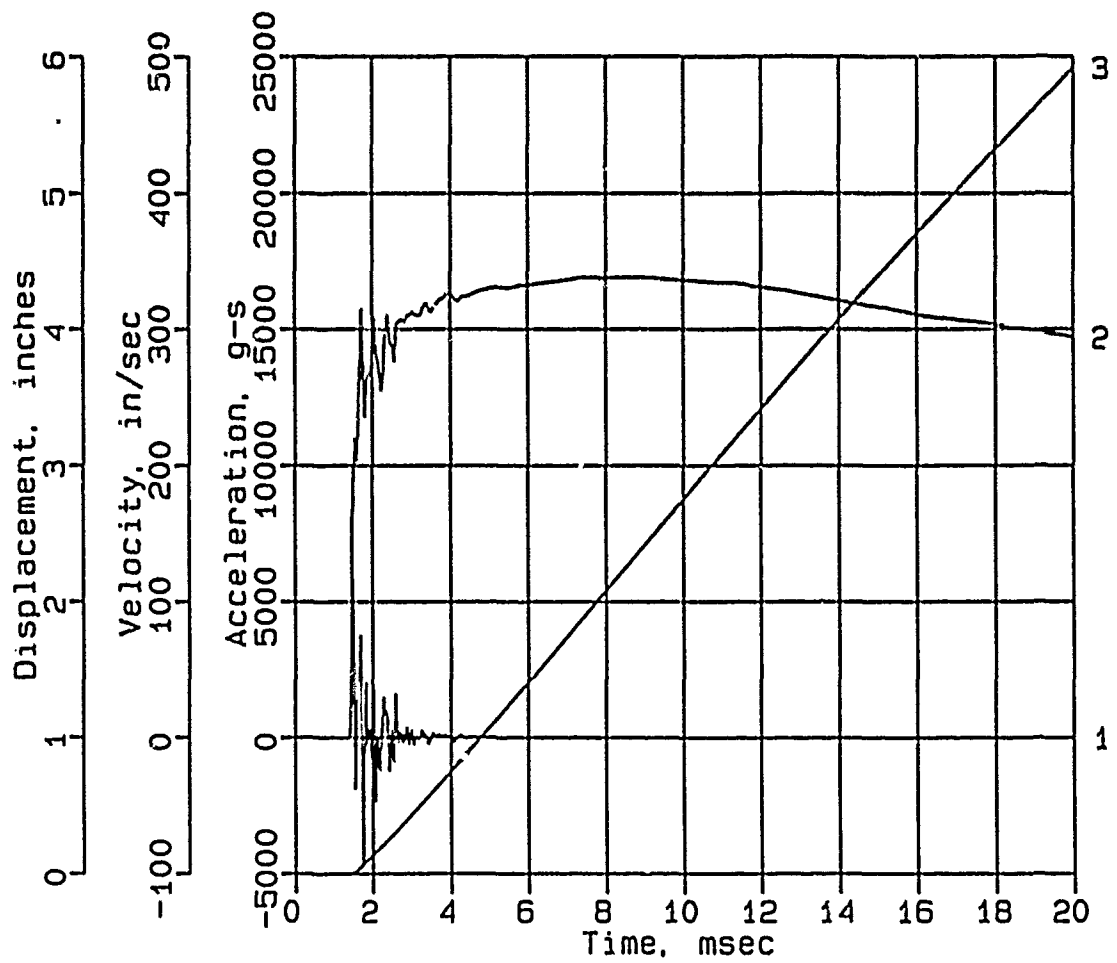
CONWEB T1
AHF-1

Digitizing rate: 200,000 Hz
Calibration: 5293
Constant Baseline Shift

CONWEB T1
AHF-3
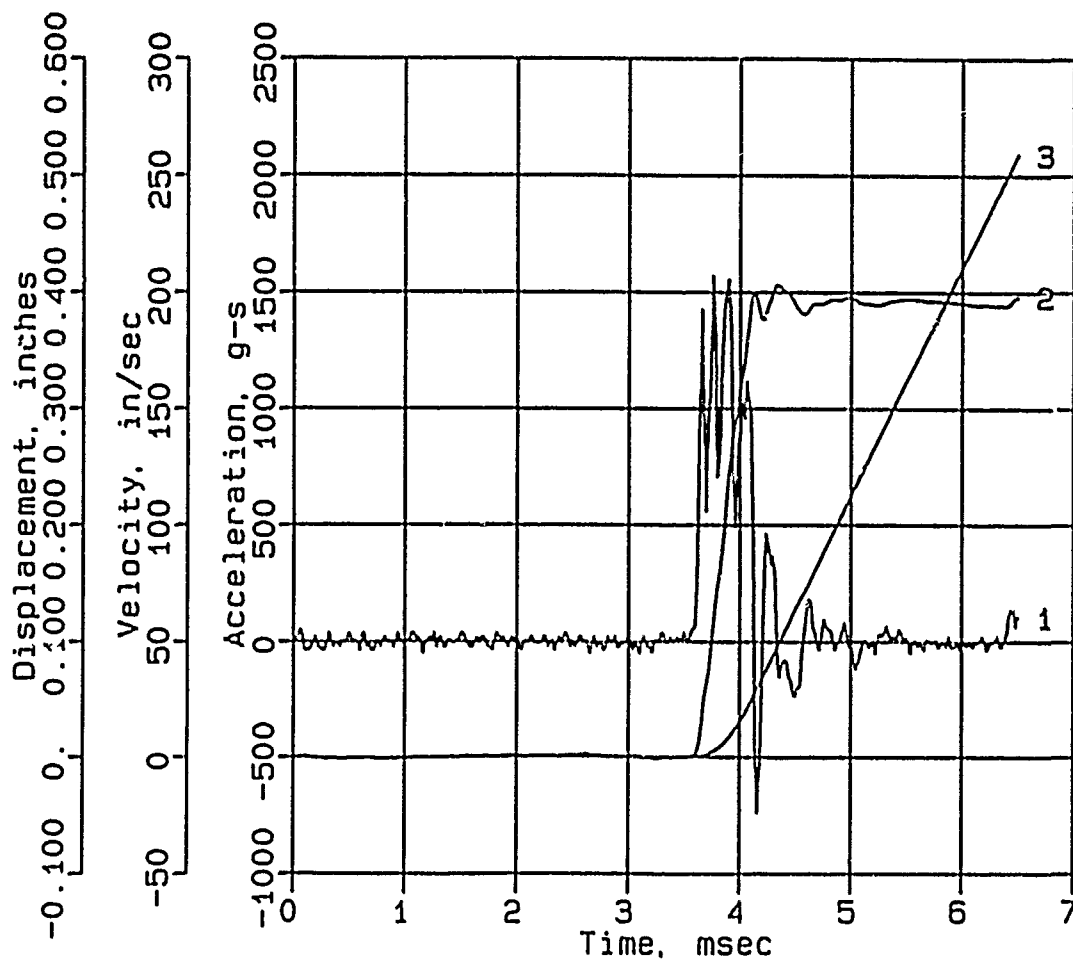
Digitizing rate: 200,000 Hz
Calibration: 10911
Constant Baseline Shift

A21

CONWEB T1

AHF-4
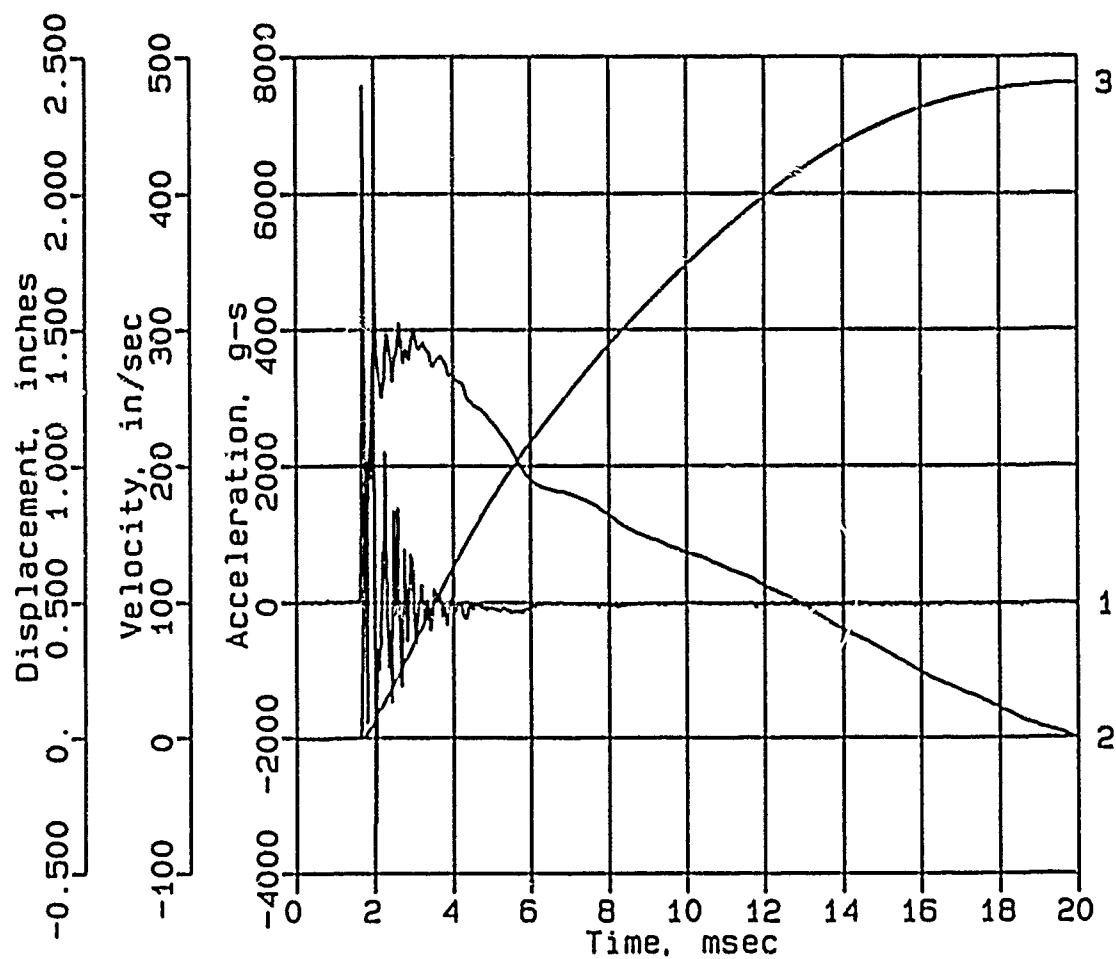
Digitizing rate: 200,000 Hz
Calibration: 11176
Constant Baseline Shift

A22
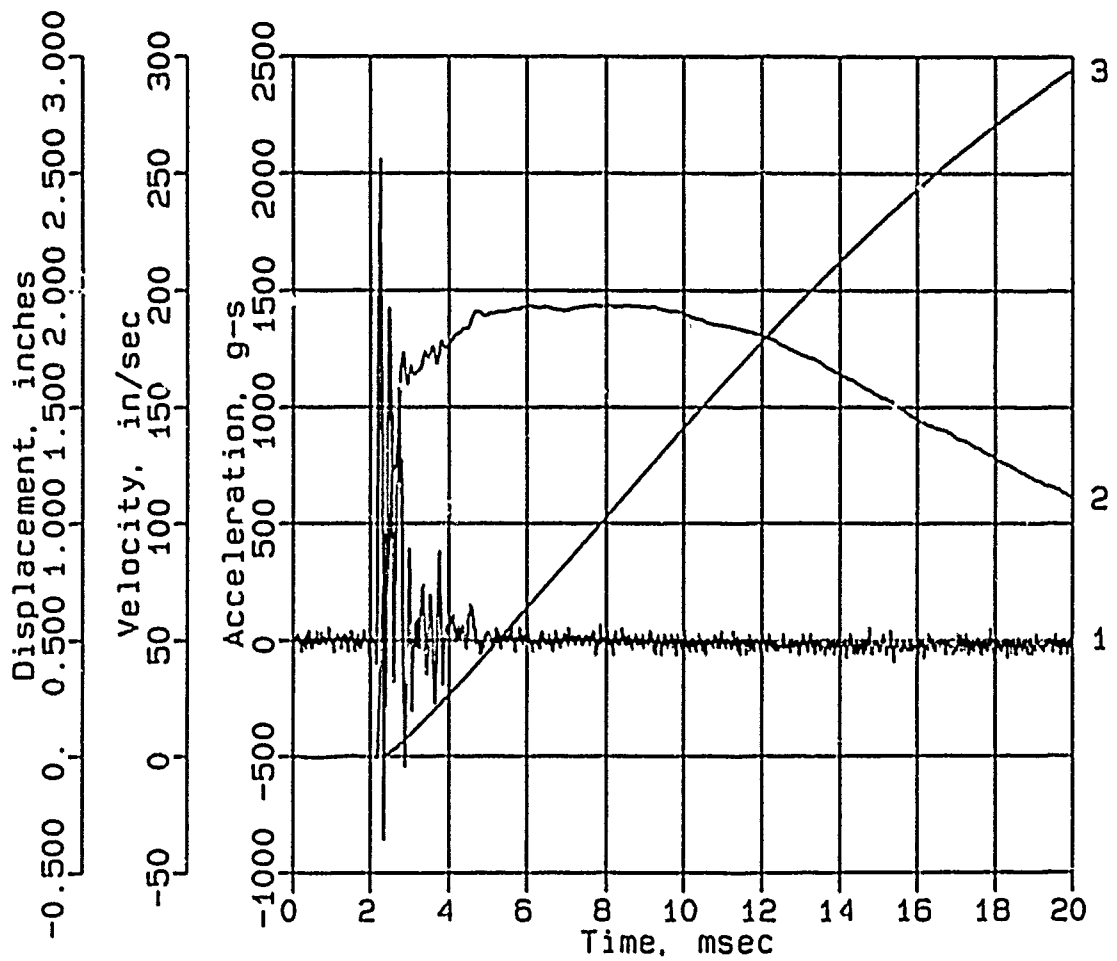
CONWEB T1
AHF-6

Digitizing rate: 200,000 Hz
Calibration: 10454
Constant Baseline Shift

A23

CONWEB T1

AHF-7
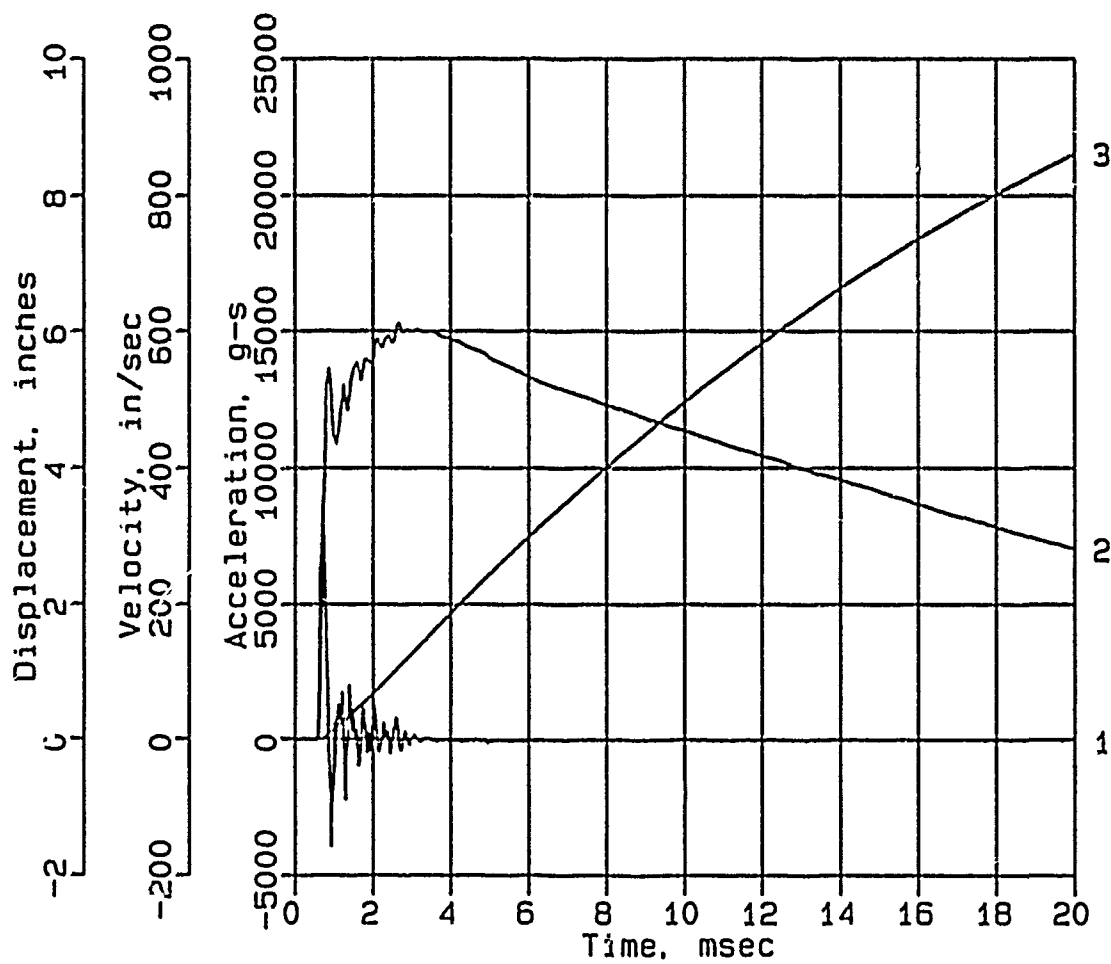
Digitizing rate: 200,000 Hz
Calibration: 10271.
Constant Baseline Shift

CONWEB T1
AHF-8
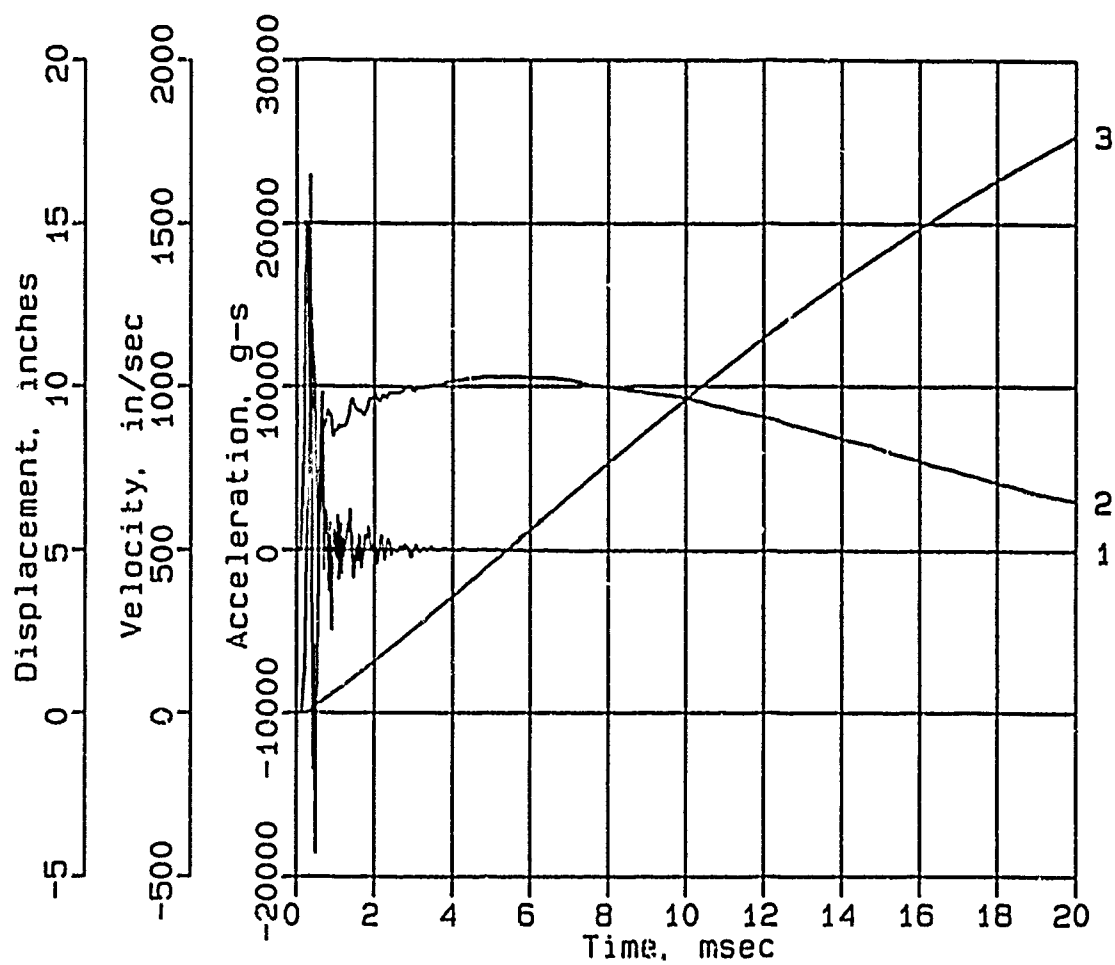
Digitizing rate: 200,000 Hz
Calibration: 24286
Constant Baseline Shift

CONWEB T1
AHF-9
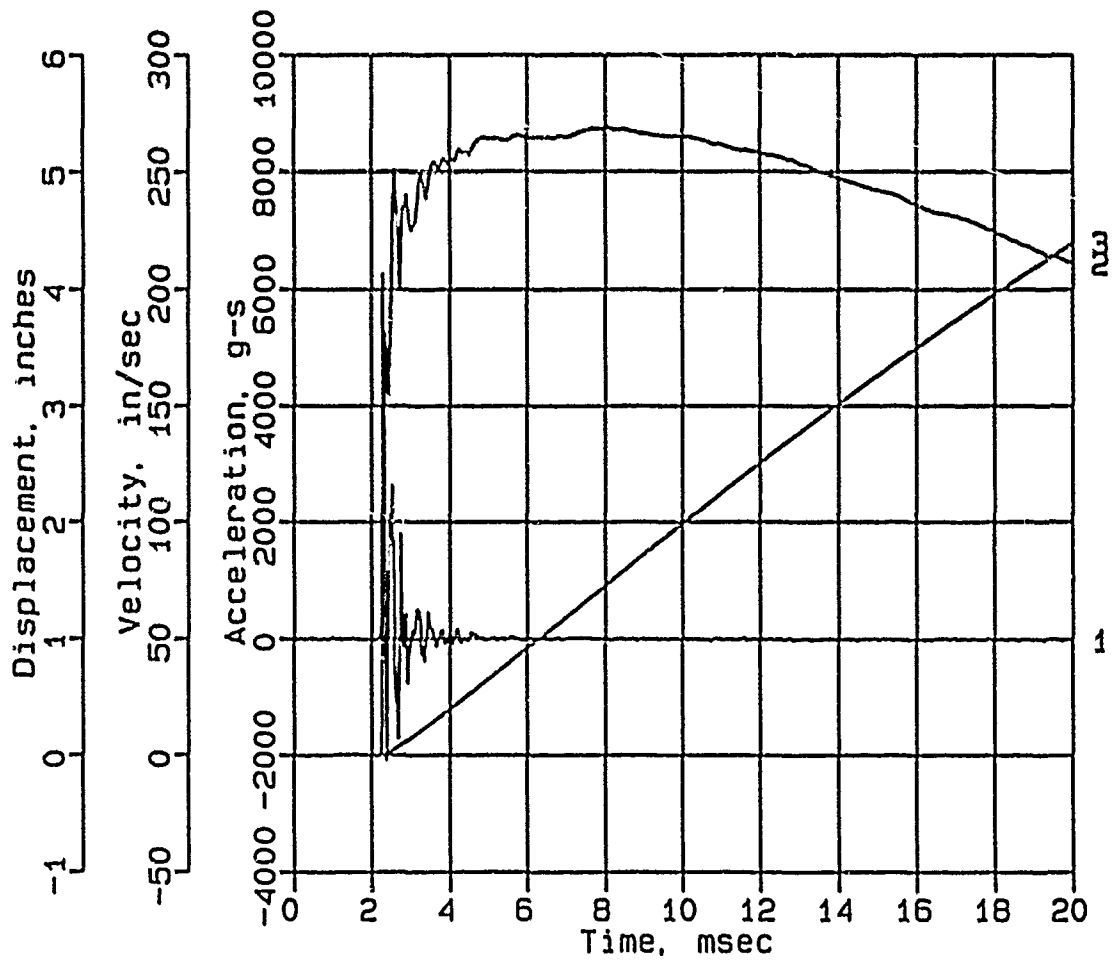
Digitizing rate: 200,000 Hz
Calibration: 11735
Constant Baseline Shift

CONWEB T1
AHF-10

Digitizing rate: 200,000 Hz
Calibration: 5928
Constant Baseline Shift

A27
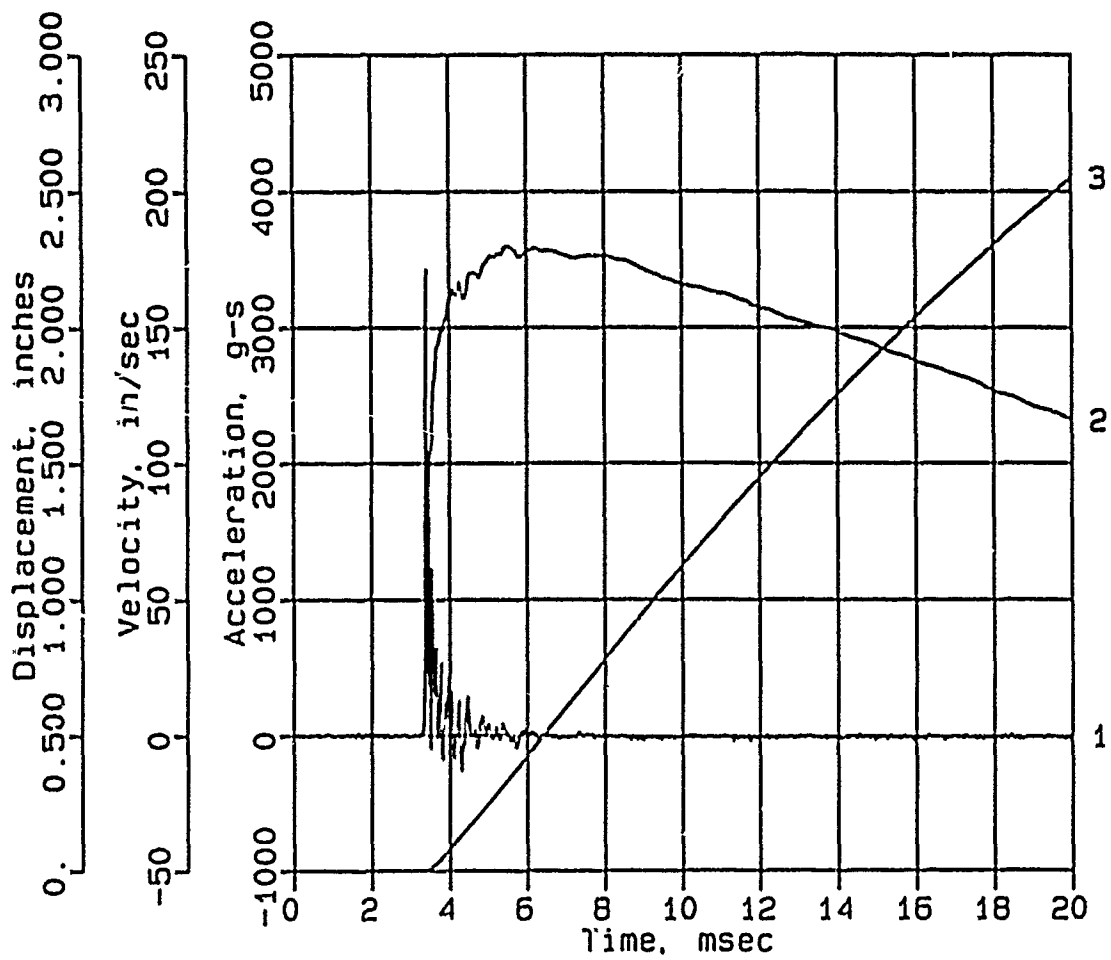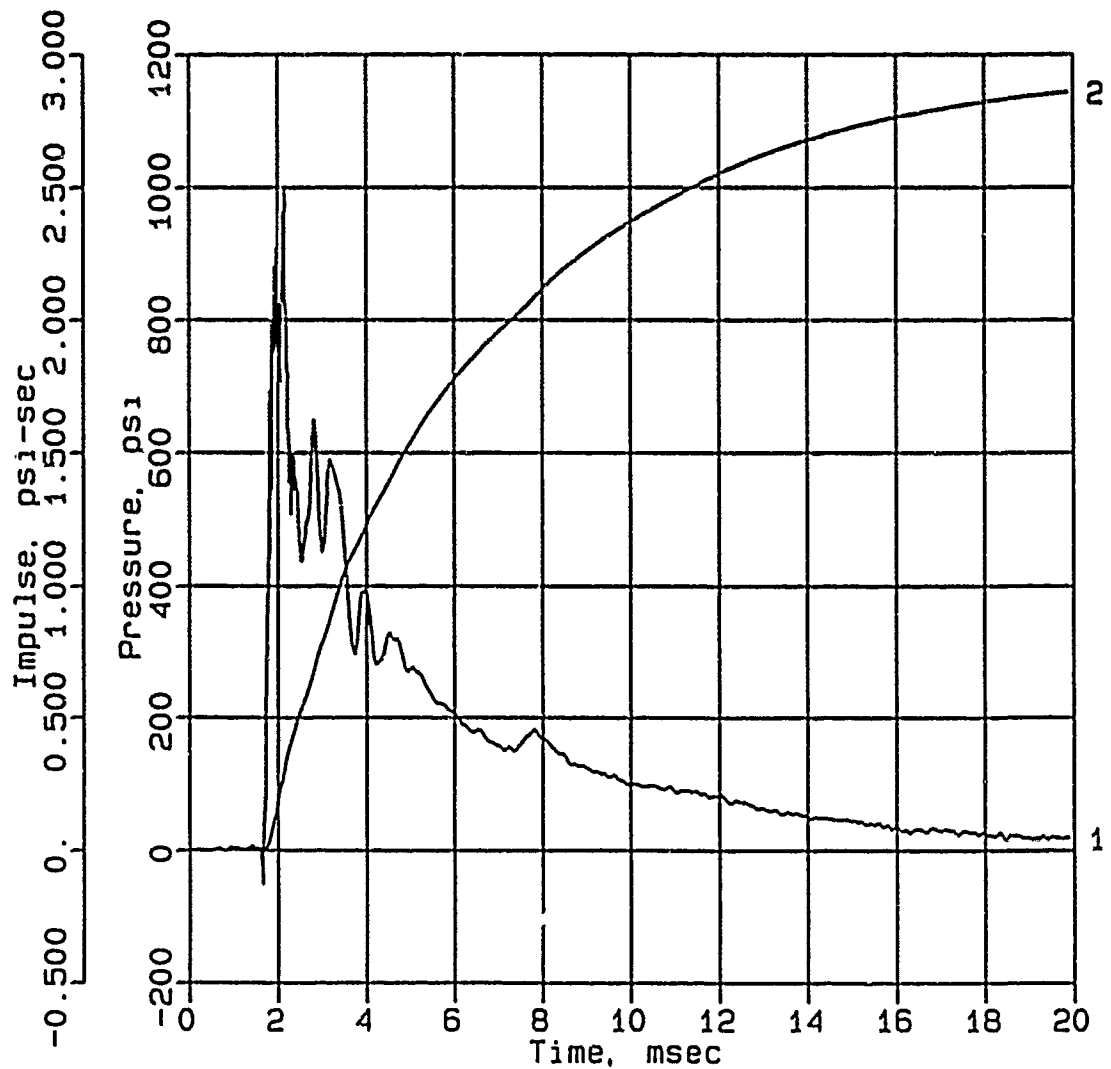
CONWEB T1
SE-1

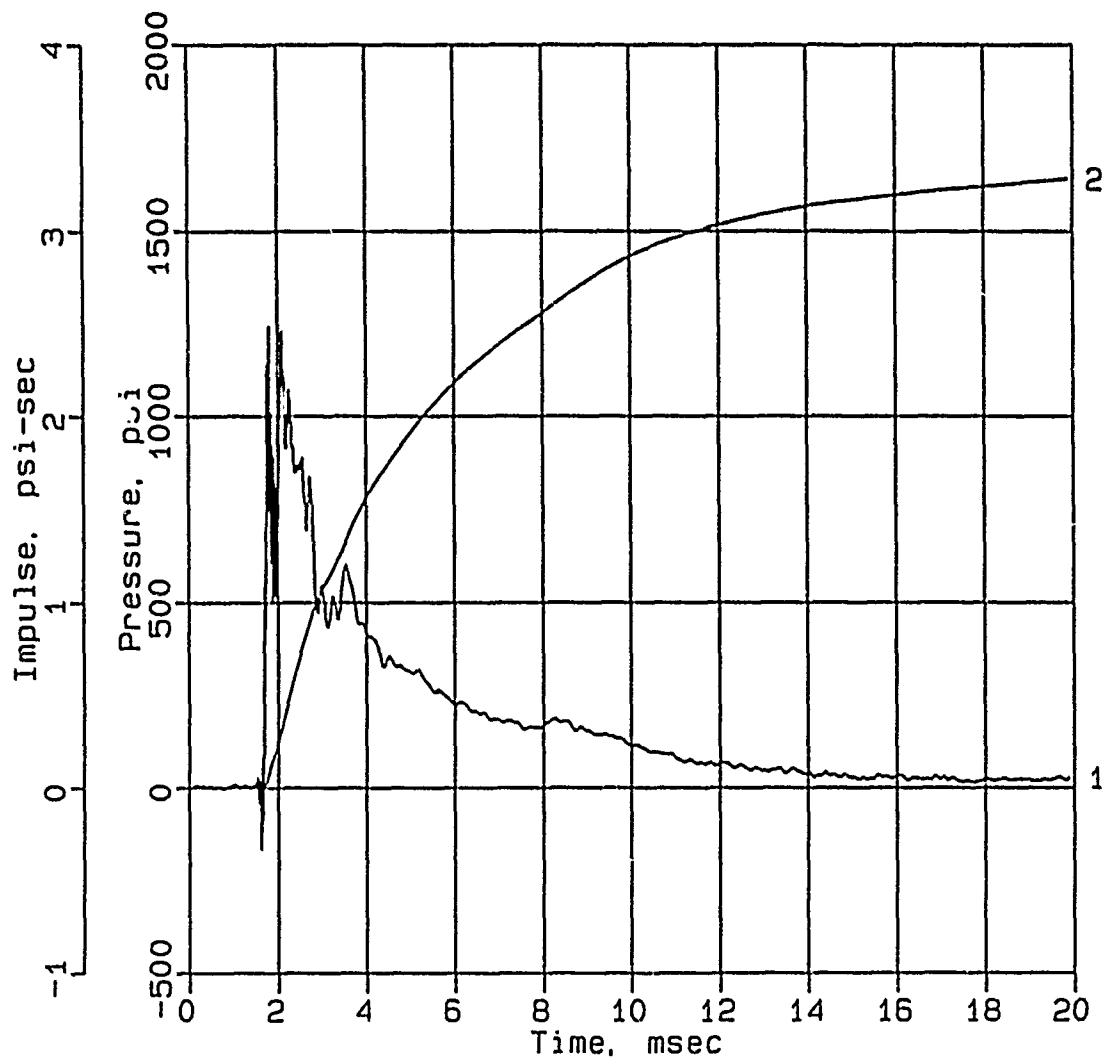Digitizing rate: 200,000 Hz
Calibration: 4555
Filtering: 20 kHz low pass filter
        5 - 17 kHz band rejection filter
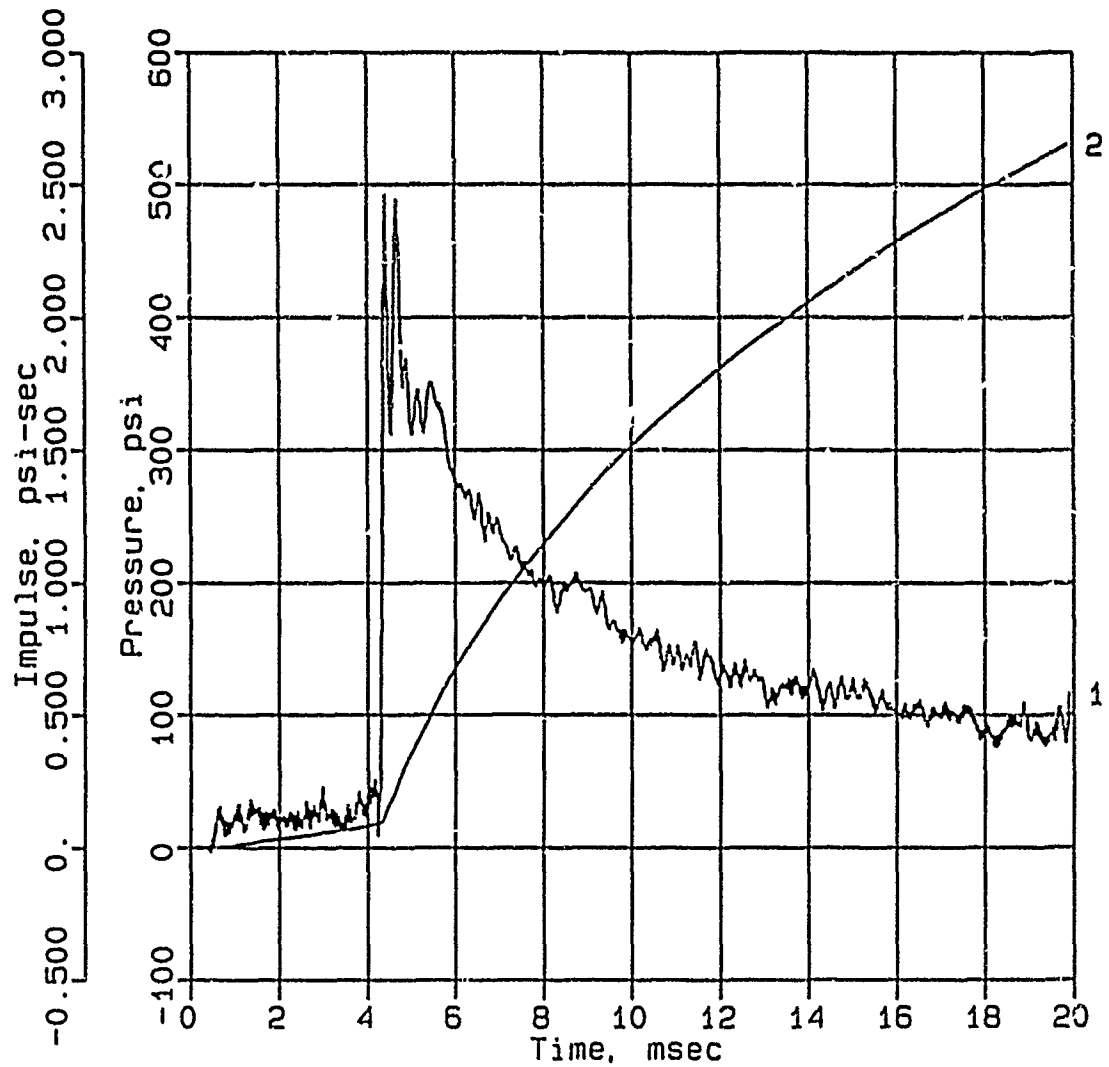
A28

CONWEB T1
SE-3

Digitizing rate: 200,000 Hz
Calibration: 10542
Filtering: 20 kHz low pass filter
            5 - 17 kHz band rejection filter

A29
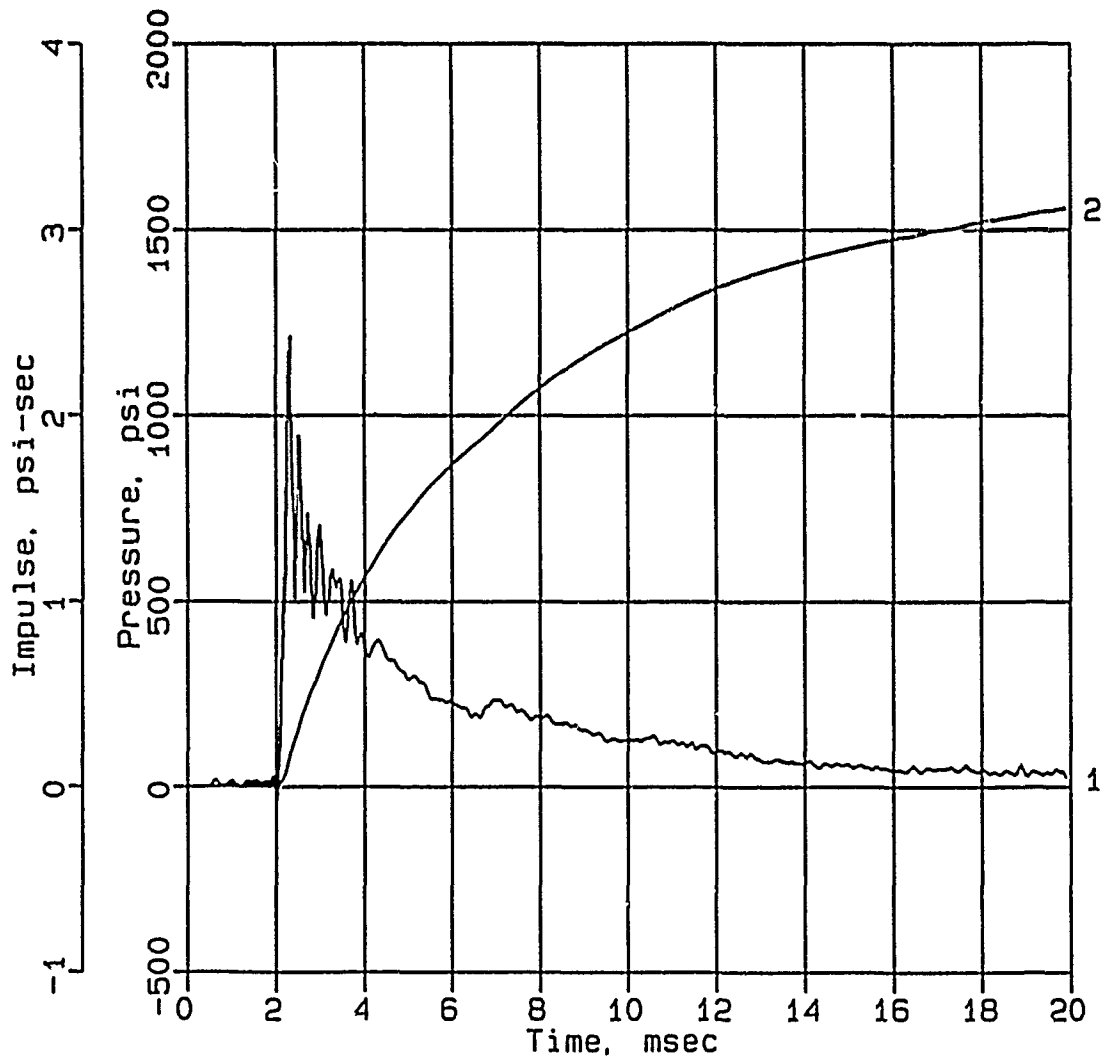
CONWEB T1
SE-4

Digitizing rate: 200,000 Hz
Calibration: 9466
Filtering: 20 kHz low pass filter
              5 - 17 kHz band rejection filter

A30
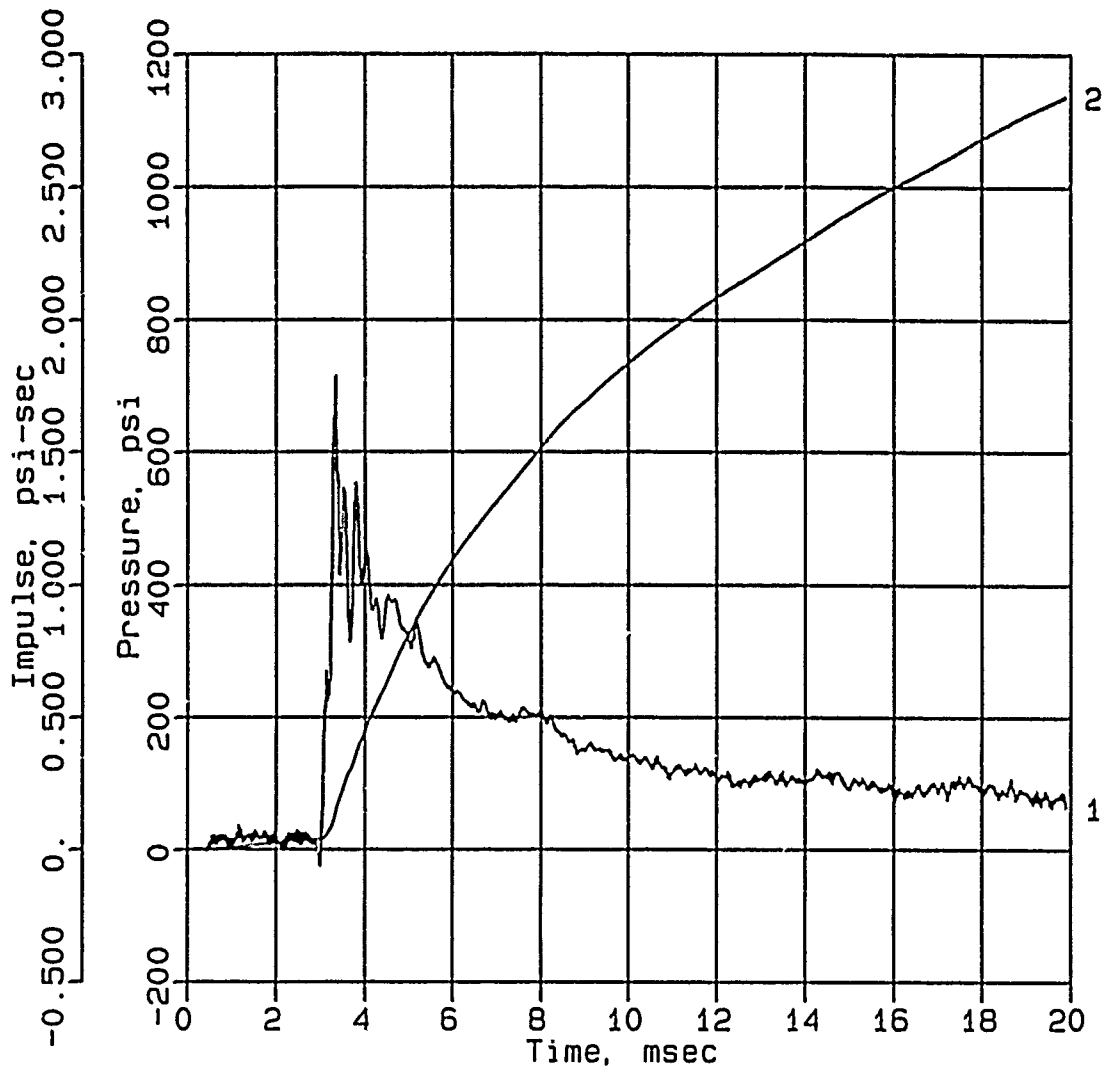
CONWEB T1
SE-6

Digitizing rate: 200,000 Hz
Calibration: 9880
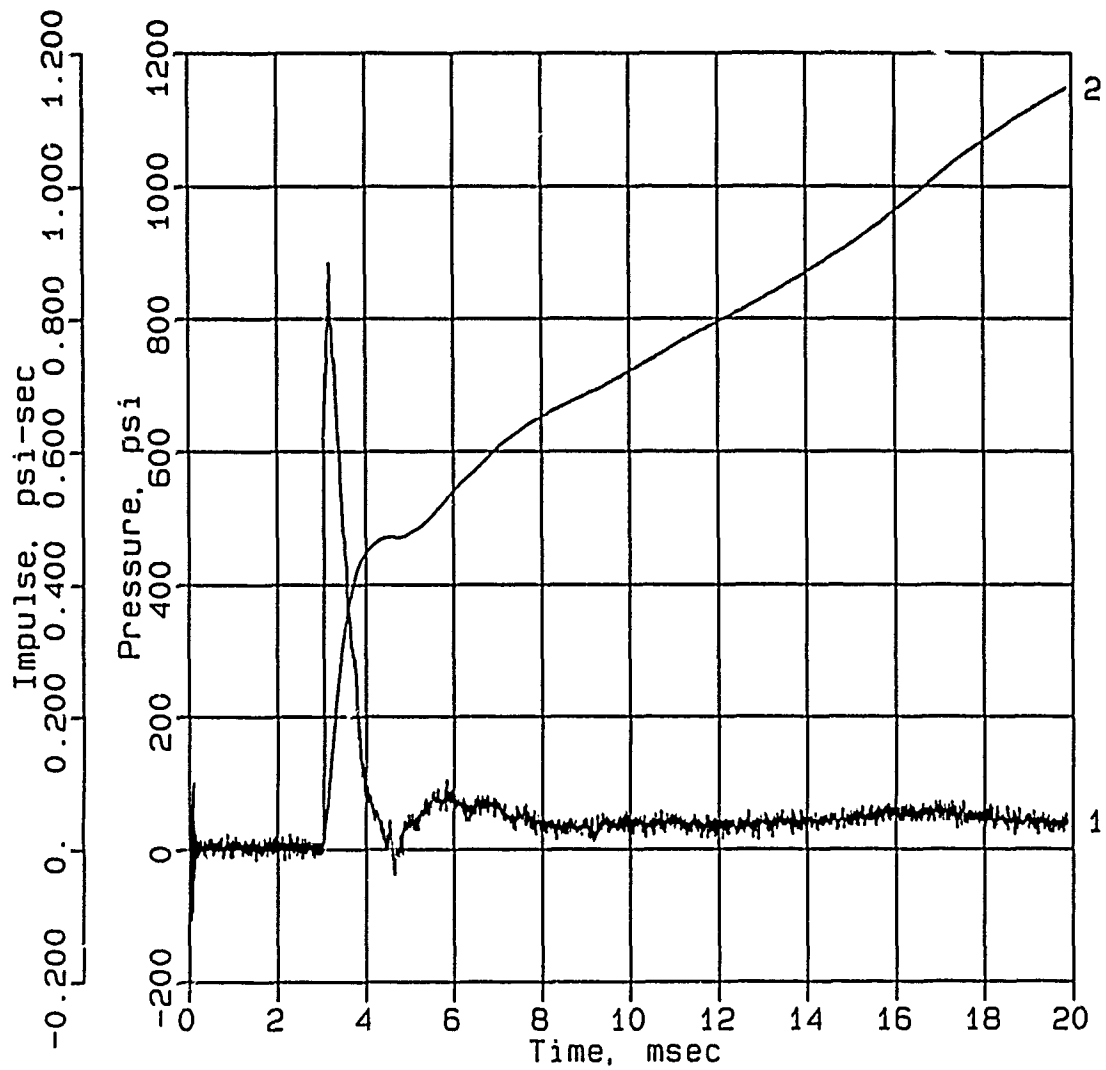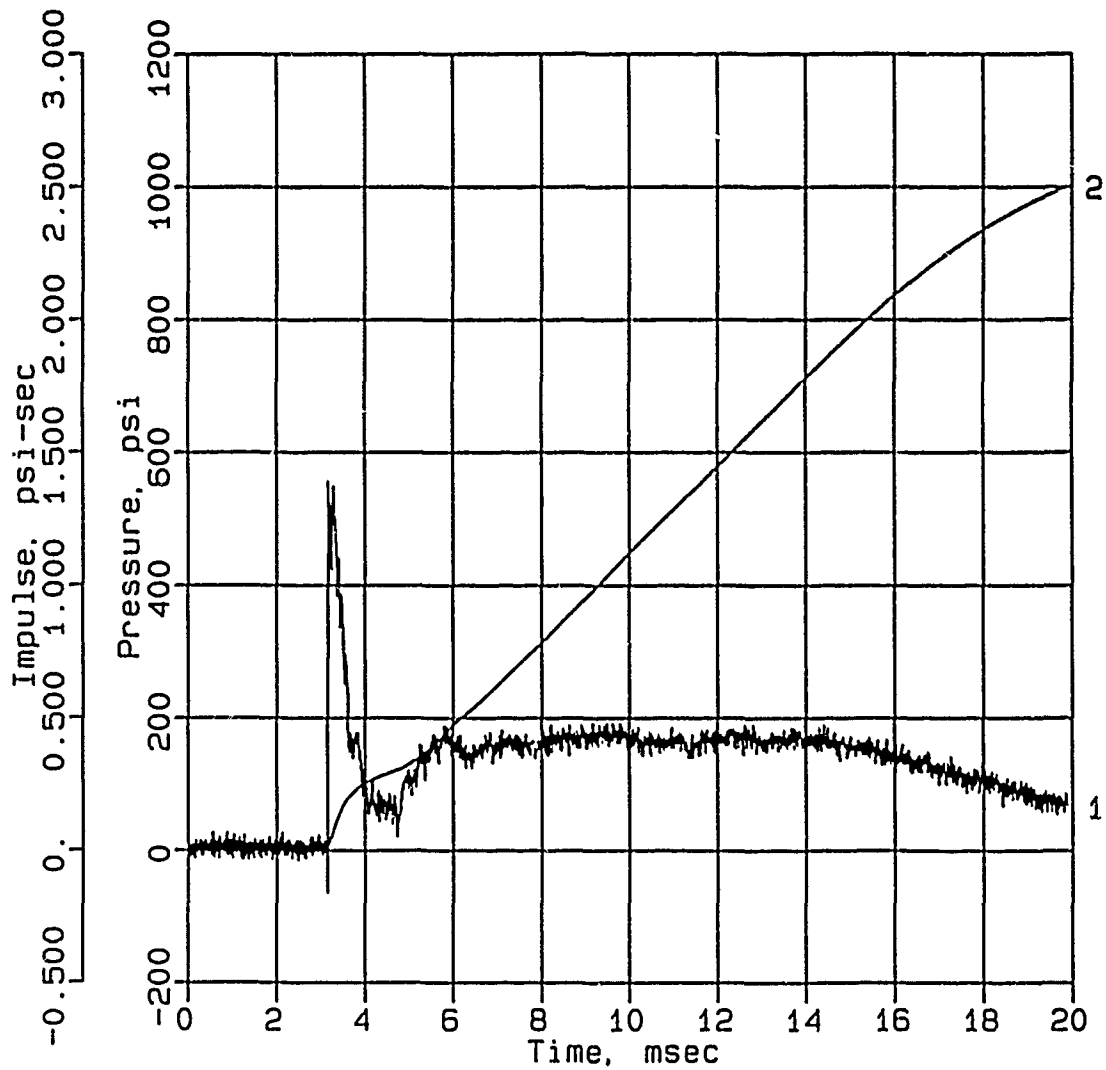Filtering: 20 kHz low pass filter
             5 - 17 kHz band rejection filter
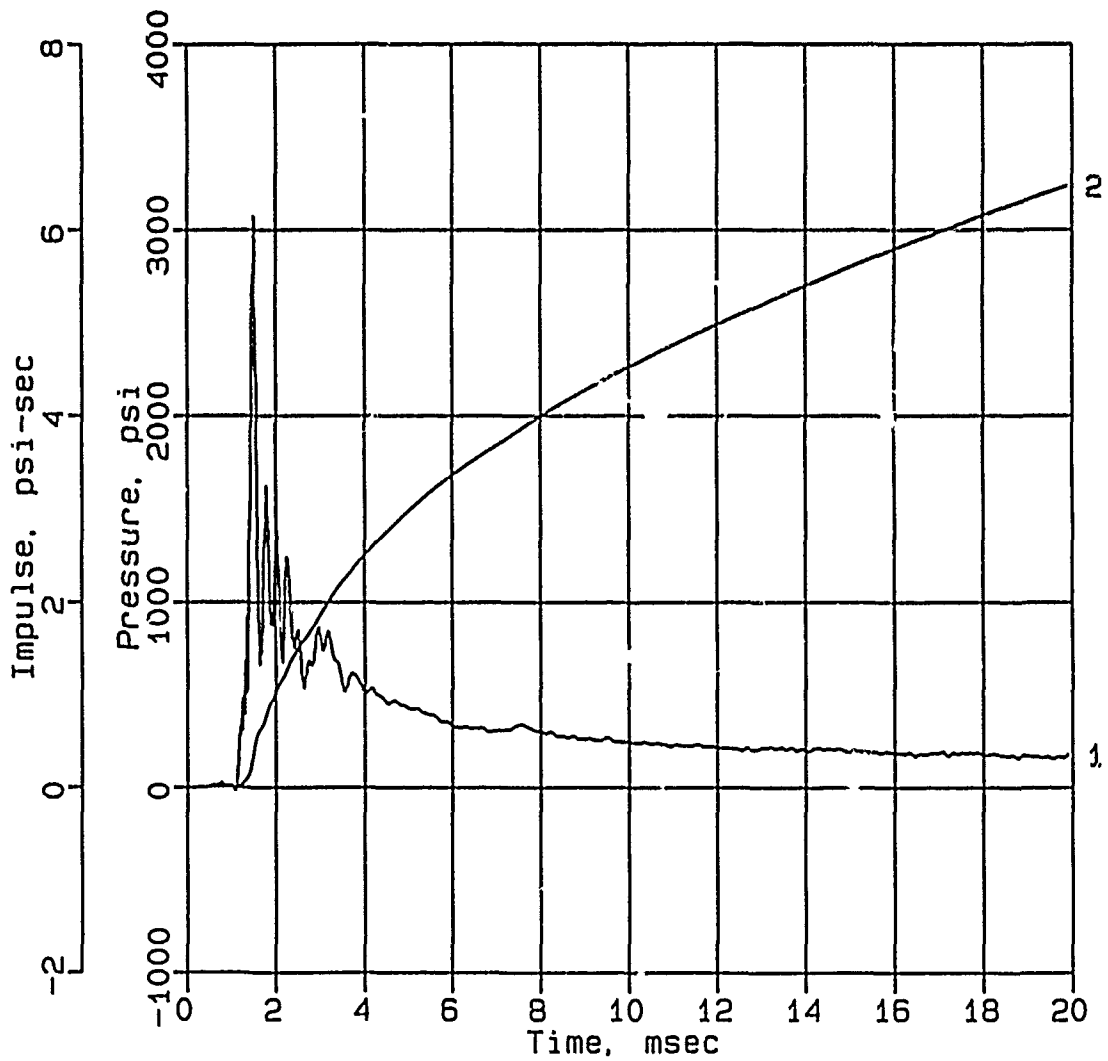
A31

CONWEB T1
SE-7

Digitizing rate: 200,000 Hz
Calibration: 10160
Filtering: 20 kHz low pass filter
5 - 17 kHz band rejection filter

CONWEB T1
SE-8
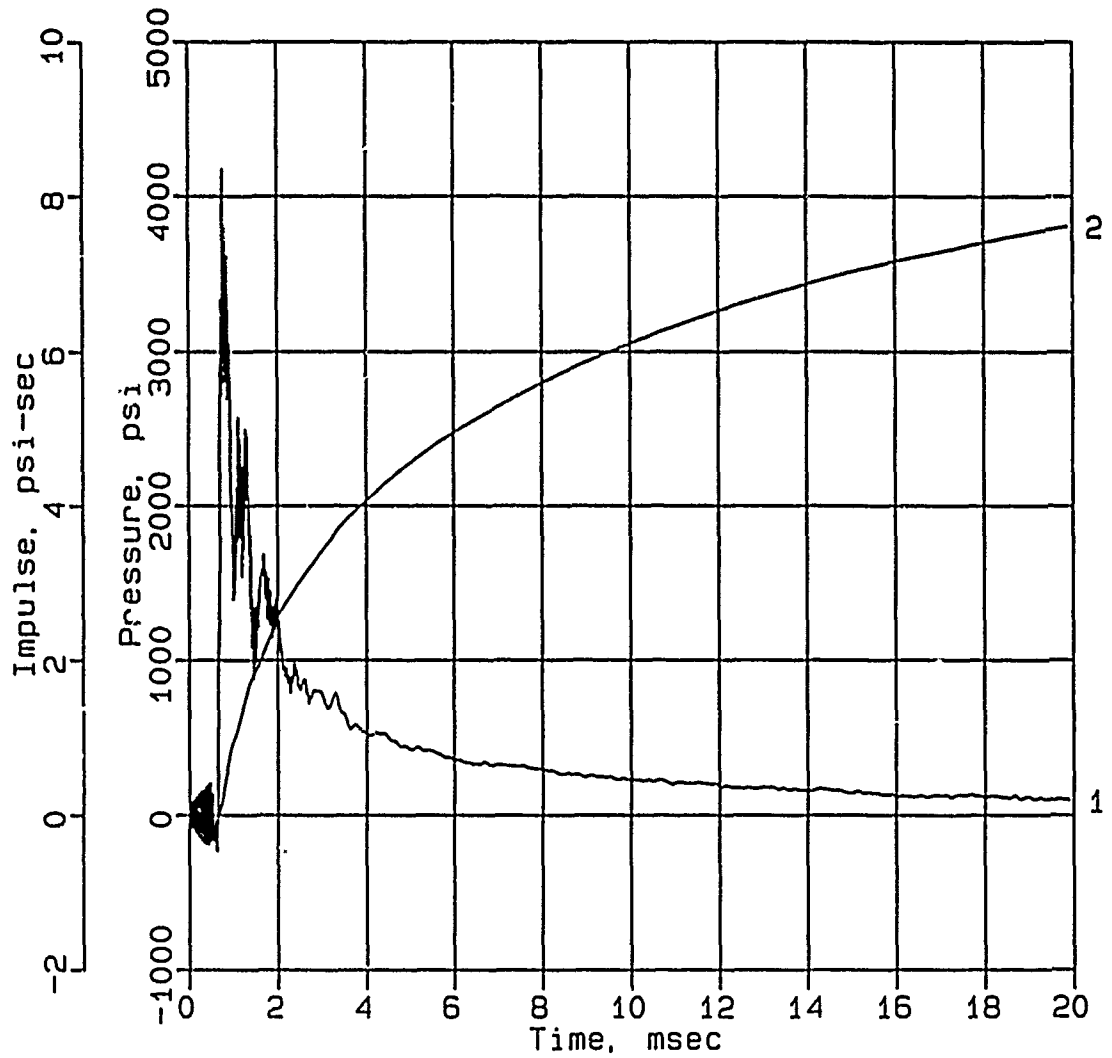
Digitizing rate: 200,000 Hz
Calibration: 9921
Filtering: 20 kHz low pass filter
            5 - 17 kHz band rejection filter
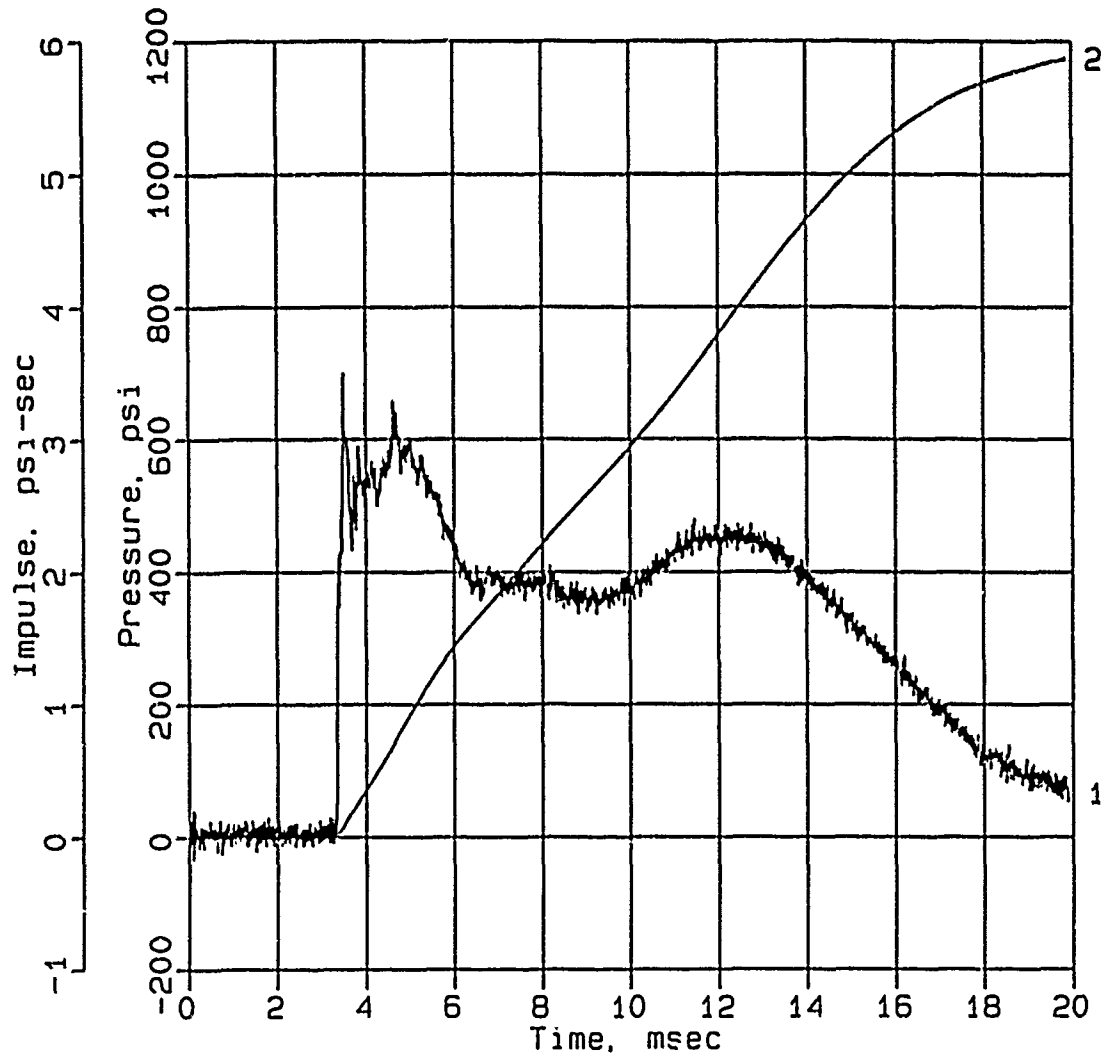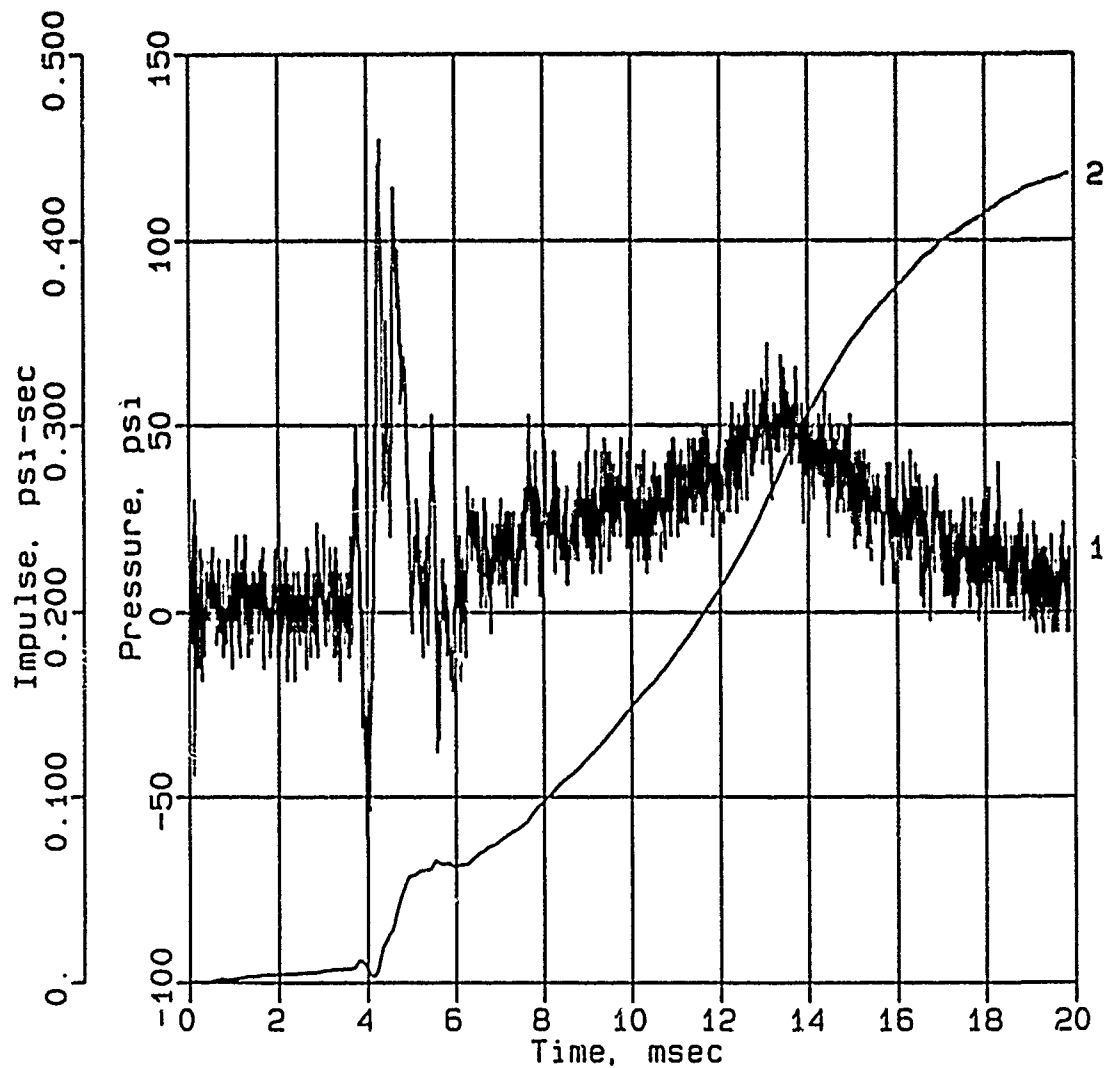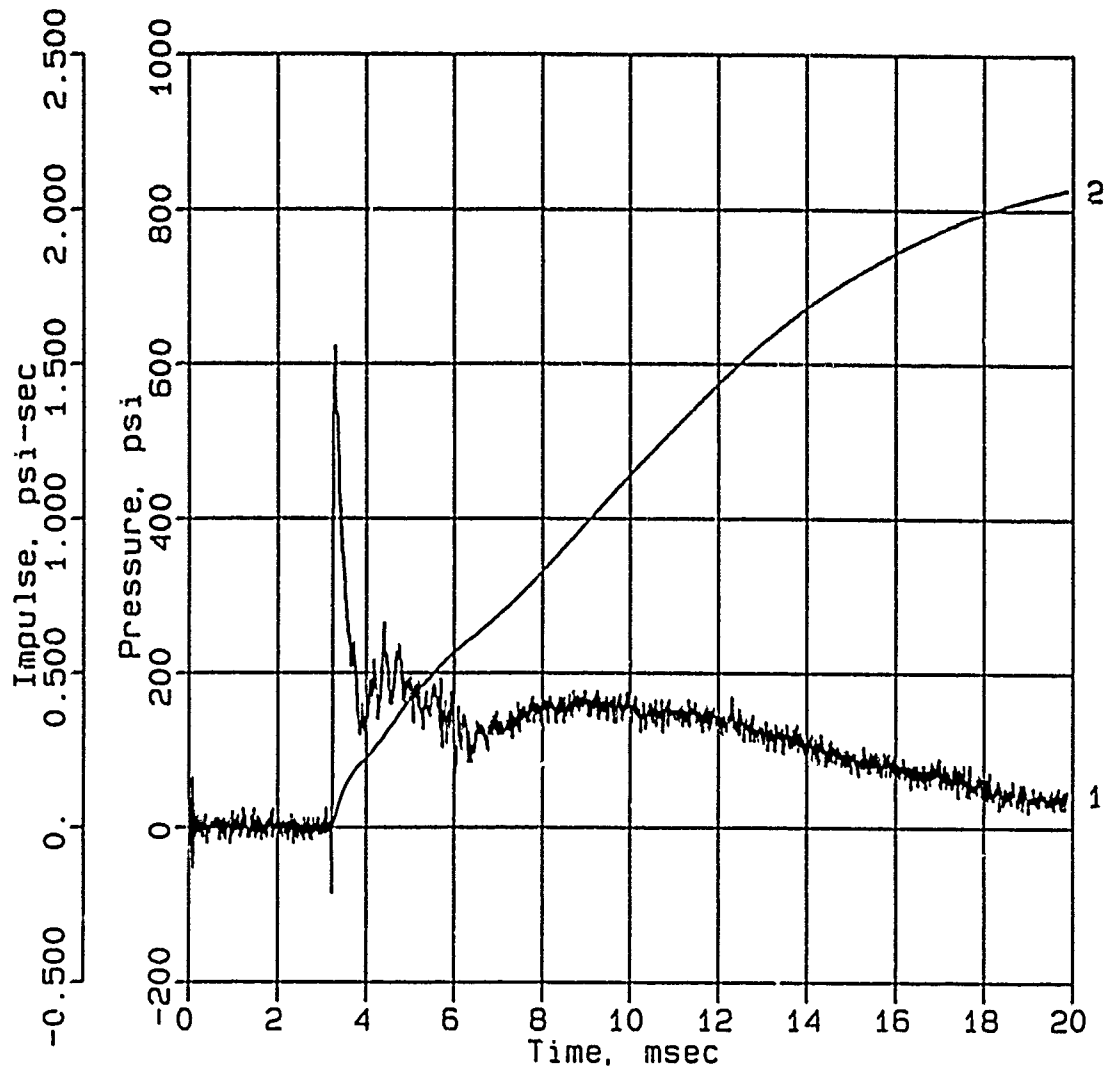
CONWEB T1
SE-9
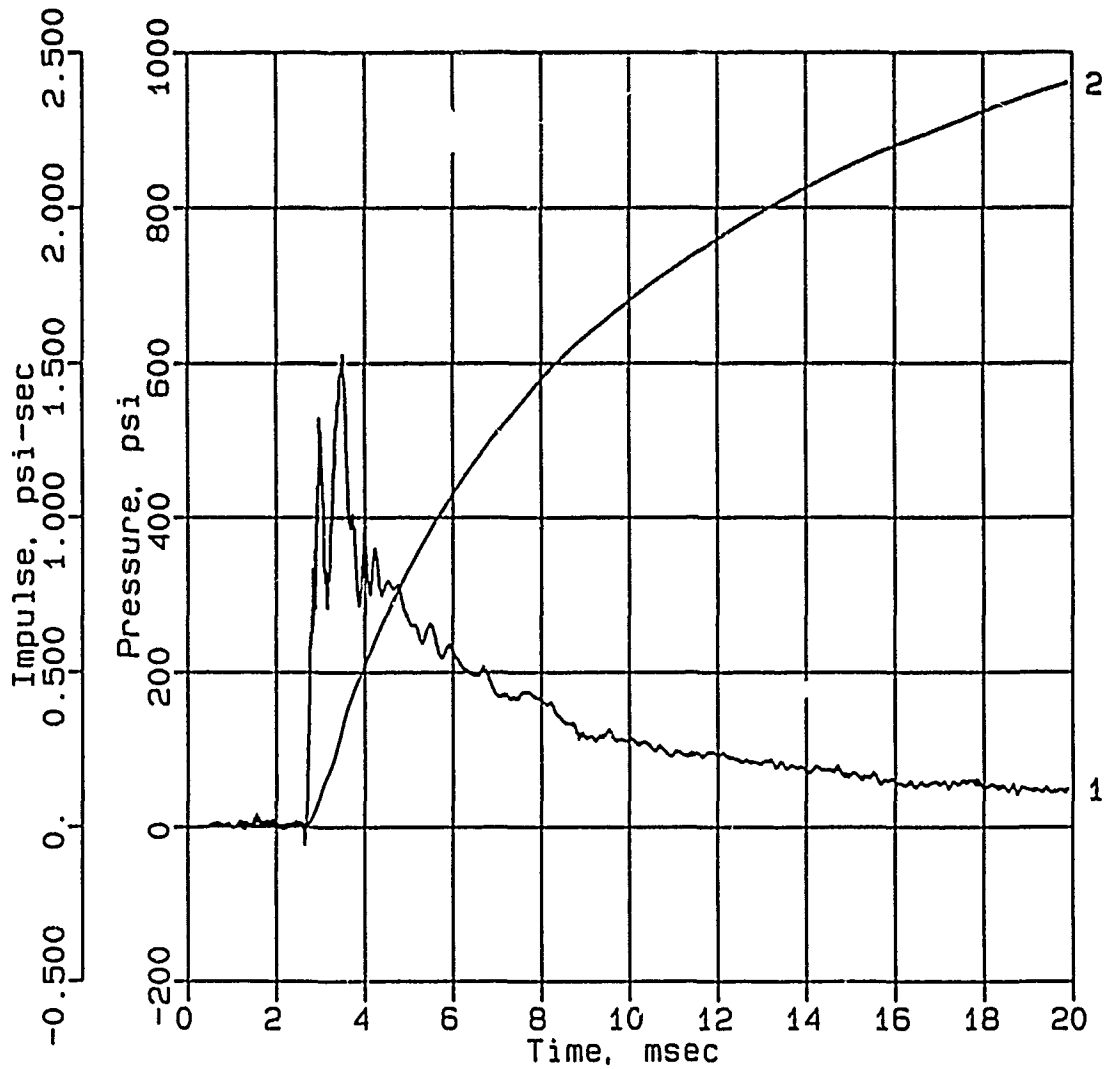
Digitizing rate: 200,000 Hz
Calibration: 5463
Filtering: 20 kHz low pass filter
            5 - 17 kHz band rejection filter

A34
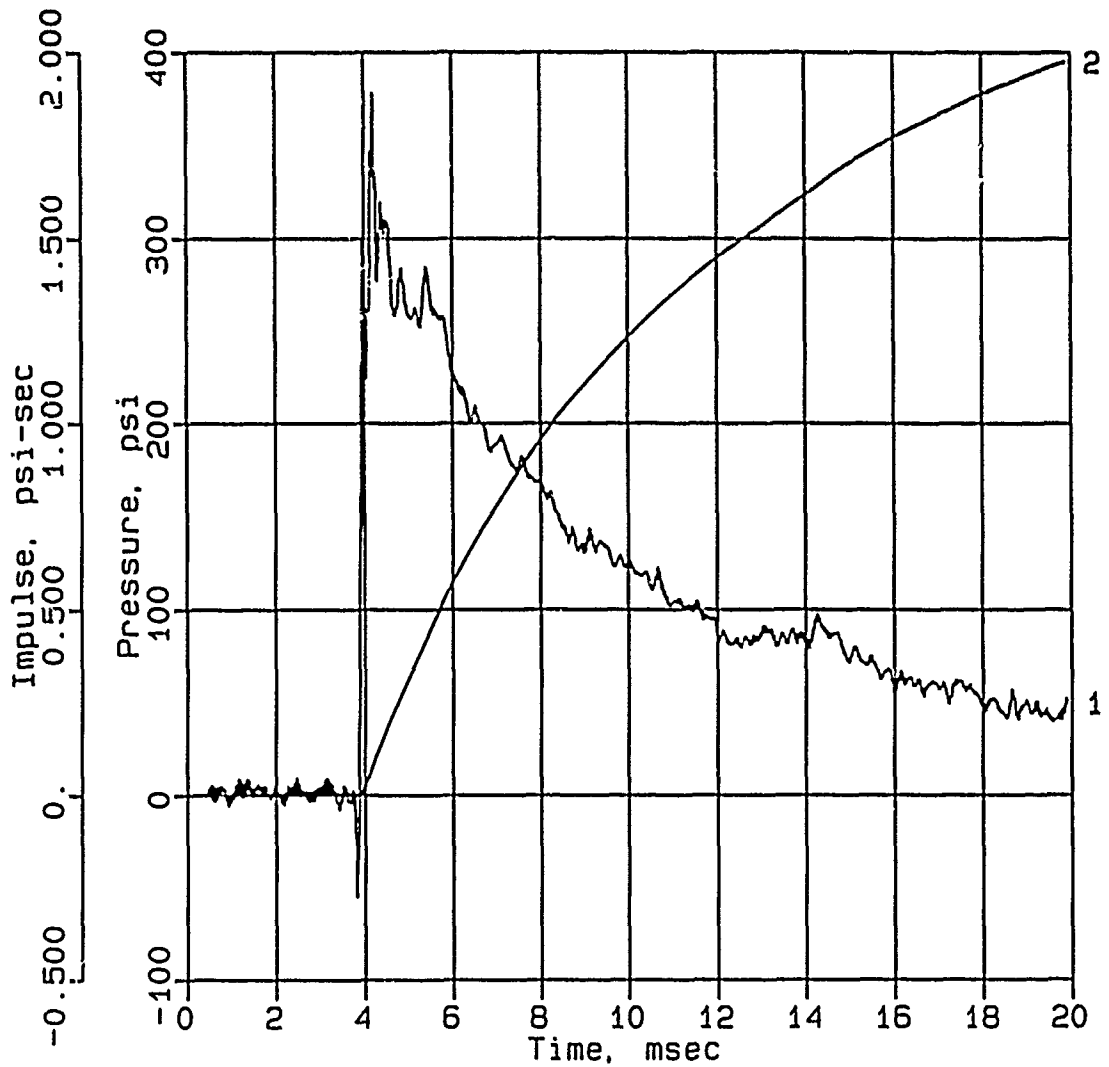
CONWEB T1
SE-10

Digitizing rate: 200,000 Hz
Calibration: 5396
Filtering: 20 kHz low pass filter
            5 - 17 kHz band rejection filter

A35
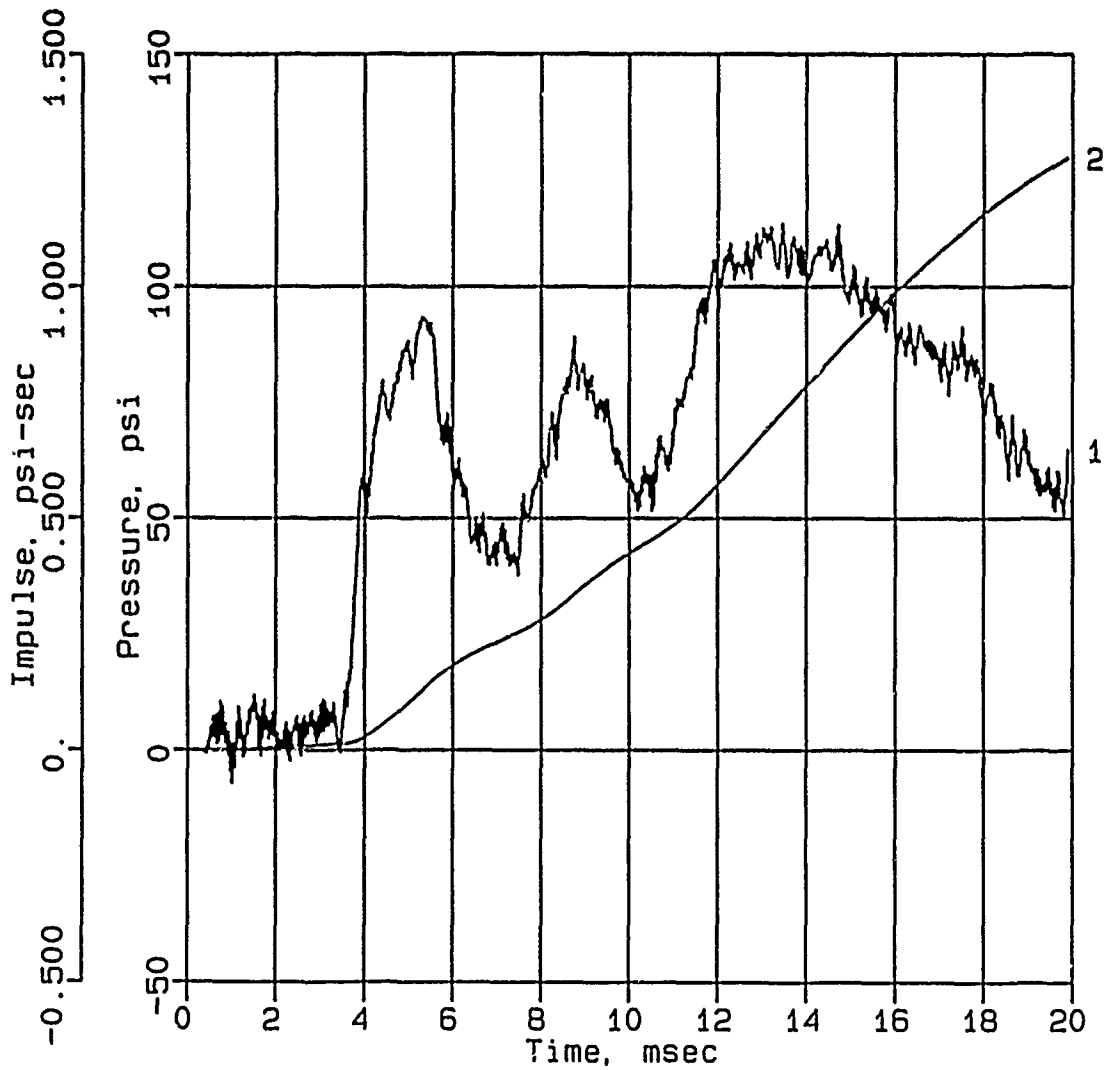
CONWEB T1
SE-11

Digitizing rate: 200,000 Hz
Calibration: 5351
Filtering: 20 kHz low pass filter
5 - 17 kHz band rejection filter

A36

APPENDIX B

DATA, BACKFILL TEST 2

Data from gages DEF-1, DEF-2, and SE-8 in Backfill Test 2 have not been included in this report.

CONWEB T2
IF-1
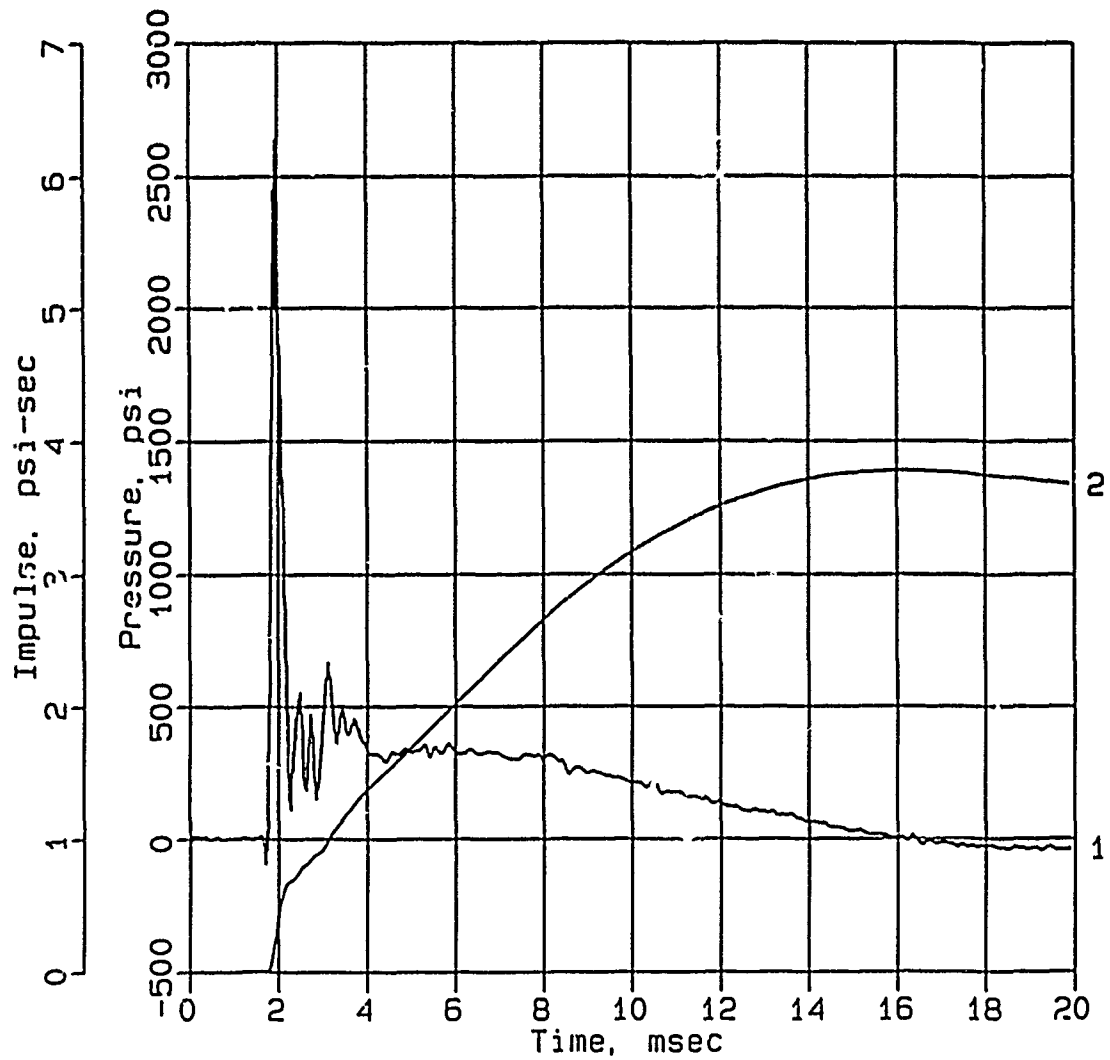
Digitizing rate: 200,000 Hz
Calibration: 4890
Filtering: 20 kHz low pass filter
            5 - 17 kHz band rejection filter

CONWEB T2
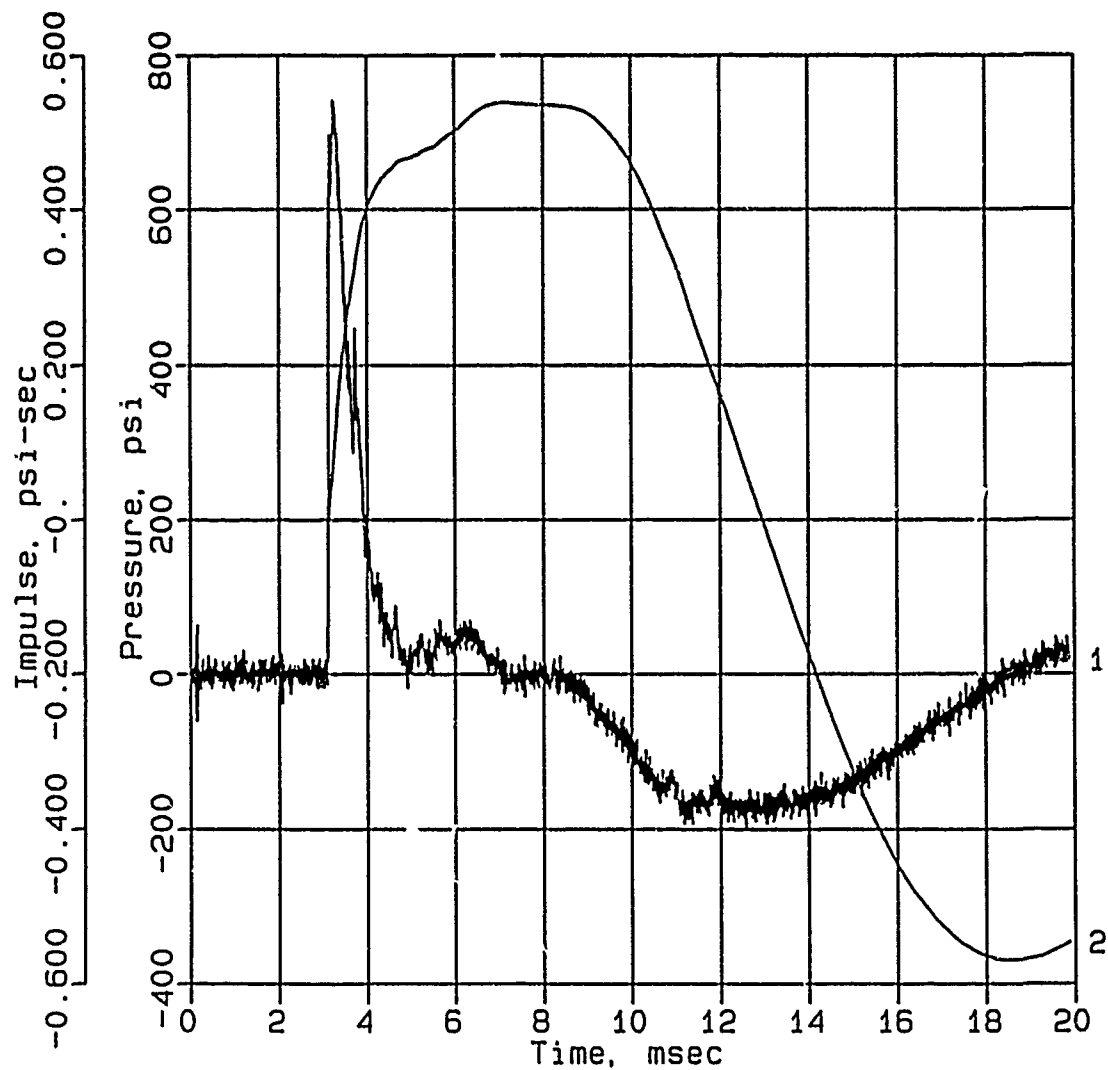## IF-2
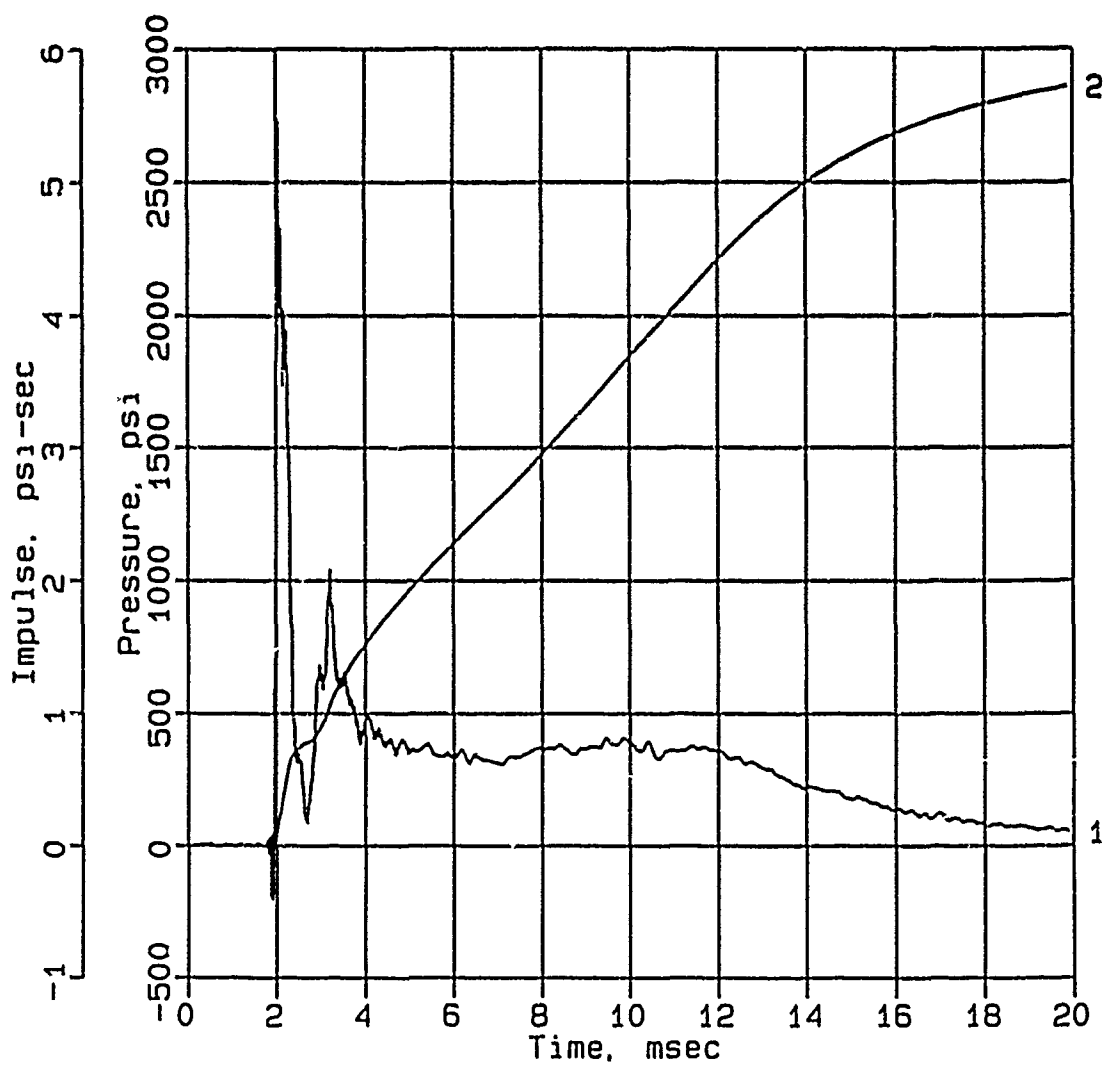
Digitizing rate: 200,000 Hz
Calibration: 5045
Filtering: 20 kHz low pass filter
5 - 17 kHz band rejection filter

B4
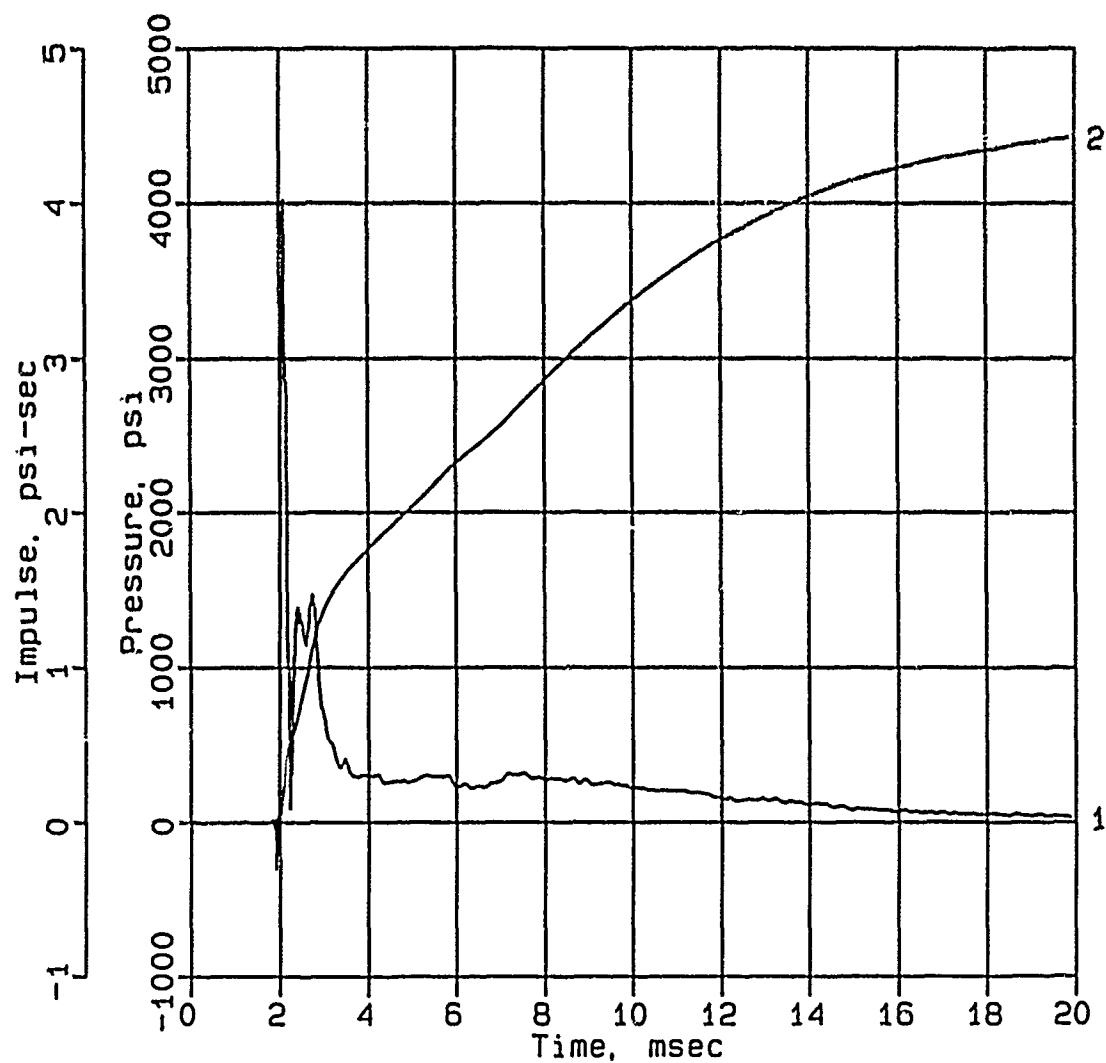
CONWEB T2
IF-3-S

Digitizing rate: 200,000 Hz
Calibration: 4932
Filtering: 20 kHz low pass filter
            5 - 17 kHz band rejection filter

CONWEB T2
IF-5
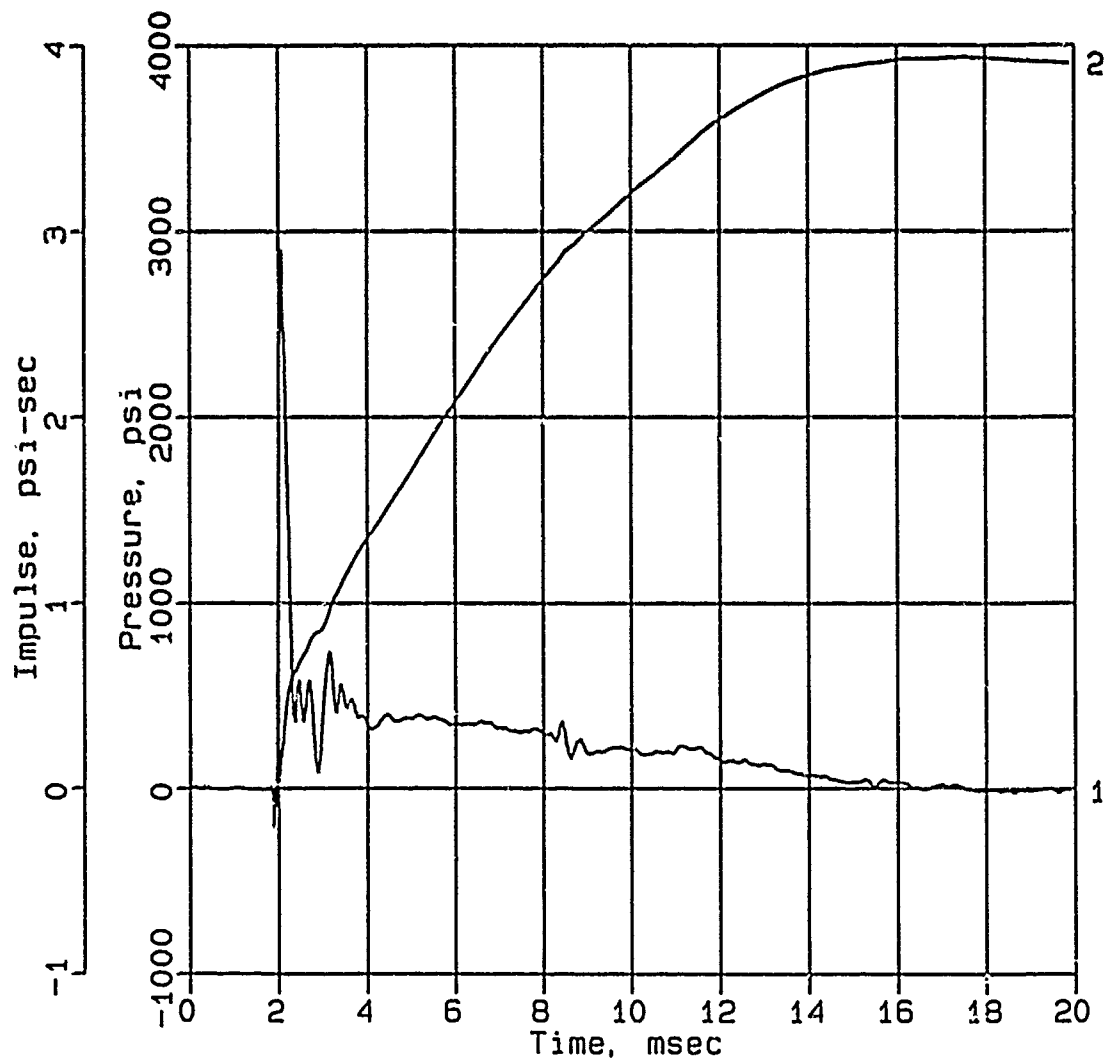
Digitizing rate: 200,000 Hz
Calibration: 5243
Filtering: 20 kHz low pass filter
            5 - 17 kHz band rejection filter

CONWEB T2
IF-6
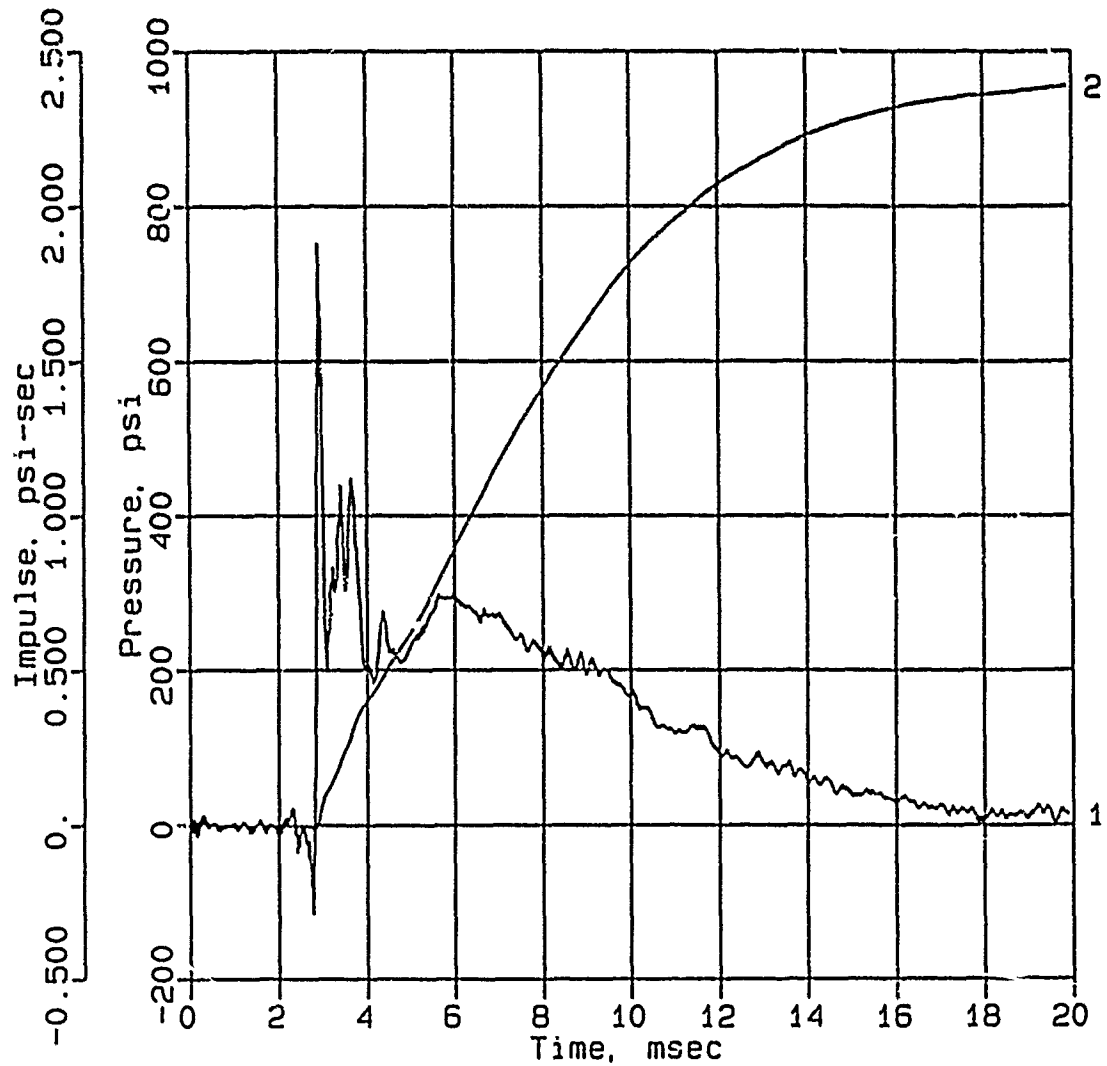
Digitizing rate: 200,000 Hz
Calibration: 5686
Filtering: 20 kHz low pass filter
        5 - 17 kHz band rejection filter

CONWEB T2
IF-8
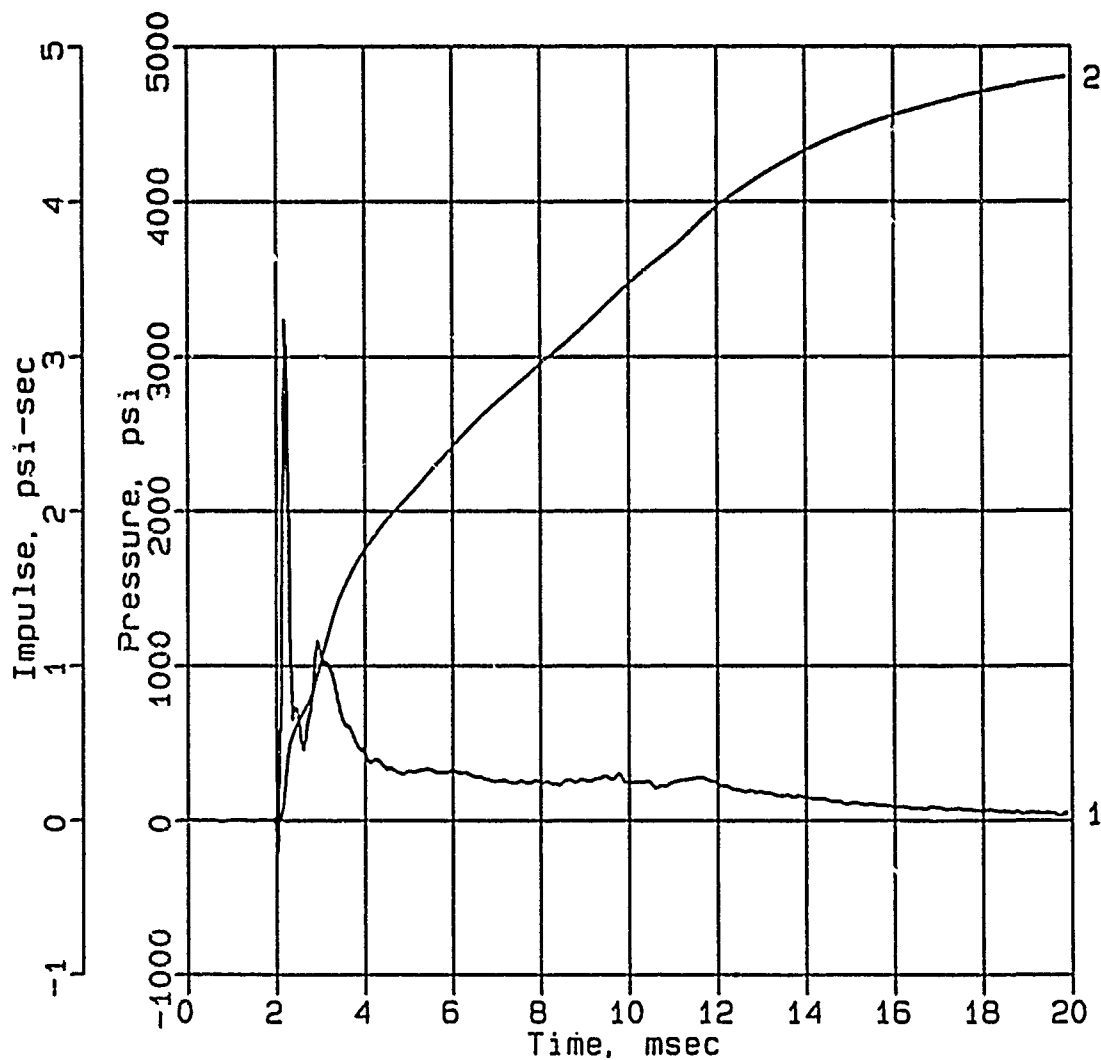
Digitizing rate: 200,000 Hz
Calibration: 4769
Filtering: 20 kHz low pass filter
            5 - 17 kHz band rejection filter

CONWEB T2
IF-9
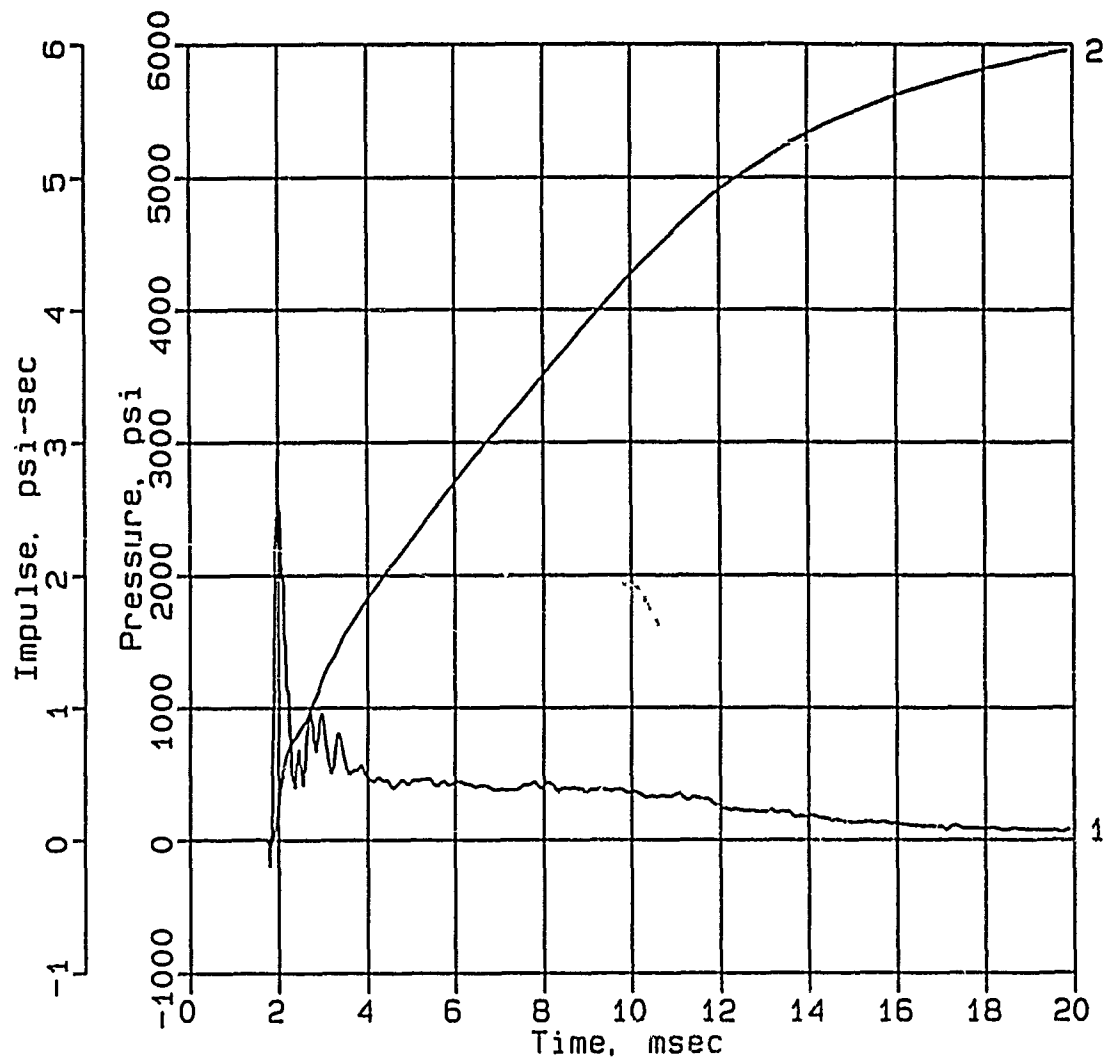
Digitizing rate: 200,000 Hz
Calibration: 4846
Filtering: 20 kHz low pass filter
            5 - 17 kHz band rejection filter

CONWEB T2

AHS-0

Digitizing rate: 200,000 Hz
Calibration: 5376
Constant Baseline Shift
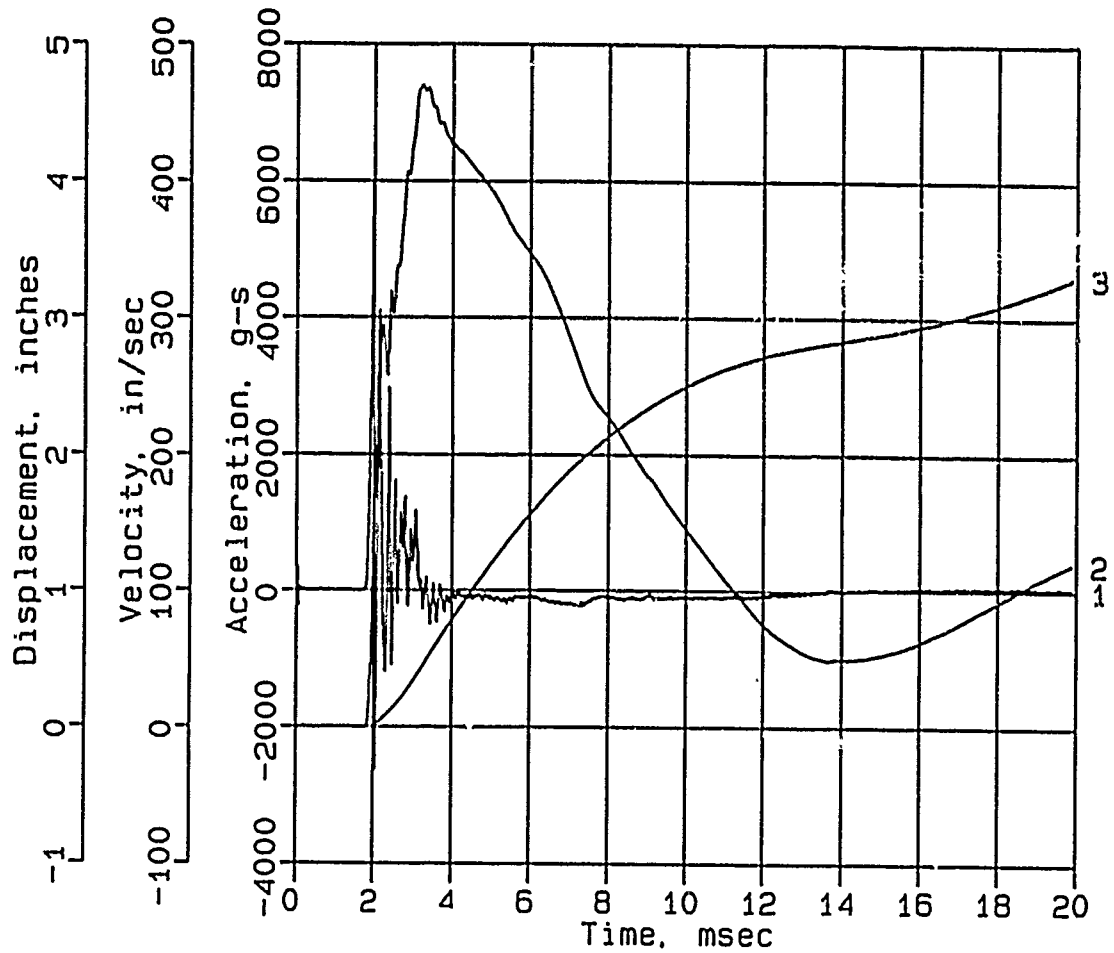
B10

CONWEB T2
AHS-1

Digitizing rate: 200,000 Hz
Calibration: 5712
Constant Baseline Shift

CONWEϹ T2
AHS-2
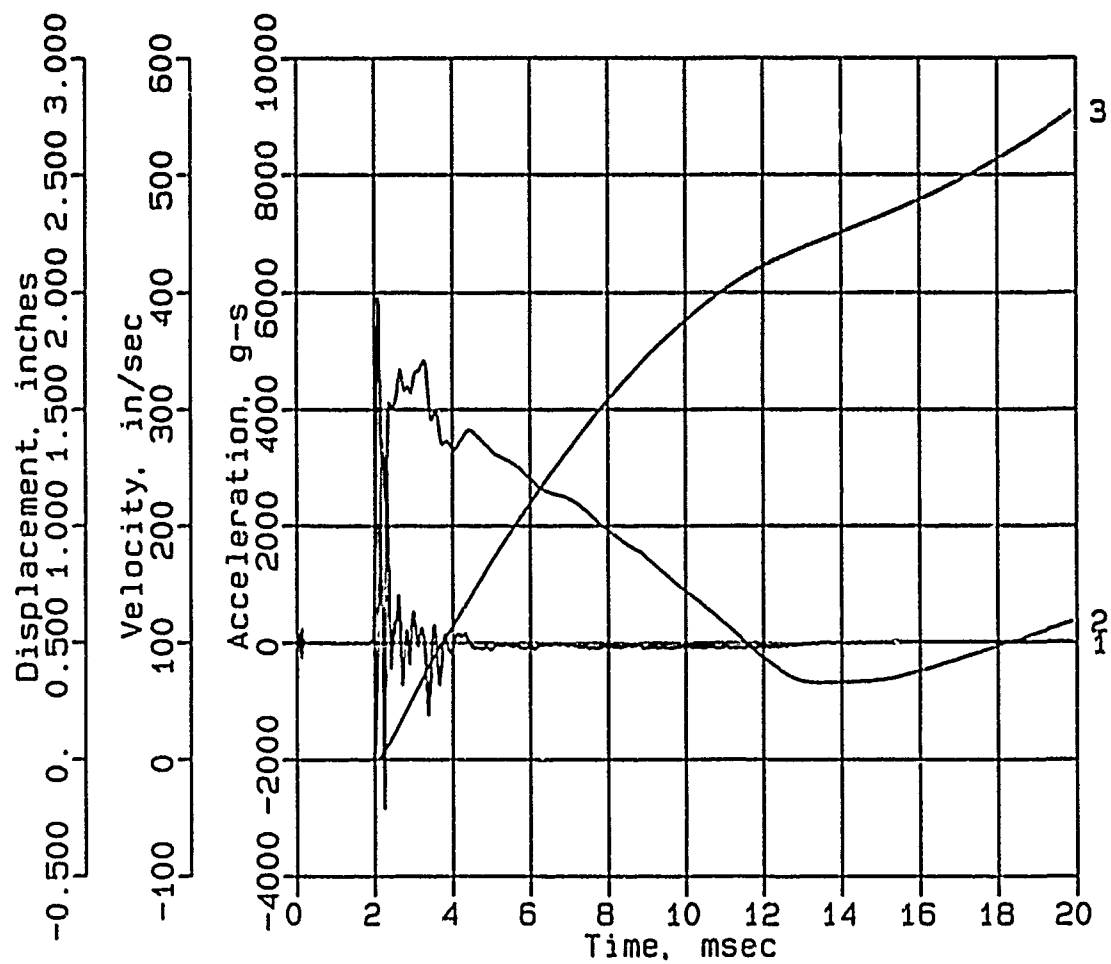
Digitizing rate: 200,000 Hz
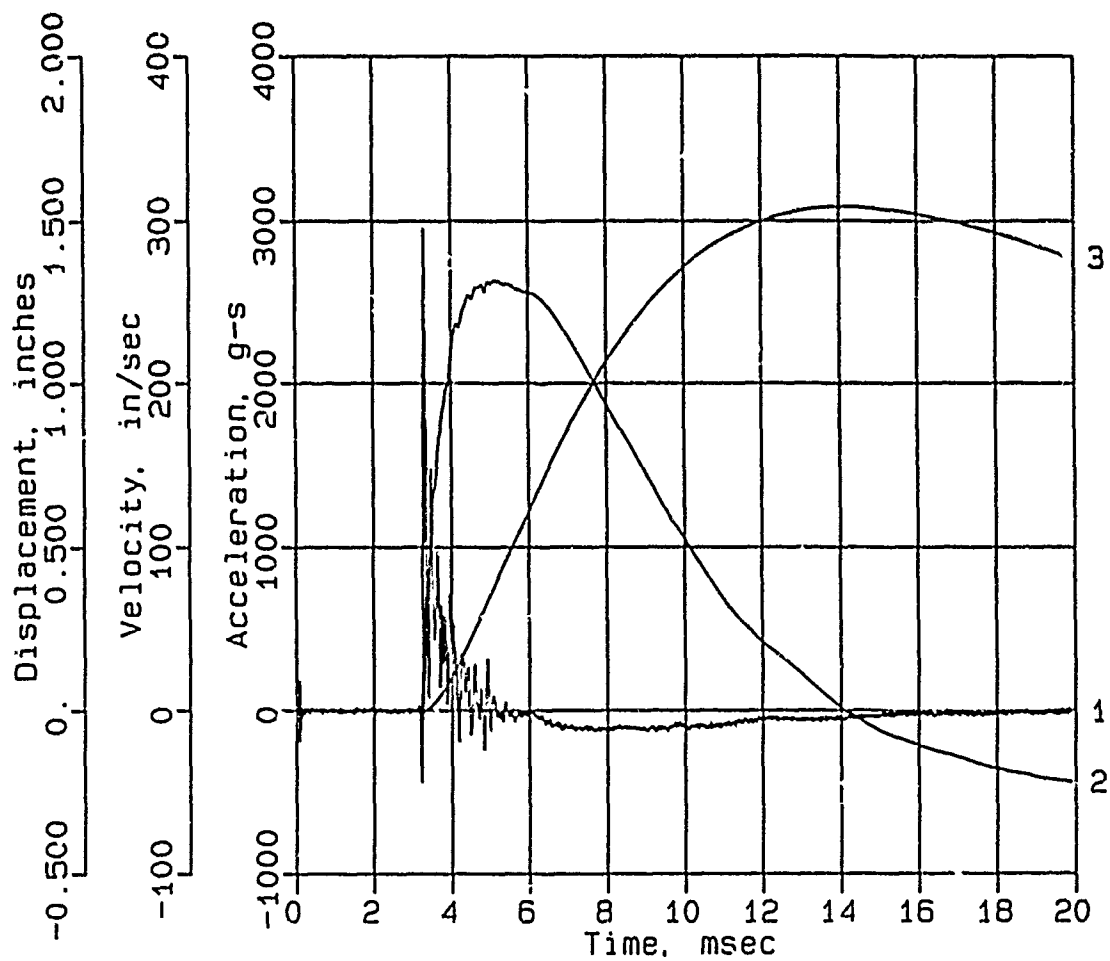Calibration: 5275
Constant Baseline Shift

CONWEB T2
AHS-3

Digitizing rate: 200,000 Hz
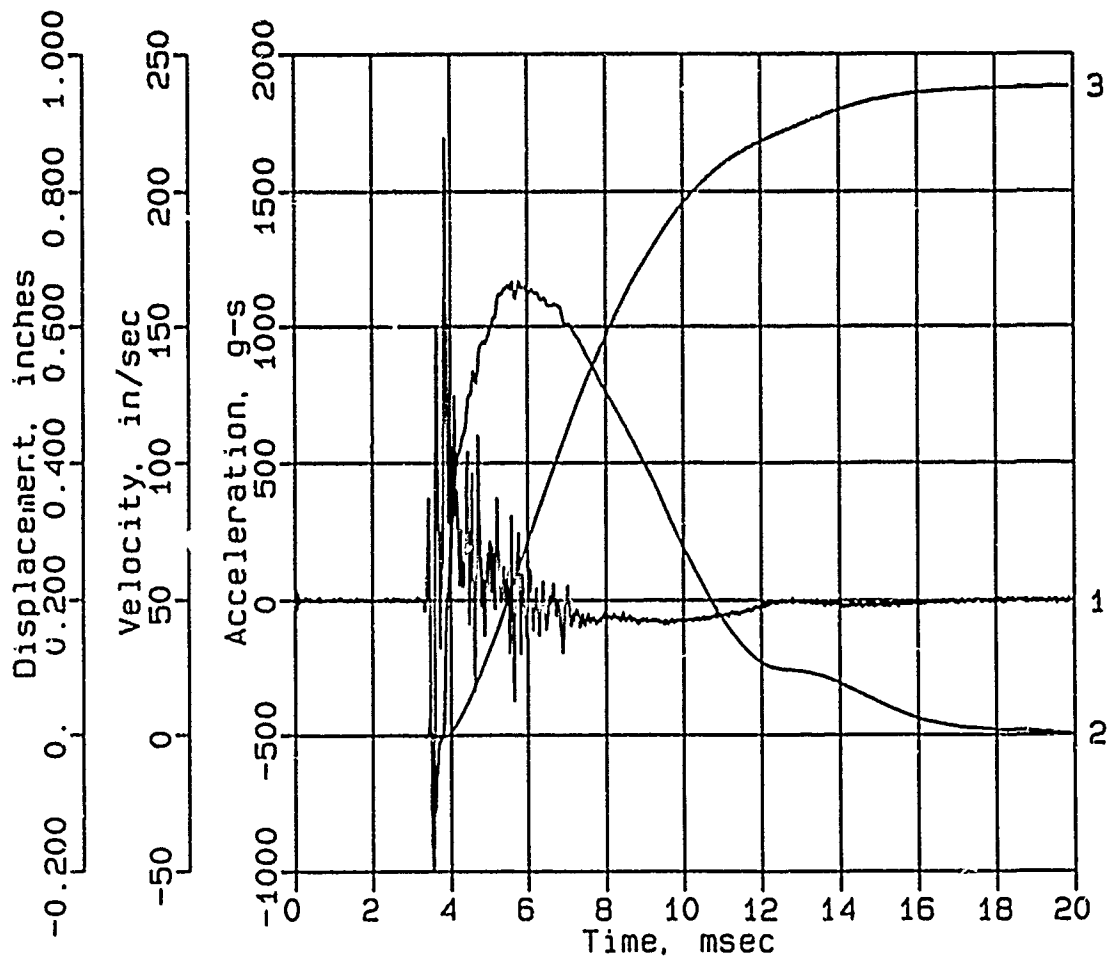Calibration: 5495
Constant Baseline Shift

B13
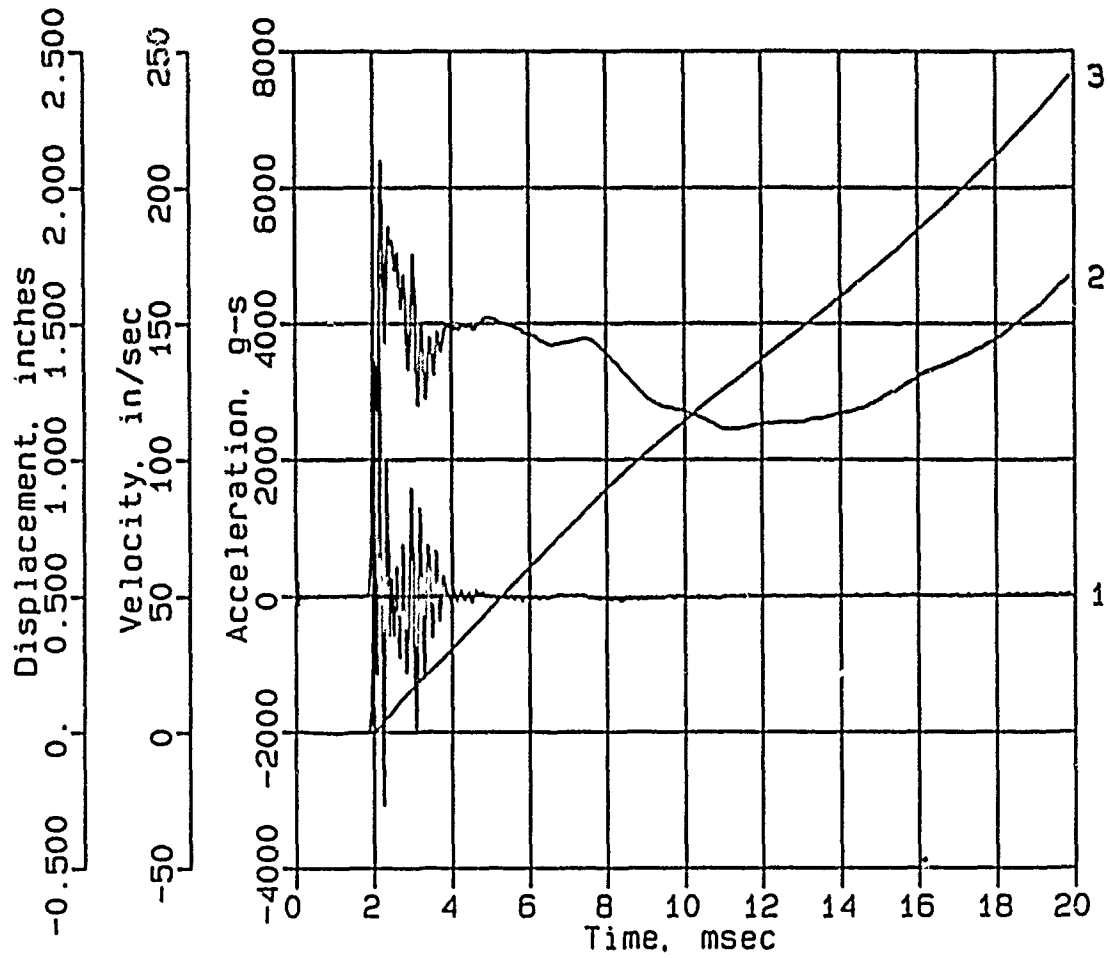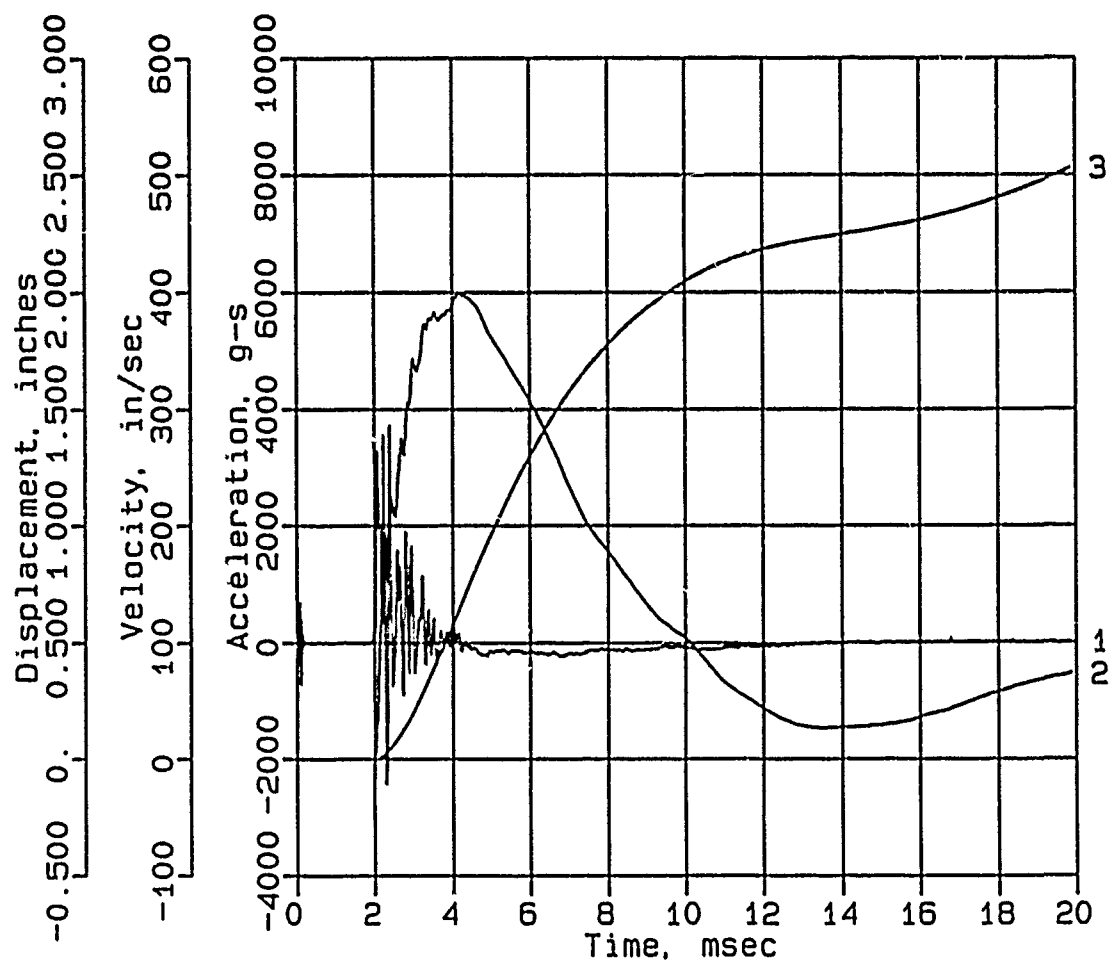
CONWEB T2
AHS-5

Digitizing rate: 200,000 Hz
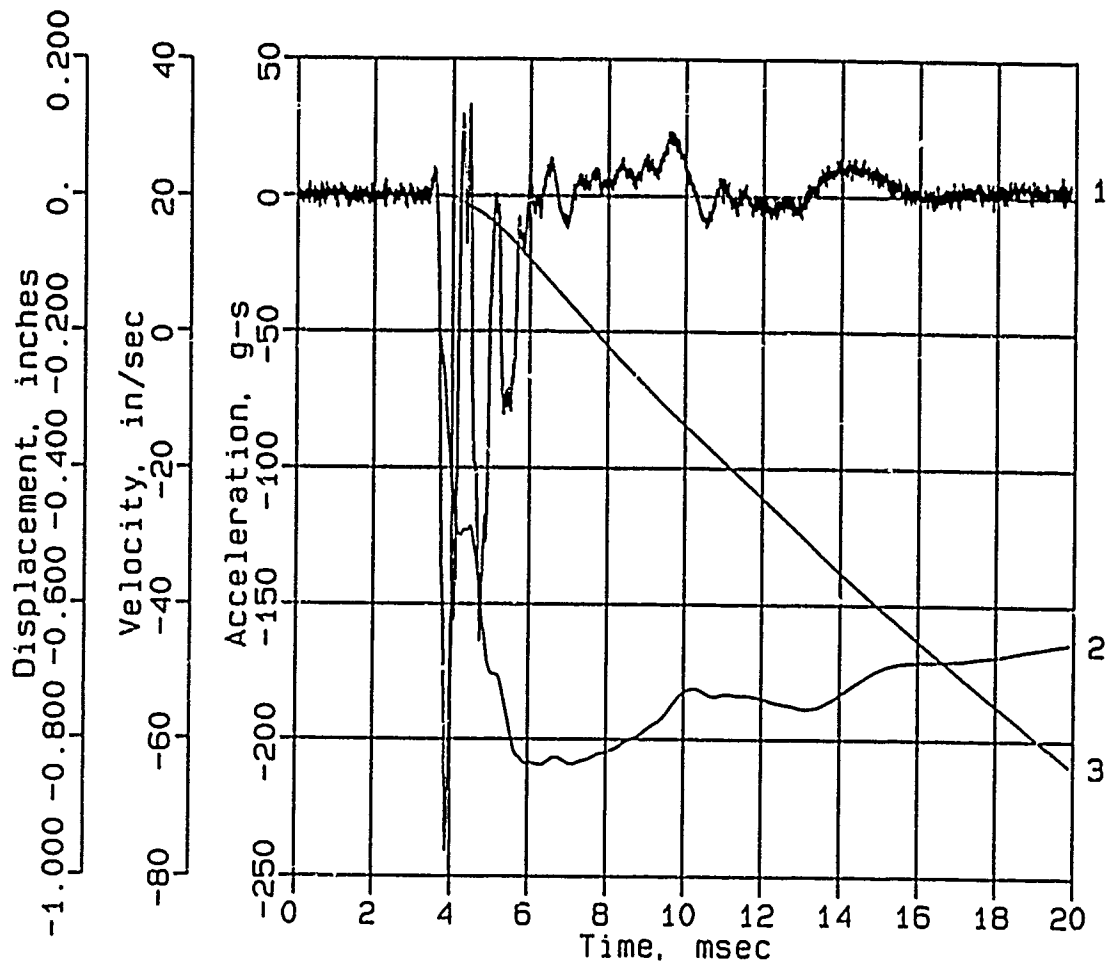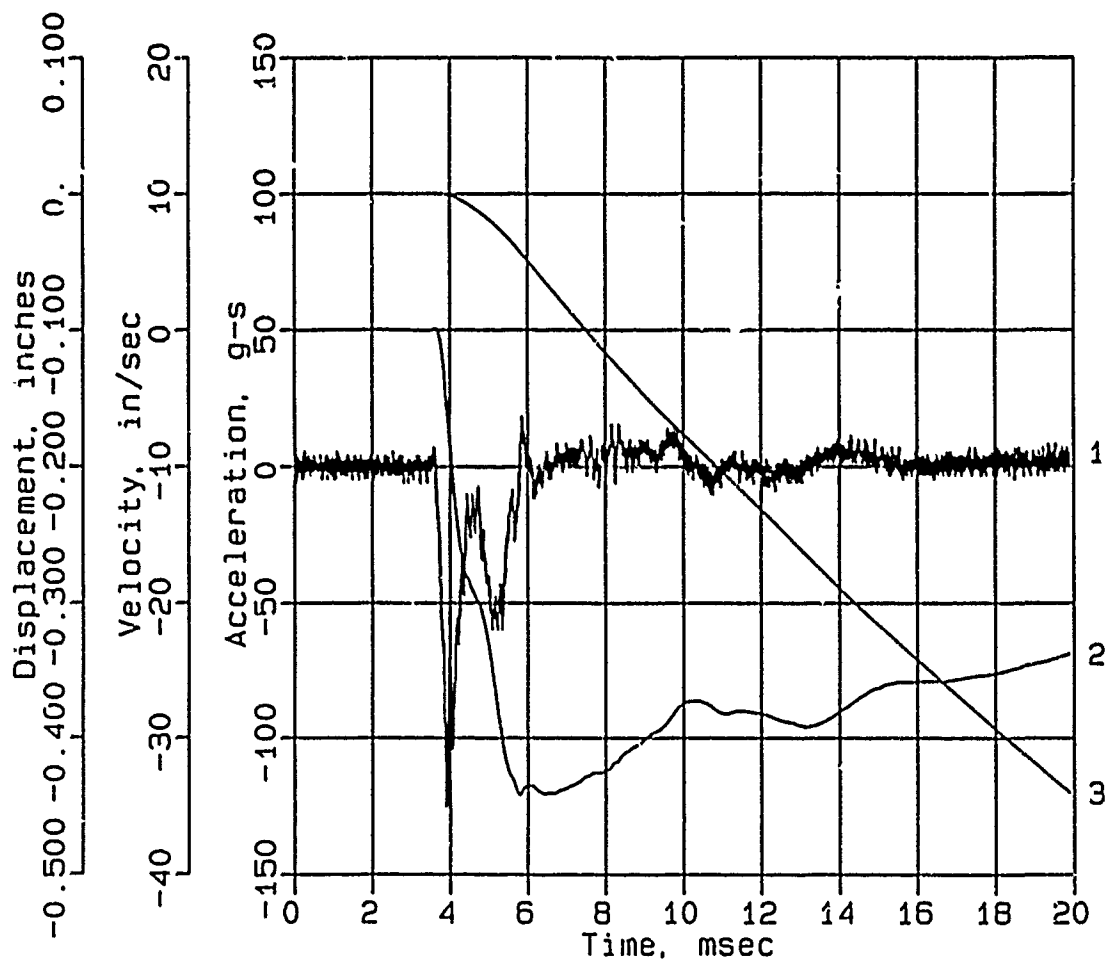Calibration: 5055
Constant Baseline Shift

CONWEB T2
AHS-6
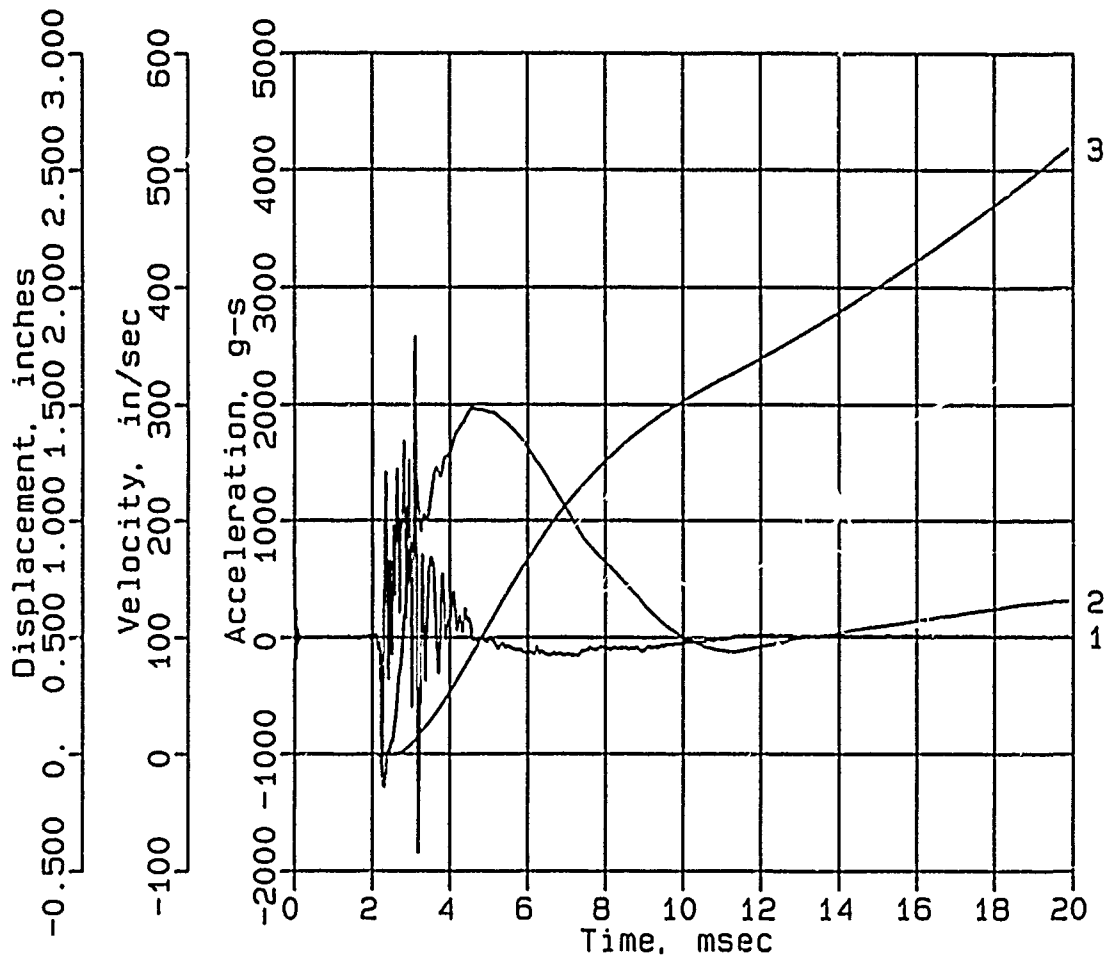
Digitizing rate: 200,000 Hz
Calibration: 2833
Constant Baseline Shift

CONWEB T2
AHS-10
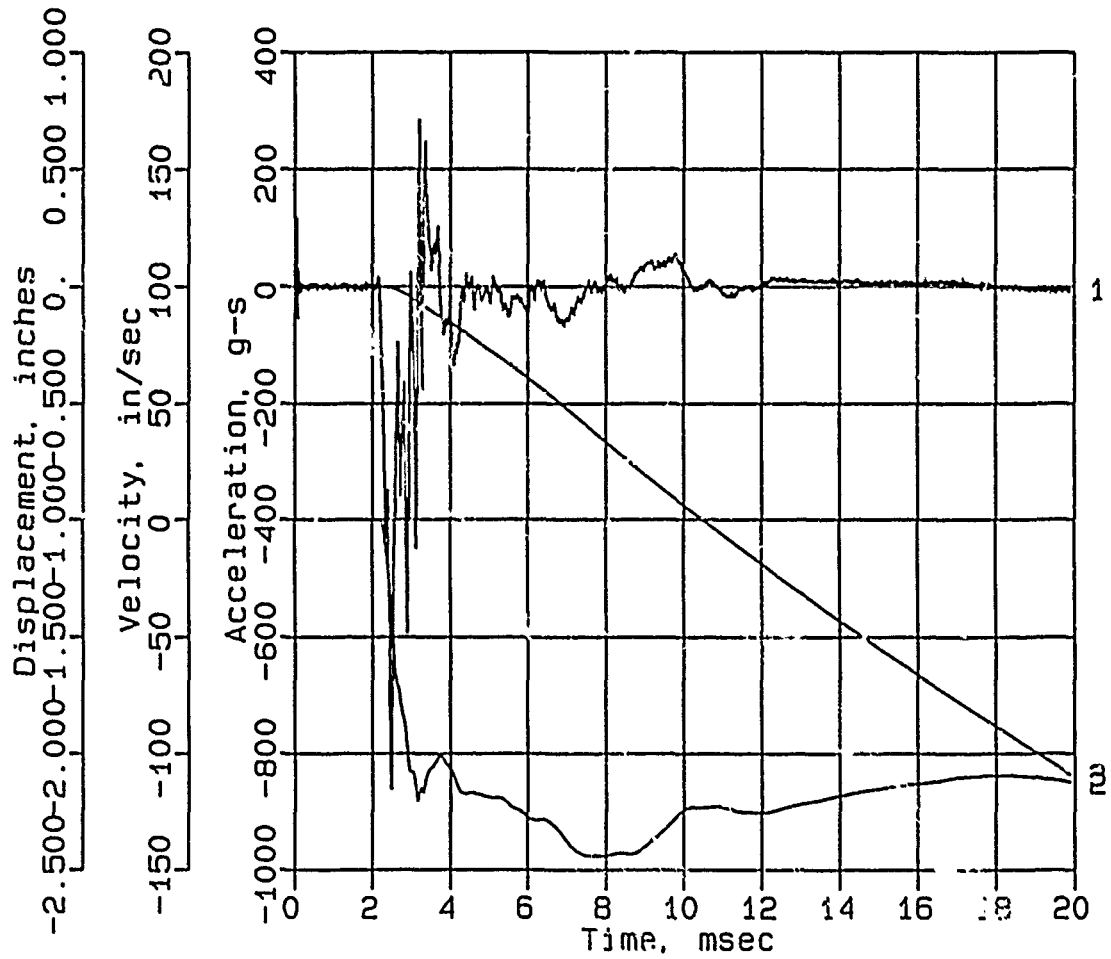
Digitizing rate: 200,000 Hz
Calibration: 1633
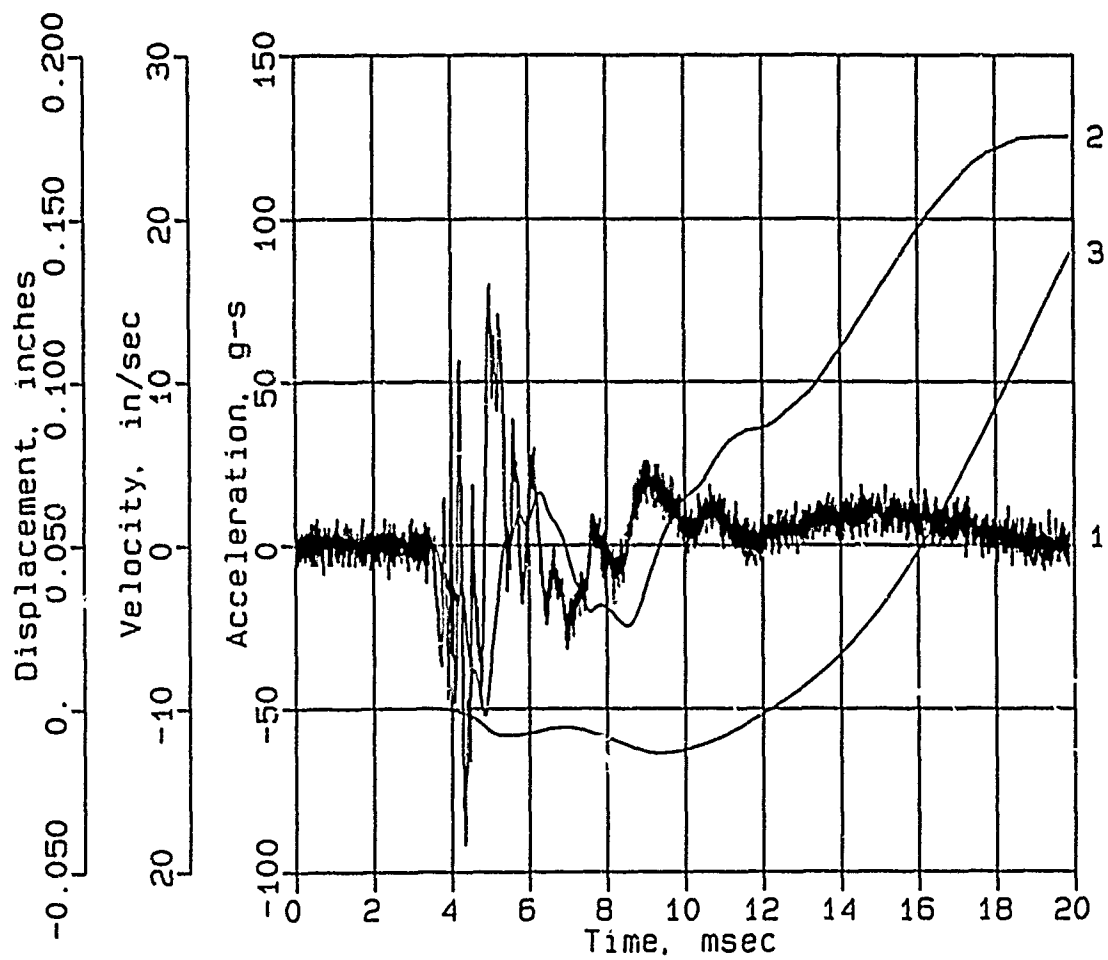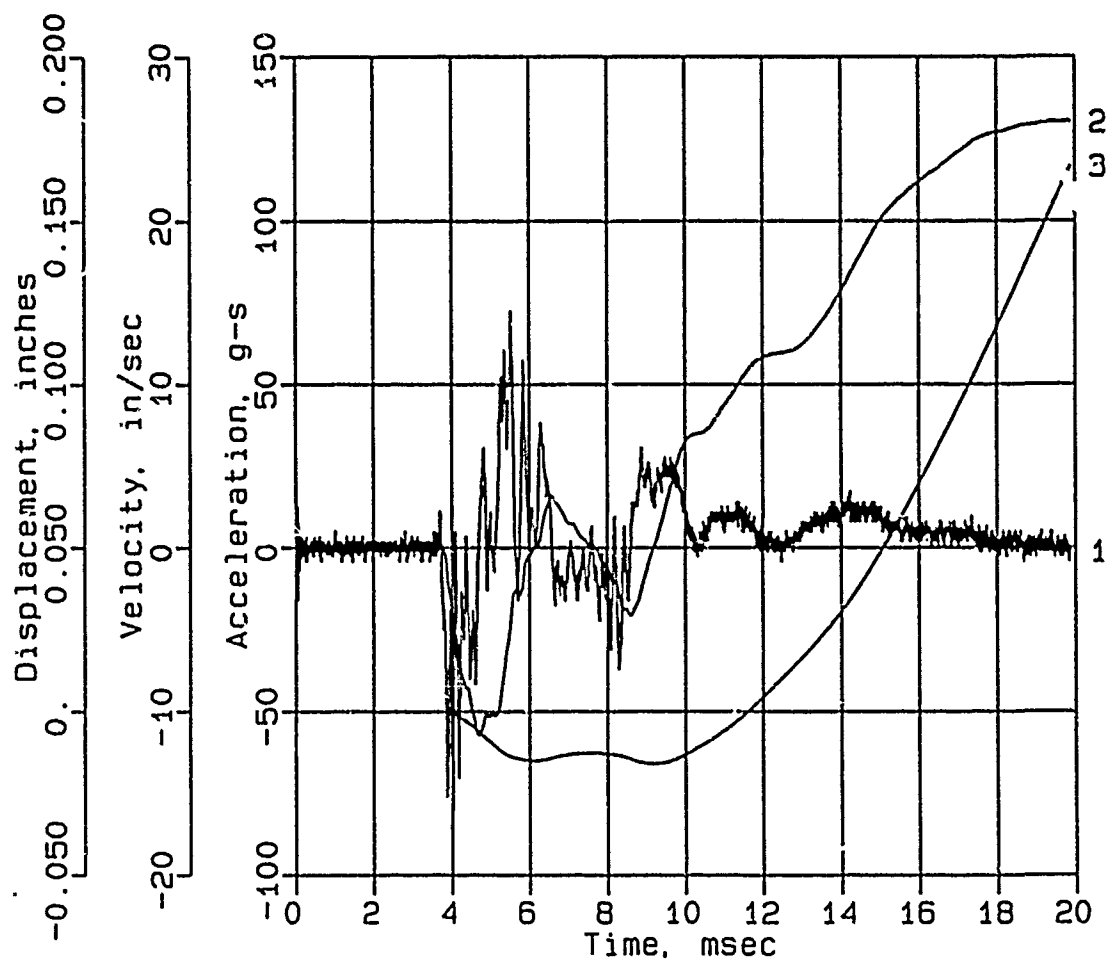Constant Baseline Shift

B16
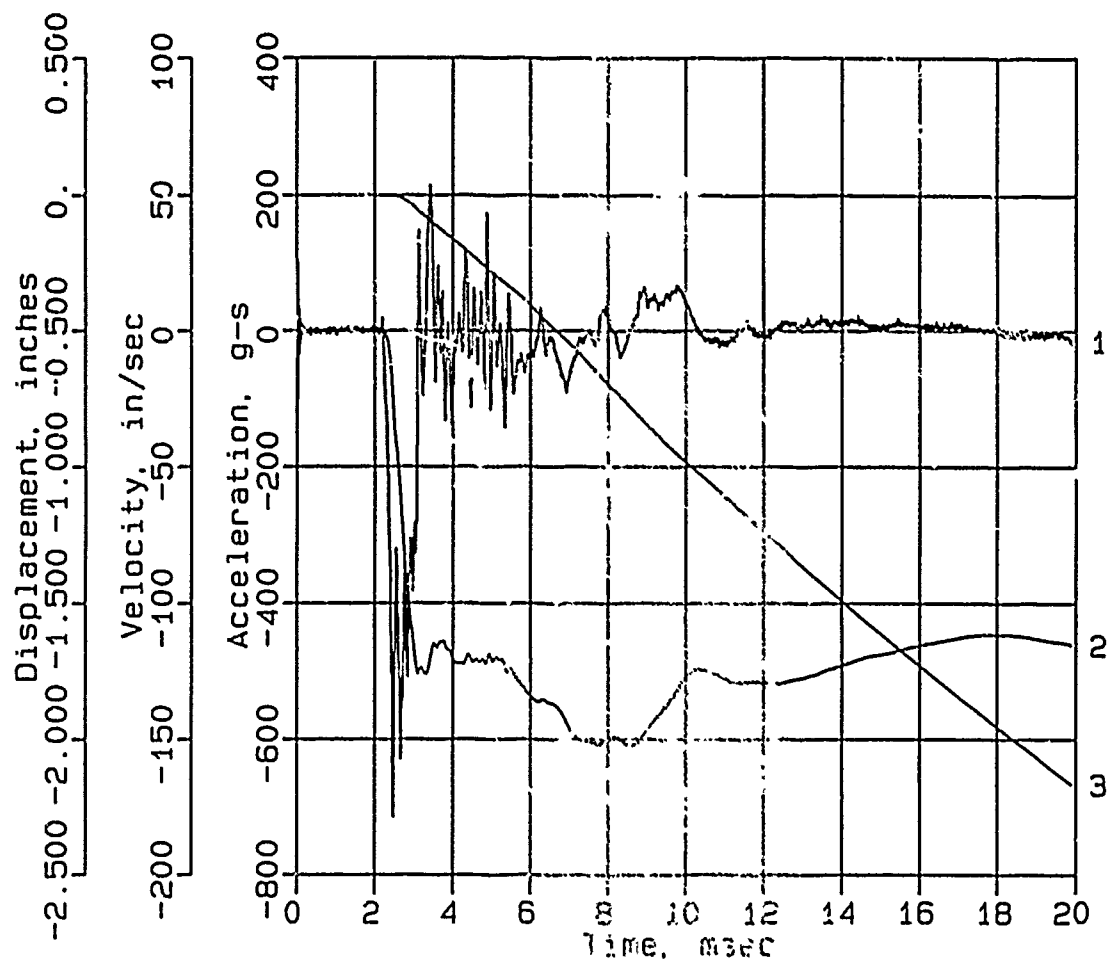
CONWEB T2
AHS-11

Digitizing rate: 200,000 Hz
Calibration: 1455
Constant Baseline Shift

CONWEB T2
AVS-10
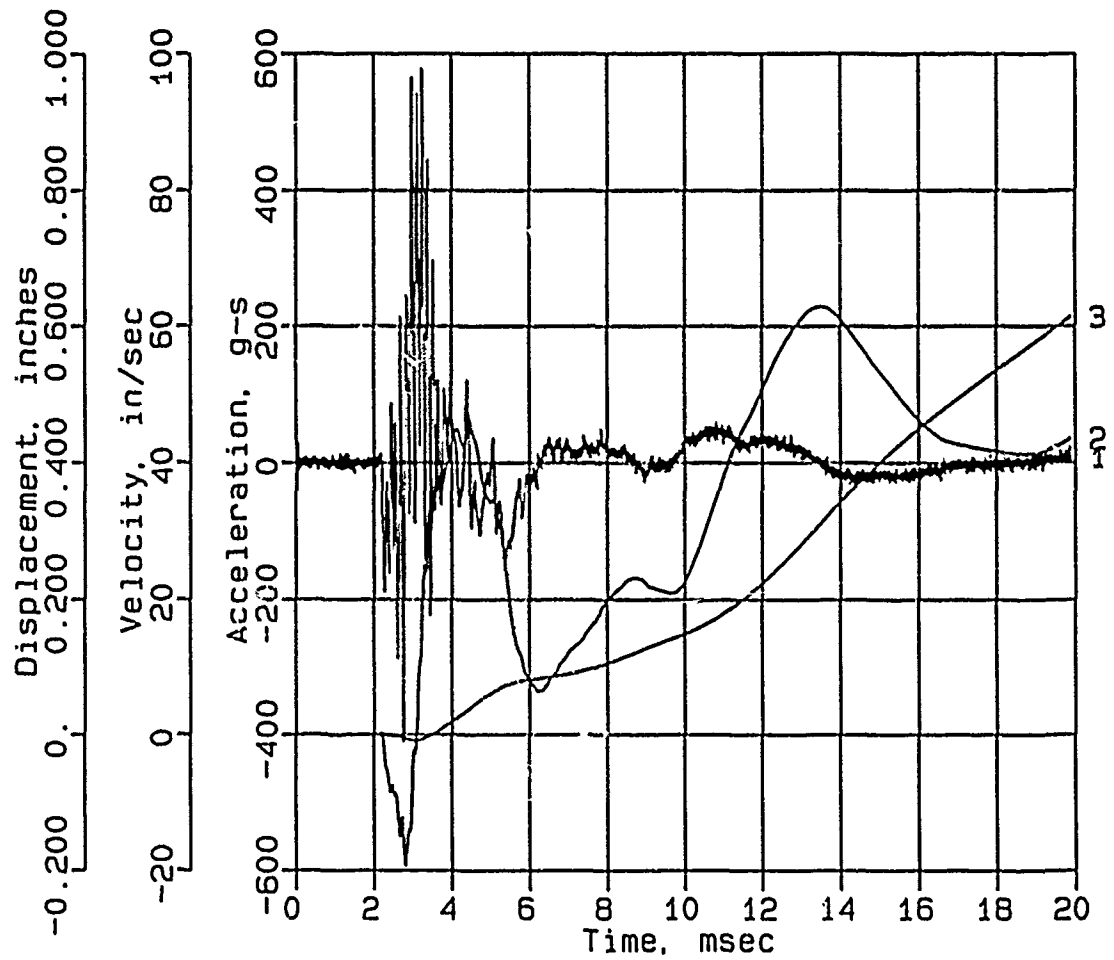
Digitizing rate: 200,000 Hz
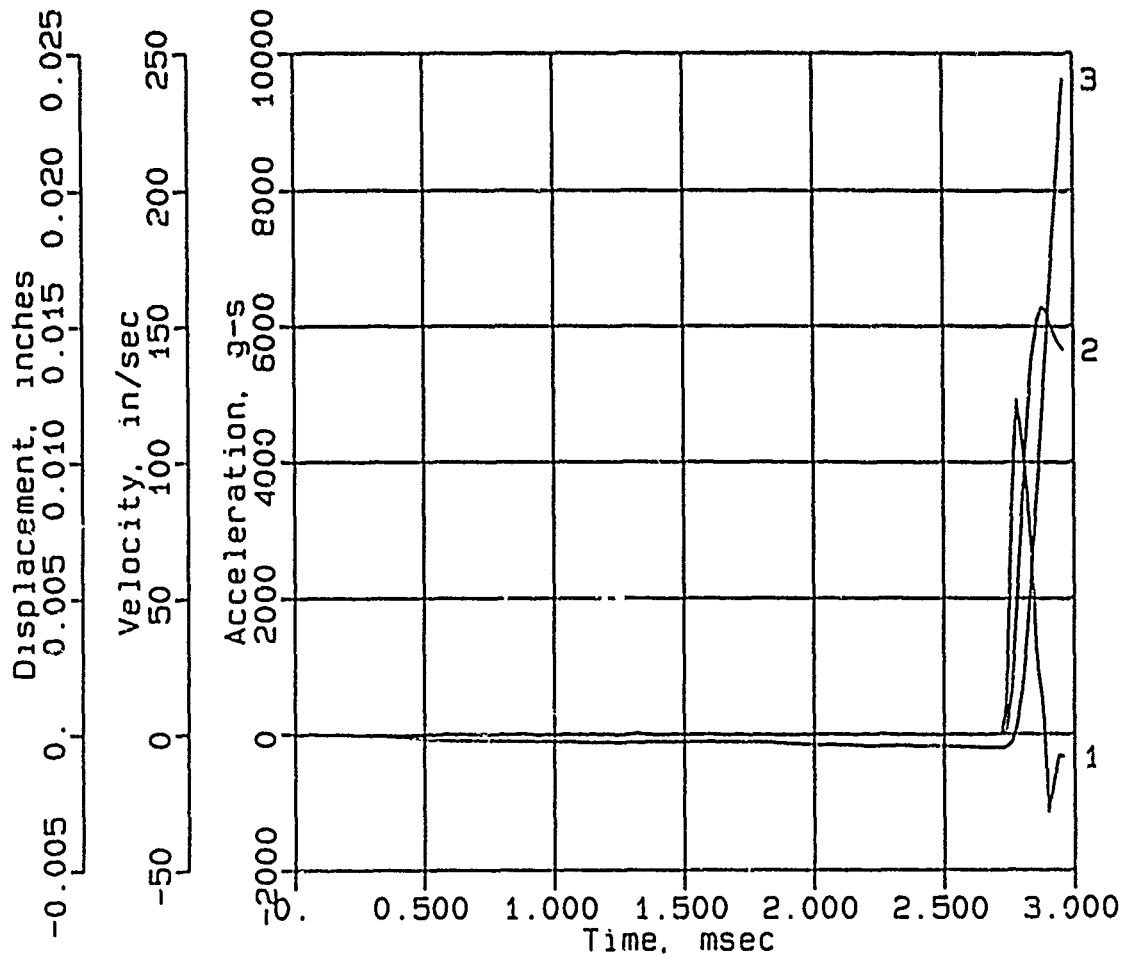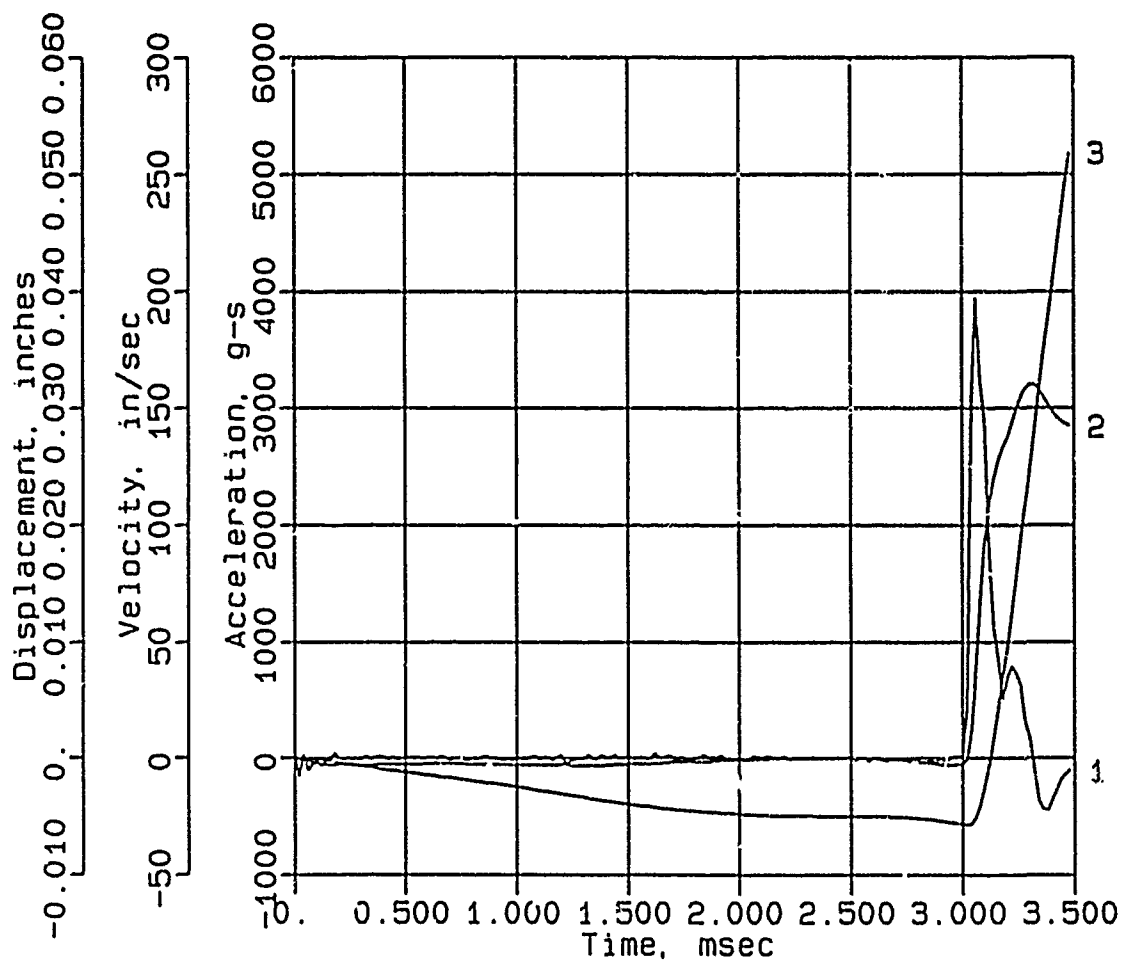Calibration: 1766
Constant Baseline Shift

CONWEB T2
AVS-12
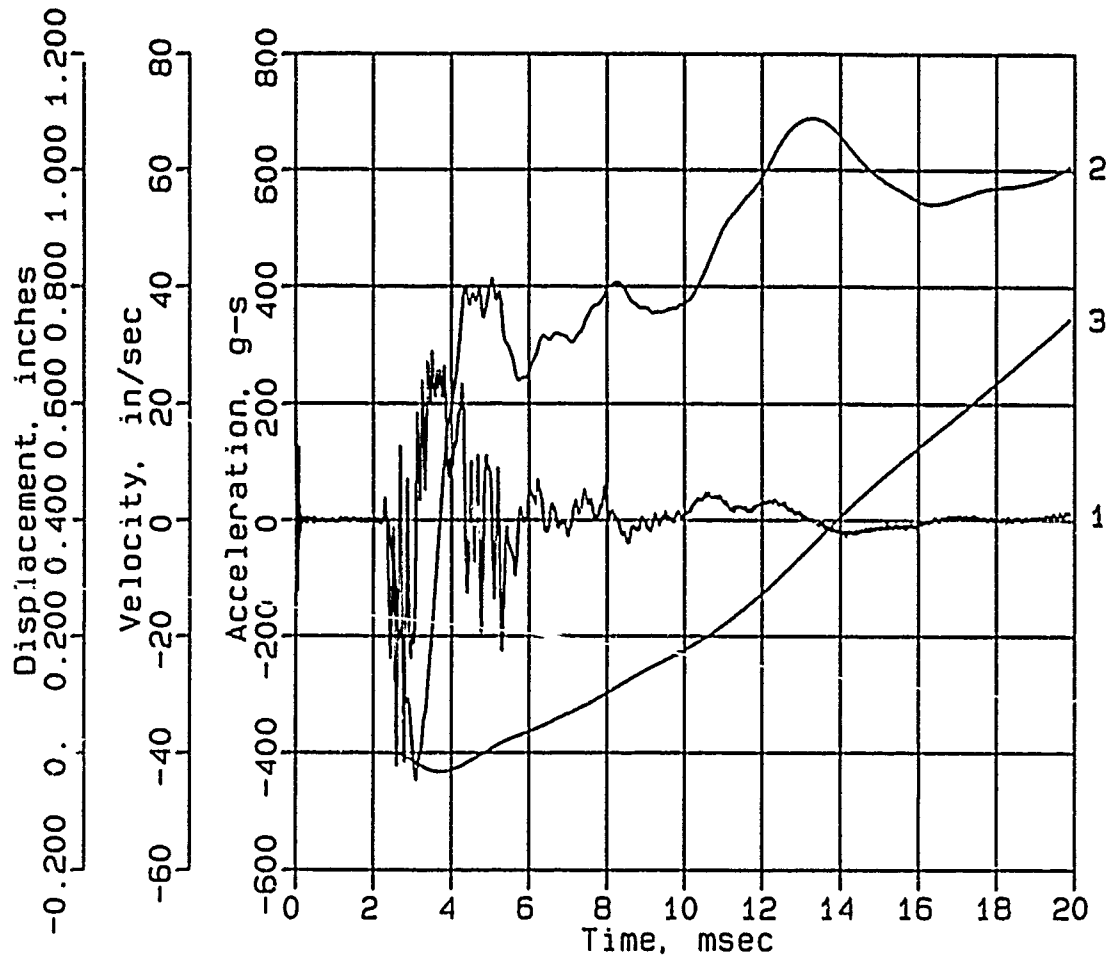
Digitizing rate: 200,000 Hz
Calibration: 1459
Constant Baseline Shift

B19

CONWEB T2

AHF-1
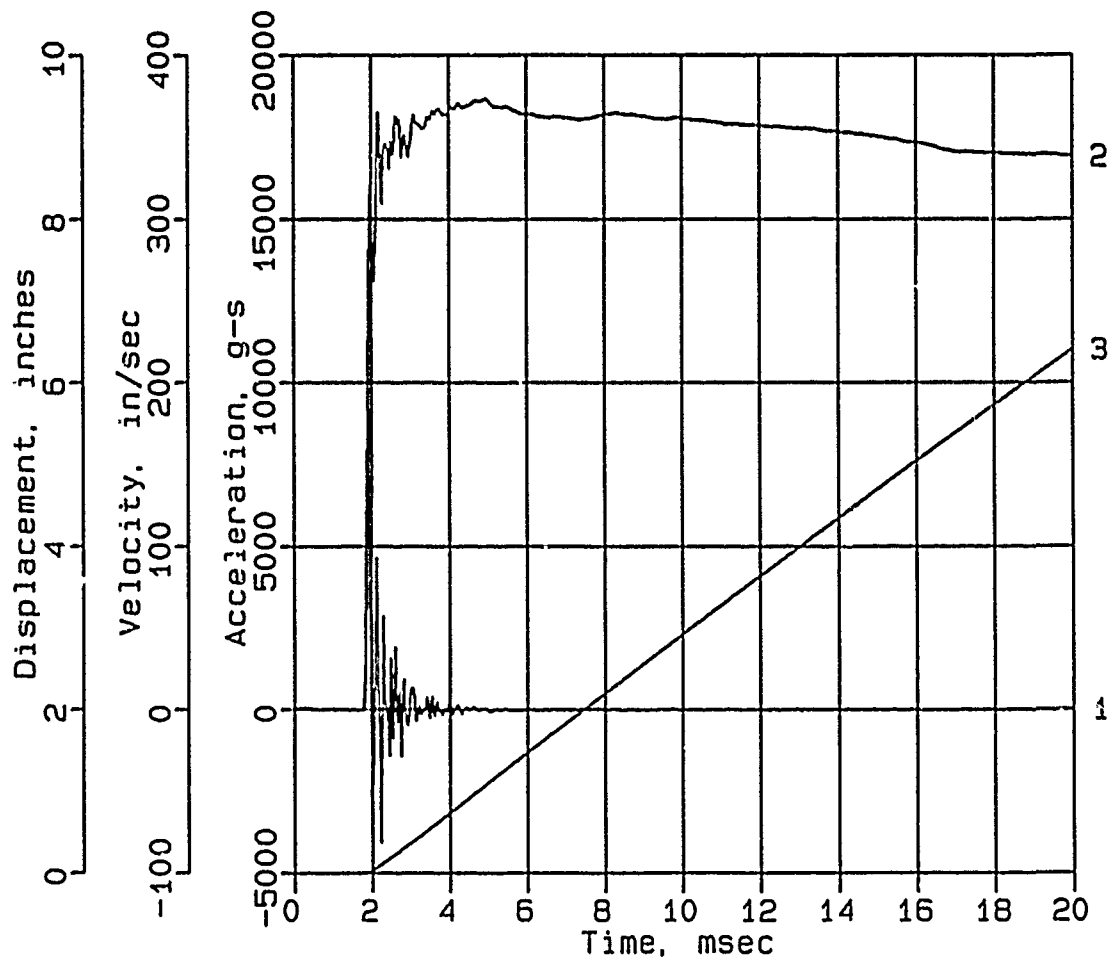
Digitizing rate: 200,000 Hz
Calibration: 12120
Constant Baseline Shift

CONWEB T2
AHF-3
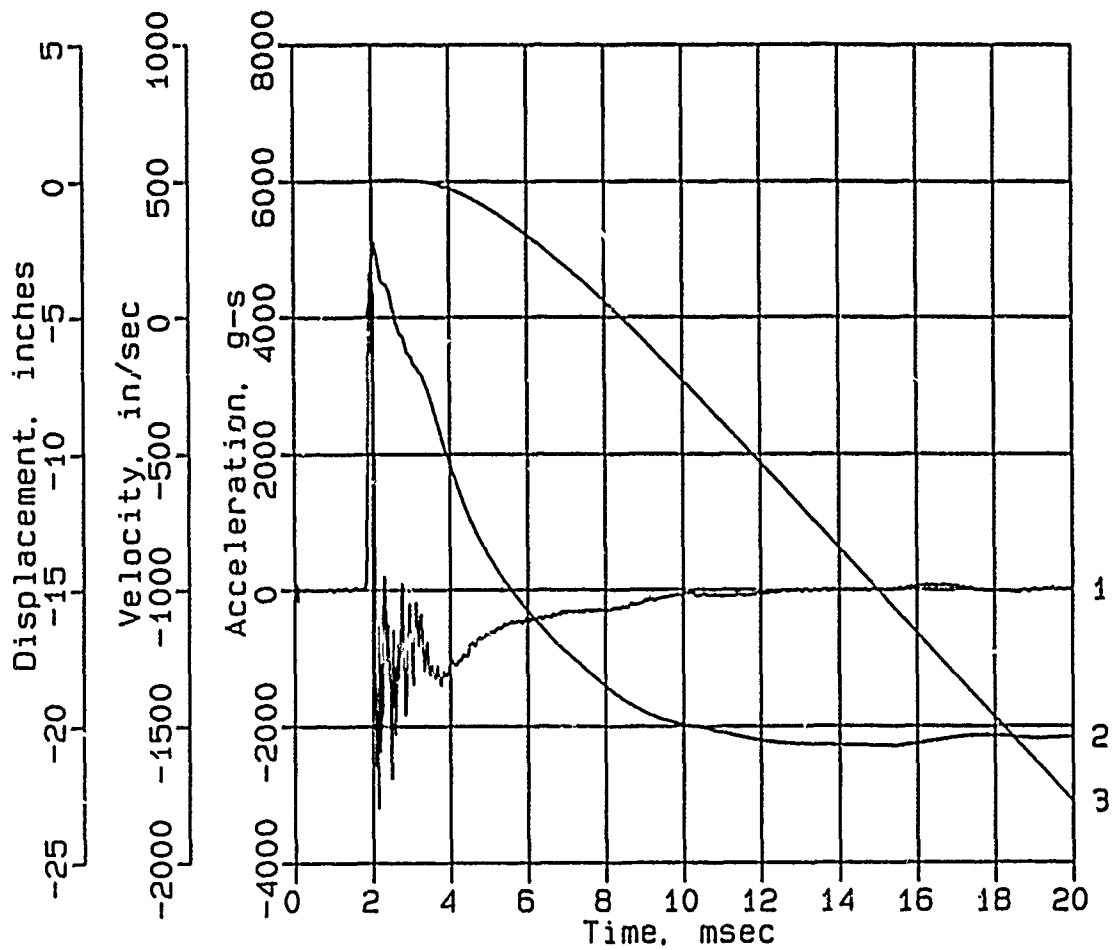
Digitizing rate: 200,000 Hz
Calibration: 7718
Constant Baseline Shift

CONWEB T2

AHF-4
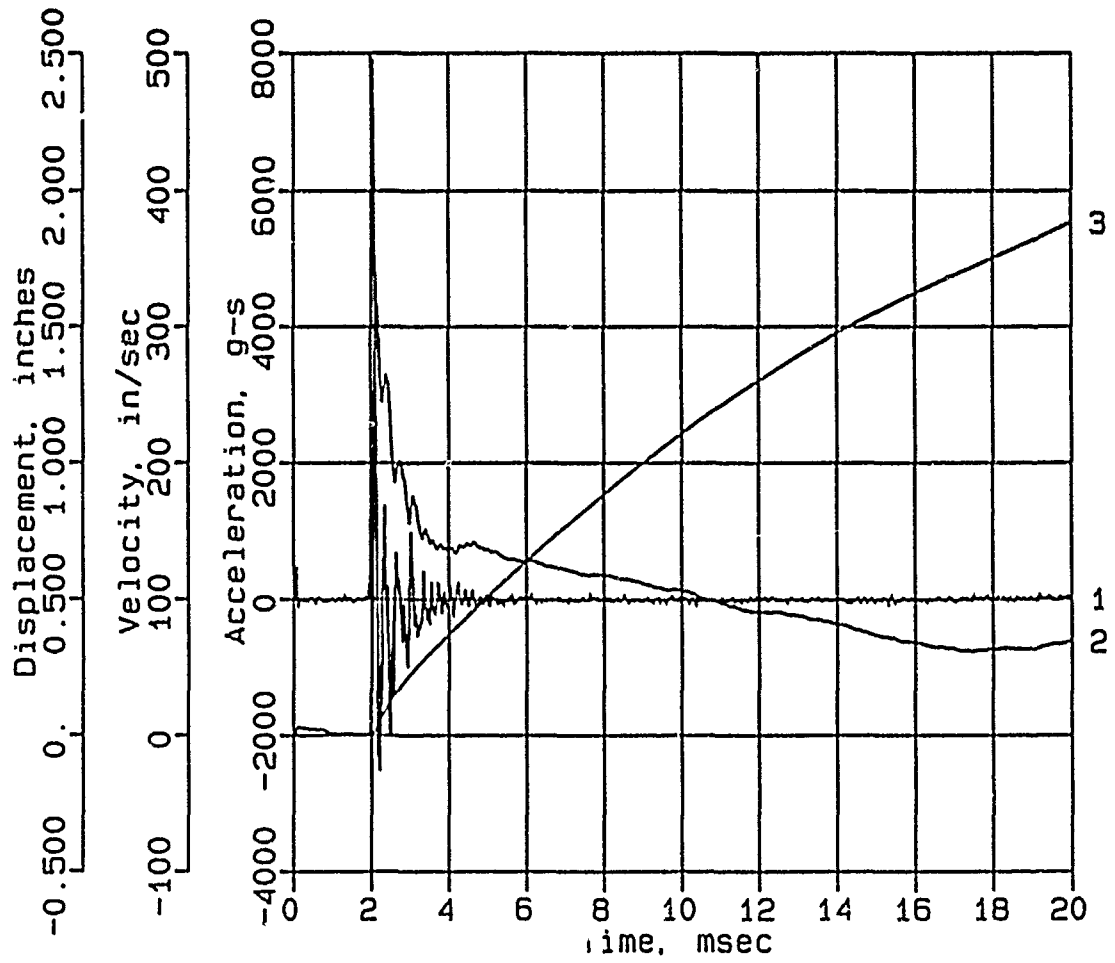
Digitizing rate: 200,000 Hz
Calibration: 18245
Constant Baseline Shift
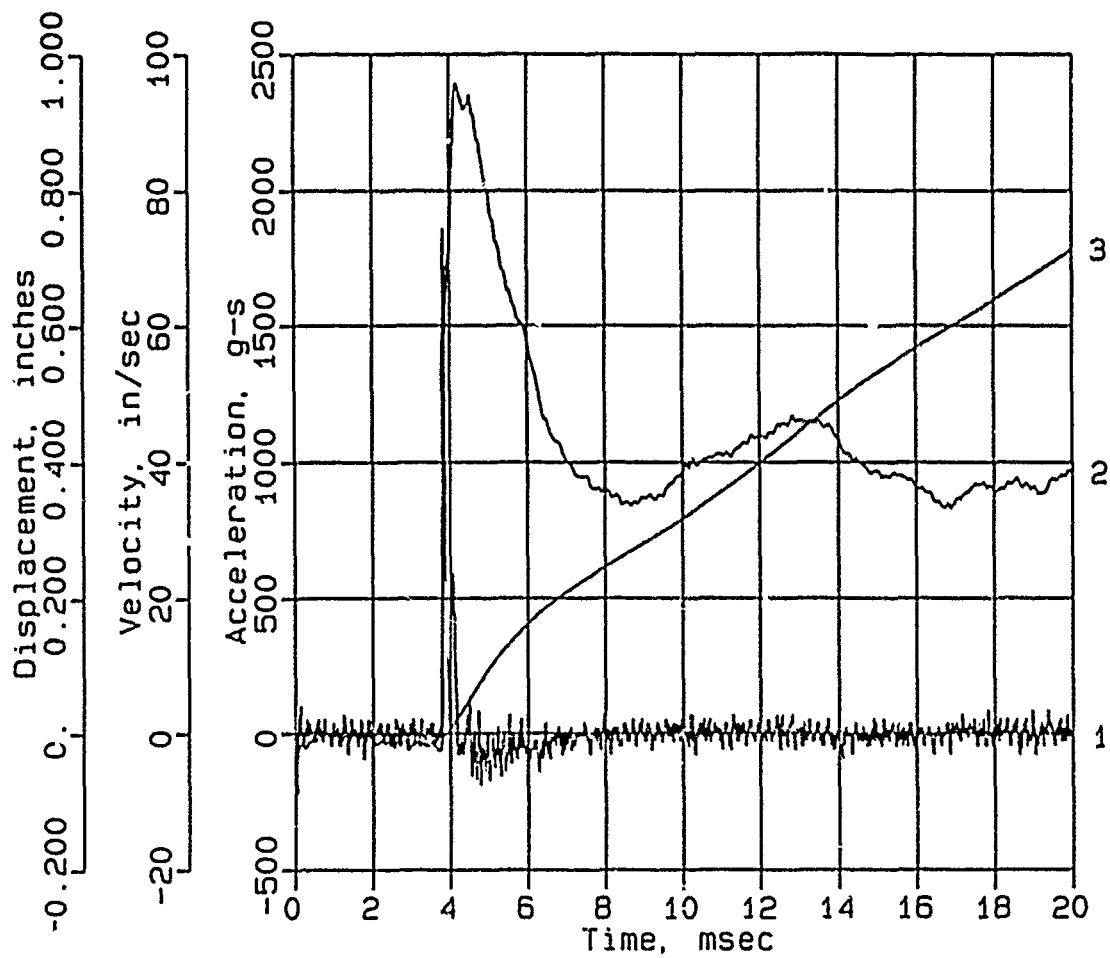
CONWEB T2
AHF-6
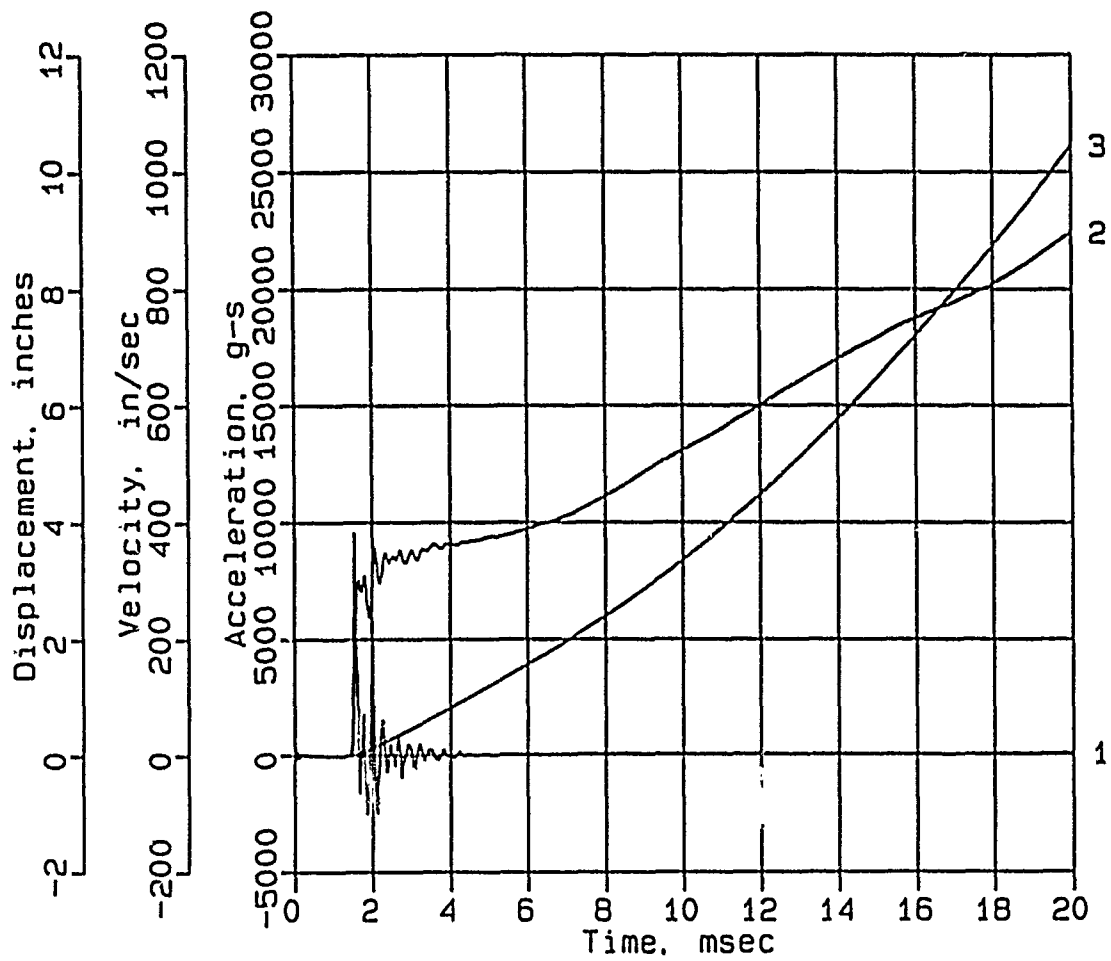
Digitizing rate: 200,000 Hz
Calibration: 7400
Constant Baseline Shift

CONWEB T2
AHF-7

Digitizing rate: 200,000 Hz
Calibration: 10271
Constant Baseline Shift

B24
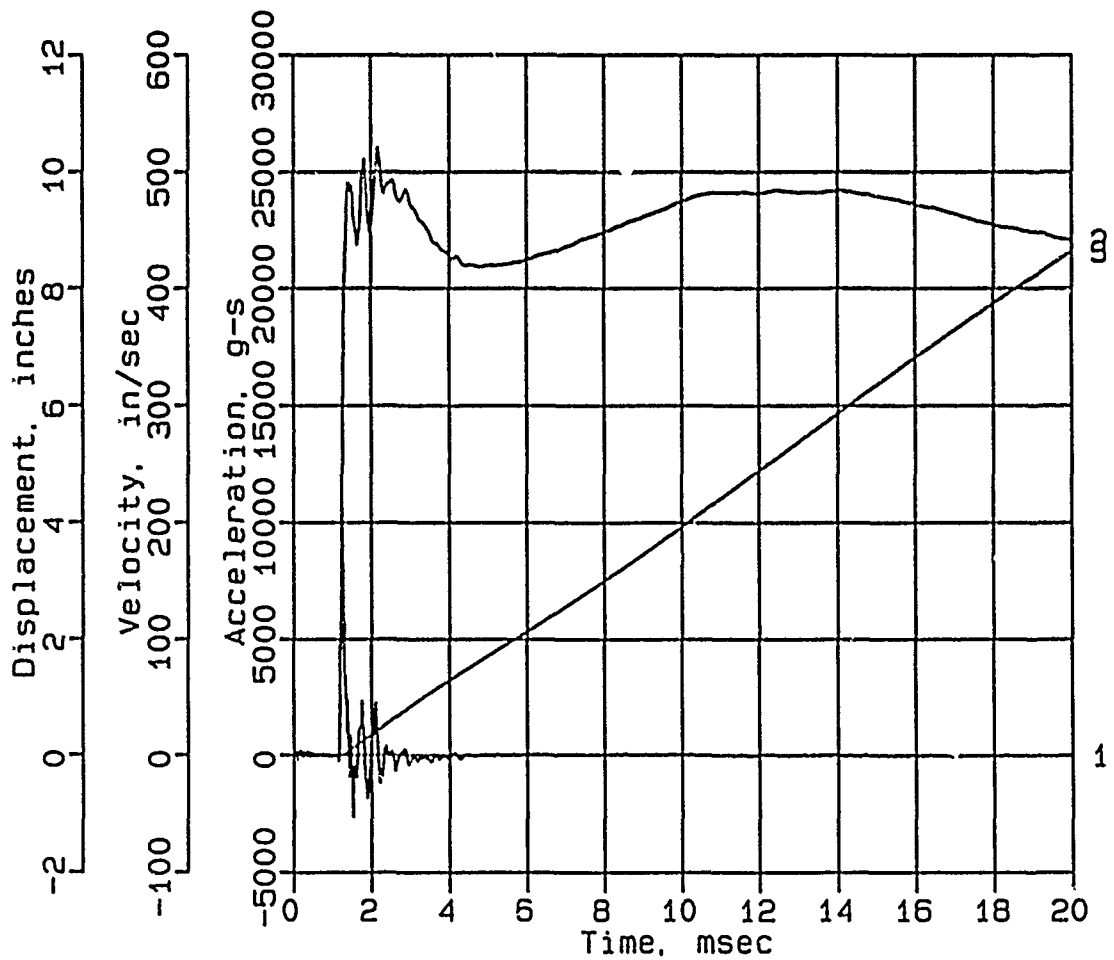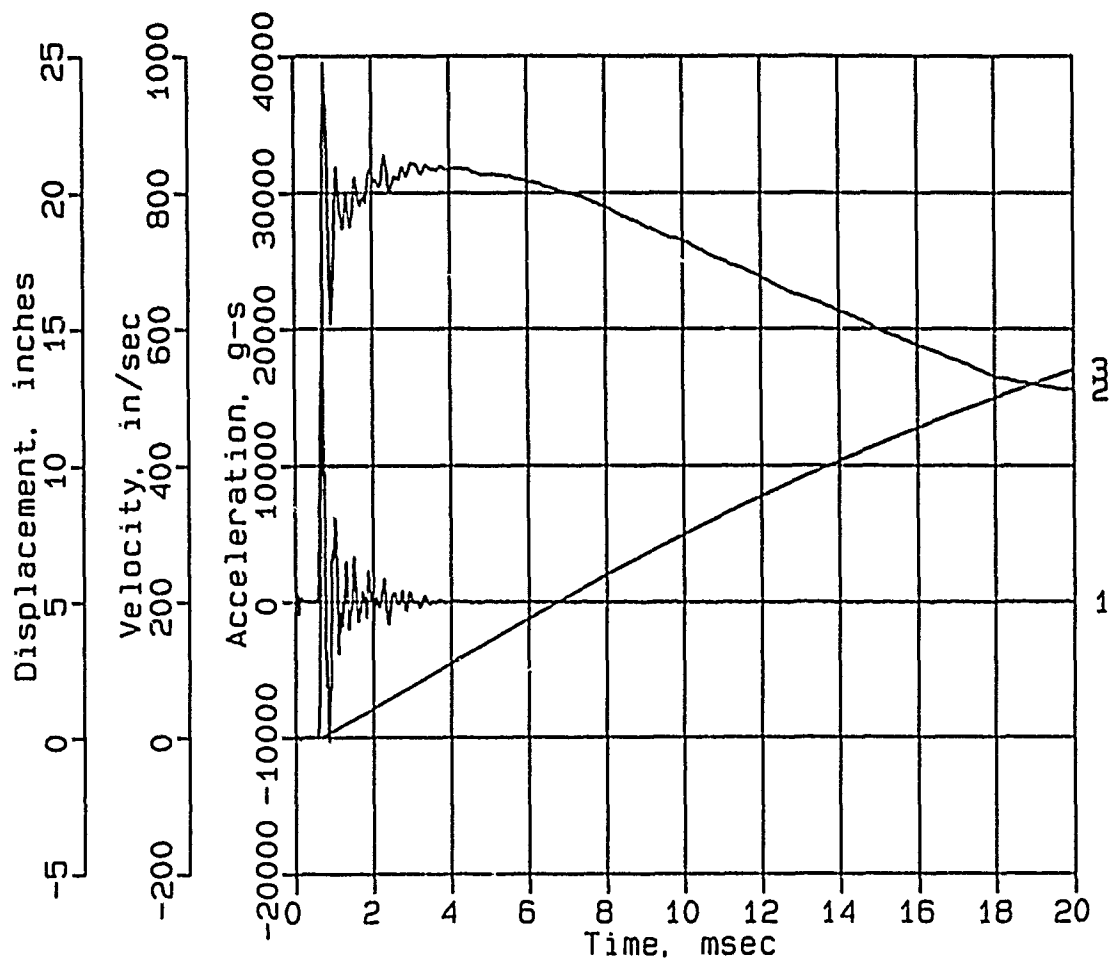
CONWEB T2
AHF-8

Digitizing rate: 200,000 Hz
Calibration: 24286
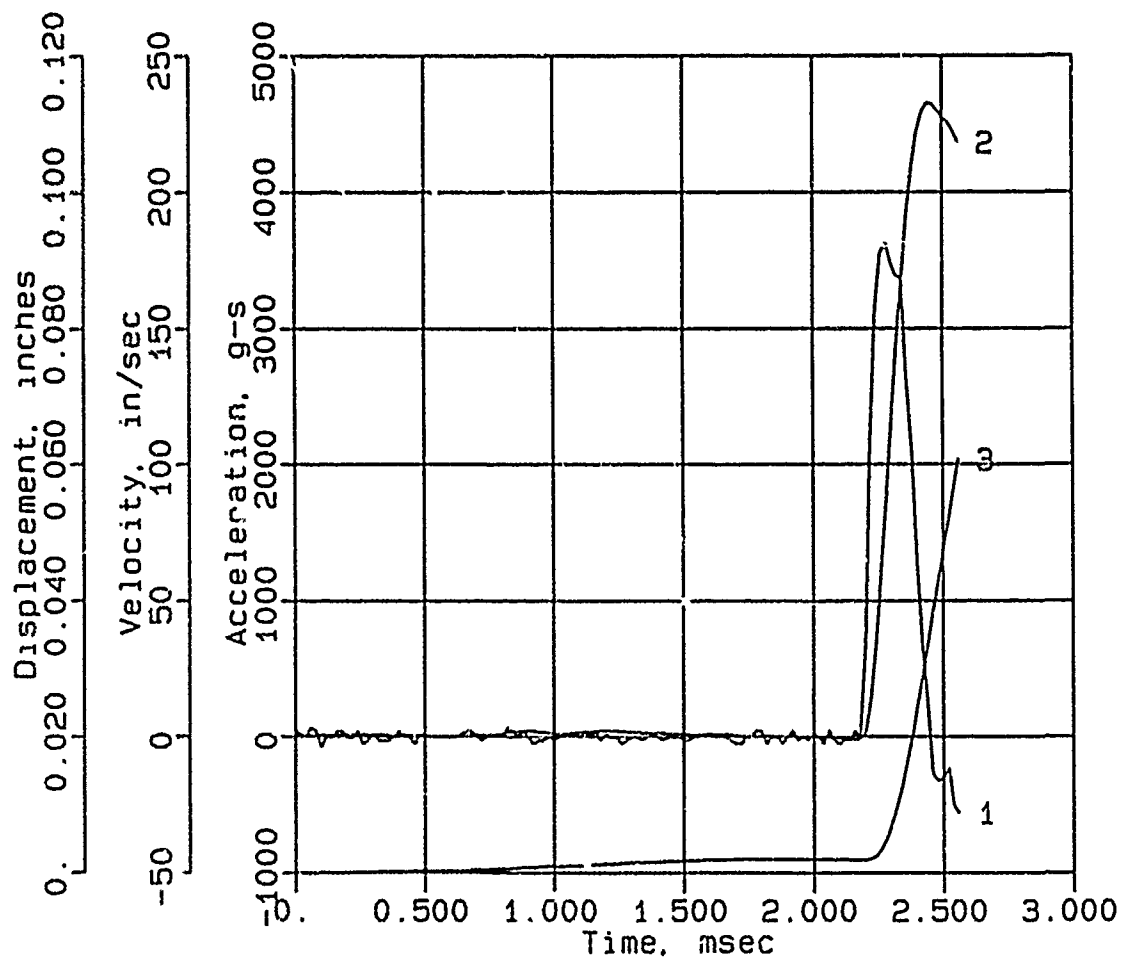Constant Baseline Shift

CONWEB T2
AHF-9
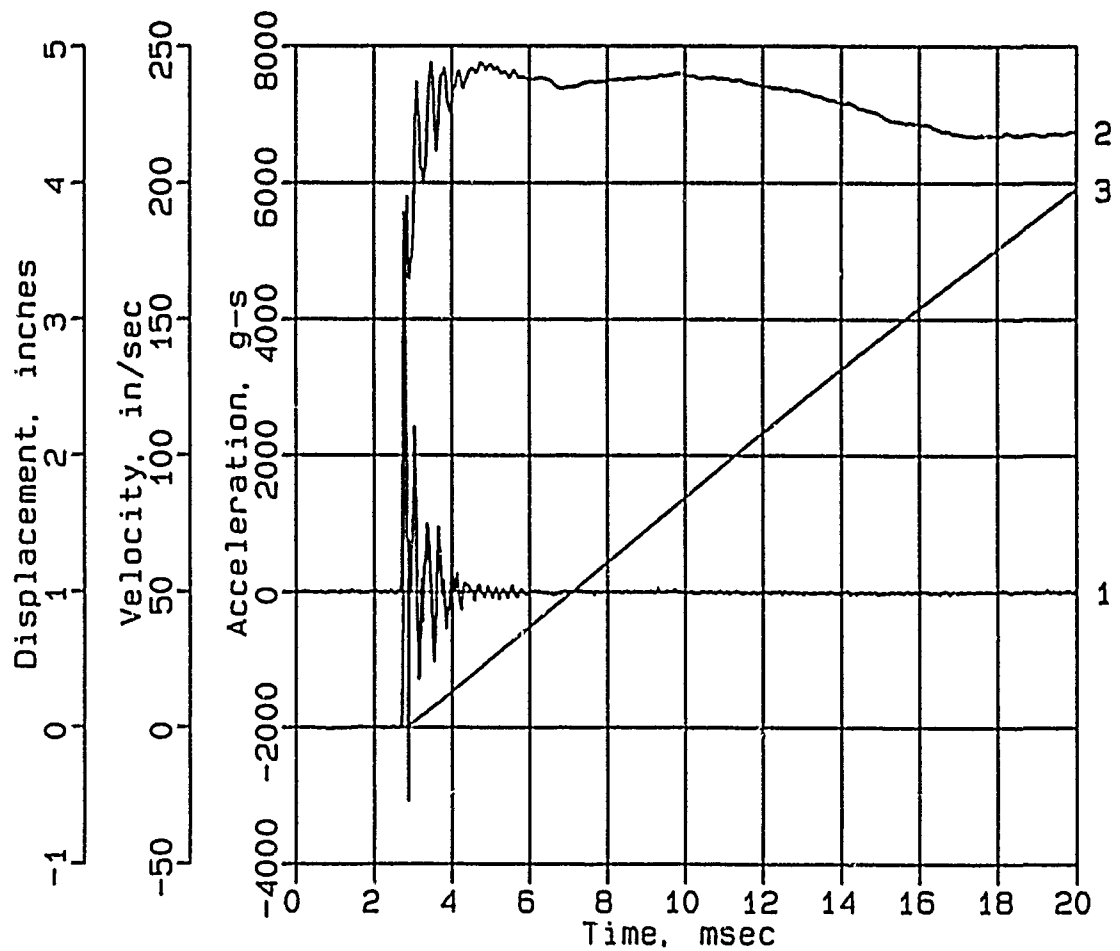
Digitizing rate: 200,000 Hz
Calibration: 11735
Constant Baseline Shift

CONWEB T2
AHF-10
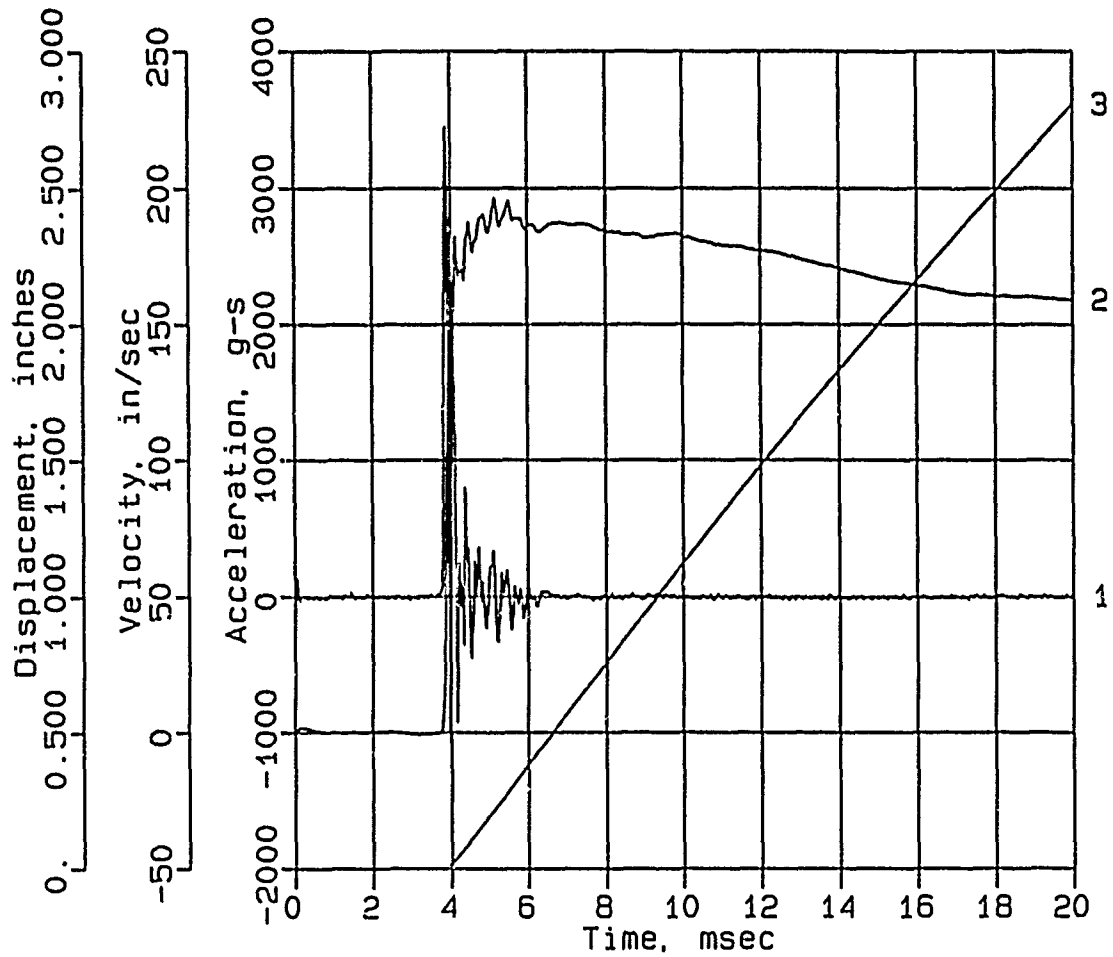
Digitizing rate: 200,000 Hz
Calibration: 5928
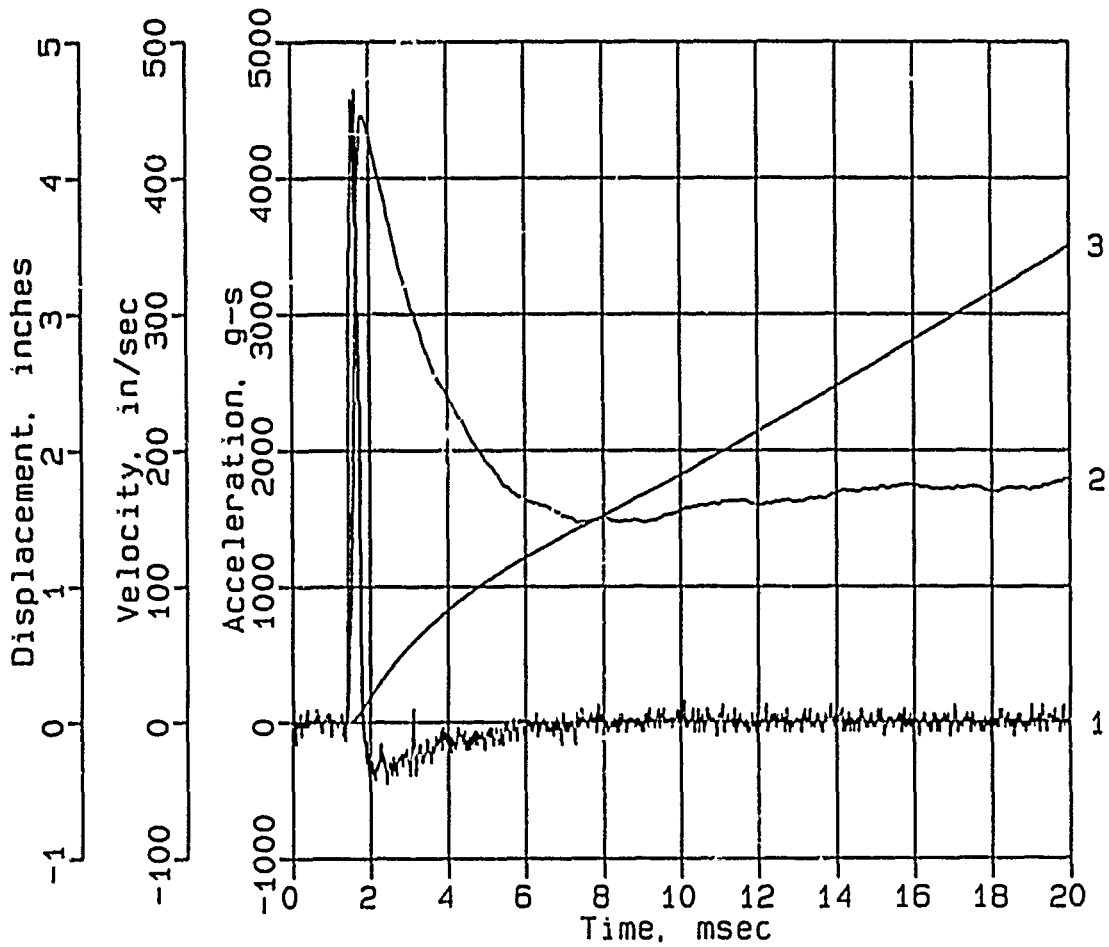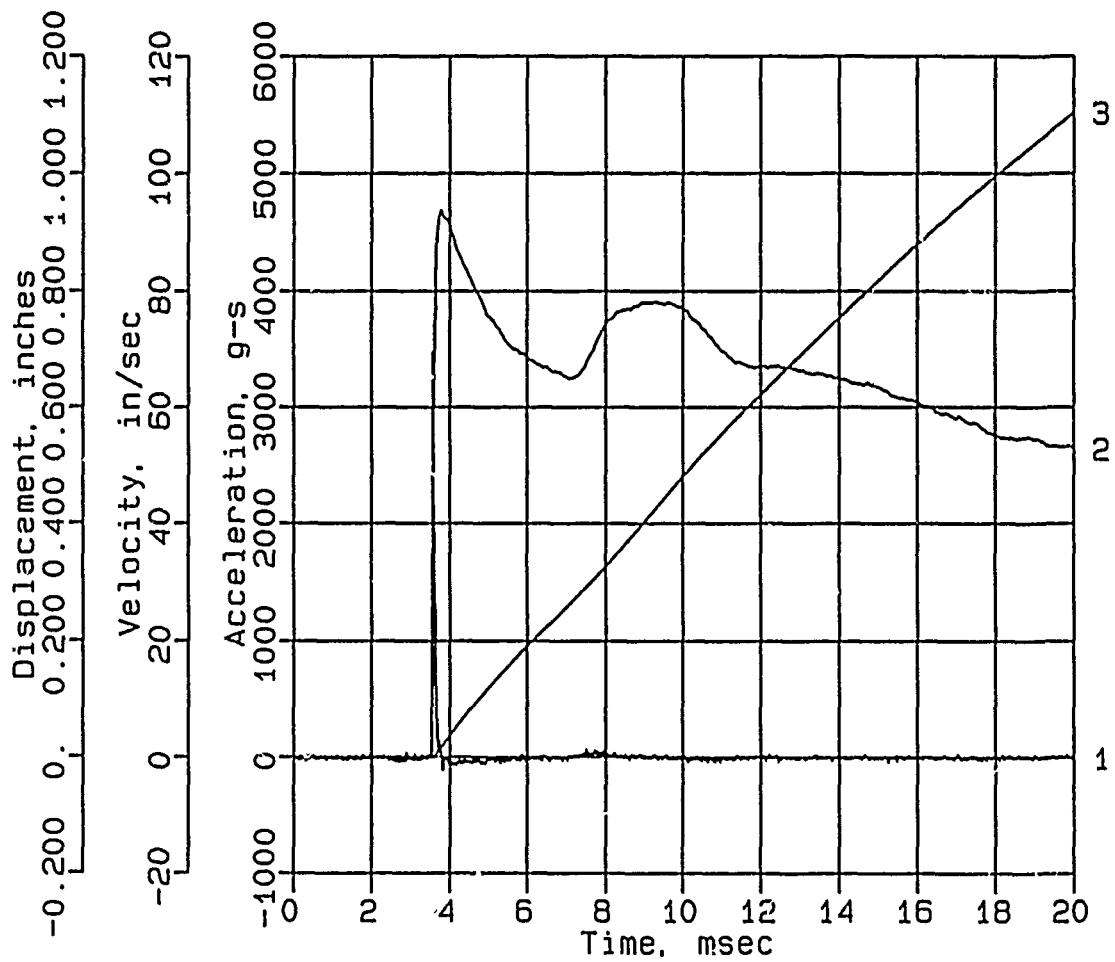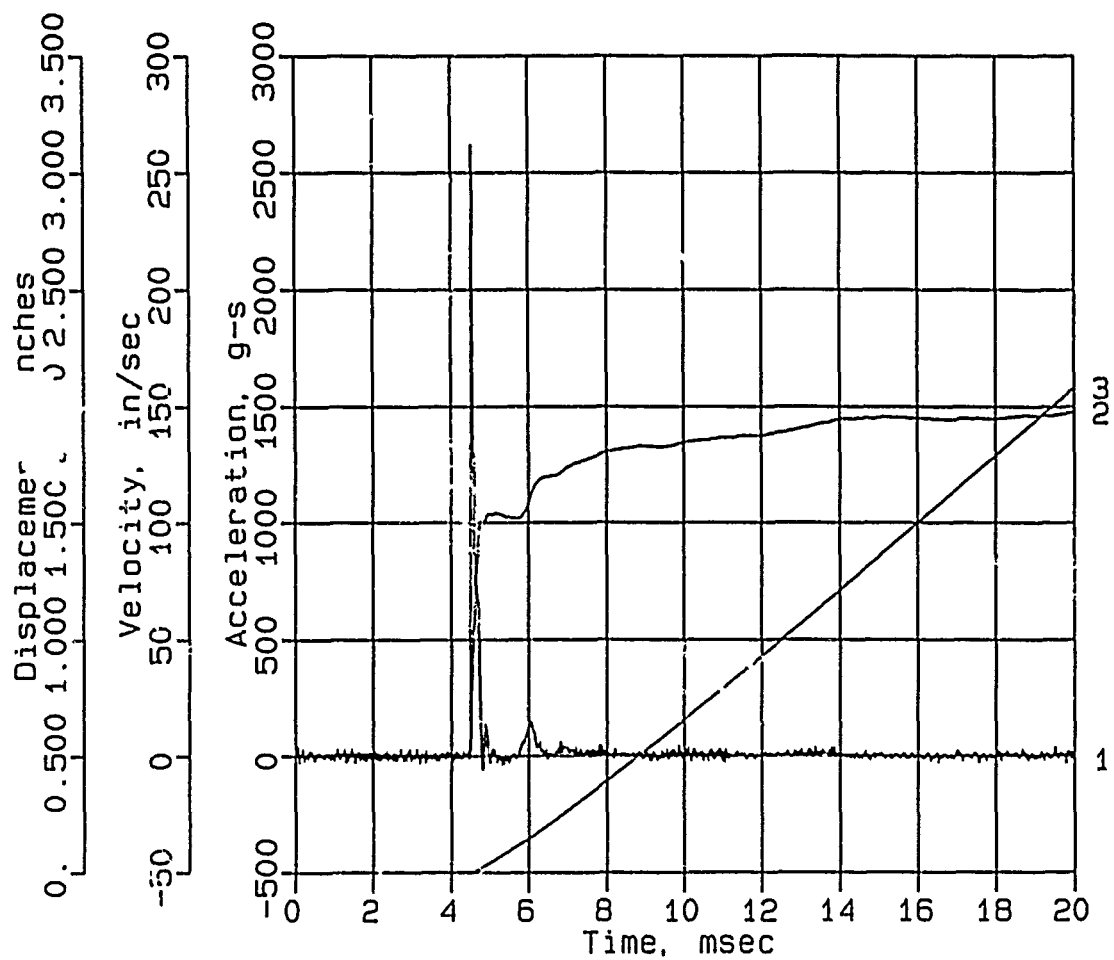Constant Baseline Shift

CONWEB T2
AHF-11
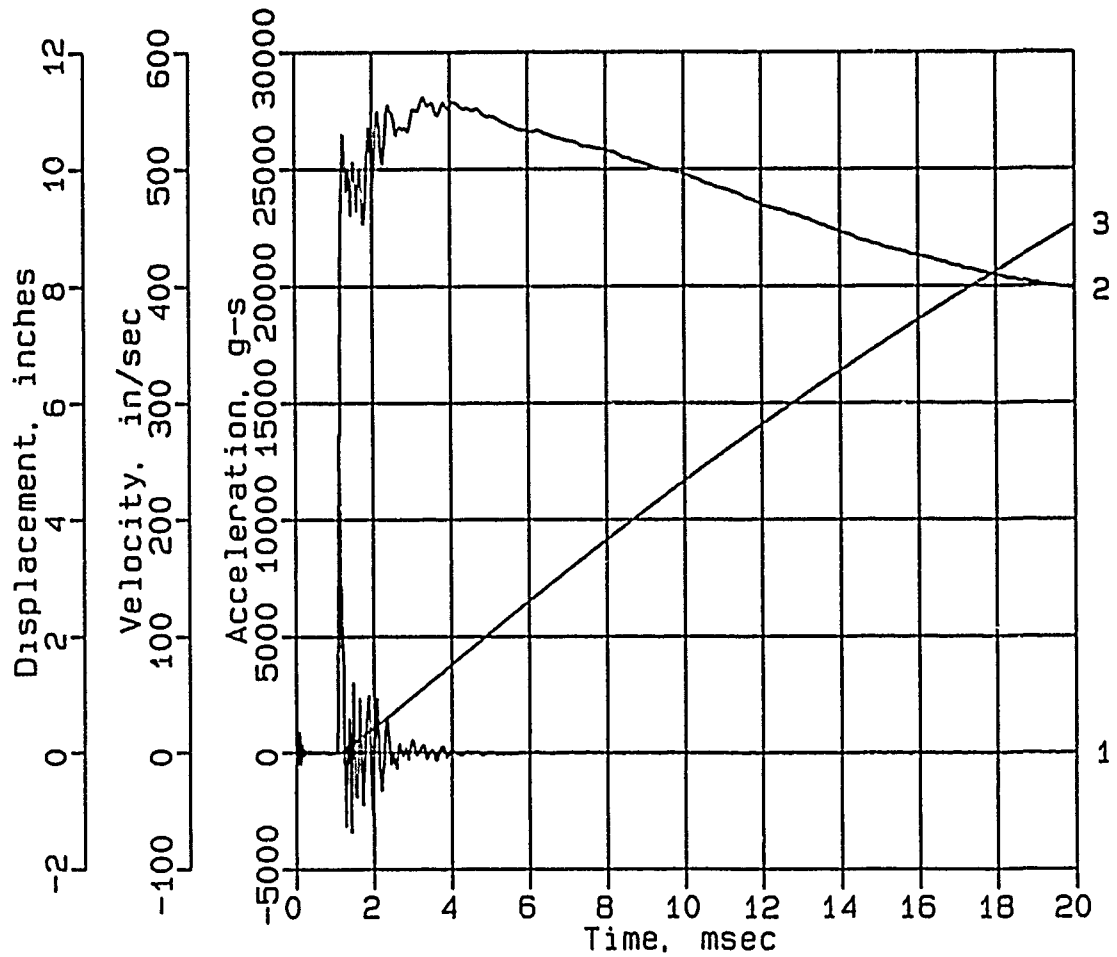
Digitizing rate: 200,000 Hz
Calibration: 12330
Constant Baseline Shift

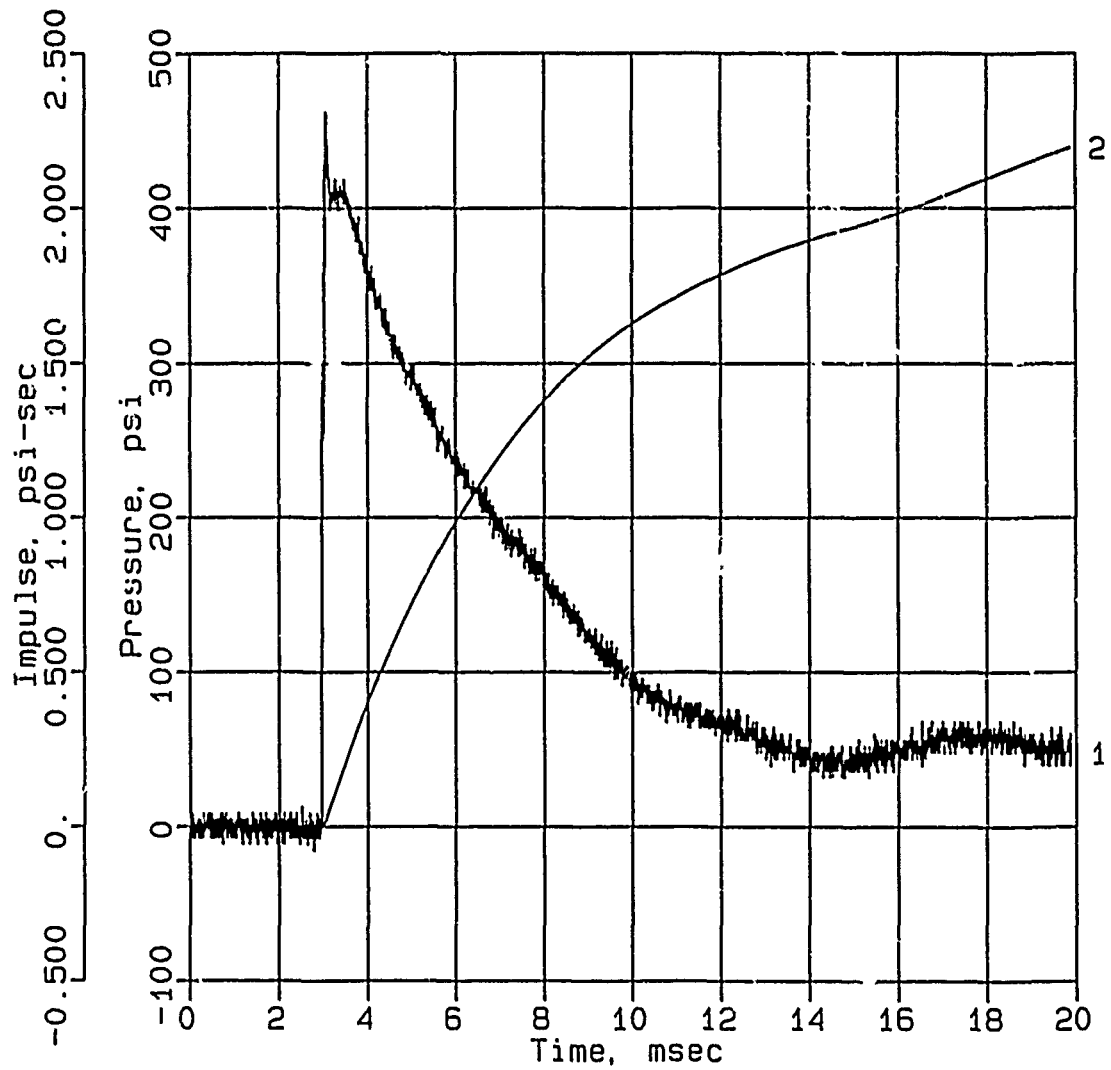# CONWEB T2
AHF-12
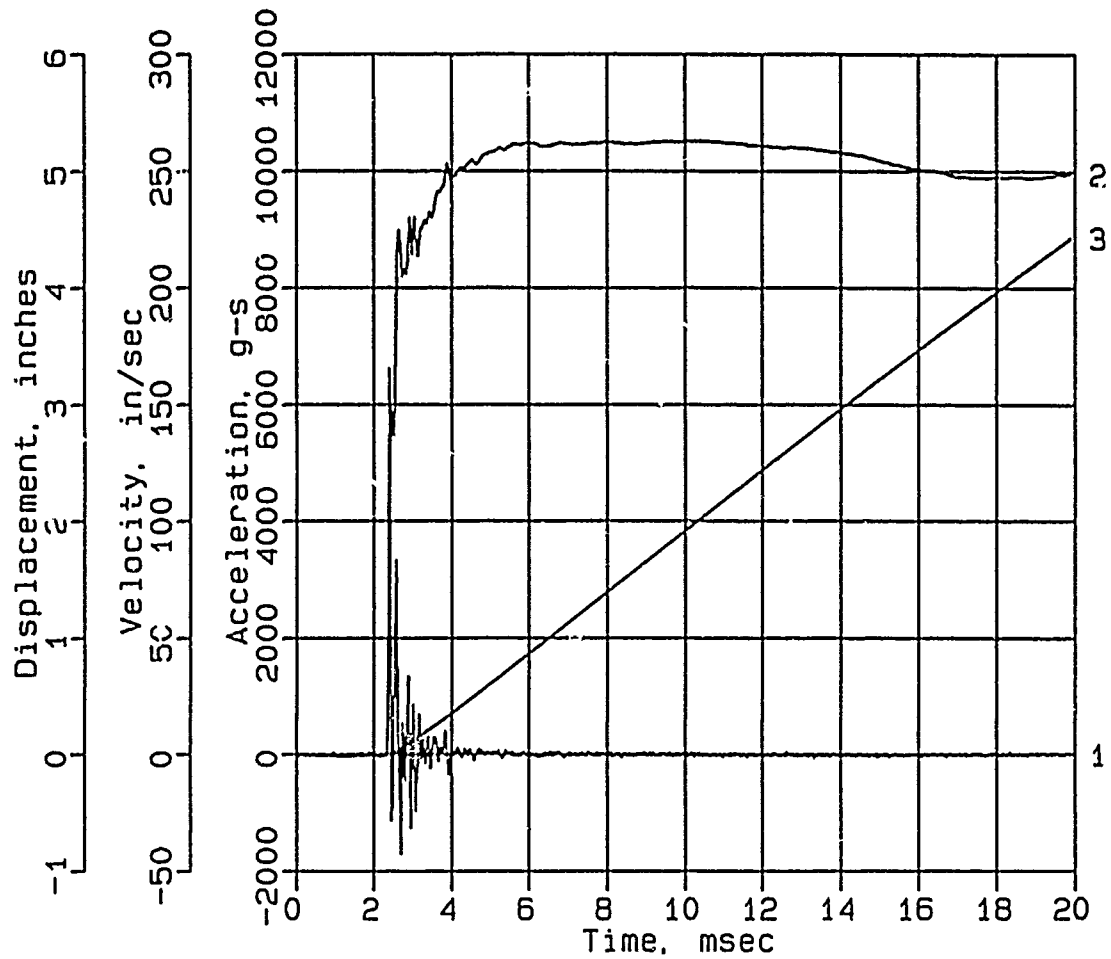
Digitizing rate: 200,000 Hz
Calibration: 9944
Constant Baseline Shift

CONWEB T2
SE-1
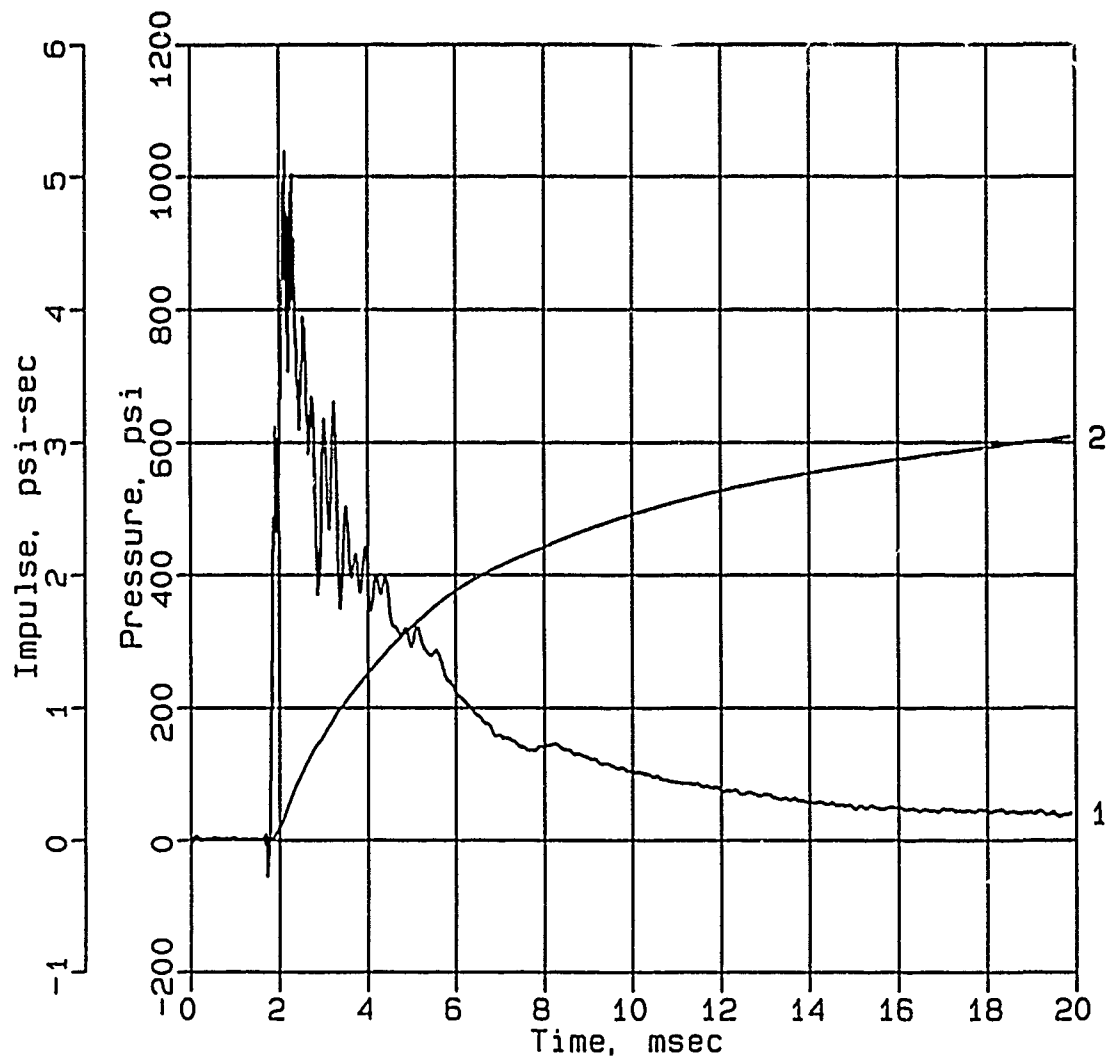
Digitizing rate: 200,000 Hz
Calibration: 3282
Filtering: 20 kHz low pass filter
           5 - 17 kHz band rejection filter

CONWEB T2
SE-3

Digitizing rate: 200,000 Hz
Calibration: 3168
Filtering: 20 kHz low pass filter
            5 - 17 kHz band rejection filter

CONWEB T2
SE-4

Digitizing rate: 200,000 Hz
Calibration: 5095
Filtering: 20 kHz low pass filter
5 - 17 kHz band rejection filter
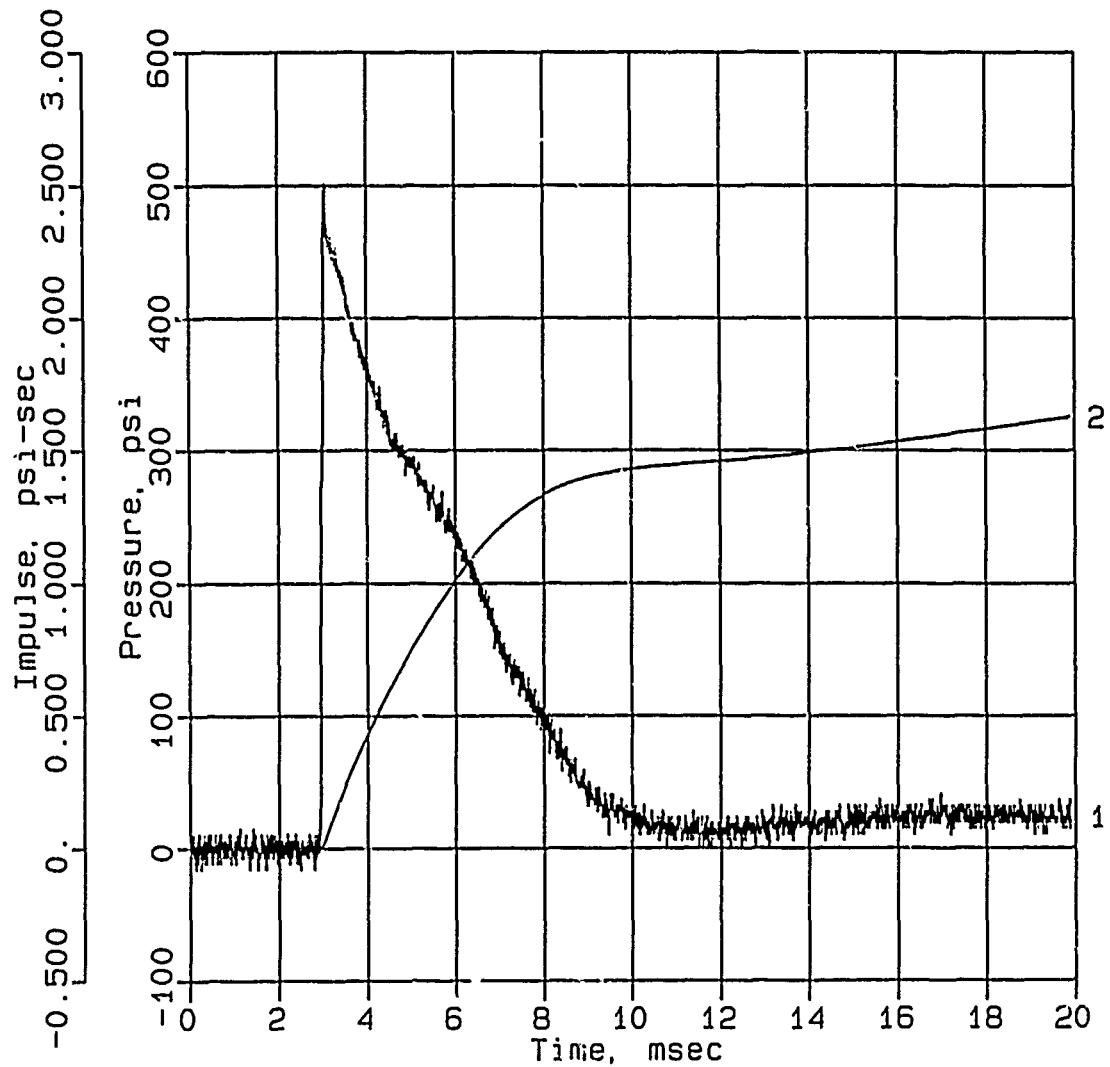
B32

CONWEB T2
SE-6

Digitizing rate: 200,000 Hz
Calibration: 2969
Filtering: 20 kHz low pass filter
5 - 17 kHz band rejection filter

CONWEB T2
SE-7

Digitizing rate: 200,000 Hz
Calibration: 10160
Filtering: 20 kHz low pass filter
5 - 17 kHz band rejection filter

CONWEB T2
SE-9

Digitizing rate: 200,000 Hz
Calibration: 2411
Filtering: 20 kHz low pass filter
            5 - 17 kHz band rejection filter

CONWEB T2

SE-10
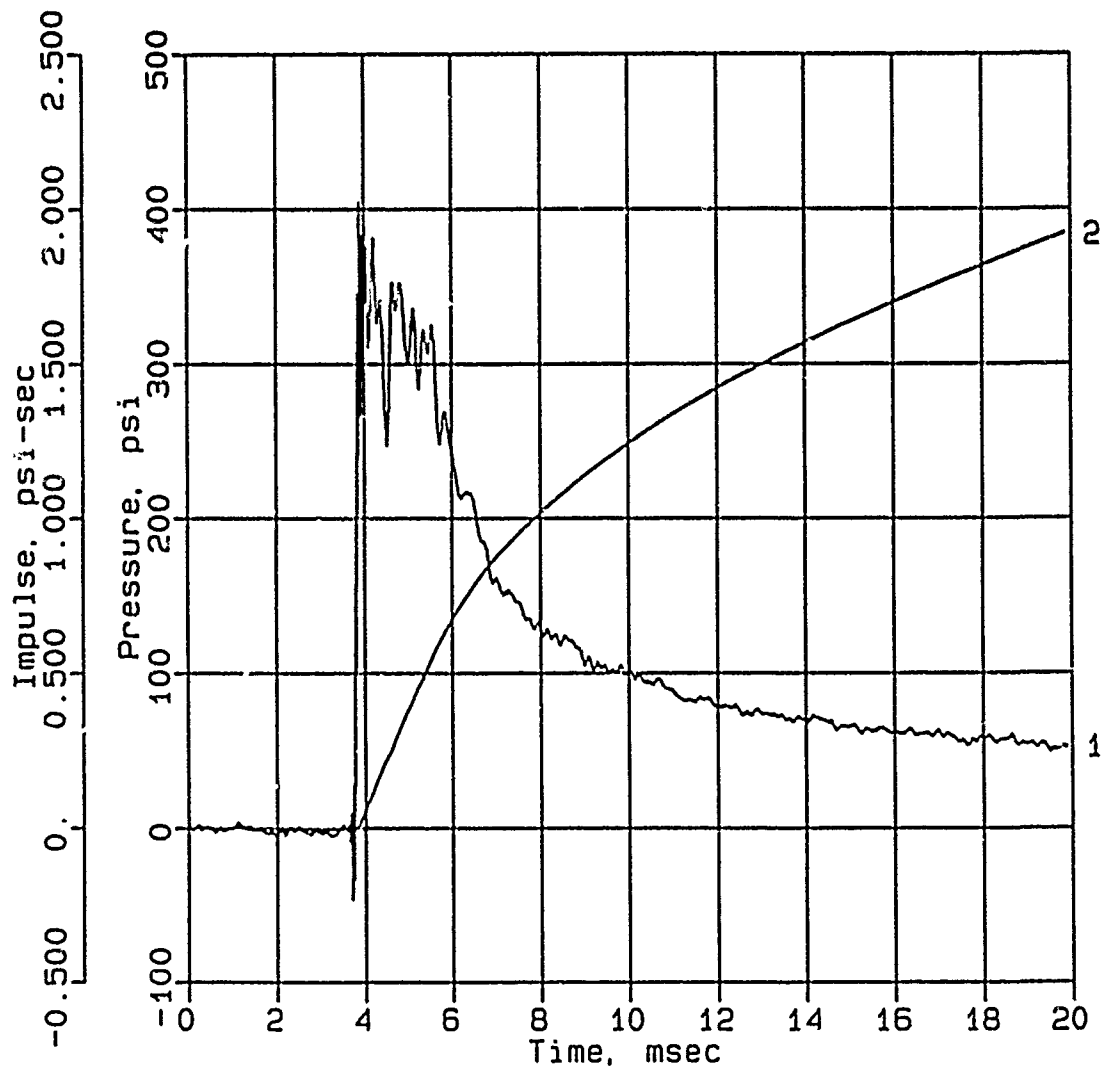
Digitizing rate: 200,000 Hz
Calibration: 2385
Filtering: 20 kHz low pass filter
            5 - 17 kHz band rejection filter

CONWEB T2
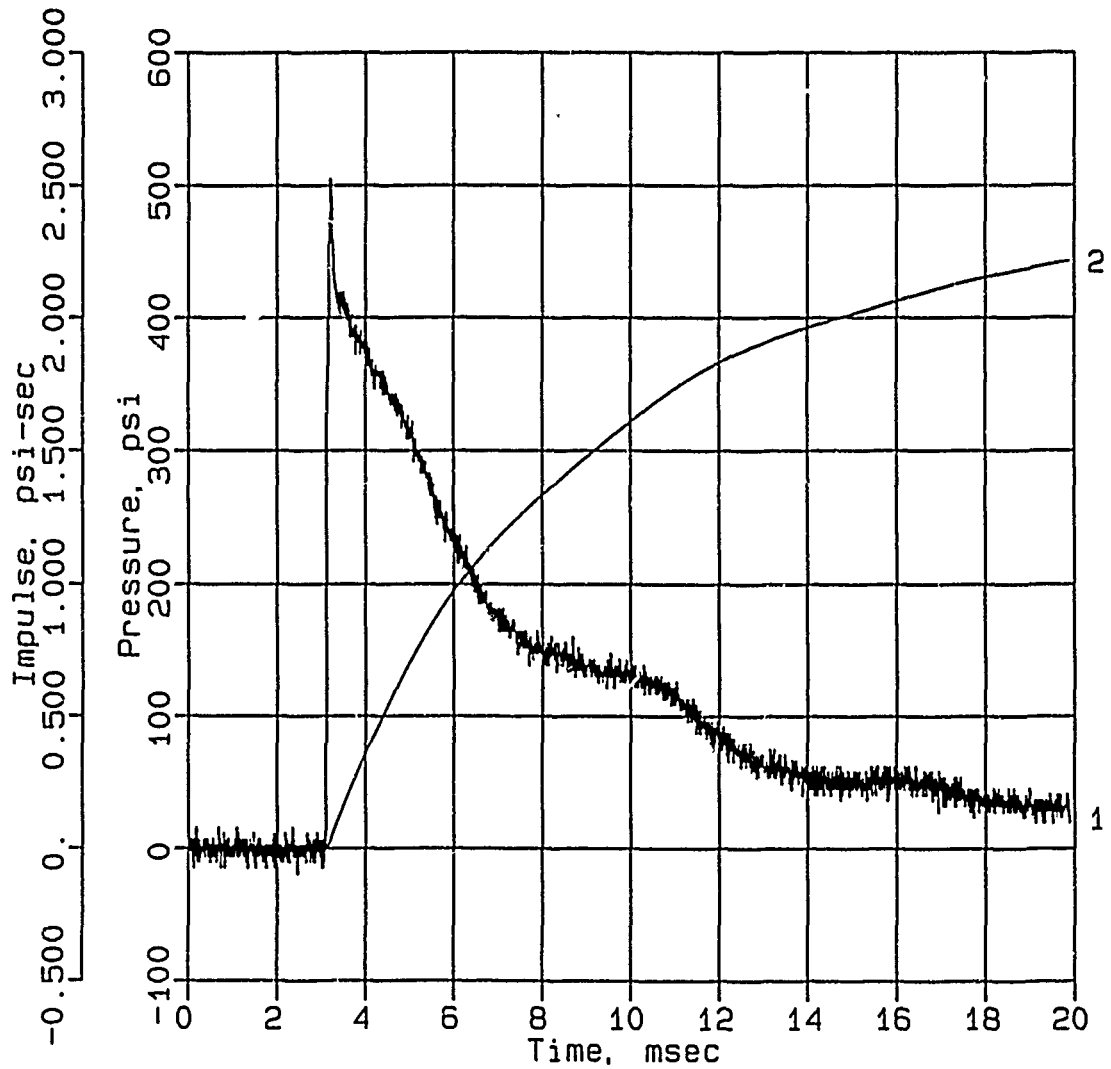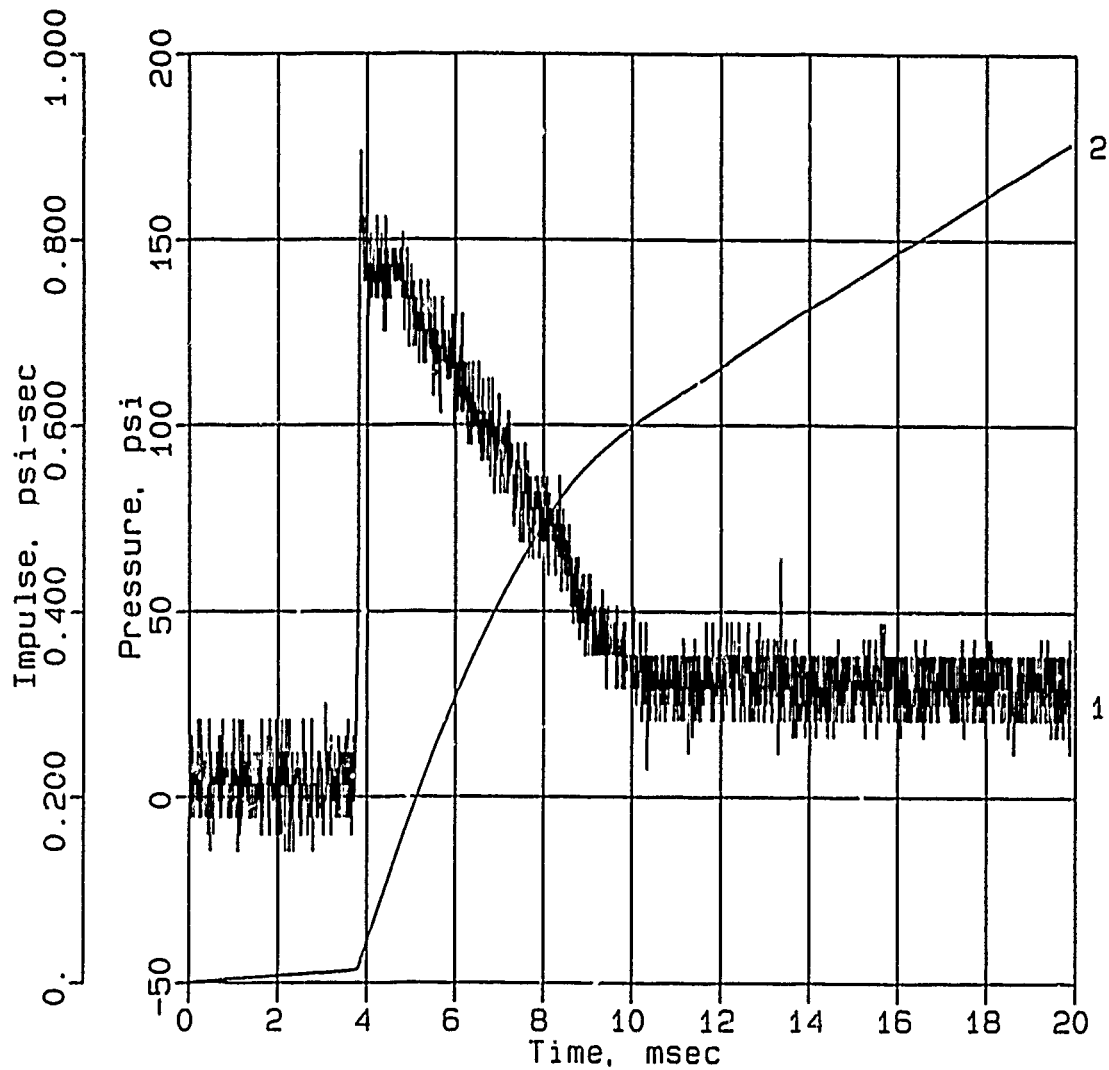## SE-11
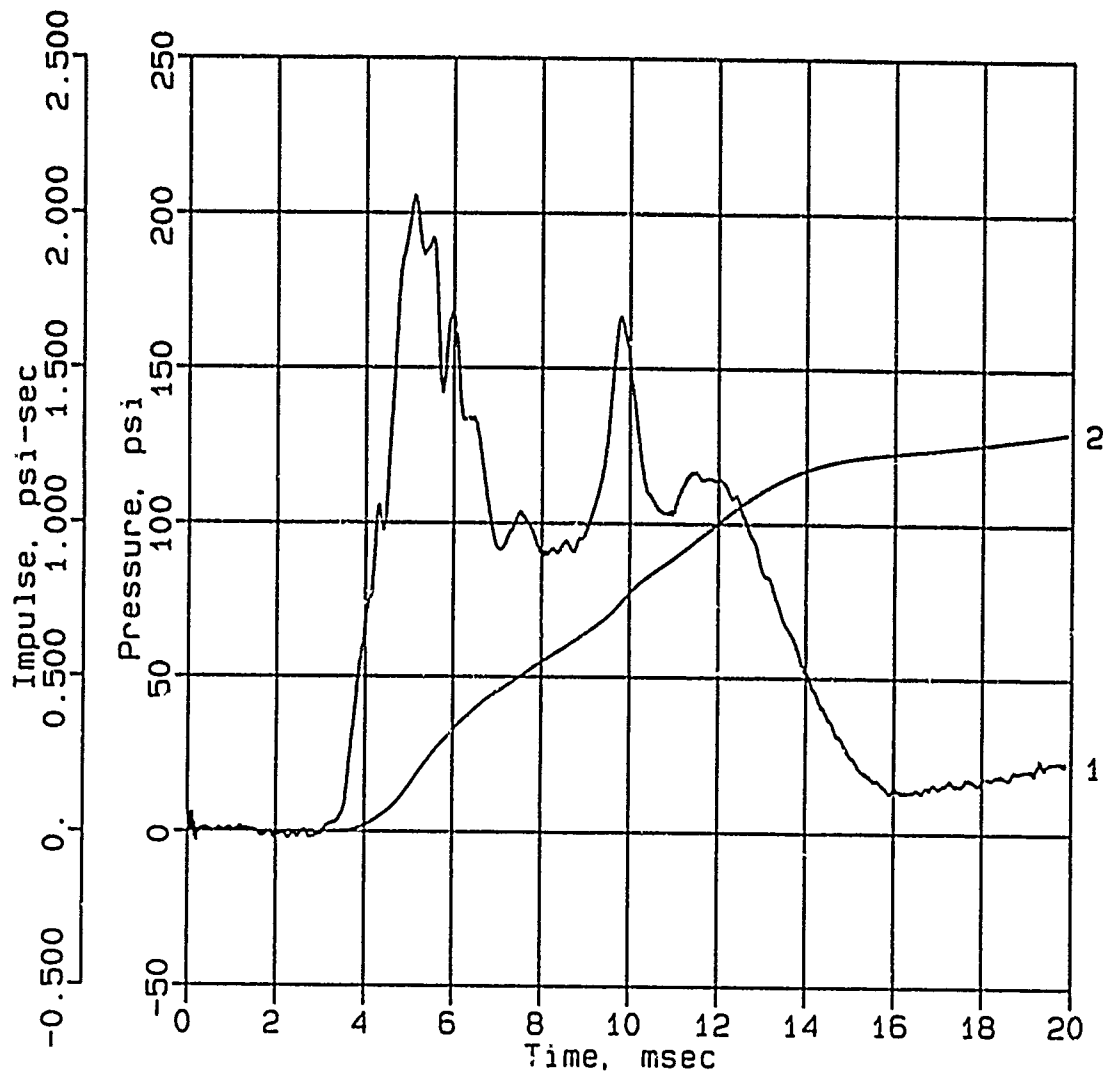
Digitizing rate: 200,000 Hz
Calibration: 866
Filtering: 20 kHz low pass filter
          5 - 17 kHz band rejection filter

CONWEB T2
SE-12
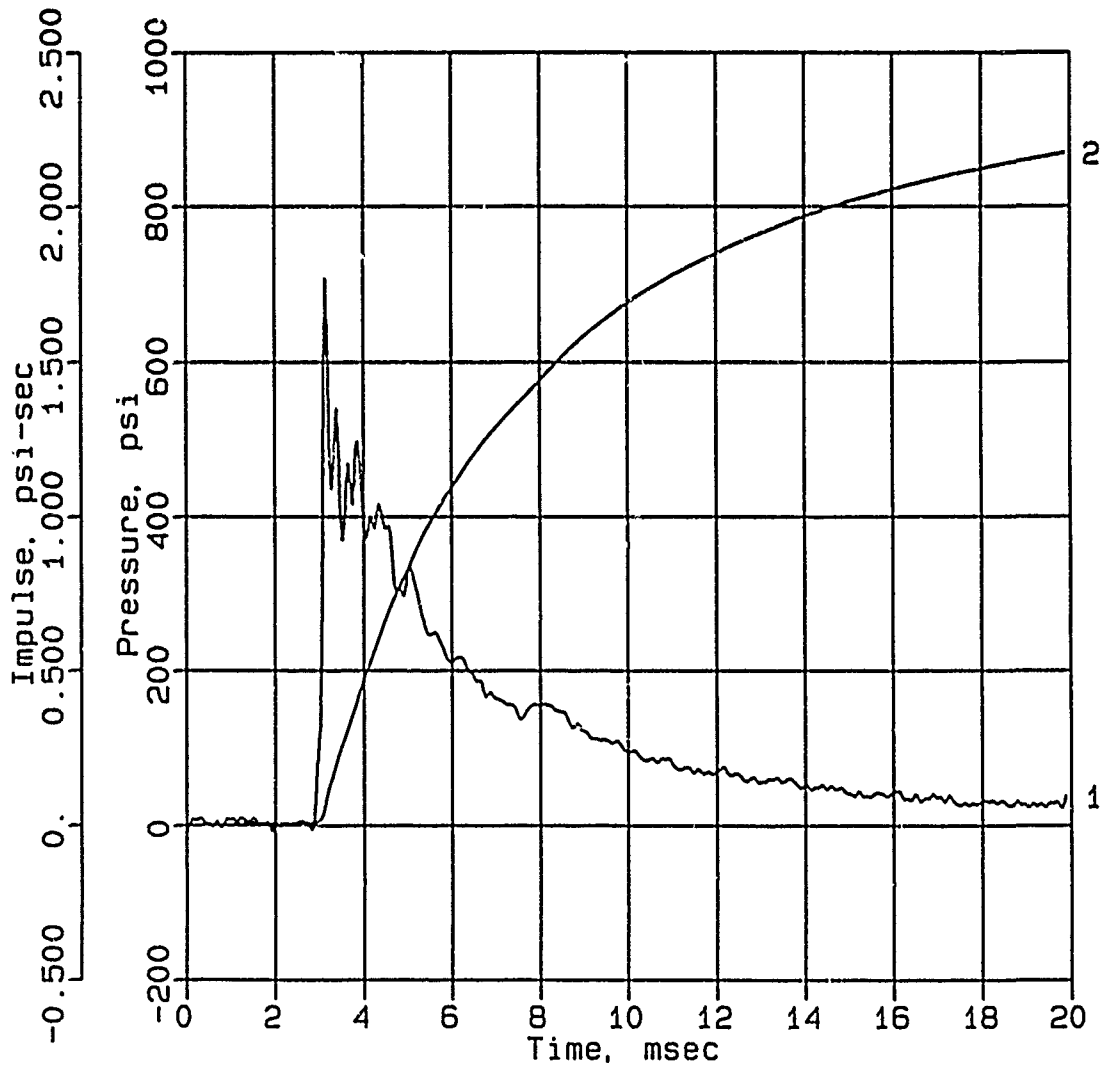
Digitizing rate: 200,000 Hz
Calibration: 5250
Filtering: 20 kHz low pass filter
        5 - 17 kHz band rejection filter
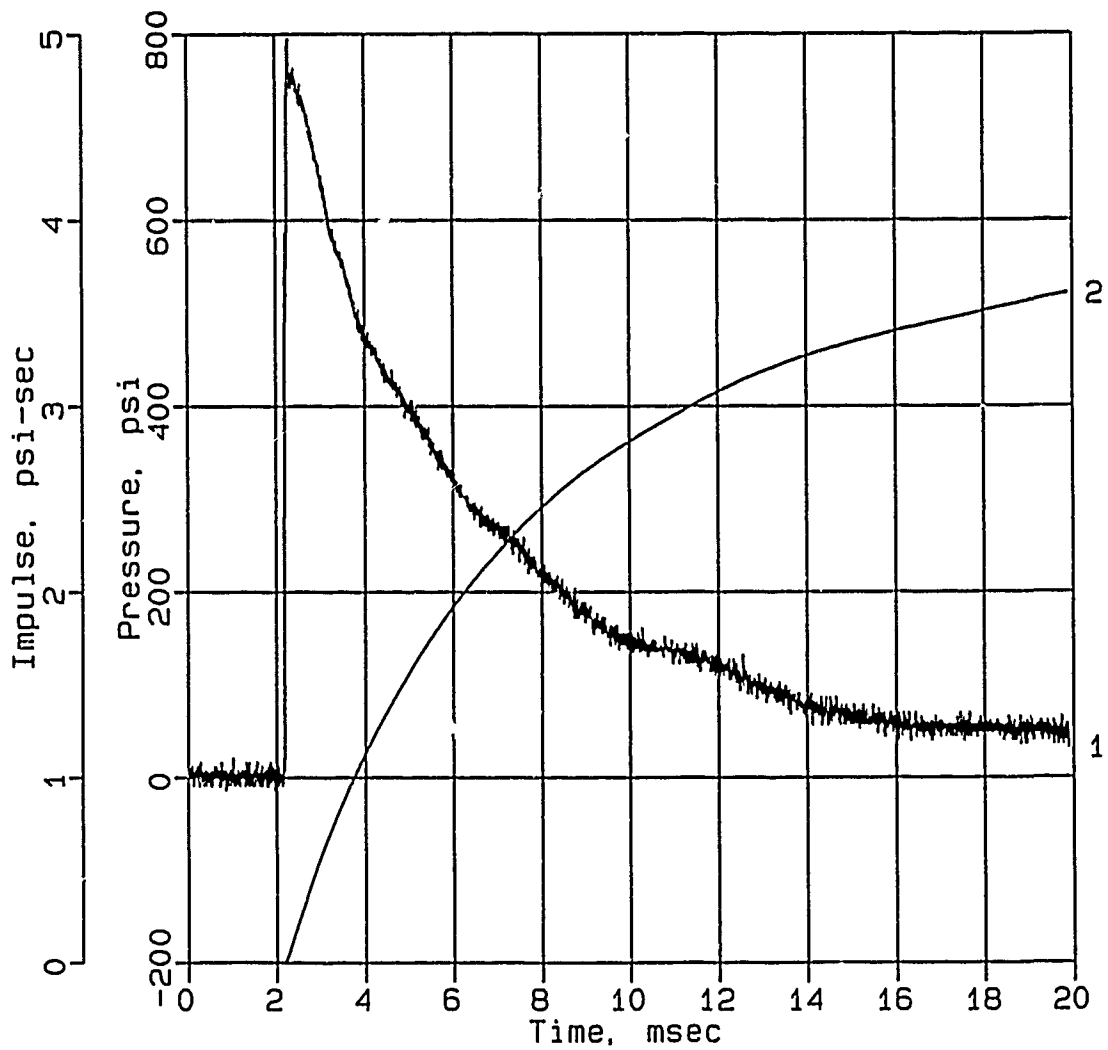
CONWEB T2
SE-13
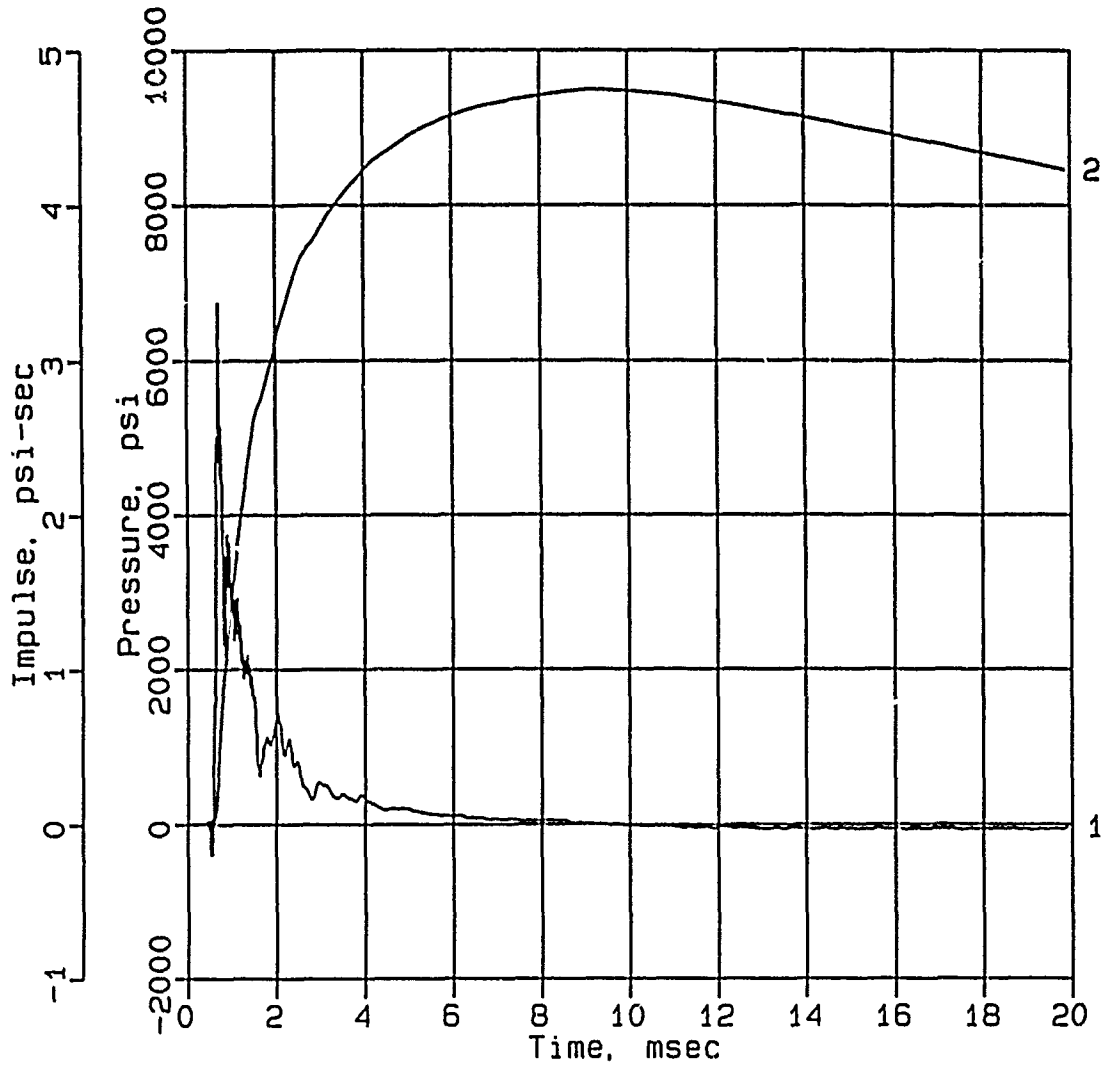
Digitizing rate: 200,000 Hz
Calibration: 10454
Filtering: 20 kHz low pass filter
        5 - 17 kHz band rejection filter

CONWEB T2
SE-14
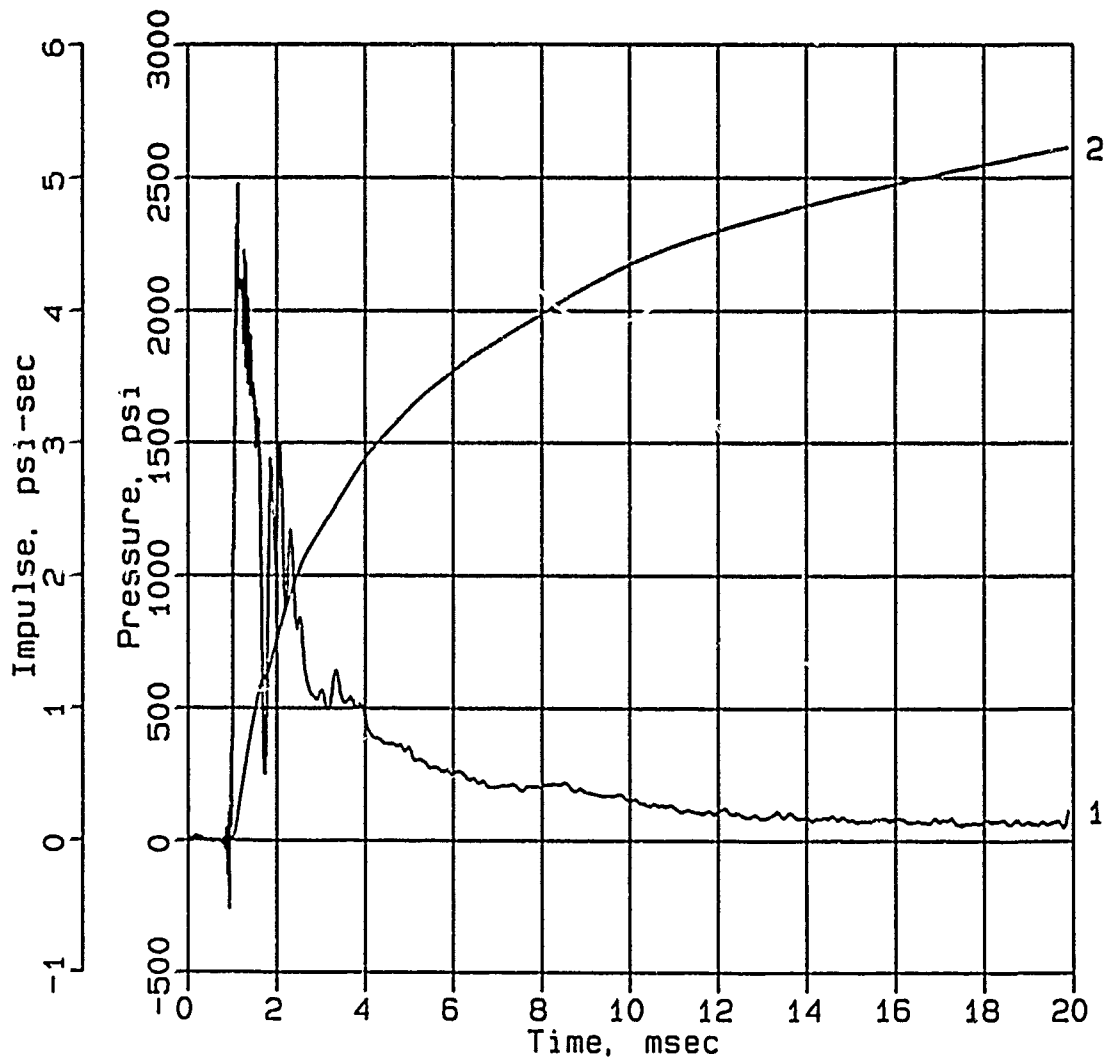
Digitizing rate: 200,000 Hz
Calibration: 10485
Filtering: 20 kHz low pass filter
            5 - 17 kHz band rejection filter
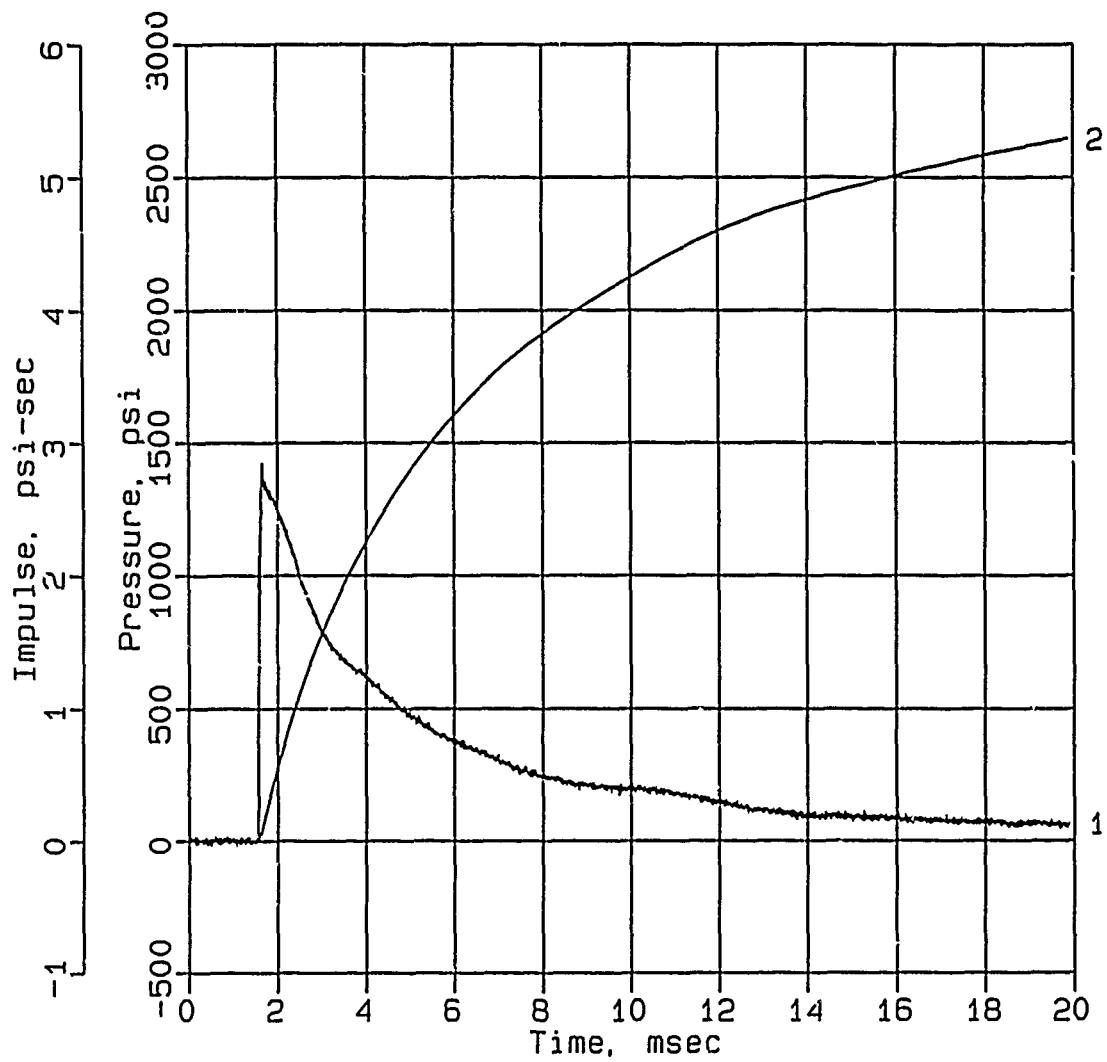
CONWEB T2
SE-15

Digitizing rate: 200,000 Hz
Calibration: 7838
Filtering: 20 kHz low pass filter
          5 - 17 kHz band rejection filter

APPENDIX C

DATA, BACKFILL TEST 3

Data from gages DEF-1, DEF-2, IF-5, and AHF-4 in Backfill Test 3 have not been included in this report.

CONWEB T3

IF-1

Digitizing rate: 200,000 Hz
Calibration: 2363
Filtering: 20 kHz low pass filter
              5 - 17 kHz band rejection filter
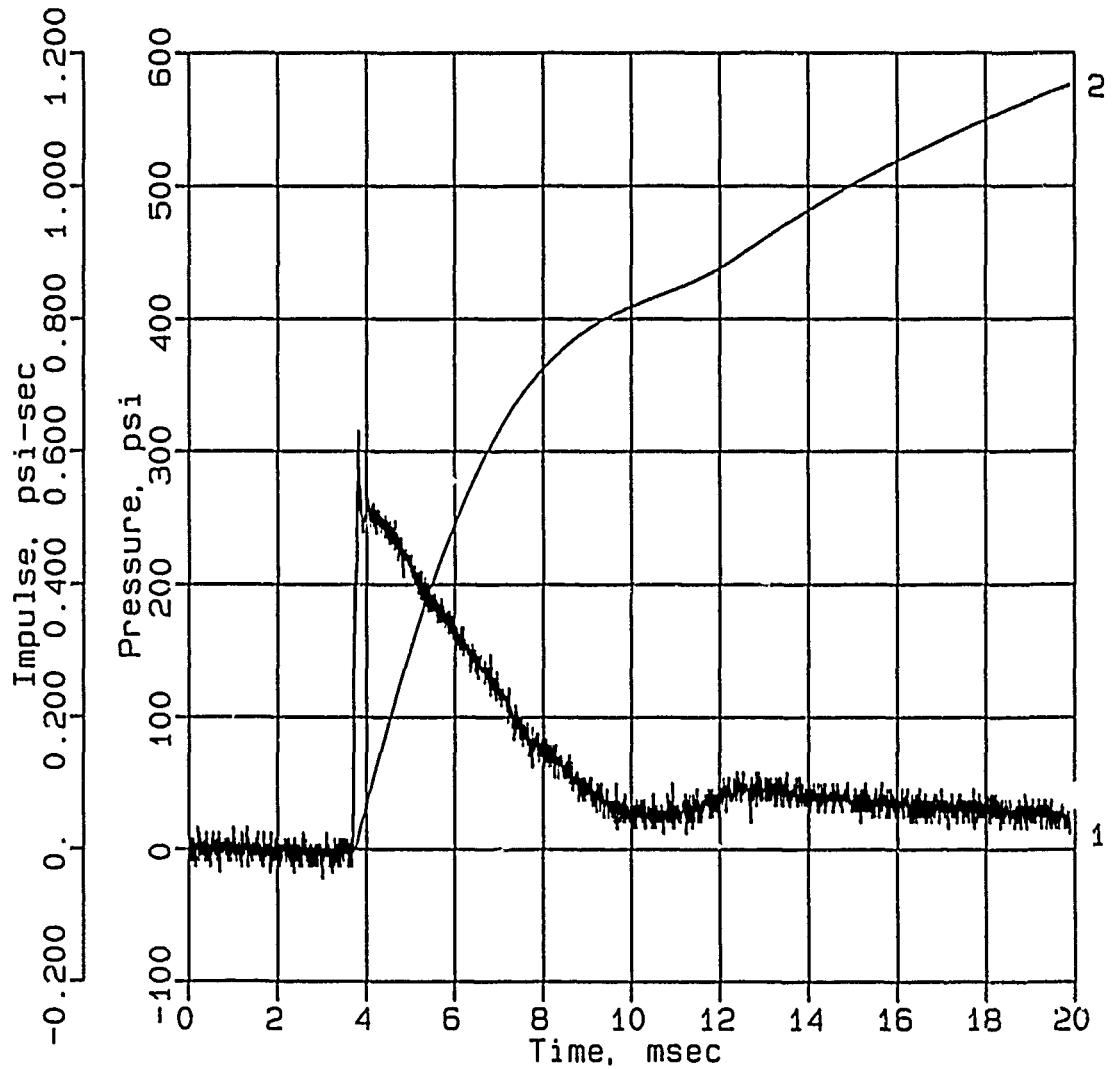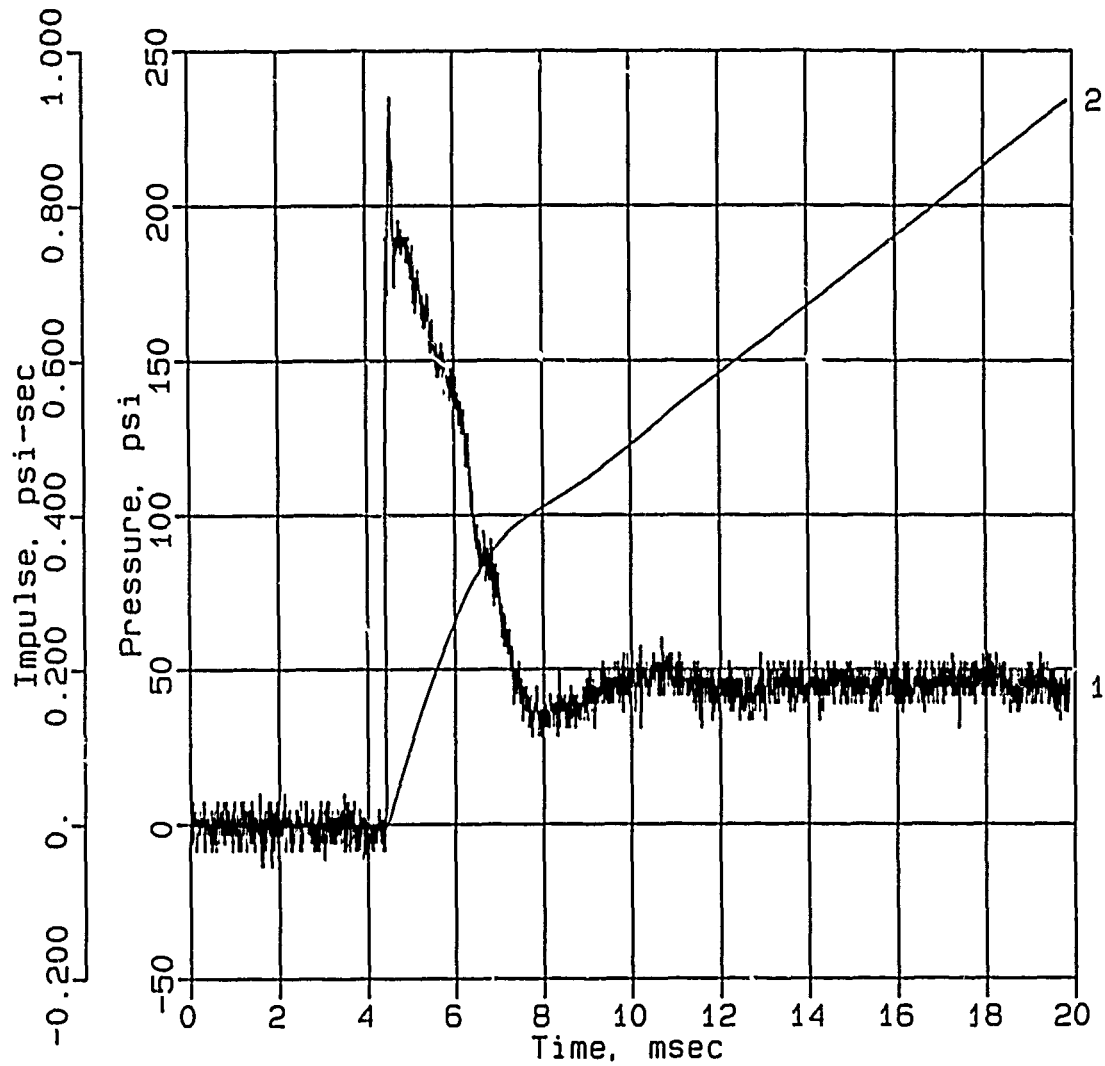
C3

CONWEB T3
IF-2

Digitizing rate: 200,000 Hz
Calibration: 2718
Filtering: 20 kHz low pass filter
            5 - 17 kHz band rejection filter
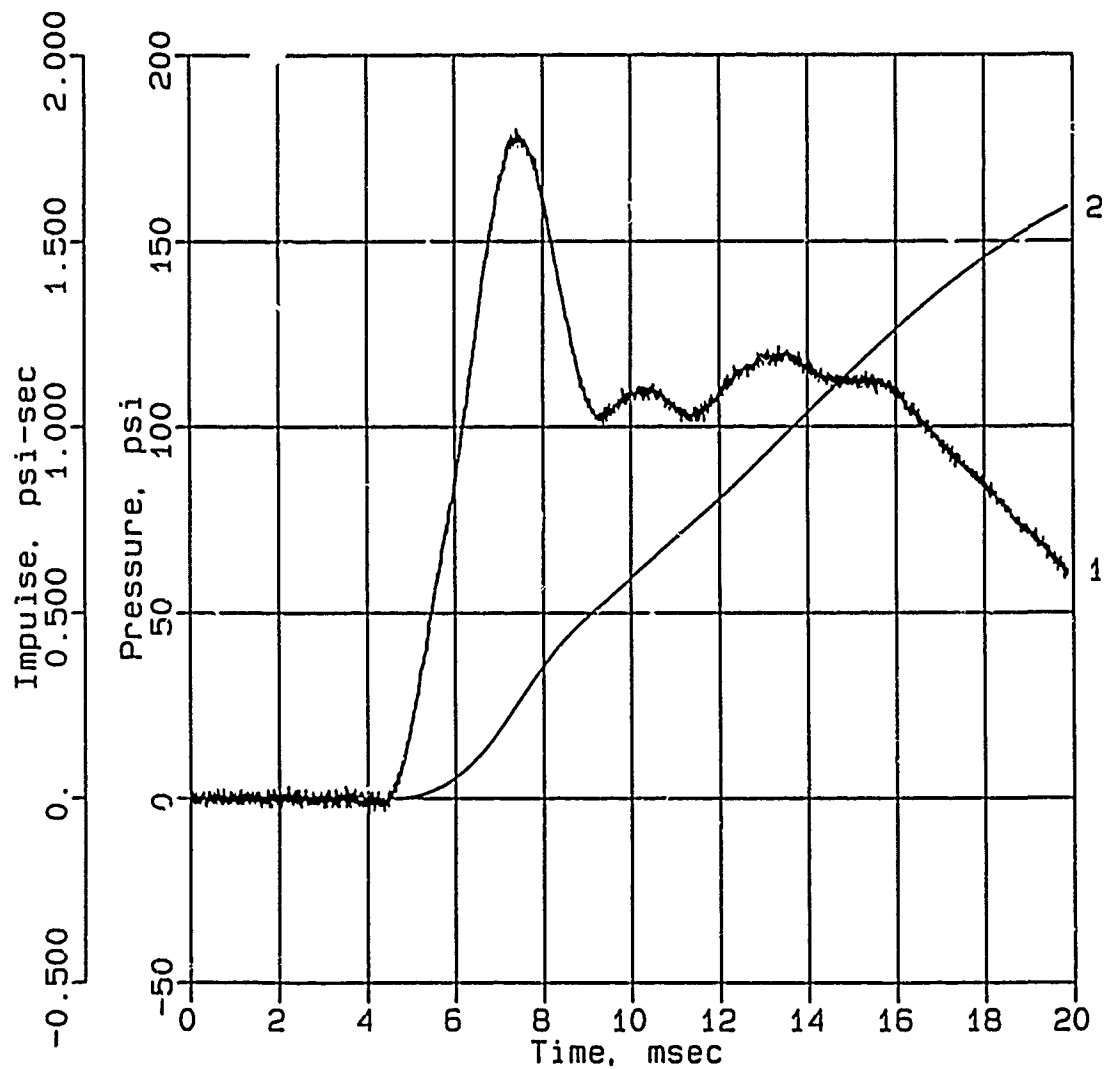
C4

CONWEB T3
IF-3

Digitizing rate: 200,000 Hz
Calibration: 2991
Filtering: 20 kHz low pass filter
        5 - 17 kHz band rejection filter

CONWEB T3
IF-6

Digitizing rate: 200,000 Hz
Calibration: 2660
Filtering: 20 kHz low pass filter
            5 - 17 kHz band rejection filter

CONWEB T3

IF-8

Digitizing rate: 200,000 Hz
Calibration: 2892
Filtering: 20 kHz low pass filter
            5 - 17 kHz band rejection filter

CONWEB T3
IF-9

Digitizing rate: 200,000 Hz
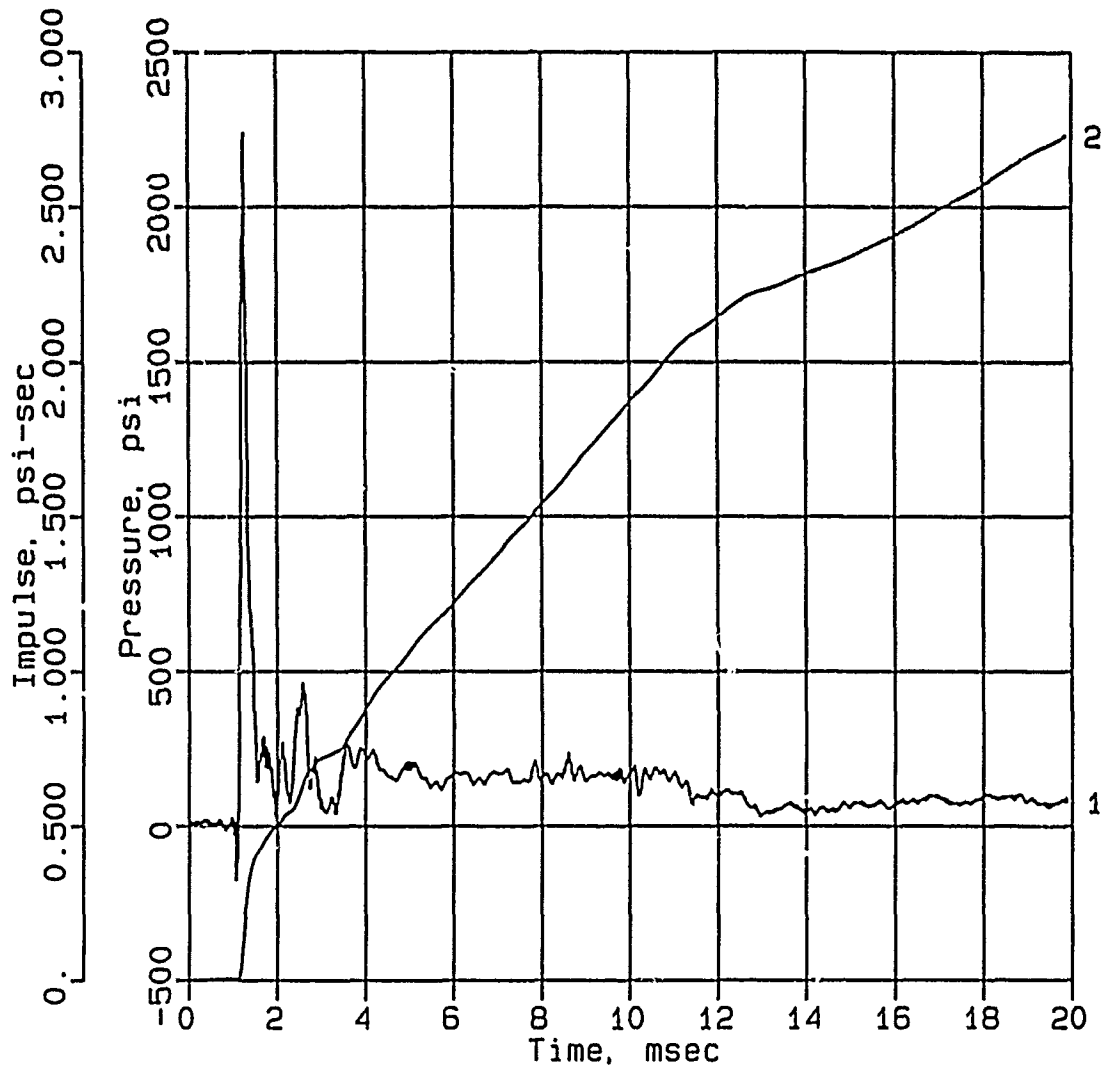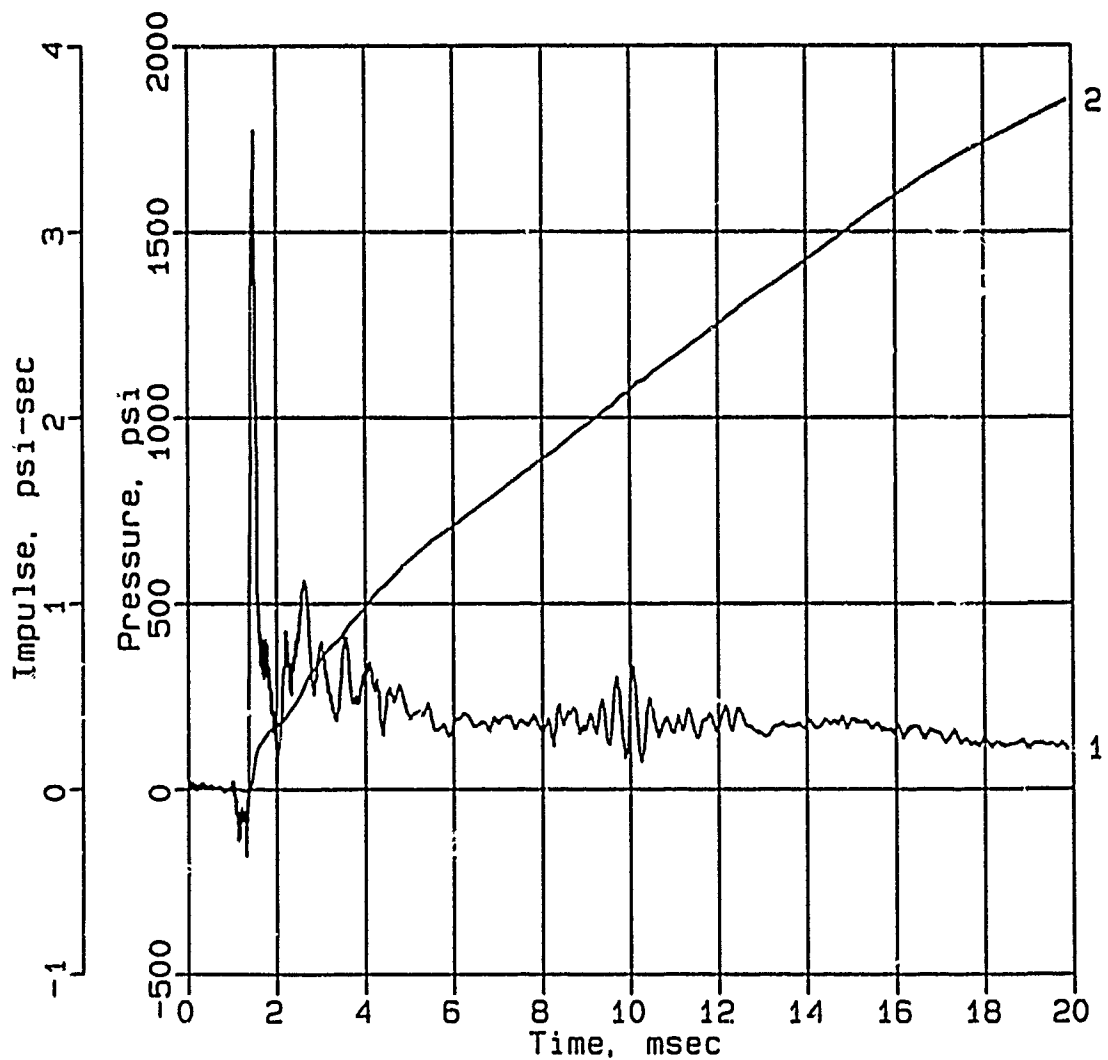Calibration: 2611
Filtering: 20 kHz low pass filter
            5 - 17 kHz band rejection filter

CONWEB T3

AHS-O
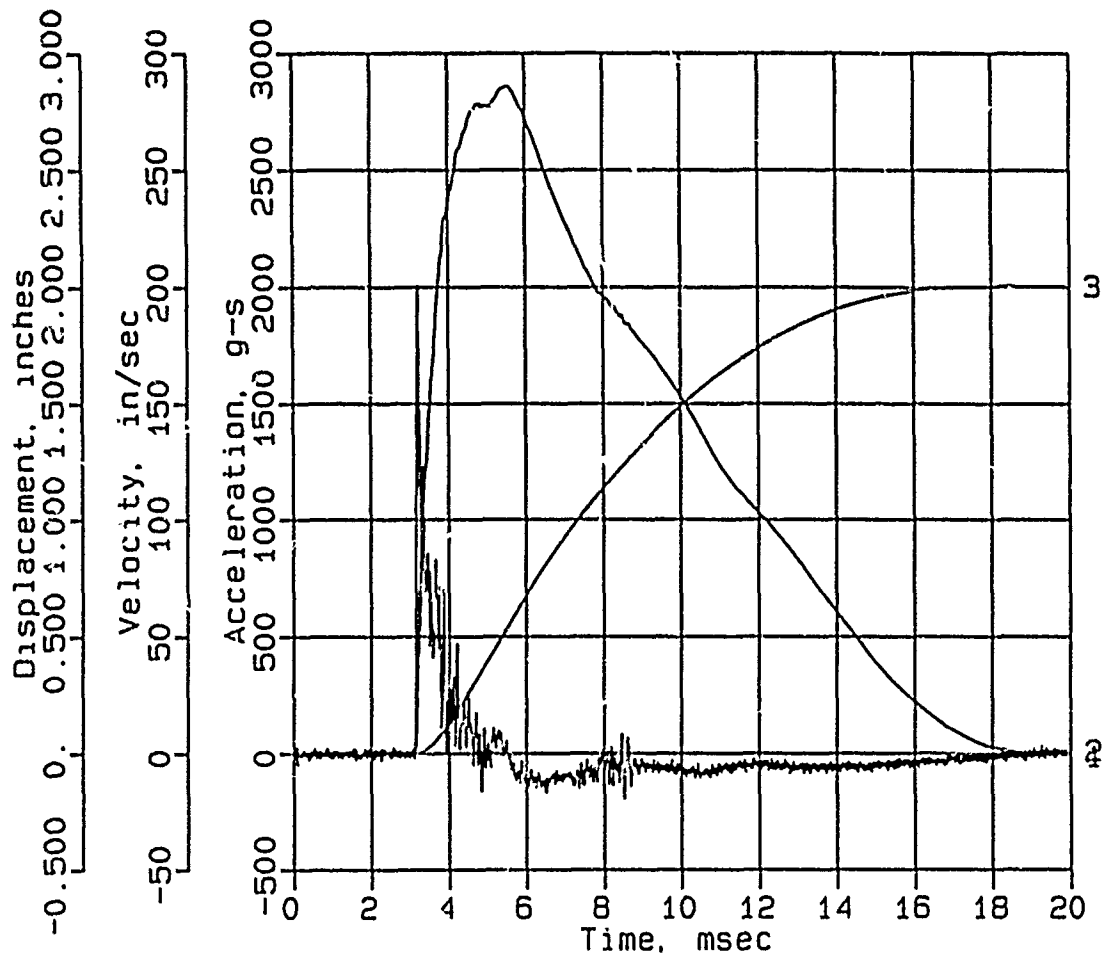
Digitizing rate: 200,000 Hz
Calibration: 3272
Constant Baseline Shift

C9

CONWEB T3

AHS-1
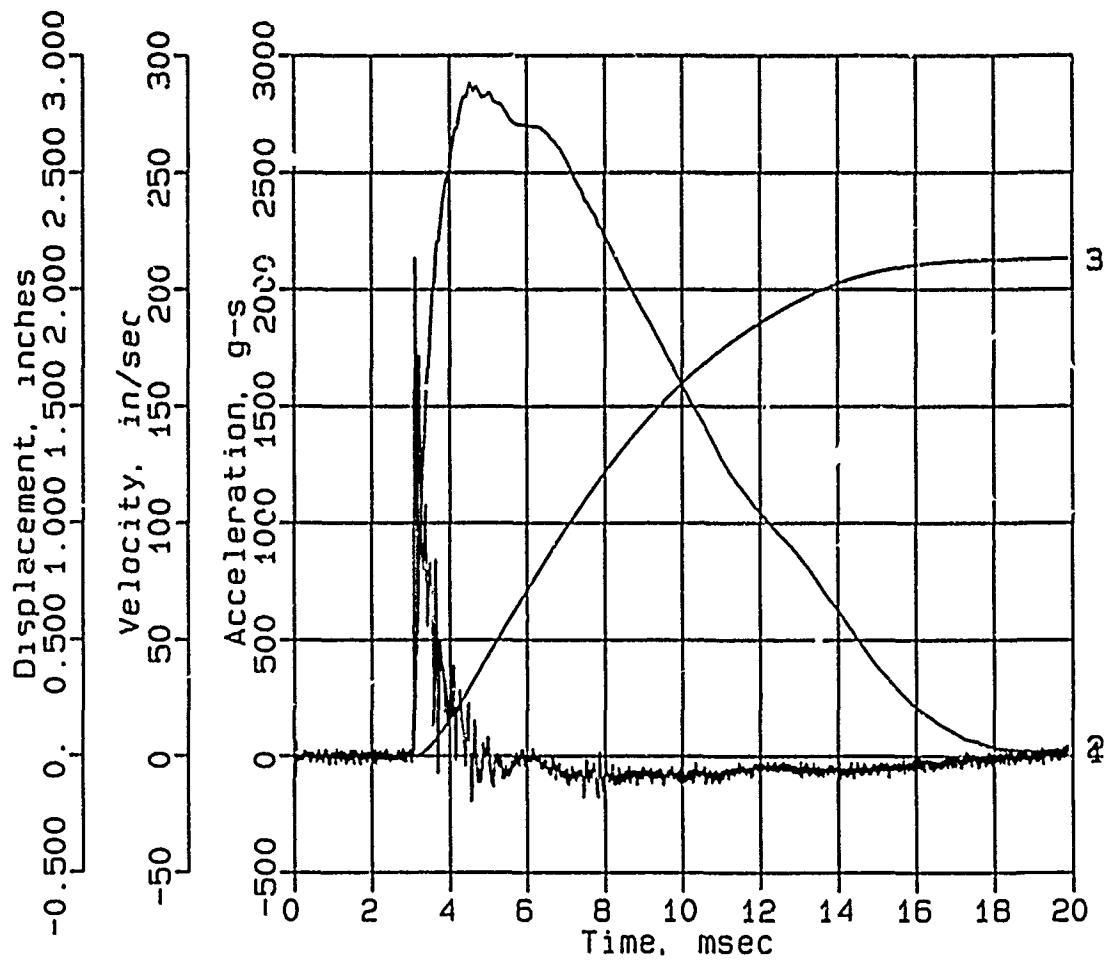
Digitizing rate: 200,000 Hz
Calibration: 5712
Constant Baseline Shift

CONWEB T3
AHS-2

Digitizing rate: 200,000 Hz
Calibration: 5275
Constant Baseline Shift

C11
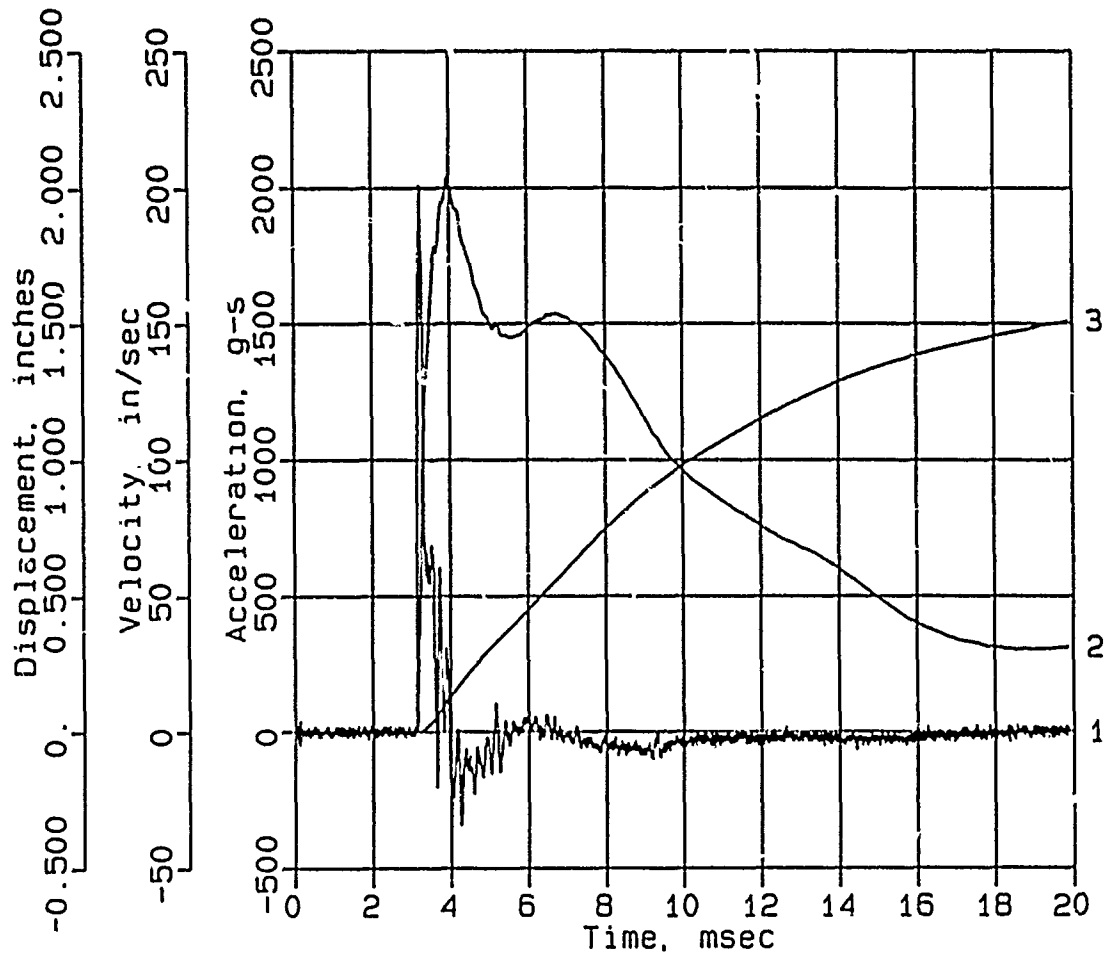
CONWEB T3

AHS-3
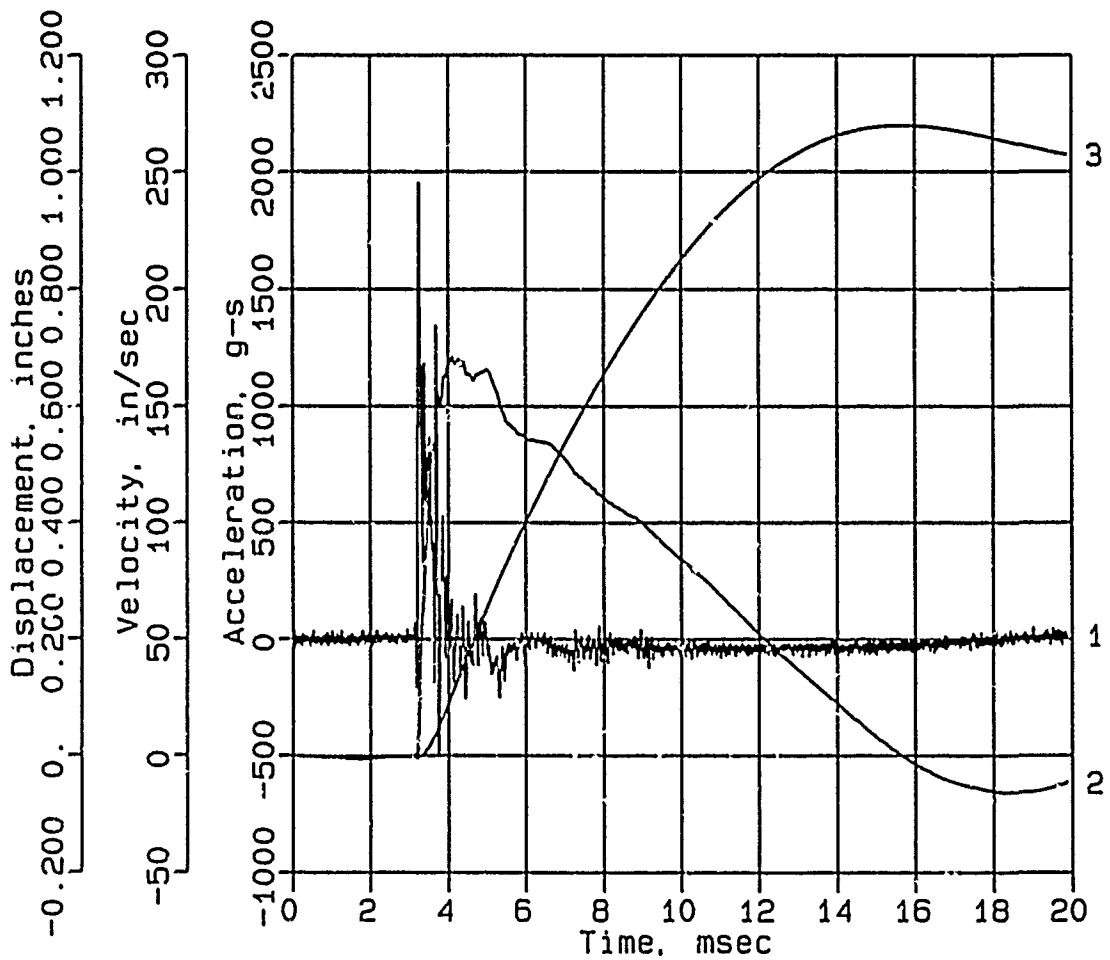
Digitizing rate: 200,000 Hz
Calibration: 5495
Constant Baseline Shift

CONWEB T3
AHS-5

Digitizing rate: 200,000 Hz
Calibration: 3073
Constant Baseline Shift

C13

CONWEB T3
AHS-6

Digitizing rate: 200,000 Hz
Calibration: 1907
Constant Baseline Shift

C14

CONWEB T3
AHS-10

Digitizing rate: 200,000 Hz
Calibration: 871
Constant Baseline Shift

CONWEB T3

AHS-11

Digitizing rate: 200,000 Hz
Calibration: 1059
Constant Baseline Shift

CONWEB T3
AVS-10

Digitizing rate: 200,000 Hz
Calibration: 942
Constant Baseline Shift

C17

CONWEB T3
AVS-12

Digitizing rate: 200,000 Hz
Calibration: 1062
Constant Baseline Shift

C18

CONWEB T3
AHF-1

Digitizing rate: 200,000 Hz
Calibration: 8539
Constant Baseline Shift

CONWEB T3
AHF-3

Digitizing rate: 200,000 Hz
Calibration: 7364
Constant Baseline Shift

C20

CONWEB T3
AHF-6

Digitizing rate: 200,000 Hz
Calibration: 11825
Constant Baseline Shift

CONWEB T3
AHF-7

Digitizing rate: 200,000 Hz
Calibration: 16426
Constant Baseline Shift

CONWEB T3
AHF-8

Digitizing rate: 200,000 Hz
Calibration: 23294
Constant Baseline Shift

CONWEB T3
AHF-9

Digitizing rate: 200,000 Hz
Calibration: 7005
Constant Baseline Shift

CONWEB T3

AHF-10

Digitizing rate: 200,000 Hz
Calibration: 5661
Constant Baseline Shift

CONWEB T3

SE-1

Digitizing rate: 200,000 Hz
Calibration: 3368
Filtering: 20 kHz low pass filter
            5 - 17 kHz band rejection filter
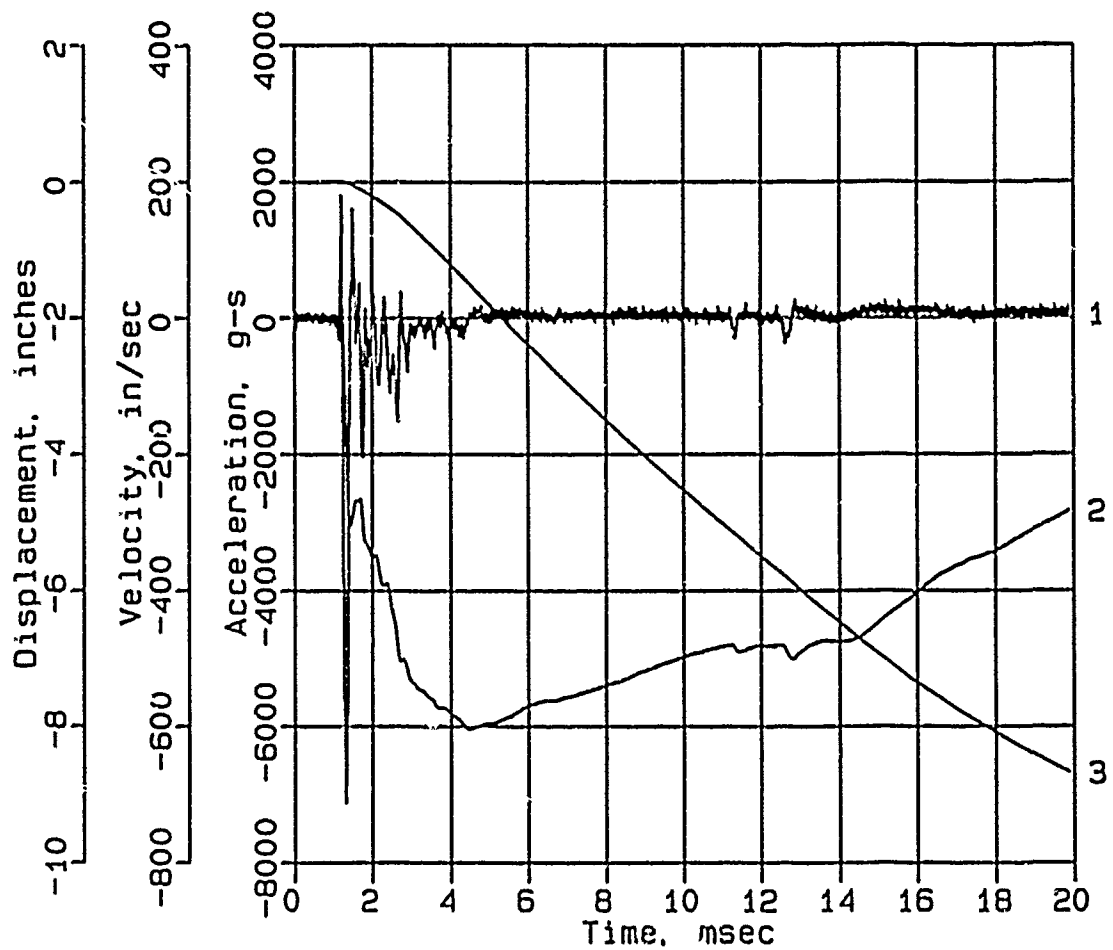
CONWEB T3
SE-3

Digitizing rate: 200,000 Hz
Calibration: 3168
Filtering: 20 kHz low pass filter
   5 - 17 kHz band rejection filter

C27

CONWEB T3

SE-4

Digitizing rate: 200,000 Hz
Calibration: 3189
Filtering: 20 kHz low pass filter
             5 - 17 kHz band rejection filter

CONWEB T3

SE-6

Digitizing rate: 200,000 Hz
Calibration: 3089
Filtering: 20 kHz low pass filter
          5 - 17 kHz band rejection filter

CONWEB T3

SE-7

Digitizing rate: 200,000 Hz
Calibration: 2990
Filtering: 20 kHz low pass filter
            5 - 17 kHz band rejection filter

C30

CONWEB T3
SE-8

Digitizing rate: 200,000 Hz
Calibration: 3520
Filtering: 20 kHz low pass filter
            5 - 1.7 kHz band rejection filter

CONWEB T3
SE-9

Digitizing rate: 200,000 Hz
Calibration: 3046
Filtering: 20 kHz low pass filter
                5 - 17 kHz band rejection filter

CONWEB T3
SE-10

Digitizing rate: 200,000 Hz
Calibration: 2109
Filtering: 20 kHz low pass filter
5 - 17 kHz band rejection filter

CONWEB T3
SE-11

Impulse, psi-sec / Pressure, psi vs Time, msec

APPENDIX D

DATA, IN-SITU TEST 4

Data from gages DEF-1, DEF-2, AHS-0, AHF-1, AHF-4, SE-4, SE-6, SE-10, and SE-12 in Backfill Test 4 have not been included in this report.

CONWEB T4

IF-1

Digitizing rate: 200,000 Hz
Calibration: 8475
Filtering: 20 kHz low pass filter
             5 - 17 kHz band rejection filter

D3

CONWEB T4

IF-2

Digitizing rate: 200,000 Hz
Calibration: 8502
Filtering: 20 kHz low pass filter
5 - 17 kHz band rejection filter

CONWEB T4
IF-3
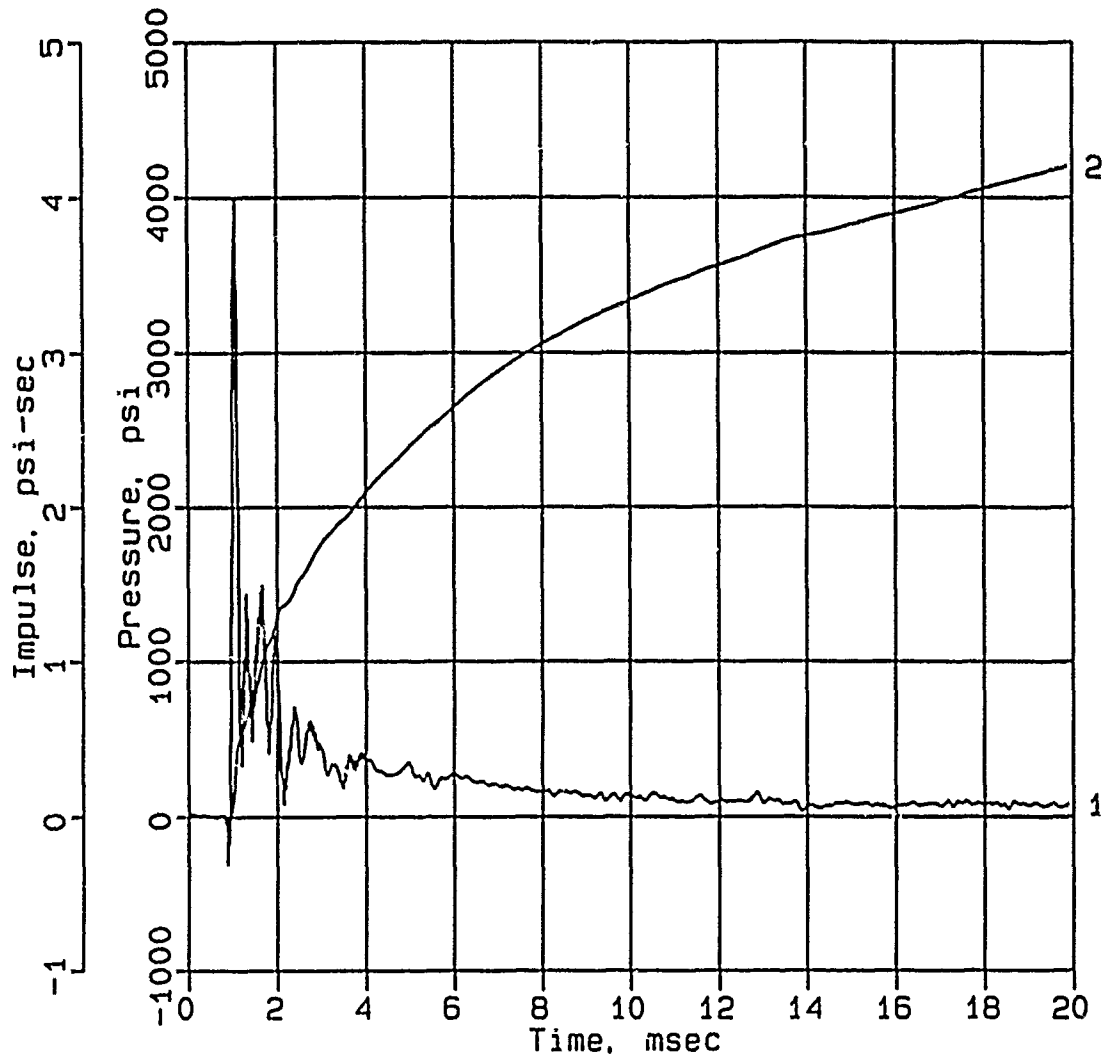
Digitizing rate: 200,000 Hz
Calibration: 8679
Filtering: 20 kHz low pass filter
        5 - 17 kHz band rejection filter

CONWEB T4
IF-5
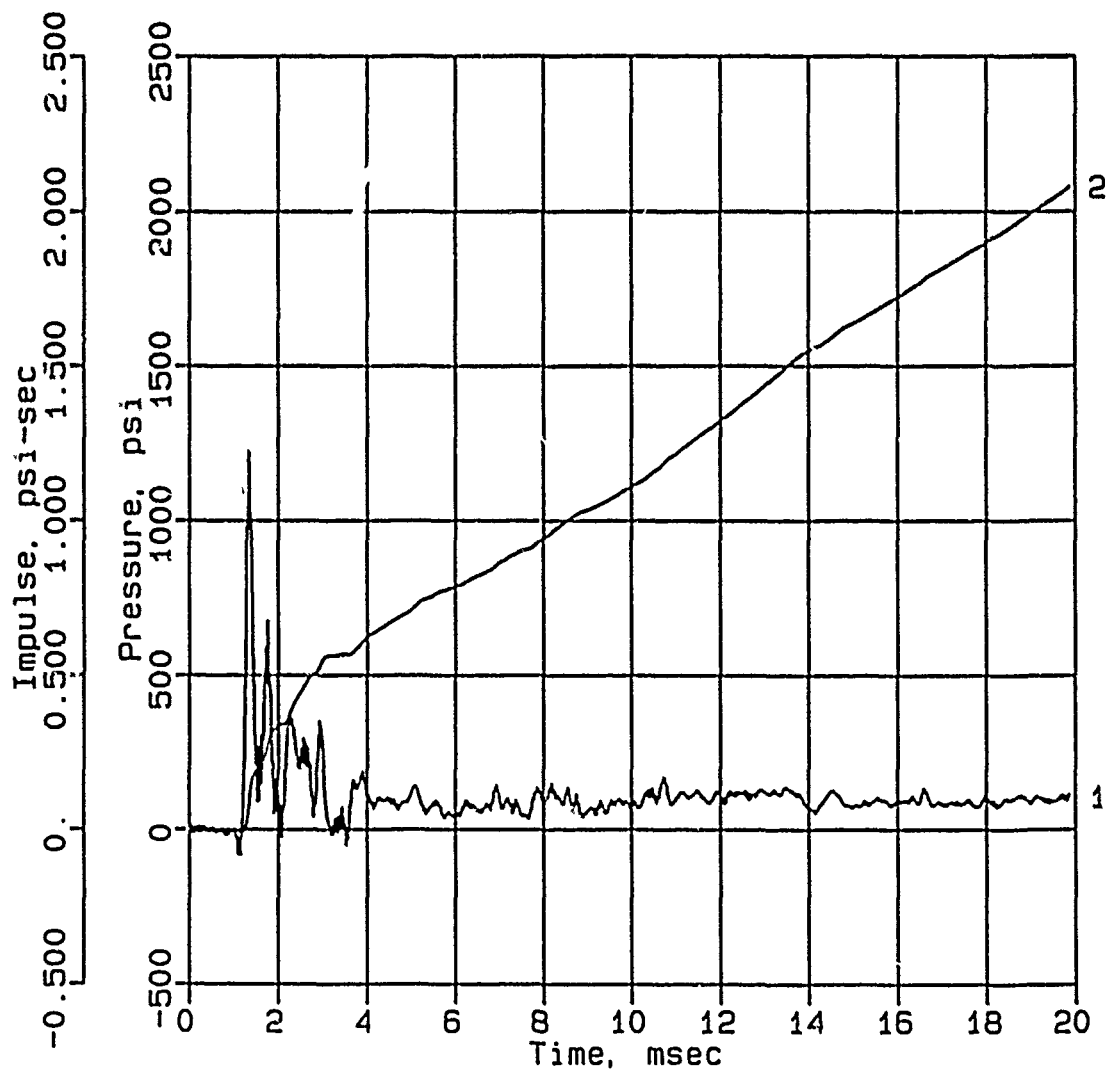
D6
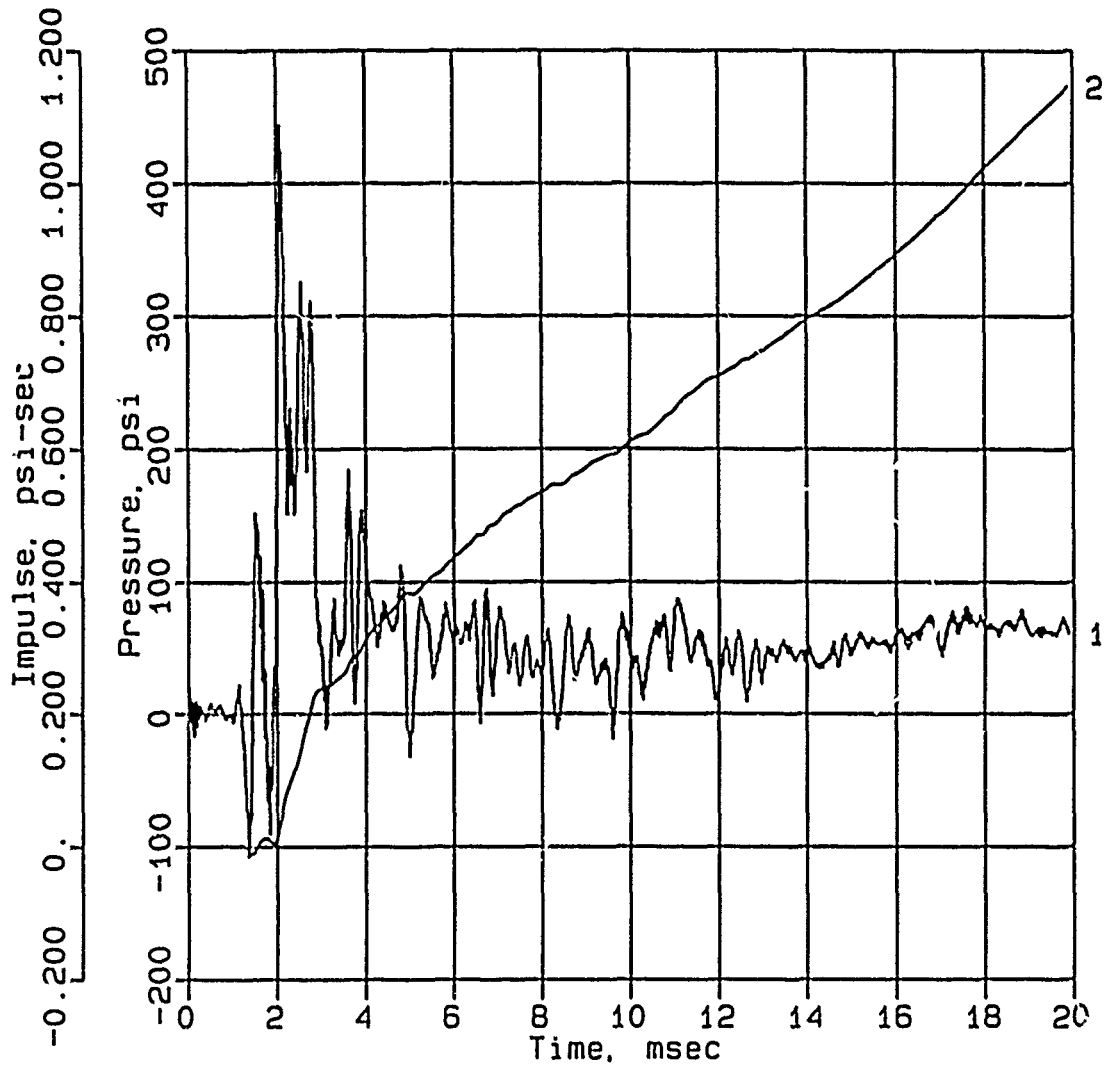
CONWEB T4
IF-6

Digitizing rate: 200,000 Hz
Calibration: 5714
Filtering: 20 kHz low pass filter
            5 - 17 kHz band rejection filter

D7
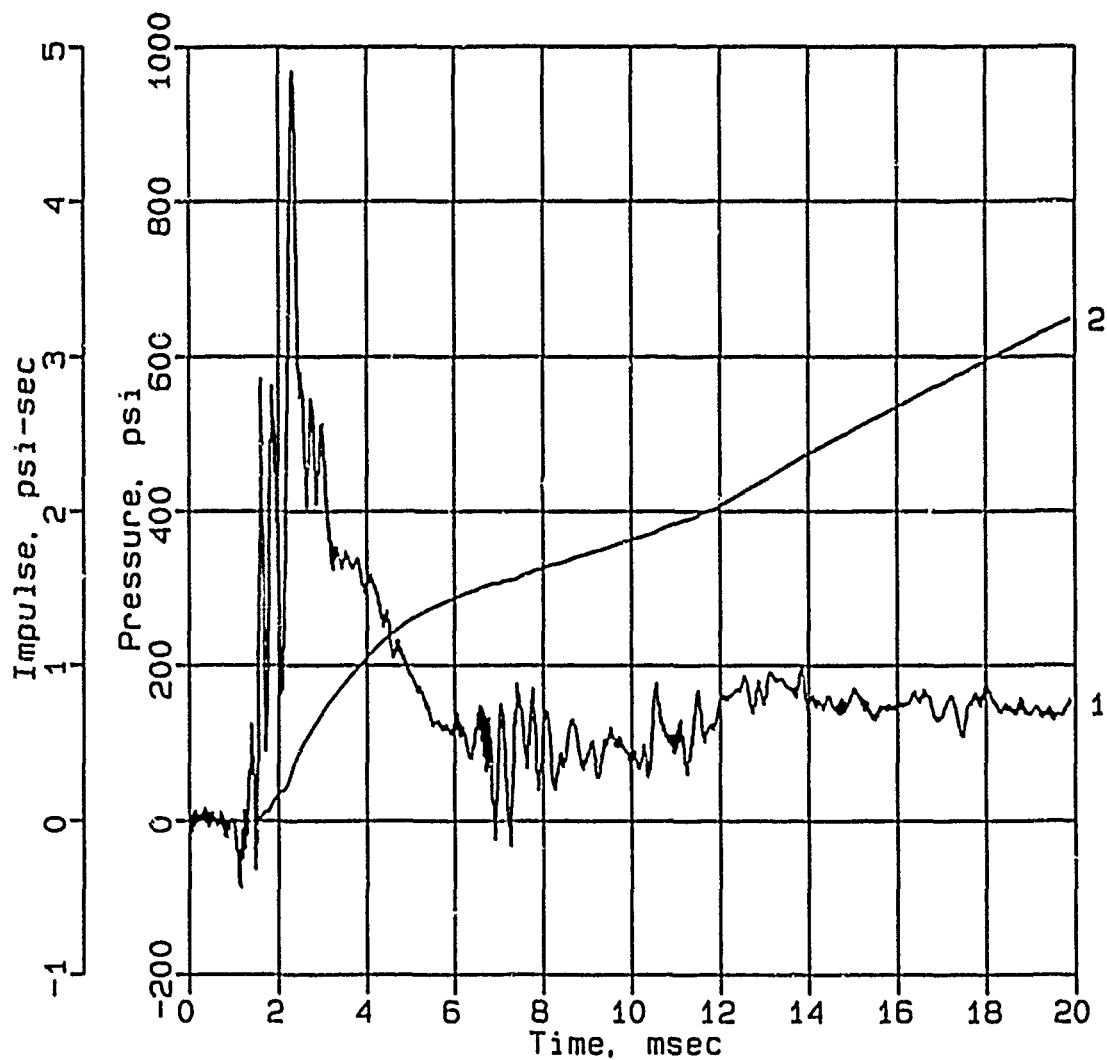
CONWEB T4
IF-8

Digitizing rate: 200,000 Hz
Calibration: 8523
Filtering: 20 kHz low pass filter
5 - 17 kHz band rejection filter

CONWEB T4
IF-9
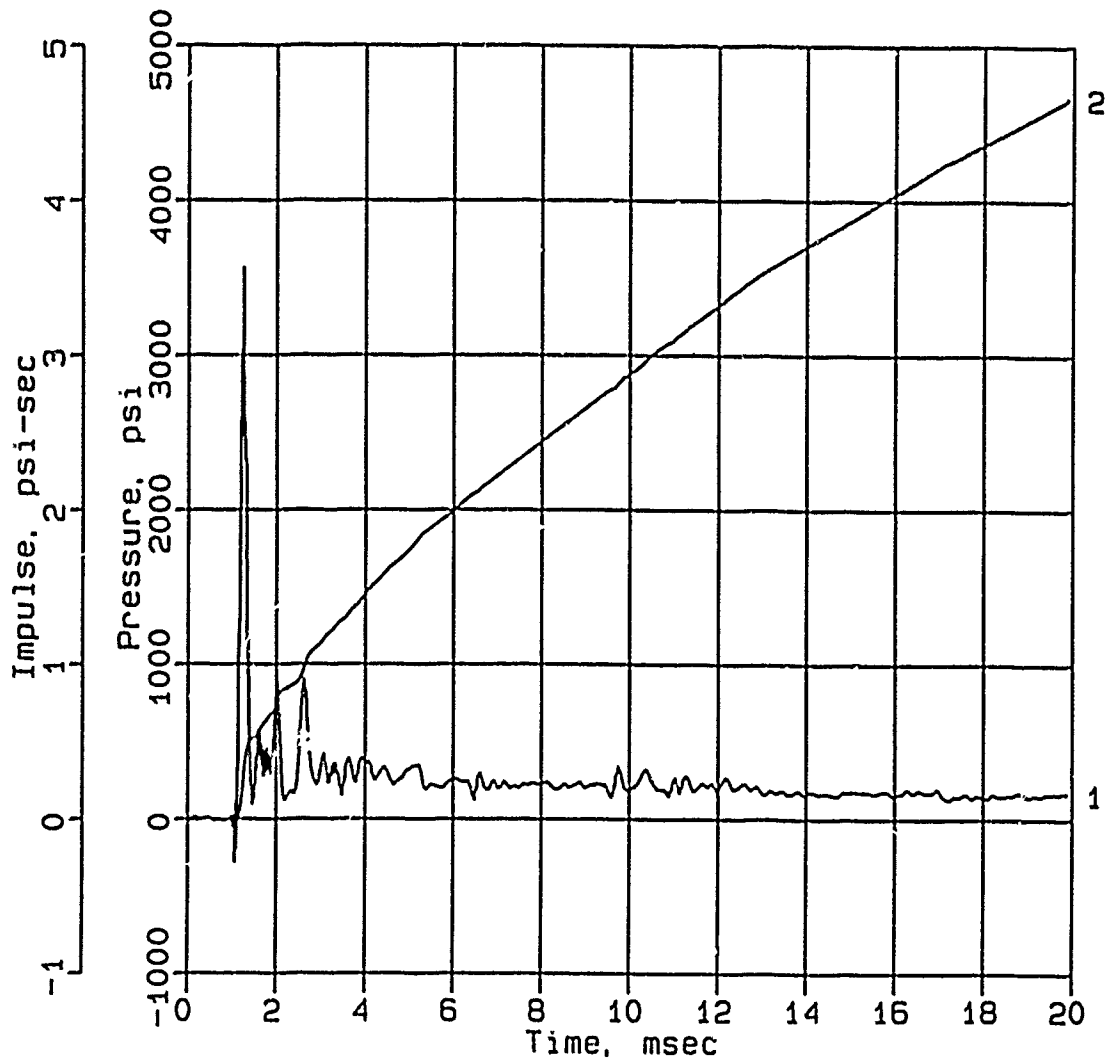
Digitizing rate: 200,000 Hz
Calibration: 8441
Filtering: 20 kHz low pass filter
      5 - 17 kHz band rejection filter

CONWEB T4
AHS-1

Digitizing rate: 200,000 Hz
Calibration: 17776
Constant Baseline Shift

CONWEB T4
AHS-2
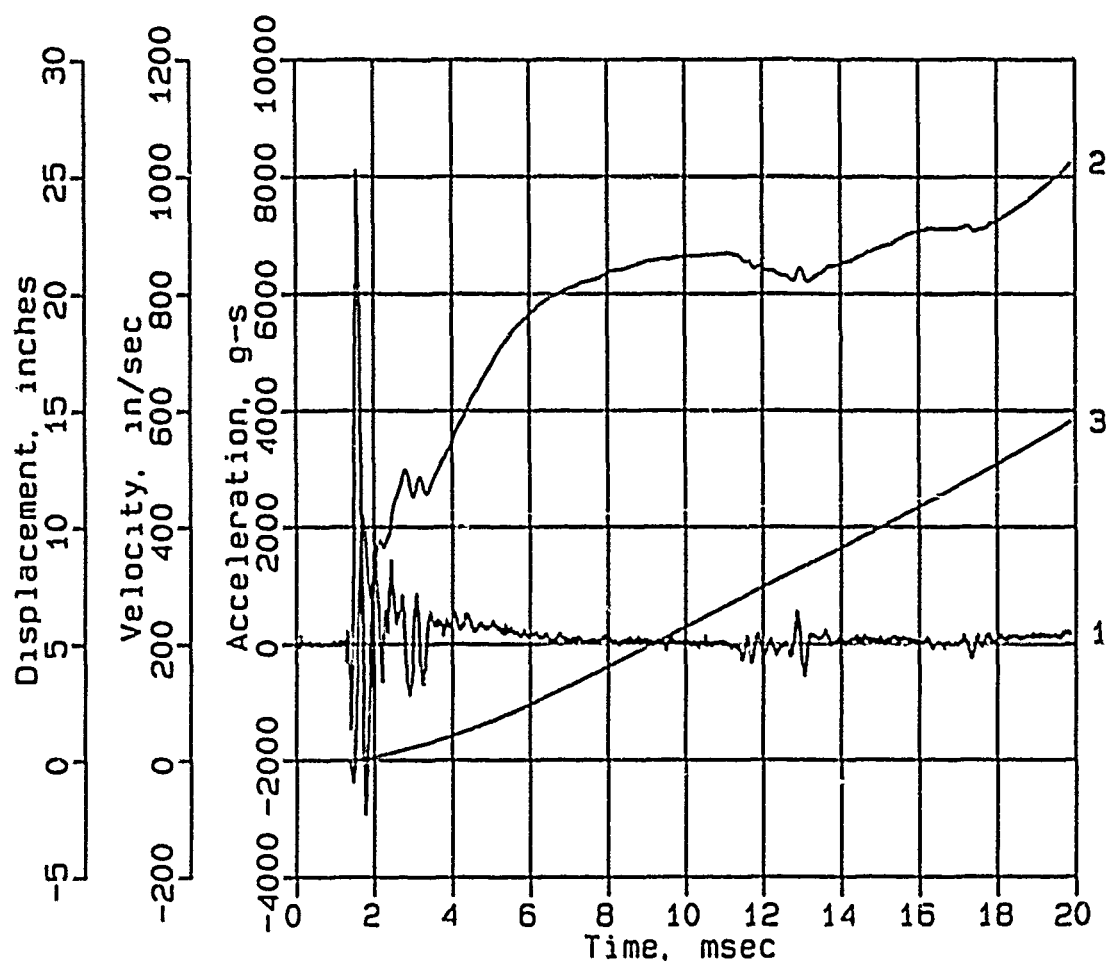
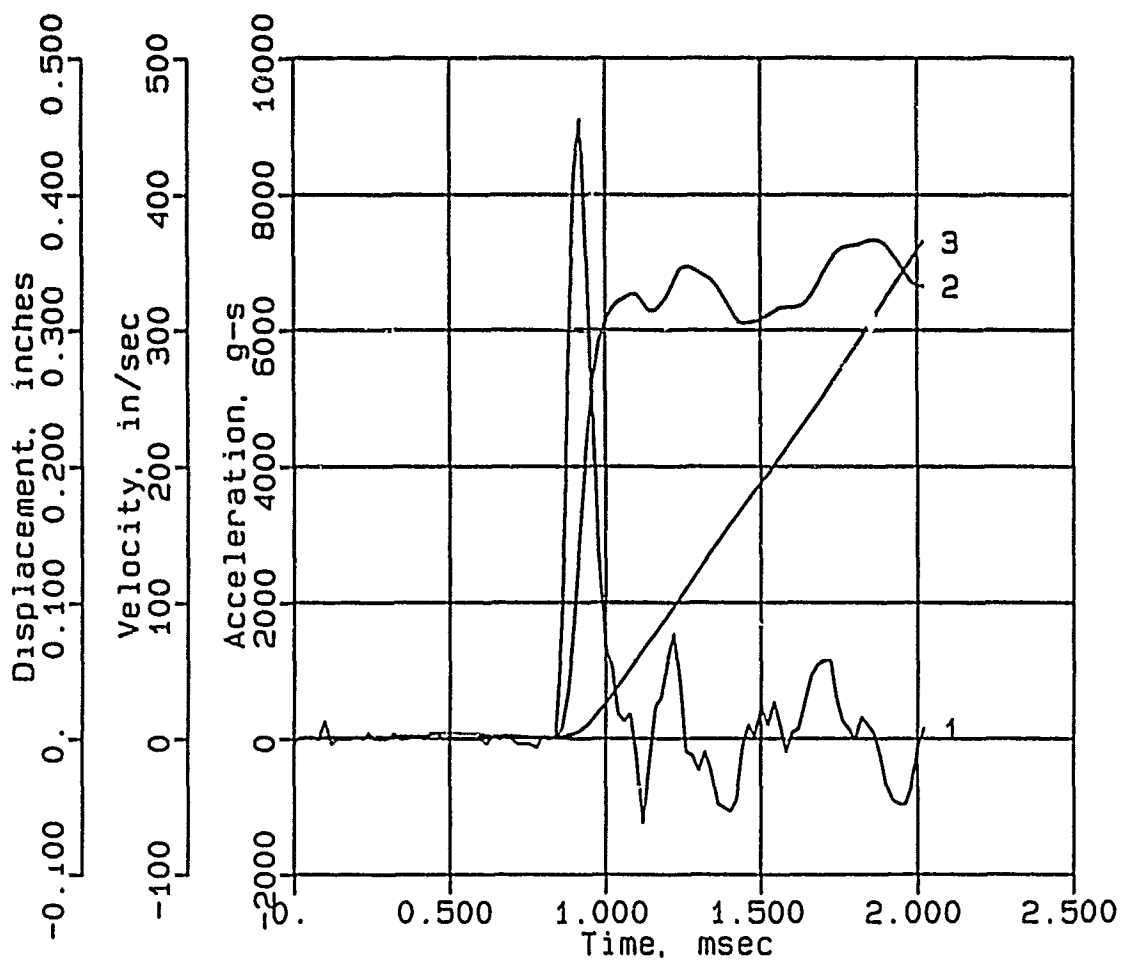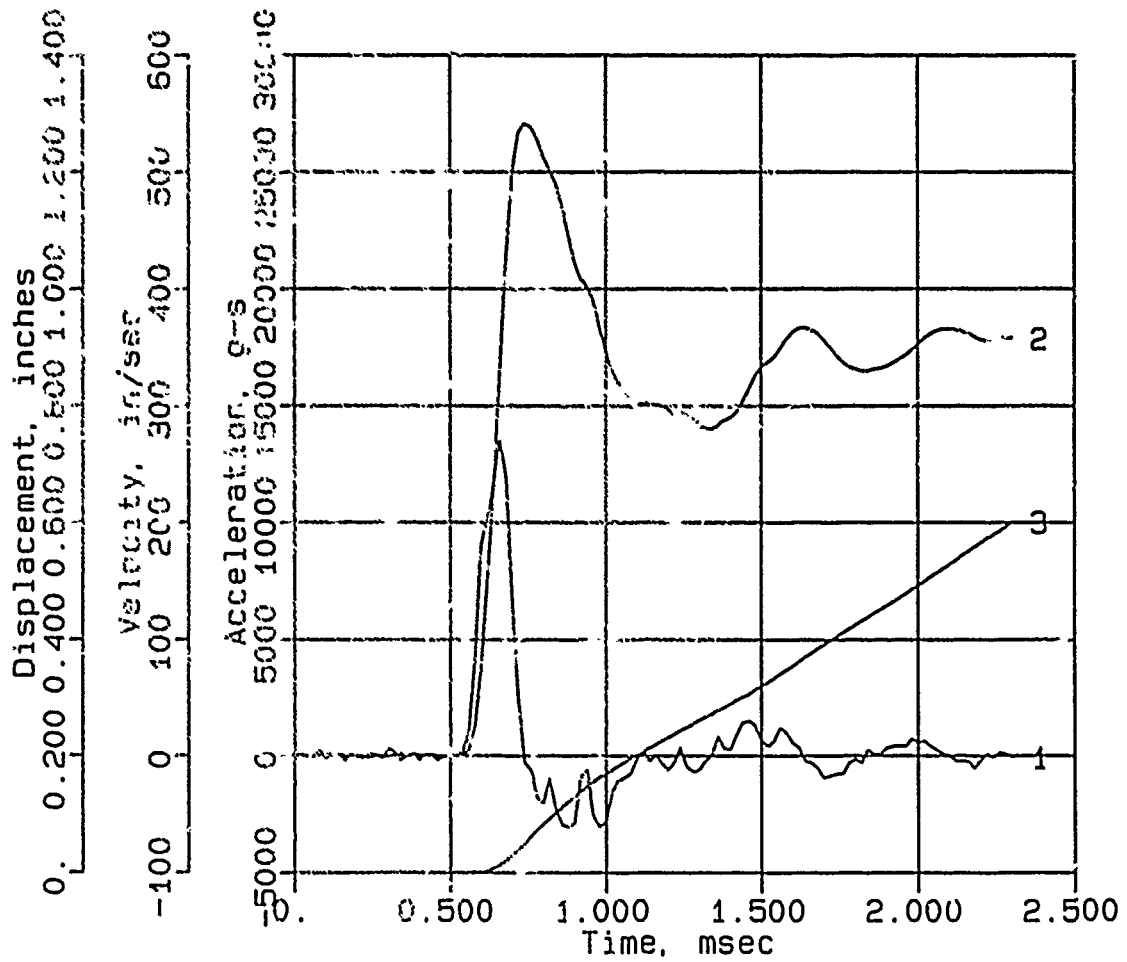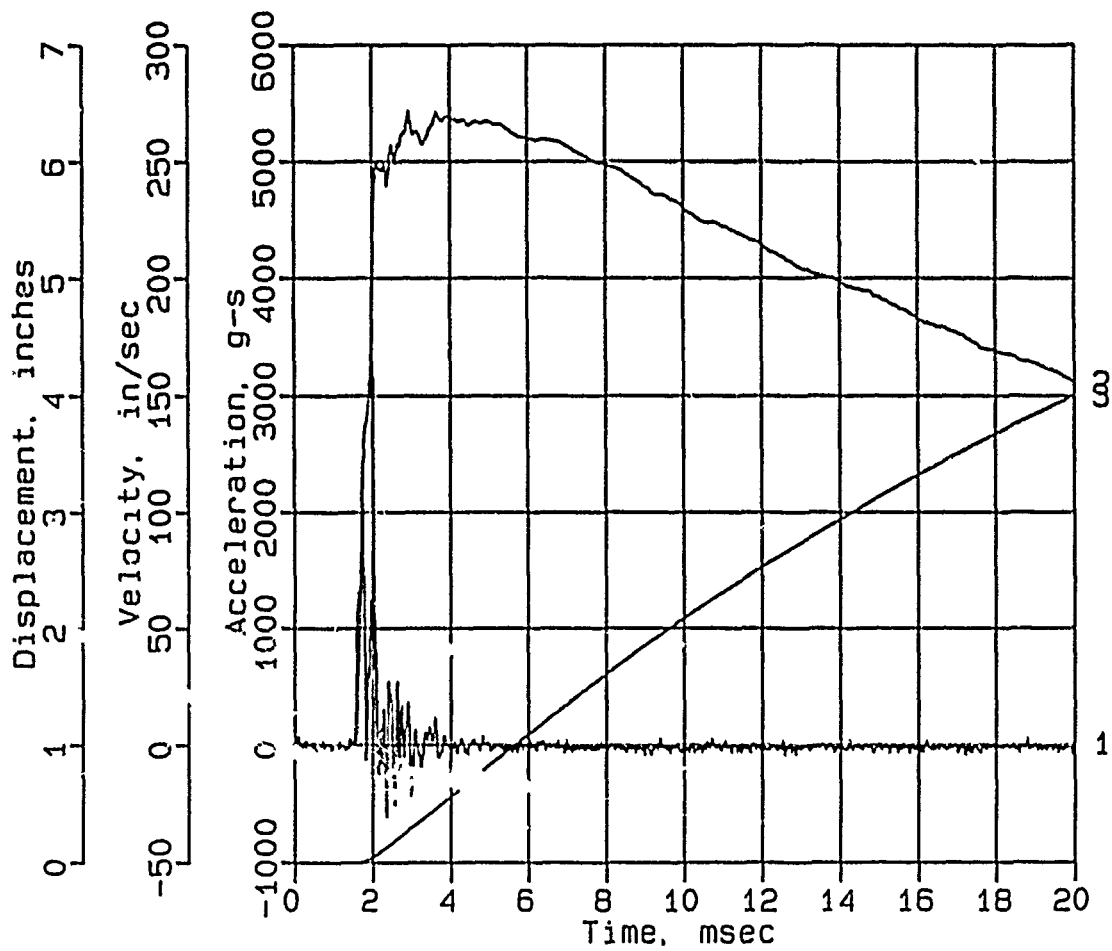Digitizing rate: 200,000 Hz
Calibration: 16416
Constant Baseline Shift
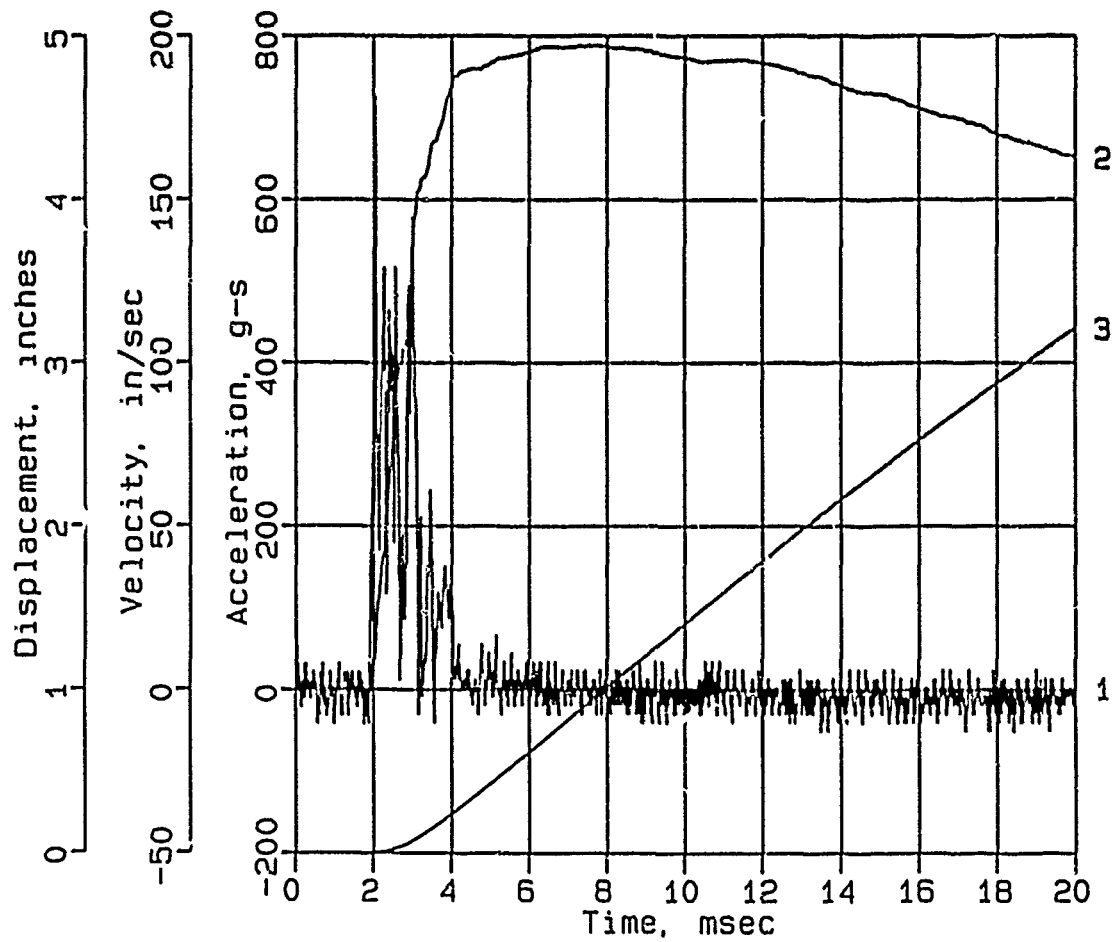
CONWEB T4
AHS-3

D12
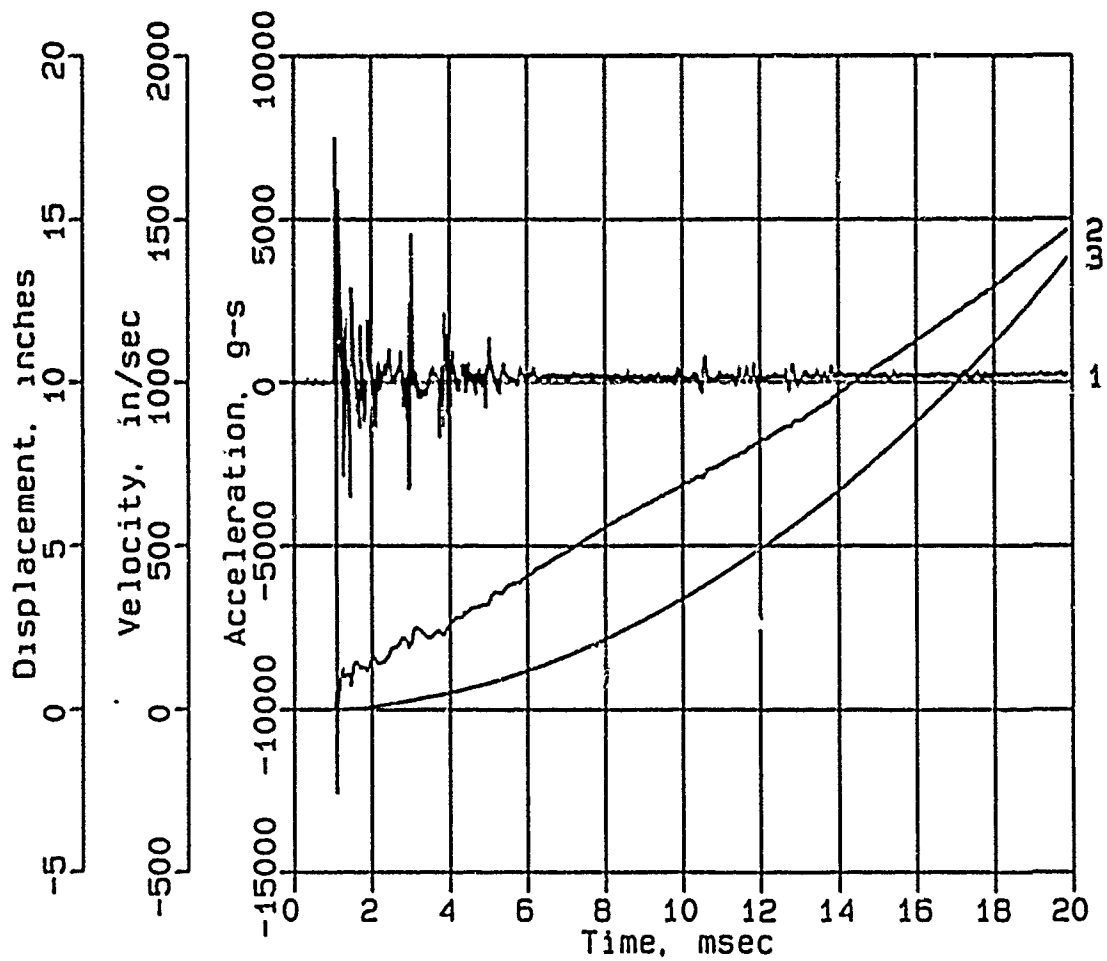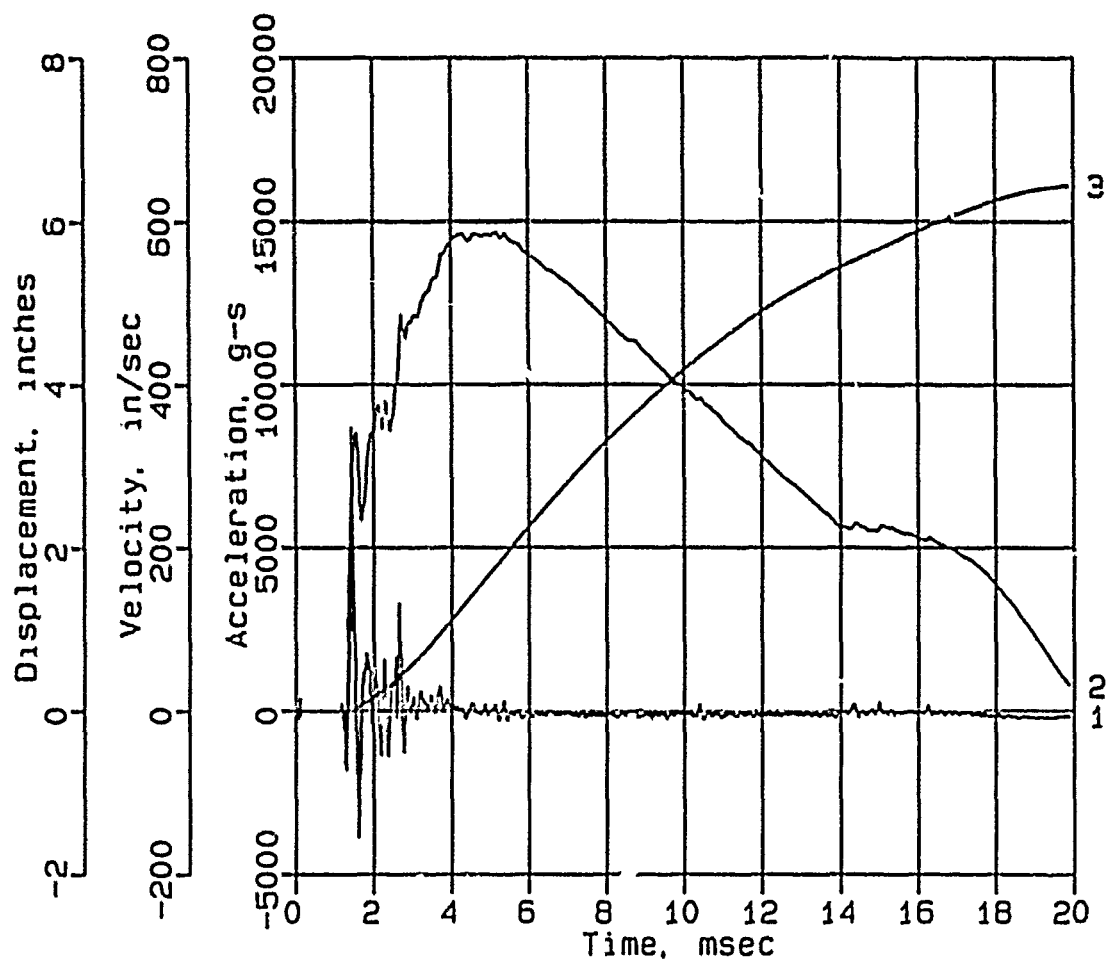
CONWEB T4
AHS-5

Digitizing rate: 200,000 Hz
Calibration: 14855
Constant Baseline Shift

CONWEB T4
AHS-6
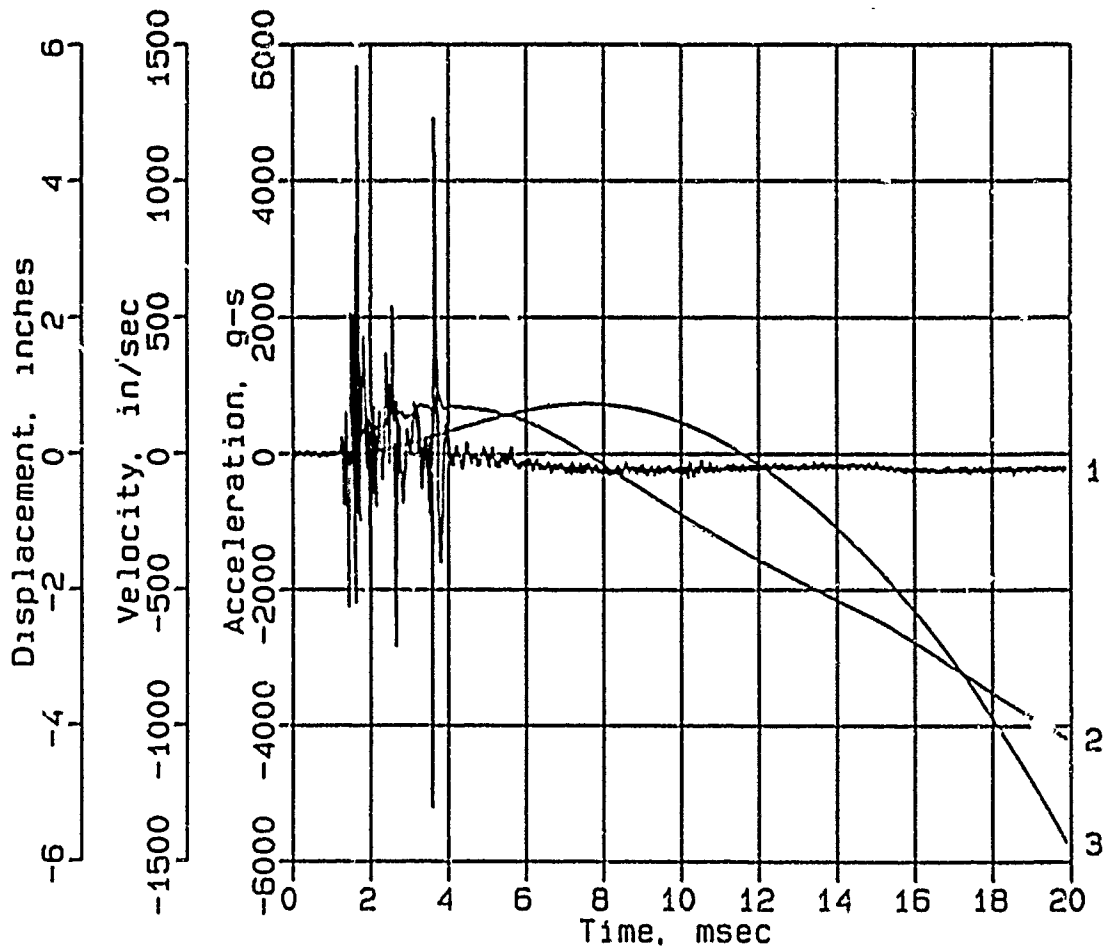
Digitizing rate: 200,000 Hz
Calibration: 8797
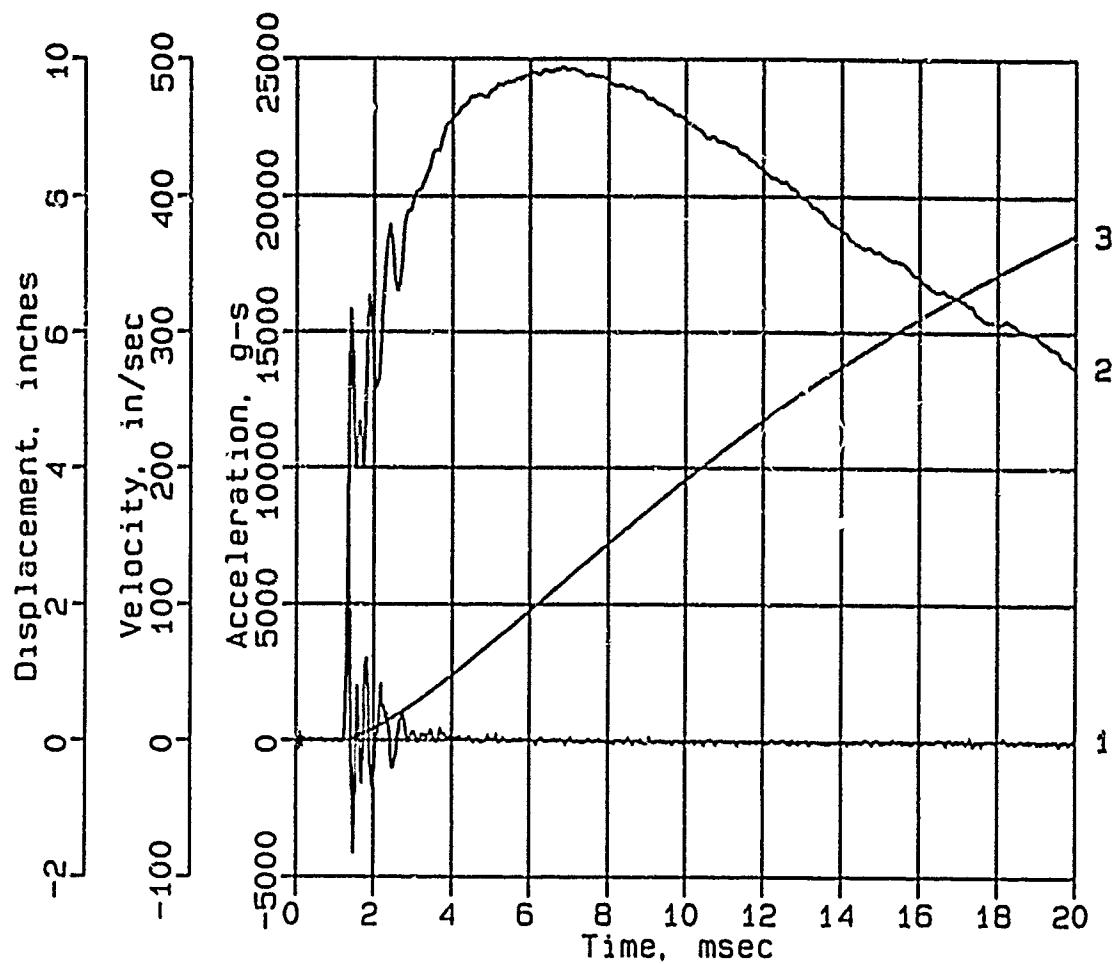Constant Baseline Shift

D14

CONWEB T4
AHS-10

Digitizing rate: 2v0,000 Hz
Calibration: 871
Constant Baseline Shift

CONWEB T4
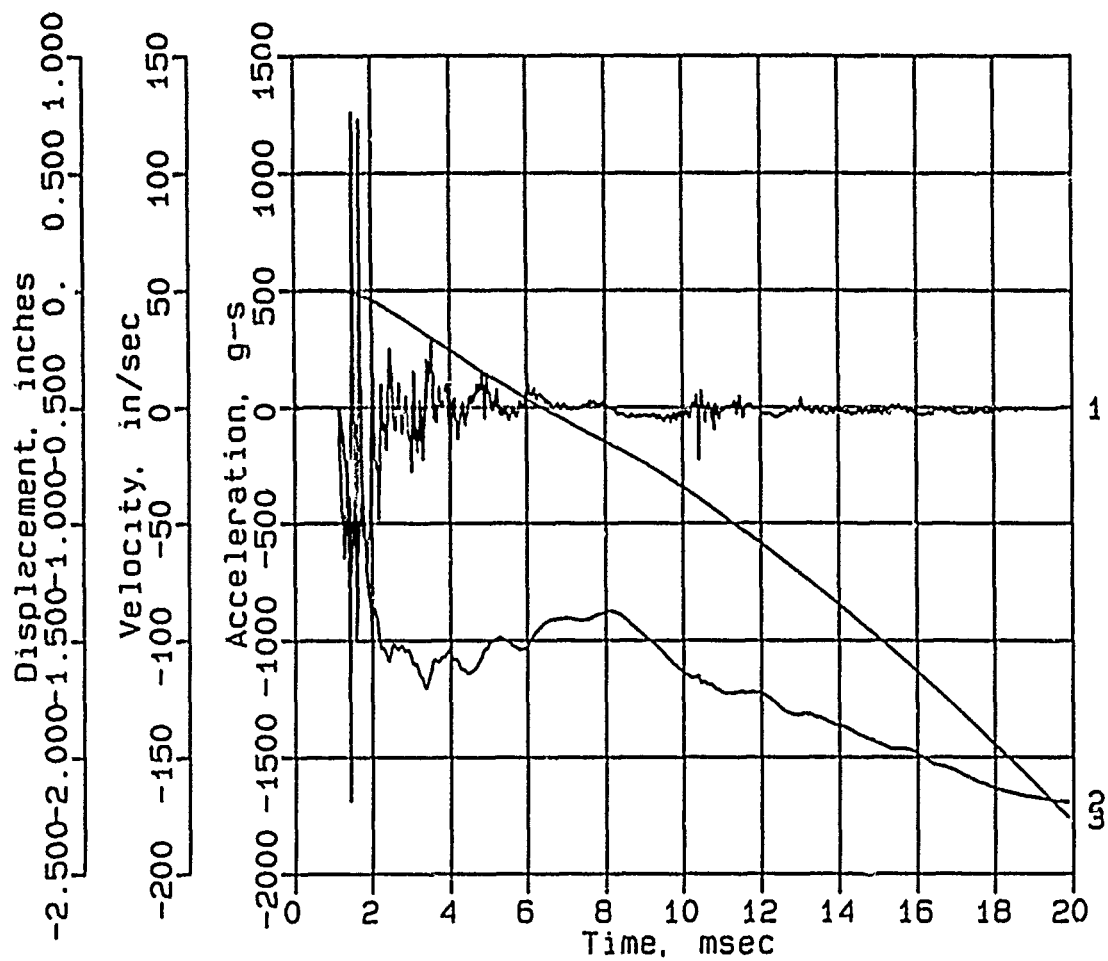
AHS-11

Digitizing rate: 200,000 Hz
Calibration: 1059
Constant Baseline Shift

D16
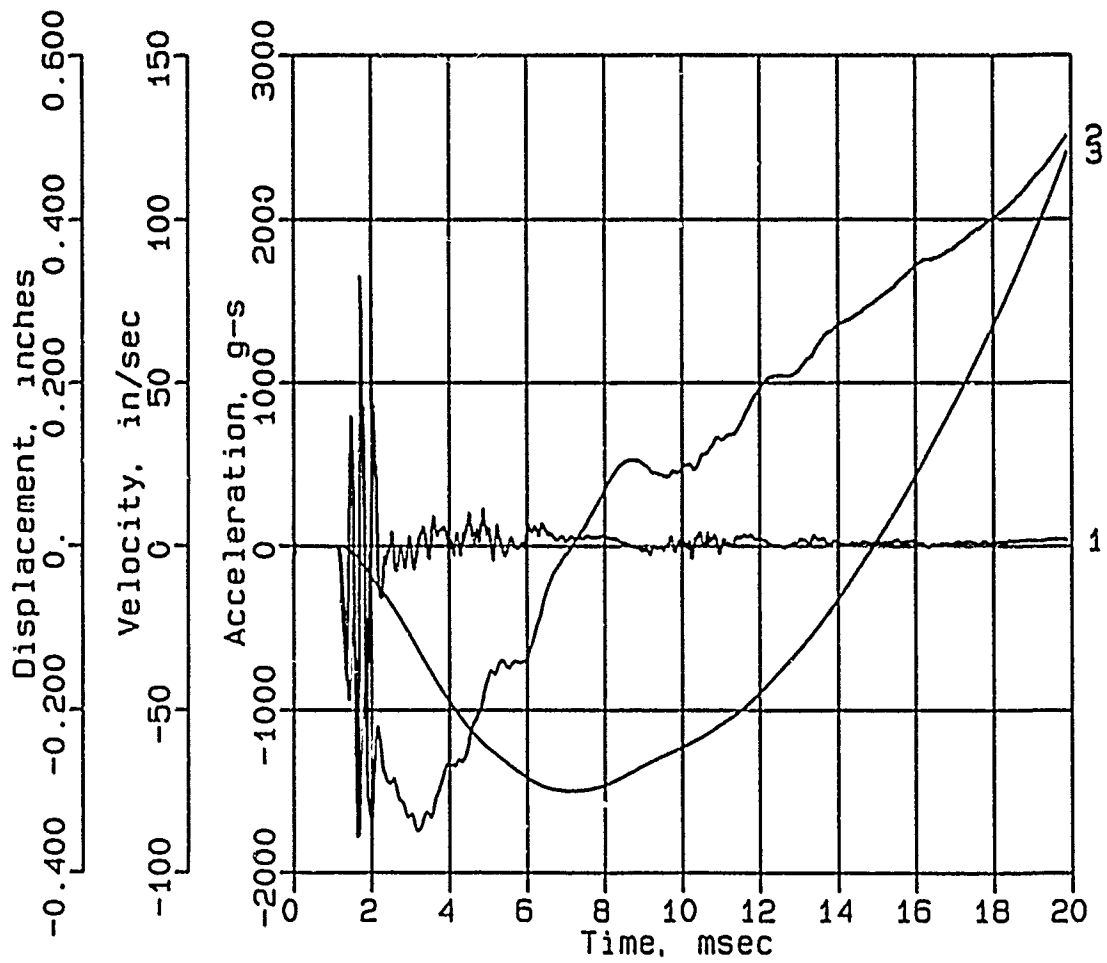
CONWEB T4

AVS-10

Digitizing rate: 200,000 Hz
Calibration: 942
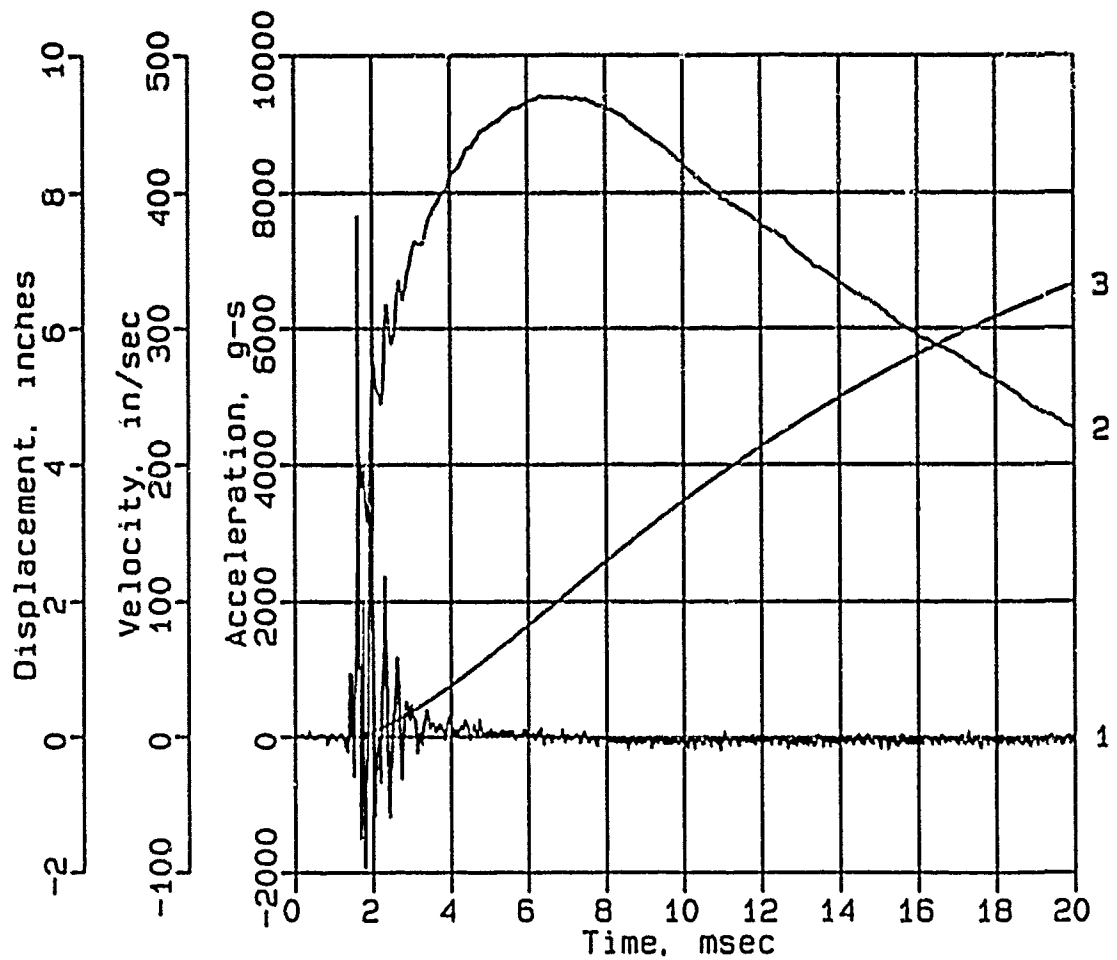Constant Baseline Shift

CONWEB T4
AVS-12
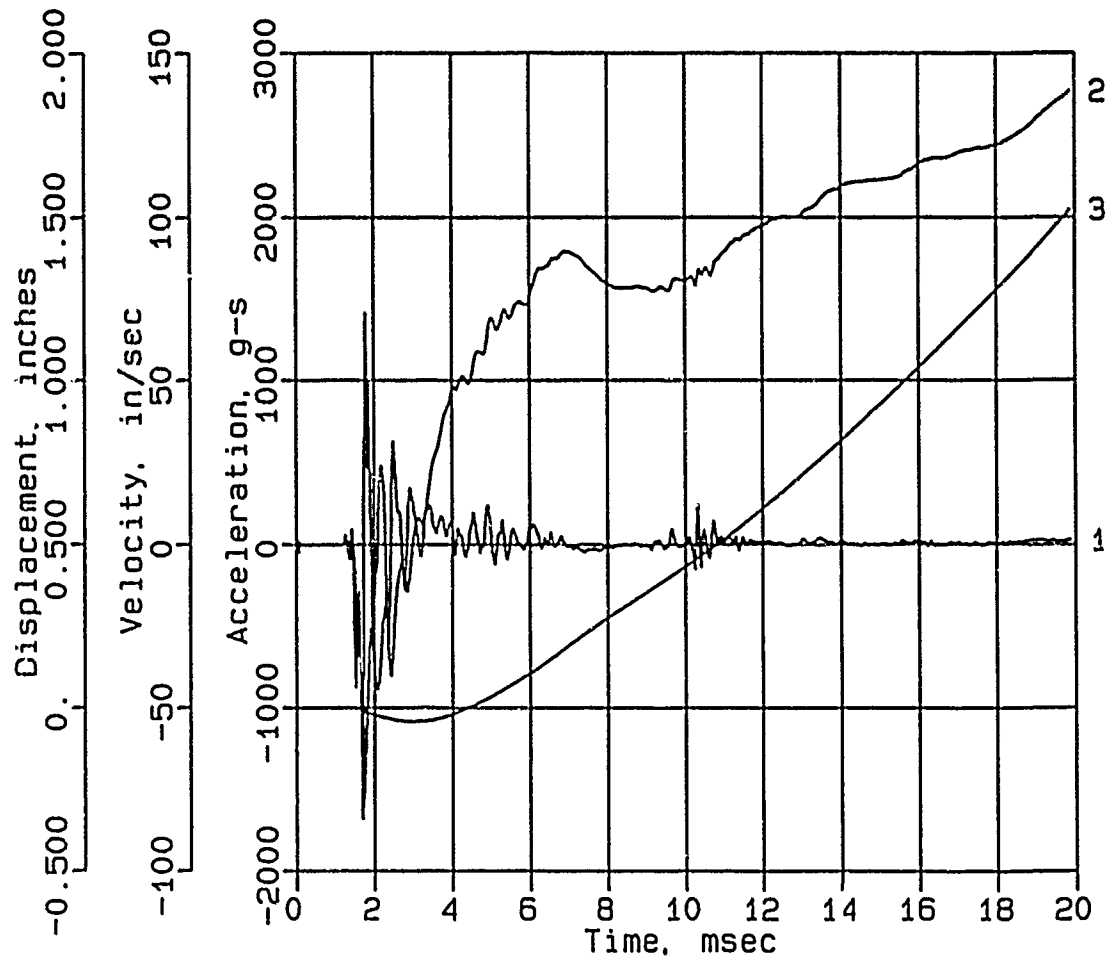
Digitizing rate: 200,000 Hz
Calibration: 1062
Constant Baseline Shift

CONWEB T4
AHF-3
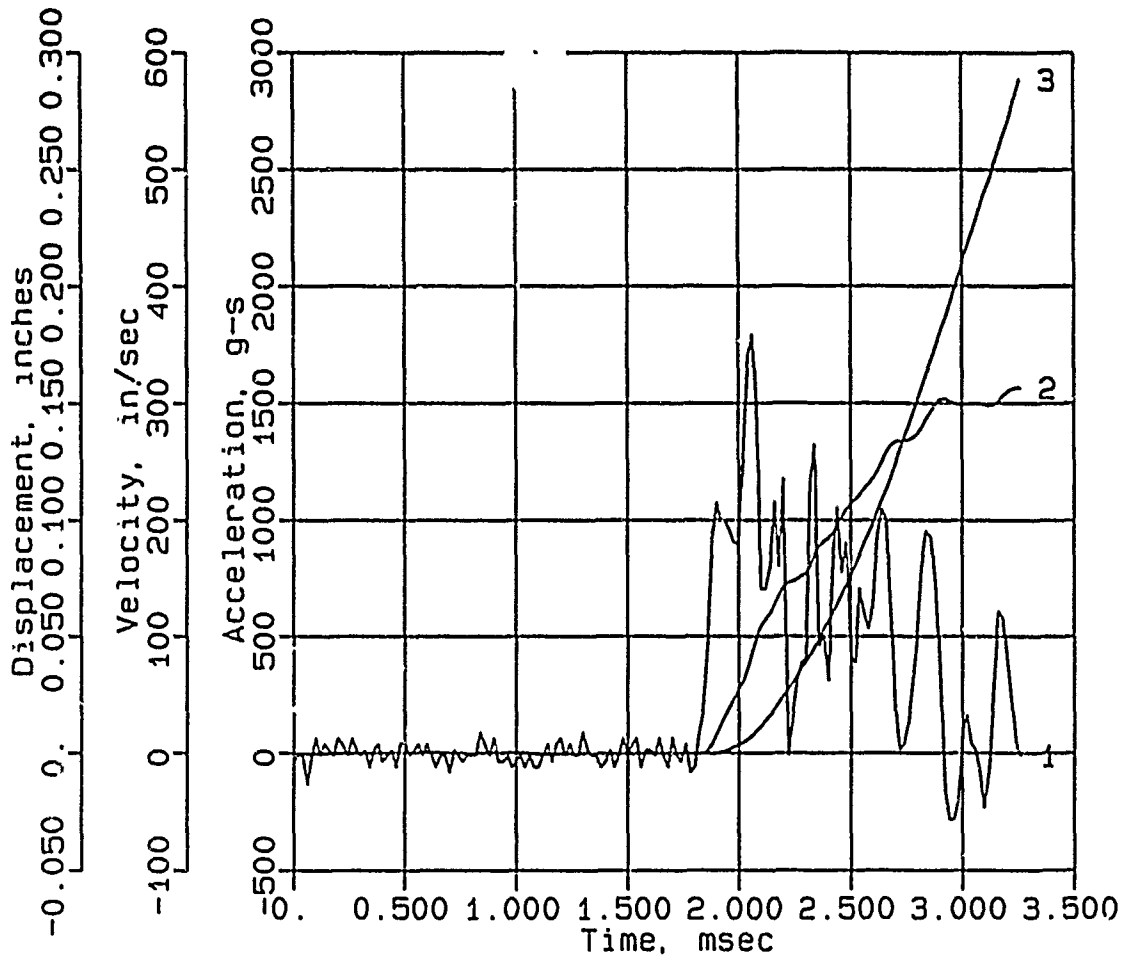
Digitizing rate: 200,000 Hz
Calibration: 18786
Constant Baseline Shift

CONWEB T4
AHF-6
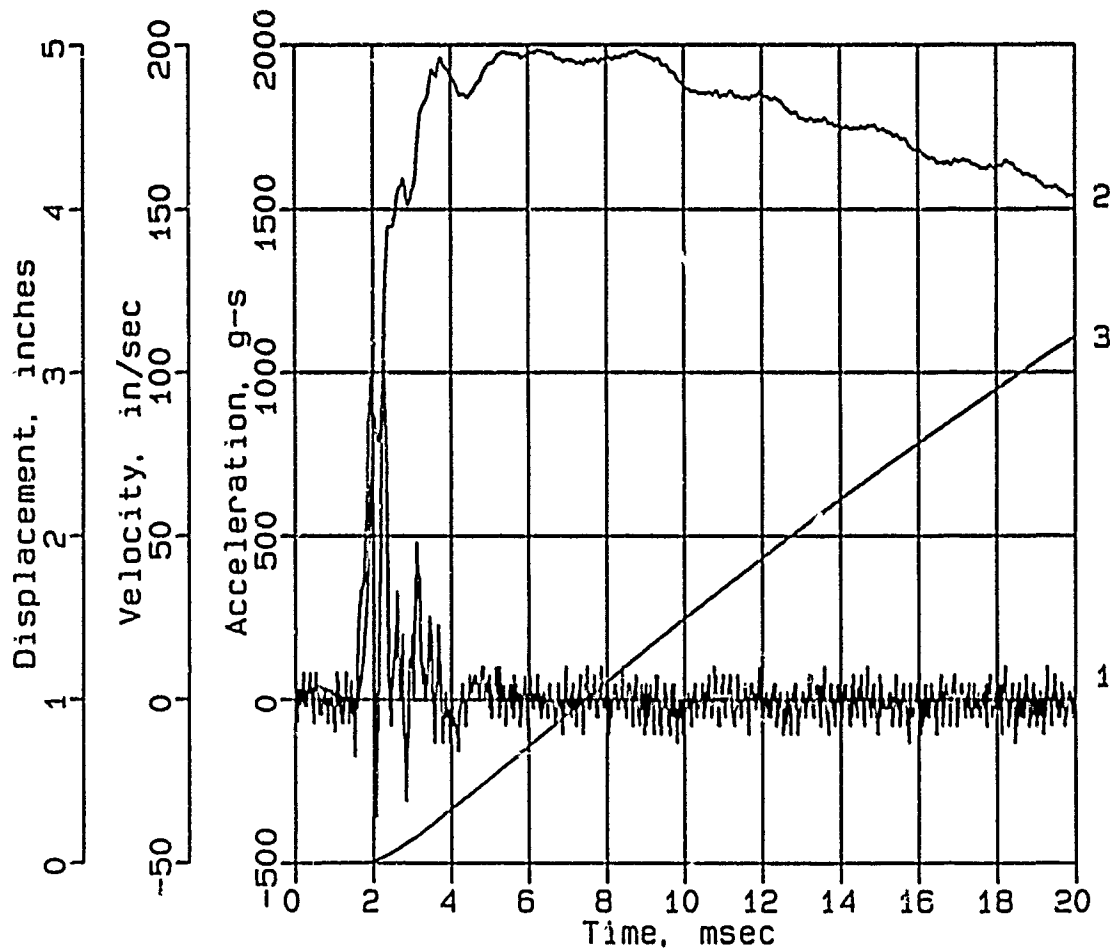
Digitizing rate: 200,000 Hz
Calibration: 18920
Constant Baseline Shift

CONWEB T4
## AHF-7

Digitizing rate: 200,000 Hz
Calibration: 38738
Constant Baseline Shift

D21

CONWEB T4
AHF-8

Digitizing rate: 200,000 Hz
Calibration: 57560
Constant Baseline Shift

CONWEB T4
AHF-9

Digitizing rate: 200,000 Hz
Calibration: 14182
Constant Baseline Shift

CONWEB T4
AHF-10

Digitizing rate: 200,000 Hz
Calibration: 7592
Constant Baseline Shift

CONWEB T4
AHF-11

Digitizing rate: 200,000 Hz
Calibration: 38606
Constant Baseline Shift

CONWEB T4
AHF-12

Digitizing rate: 200,000 Hz
Calibration: 21008
Constant Baseline Shift

CONWEB T4
SE-1
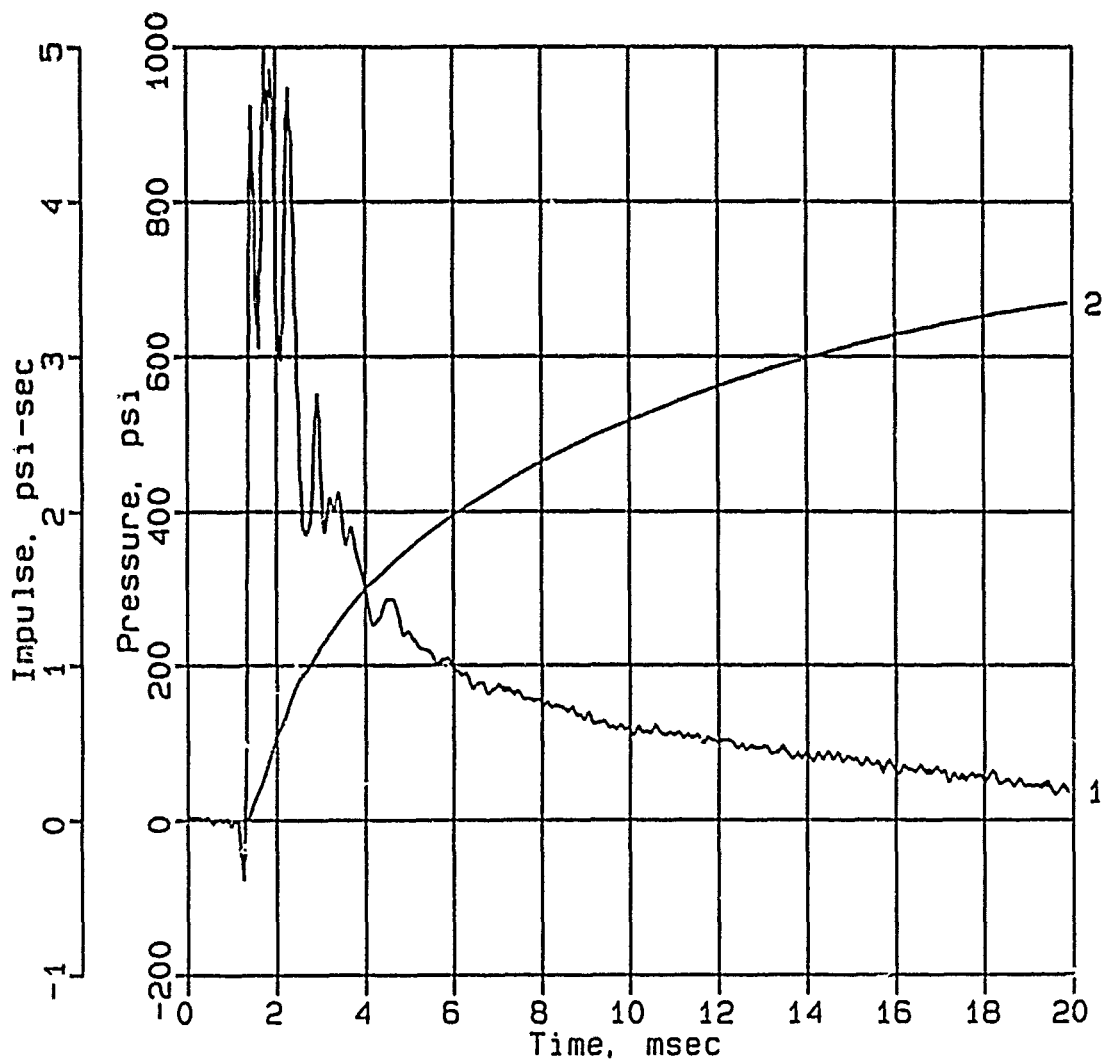
Digitizing rate: 200,000 Hz
Calibration: 7239
Filtering: 20 kHz low pass filter
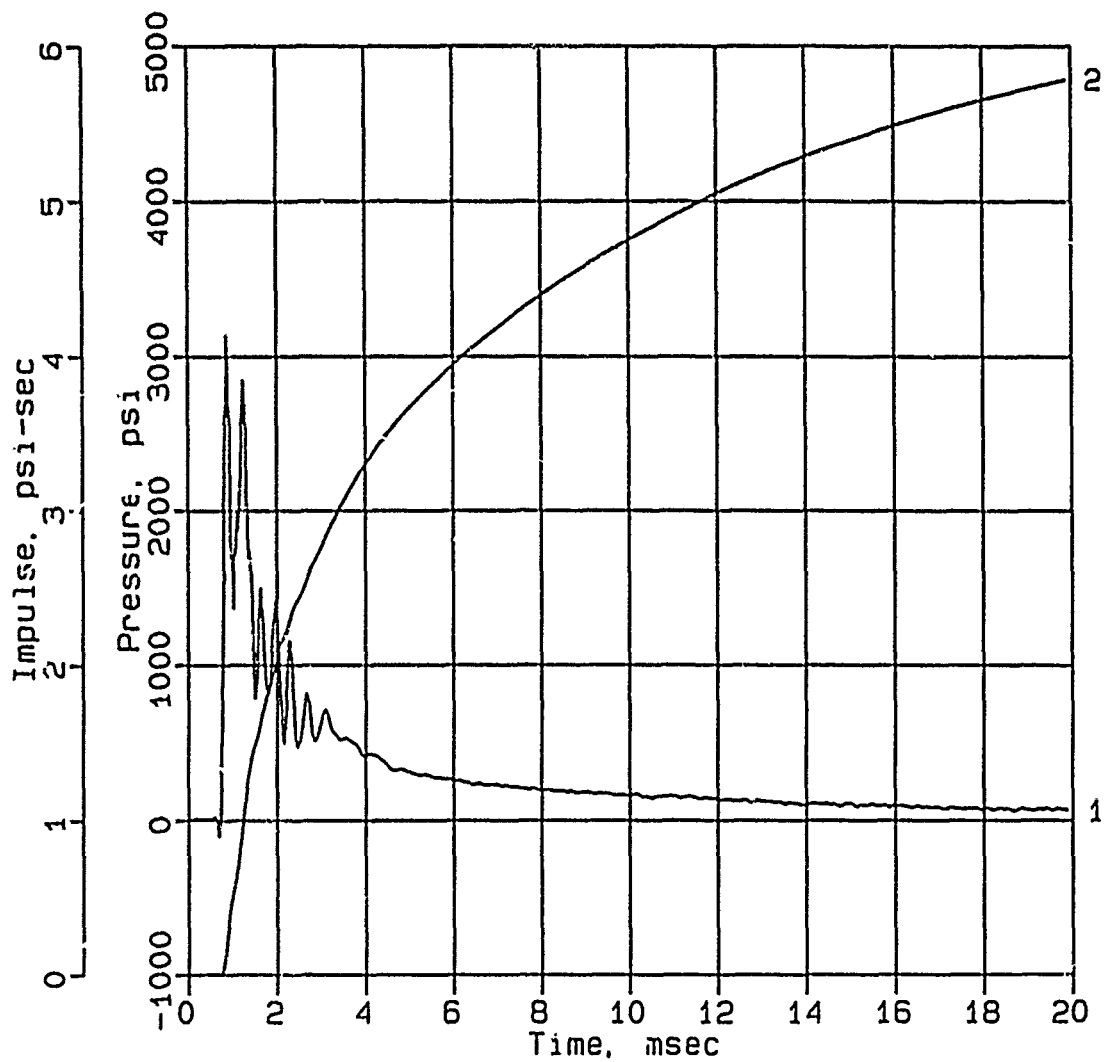   5 - 17 kHz band rejection filter

CONWEB T4

SE-3
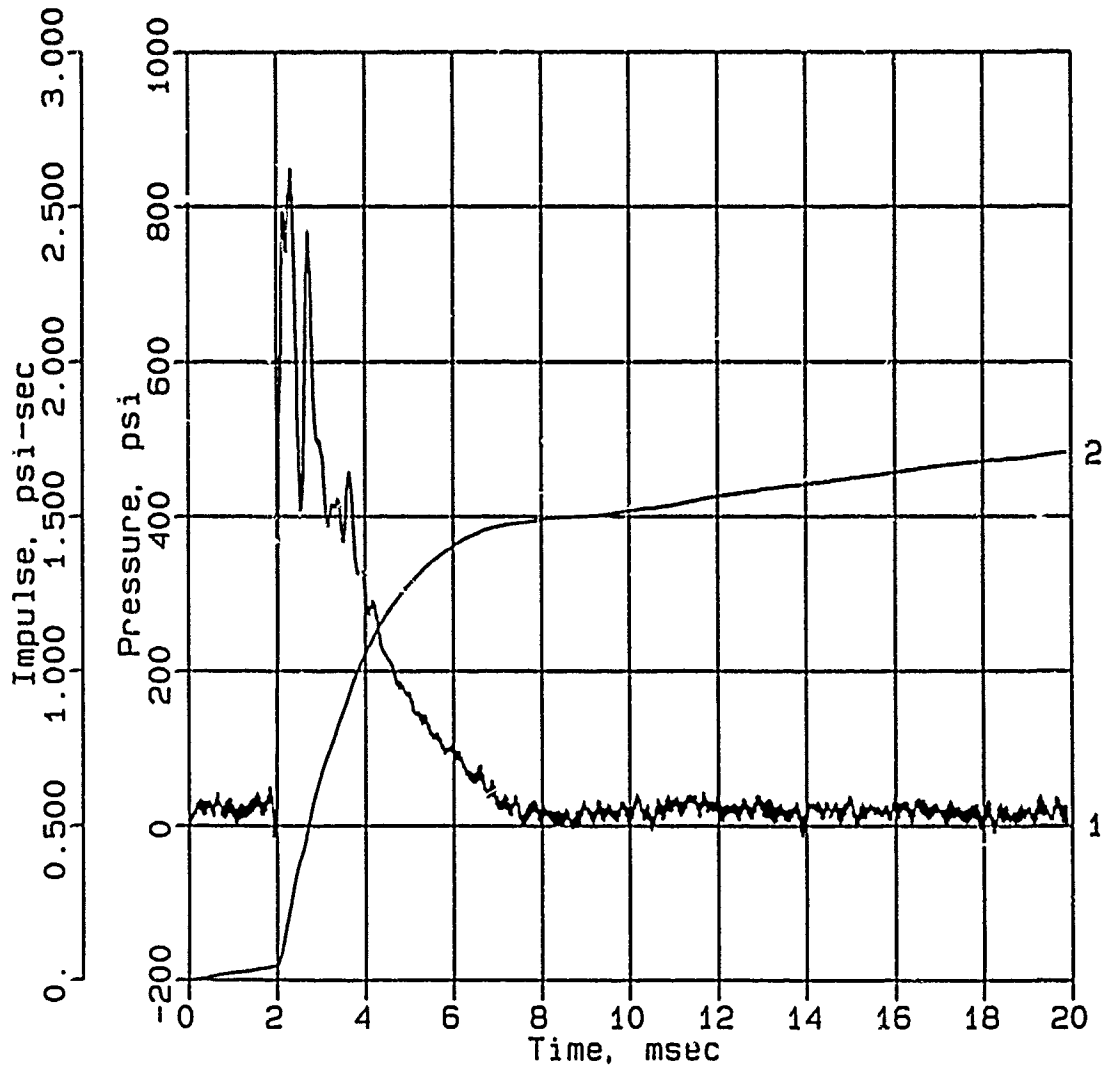
Digitizing rate: 200,000 Hz
Calibration: 10542
Filtering: 20 kHz low pass filter
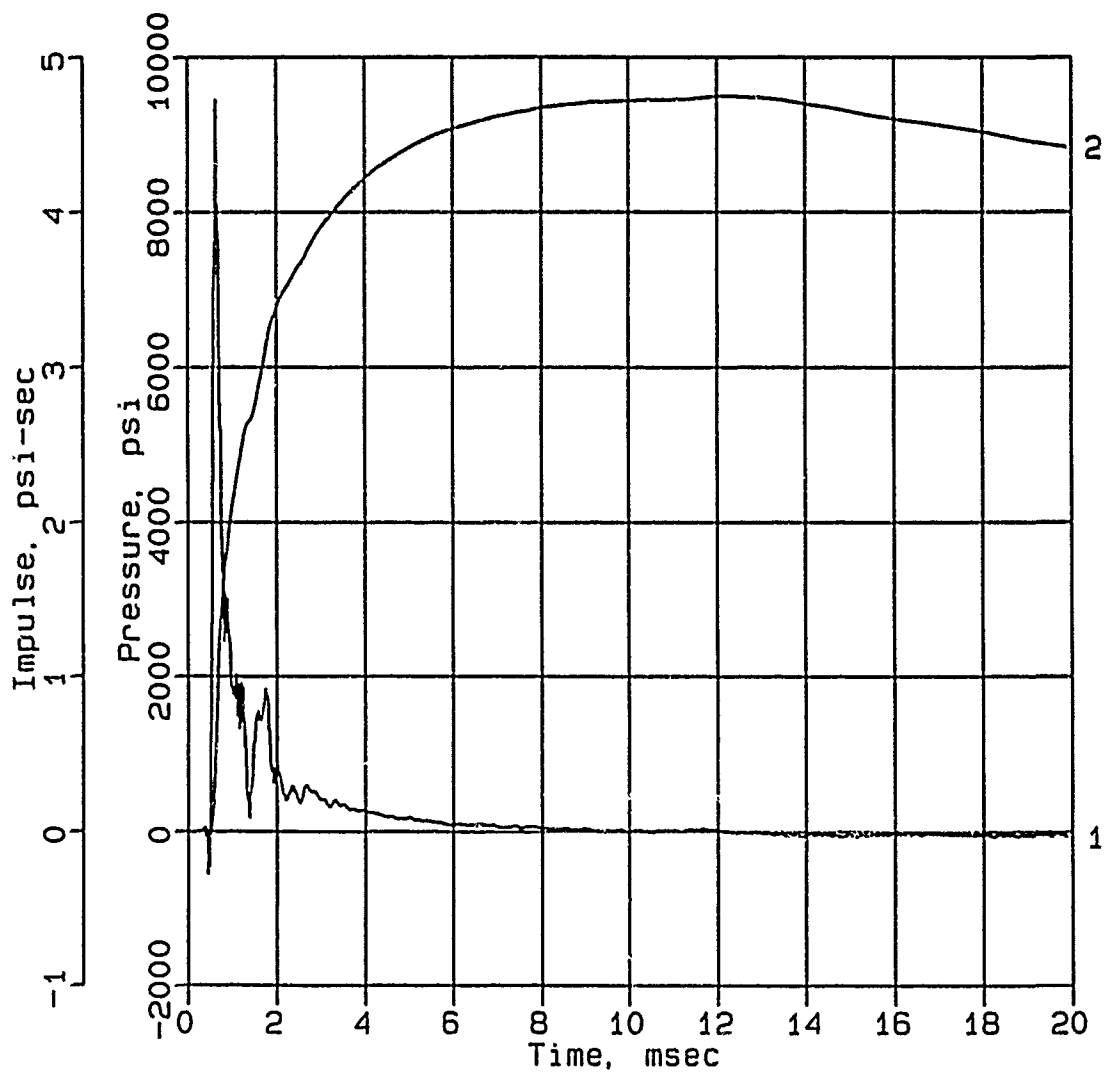   5 - 17 kHz band rejection filter

CONWEB T4

SE-7

Digitizing rate: 200,000 Hz
Calibration: 10160
Filtering: 20 kHz low pass filter
            5 - 17 kHz band rejection filter

CONWEB T4
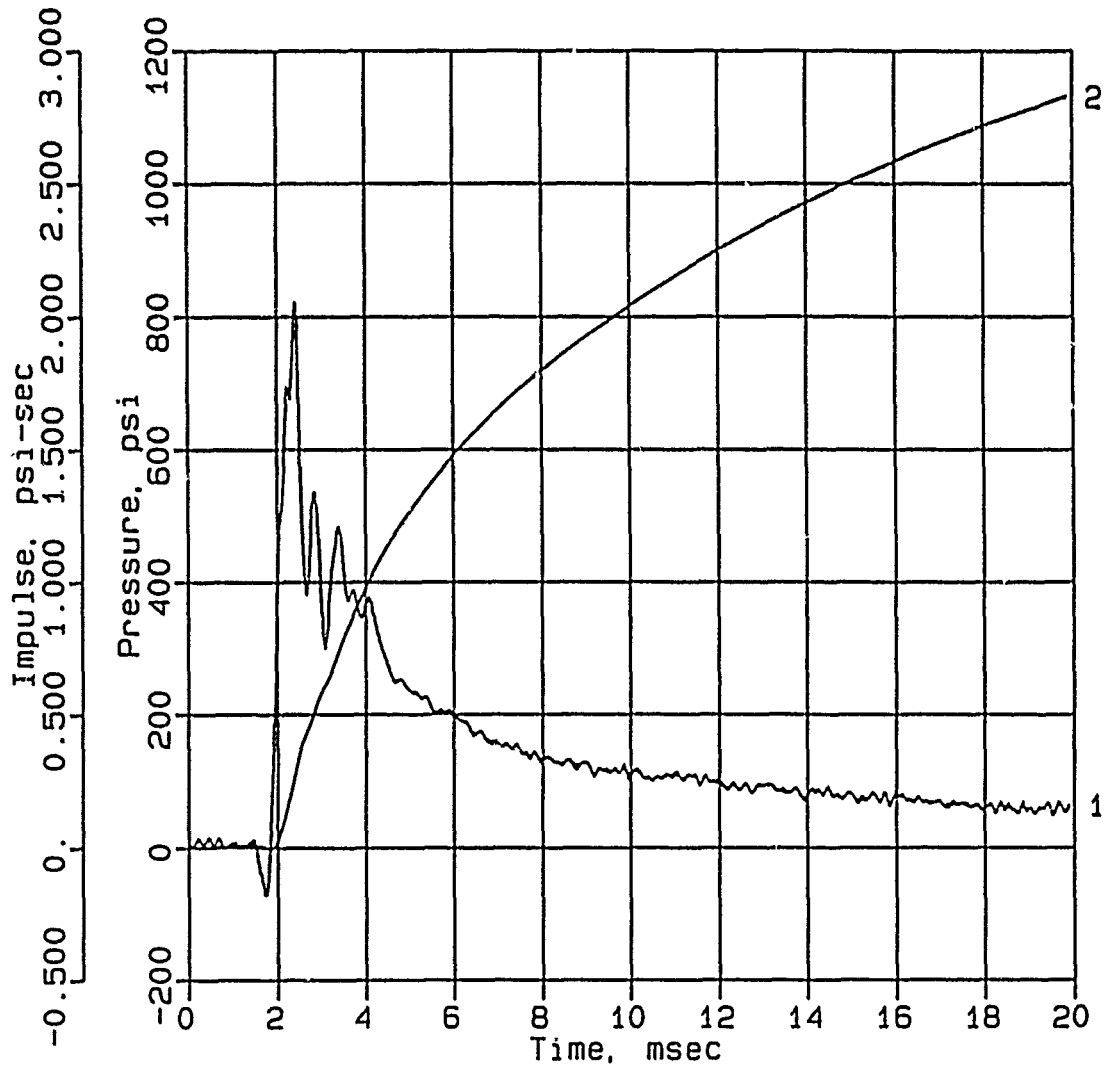
SE-8

Digitizing rate: 200,000 Hz
Calibration: 13827
Filtering: 20 kHz low pass filter
        5 - 17 kHz band rejection filter

CONWEB T4
SE-9
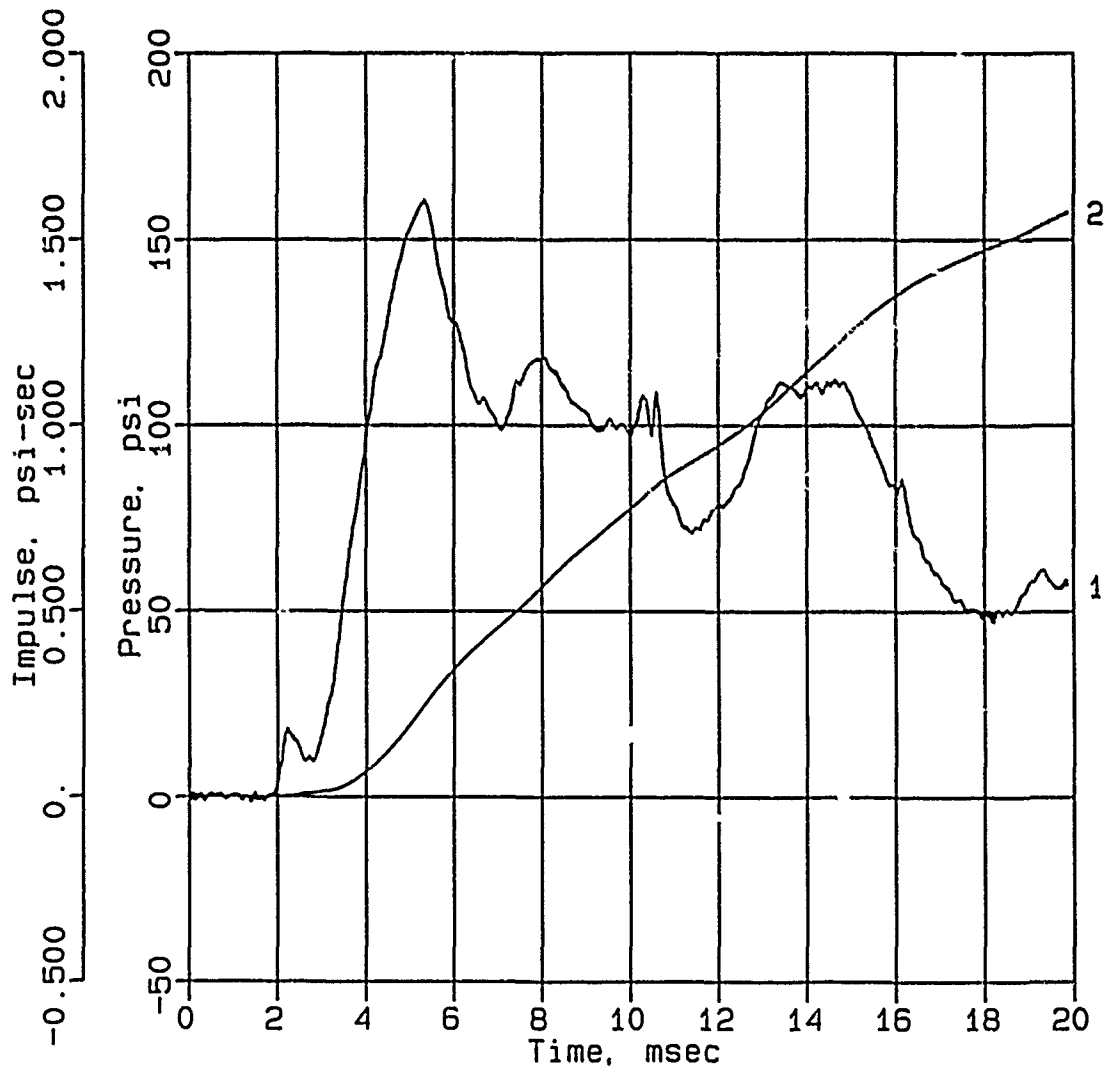

Digitizing rate: 200,000 Hz
Calibration: 7905
Filtering: 20 kHz low pass filter
            5 - 17 kHz band rejection filter

CONWEB T4
SE-11
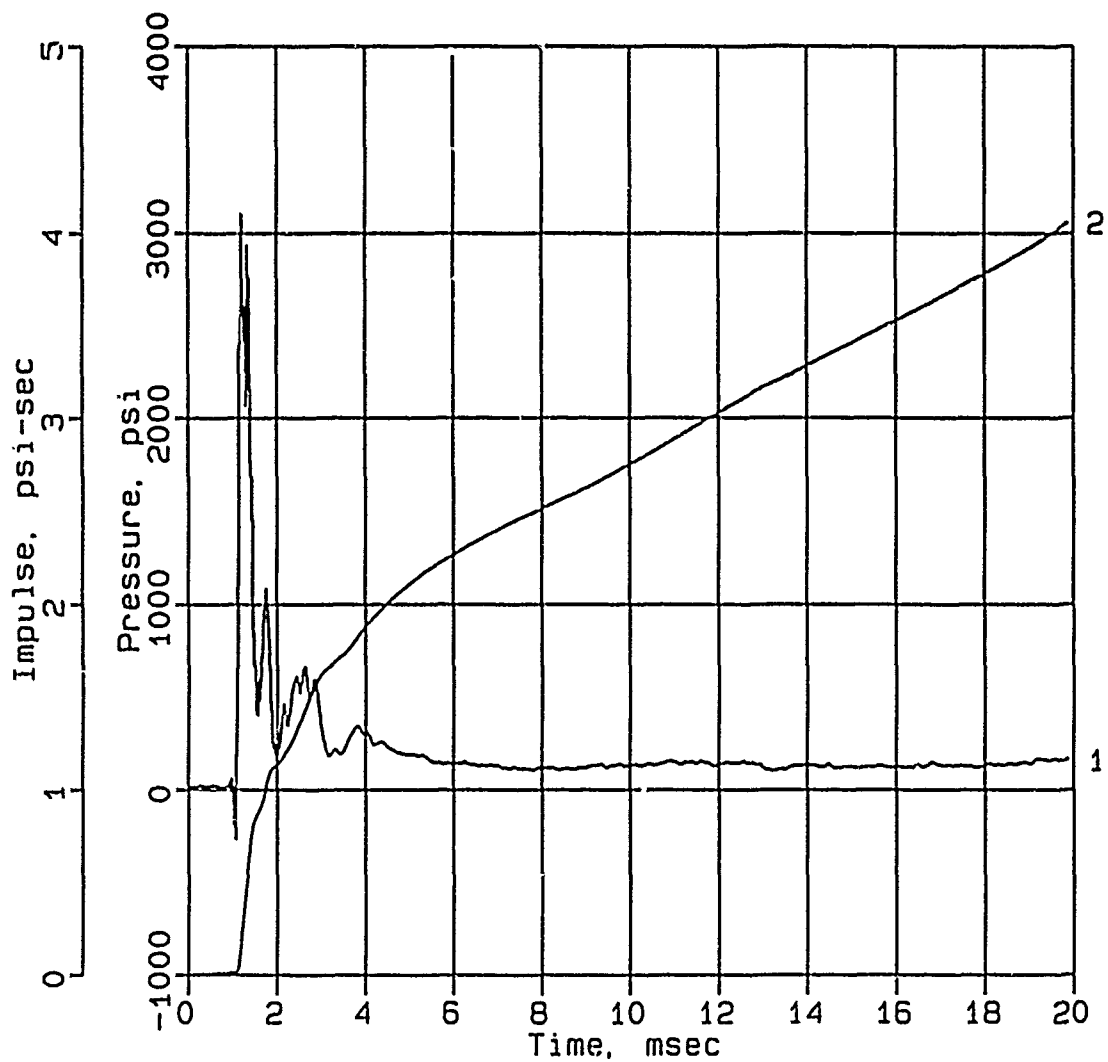

Digitizing rate: 200,000 Hz
Calibration: 866
Filtering: 20 kHz low pass filter
            5 - 17 kHz band rejection filter
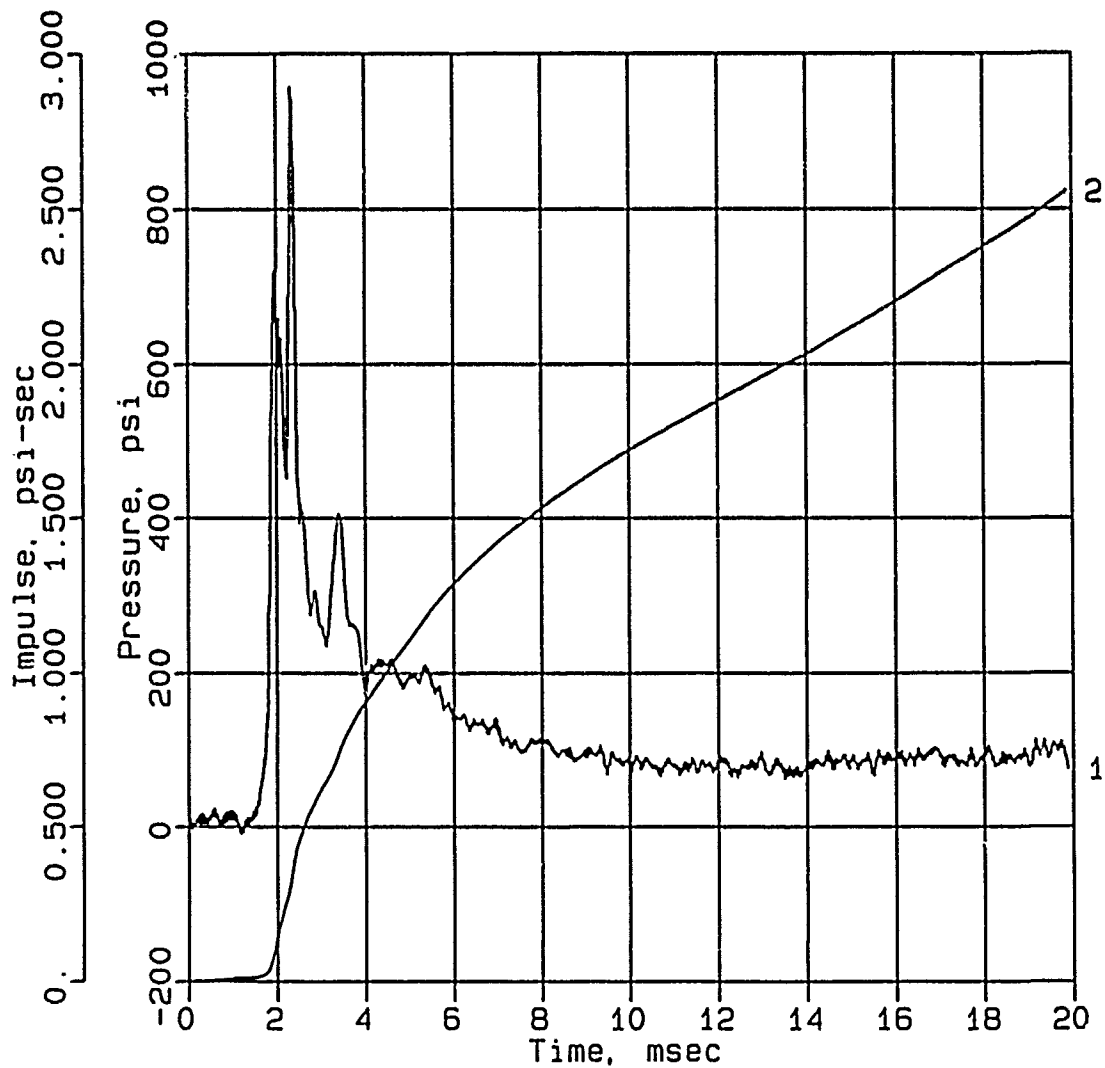
CONWEB T4
SE-13

Digitizing rate: 200,000 Hz
Calibration: 10020
Filtering: 20 kHz low pass filter
        5 - 17 kHz band rejection filter
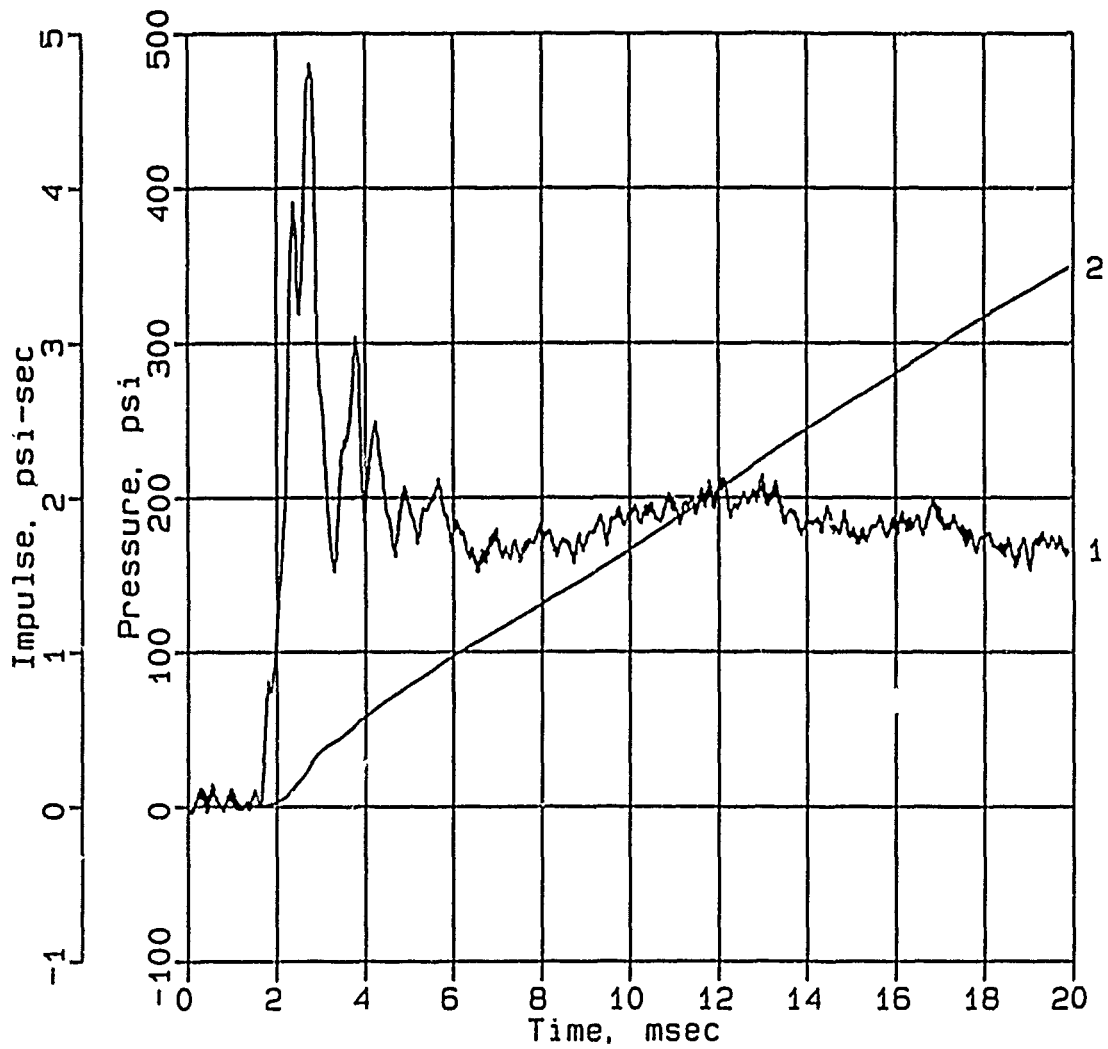
CONWEB T4

SE-14

Digitizing rate: 200,000 Hz
Calibration· 10485
Filtering: 20 kHz low pass filter
5 - 17 kHz band rejection filter

CONWEB T4
SE-15

Digitizing rate: 200,000 Hz
Calibration: 10097
Filtering: 20 kHz low pass filter
        5 - 17 kHz band rejection filter